



Role of CBP and p300 in the establishment and maintenance of transcriptional programs in adult excitatory neurons

PhD Thesis | Michał Lipiński

Role of CBP and p300 in the establishment and maintenance of transcriptional programs in adult excitatory neurons

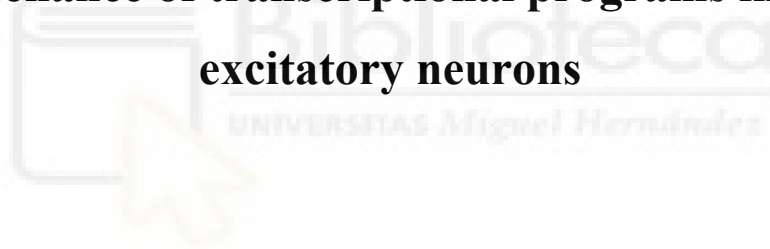
PhD Thesis | Michał Lipiński





Instituto de Neurociencias (CSIC-UMH)
Programa de Doctorado en Neurociencias
Universidad Miguel Hernández de Elche, Alicante (España)

**Role of CBP and p300 in the establishment and
maintenance of transcriptional programs in adult
excitatory neurons**



Doctoral thesis
Presented by:
Michał Lipiński

Director:
Angel Barco, CSIC

Co-director:
Jose Pascual López-Atalaya, CSIC

San Juan de Alicante, 2019



DOCTORAL THESIS BY COMPENDIUM OF PUBLICATIONS

To whom it may concern:

The doctoral thesis developed by me, Michał Lipiński, entitled *Role of CBP and p300 in the establishment and maintenance of transcriptional programs in adult excitatory neurons* is a compendium of publications and includes the following publications:

Lipinski, M., Del Blanco, B. and **Barco, A.** (2019). "CBP/p300 in brain development and plasticity: Disentangling the KAT's cradle."
Current Opinion in Neurobiology 2019 Mar 8; 59:1-8.
DOI: 10.1016/j.conb.2019.01.023

Ito S, Magalska A, Alcaraz-Iborra M, **Lopez-Atalaya JP**, Rovira V, Contreras-Moreira B, **Lipinski M**, Olivares R, Martinez-Hernandez J, Ruszczycki B, Lujan R, Geijo-Barrientos E, Wilczynski GM, **Barco A.** "Loss of neuronal 3D chromatin organization causes transcriptional and behavioural deficits related to serotonergic dysfunction."
Nature Communications 2014 Jul 18; 5:4450.
DOI: 10.1038/ncomms5450. PMID: 25034090.

I declare that these publications will not be used in any other thesis.

Yours sincerely,

San Juan de Alicante, 23th of June 2019

Michał Lipiński



A QUIEN CORRESPONDA:

Prof. Miguel Valdeolmillos López, Coordinador del Programa de Doctorado en Neurociencias del Instituto de Neurociencias, Centro Mixto de la Universidad Miguel Hernández-UMH y la Agencia Estatal Consejo Superior de Investigaciones Científicas-CSIC,

CERTIFICA:



Que la Tesis Doctoral presentada por compendio de publicaciones “**Role of CBP and p300 in the establishment and maintenance of transcriptional programs in adult excitatory neurons**” ha sido realizada por D. Michał Lipiński (NIE: Y2459039P) bajo la dirección del Prof. Angel Barco y codirección de Dr. Jose Pascual López-Atalaya y da su conformidad para que sea presentada a la Comisión de Doctorado de la Universidad Miguel Hernández de Elche.

Para que así conste a los efectos oportunos, firma el presente certificado en San Juan de Alicante a 23 de Junio de 2019.

Miguel Valdeolmillos López



A QUIEN CORRESPONDA:

Dr. Angel Barco, Profesor de Investigación del Consejo Superior de Investigaciones Científicas,

Autoriza la presentación de la Tesis Doctoral por compendio de publicaciones **“Role of CBP and p300 in the establishment and maintenance of transcriptional programs in adult excitatory neurons”** realizada por D. Michał Lipiński (NIE: Y2459039P) bajo su dirección y supervisión en el Instituto de Neurociencias de Alicante, centro mixto CSIC-UMH, presentada para la obtención del grado de Doctor por la Universidad Miguel Hernández de Elche.

Para que así conste a los efectos oportunos, firma el presente certificado en San Juan de Alicante a 23 de Junio de 2019.

Angel Barco



A QUIEN CORRESPONDA:

Dr. Jose Pascual López-Atalaya, Investigador Ramon y Cajal del Consejo Superior de Investigaciones Científicas,

Autoriza la presentación de la Tesis Doctoral por compendio de publicaciones **“Role of CBP and p300 in the establishment and maintenance of transcriptional programs in adult excitatory neurons”** realizada por D. Michał Lipiński (NIE: Y2459039P) en el Instituto de Neurociencias de Alicante, centro mixto CSIC-UMH y presentada para la obtención del grado de Doctor por la Universidad Miguel Hernández de Elche, en la que ha participado como co-director supervisando aspectos concretos del estudio,

Para que así conste a los efectos oportunos, firma el presente certificado en San Juan de Alicante a 23 de Junio de 2019.

Jose Pascual López-Atalaya

“The moment when you step out into the open is also a moment of risk-taking. Letting go of the old is part of the new beginning. There is no beginning without an end.”

Chancellor Angela Merkel, *Speech at the Harvard Commencement Day 2019*

“Traveling is the antidote to ignorance (...). It changes your mind, your perspective, how you believe, what you believe.”

Trevor Noah, *Afraid of the Dark*

“Science is more than a body of knowledge. It’s a way of thinking. A way of skeptically interrogating the universe with a fine understanding of human fallibility.”

Carl Sagan, *Interview with Charlie Rose 1996*



“I’m not trying to prove anything here. I’m a scientist, I know what constitutes proof. I use my childhood name to remind myself that a scientist must also be like a child. If he sees a thing he must say that he sees it, whether it’s what he was expecting to see or not. Otherwise he’ll only see what he is expecting.”

Douglas Adams, *The Hitchhiker’s Guide to The Galaxy, Quandary Phase*

“So, in the face of overwhelming odds, I’m left with only one option:
I’m going to have to science the sh*t out of this.”

Andy Weir, *The Martian*

ACKNOWLEDGEMENTS

First of all, I would like to thank my thesis Director, Angel, for giving me the amazing opportunity of working in his lab, using his resources and most of all learning how to do solid science. If not because of you I would not be where I am right now. Metaphorically, but also literally. The critical thinking, problem solving and my knowledge are definitely the things I am carrying with me from this lab thanks to you. Thank you for all the professional and personal support you gave me.

Second, I need to thank my Co-Director Jose, who has been closely mentoring me for the last 7 years. You taught me both how to plan the experiments and how to perform them. Taught me how to improve based on my experiences. Guided me through the decisions I needed to make. I will always remember these hours of you explaining me the smallest details of science. Thank you for every minute of these hours.

I would like to thank all my labmates, and in these 7 years there were many: Marilyn, Sven, Manu, Deisy, Anna, Satomi, Luismi, Román, Bea, Alejandro, Jordi, Juan, Ana, Nuria, Rafa, Paula, Marta, Marián, Emanuele, Miguel, Romana, Victor, Carmen, Jeiny and Angel. Thank you all for being there with me, teaching me things, learning with me and listening to me playing smart. Thank you for becoming my friends. I cannot acknowledge you enough. Here, I owe my special thanks to all the people who participated in the experiments performed in this PhD thesis: Rafa, Bea, Alejandro, Juan, Nuria, Jordi, Román, Marián and Antonio. Thanks also to Chema and Santiago from Canals lab, Andrzej and Grzegorz from Wilczynski lab. This work could not have been completed without you.

Thanks to all my out-of-the-lab friends. Especially those who never let me down and will hopefully stay my friends forever. Just to mention a few: Sergio J, Ada, Sergio V, Giovanni, Sempere, Anton, Ugo, Cris and Leti. I know I could always count on you. Rogal, Misia, Os i Ania – dziękuję Wam za dodatkowy powód by wracać do Polski.

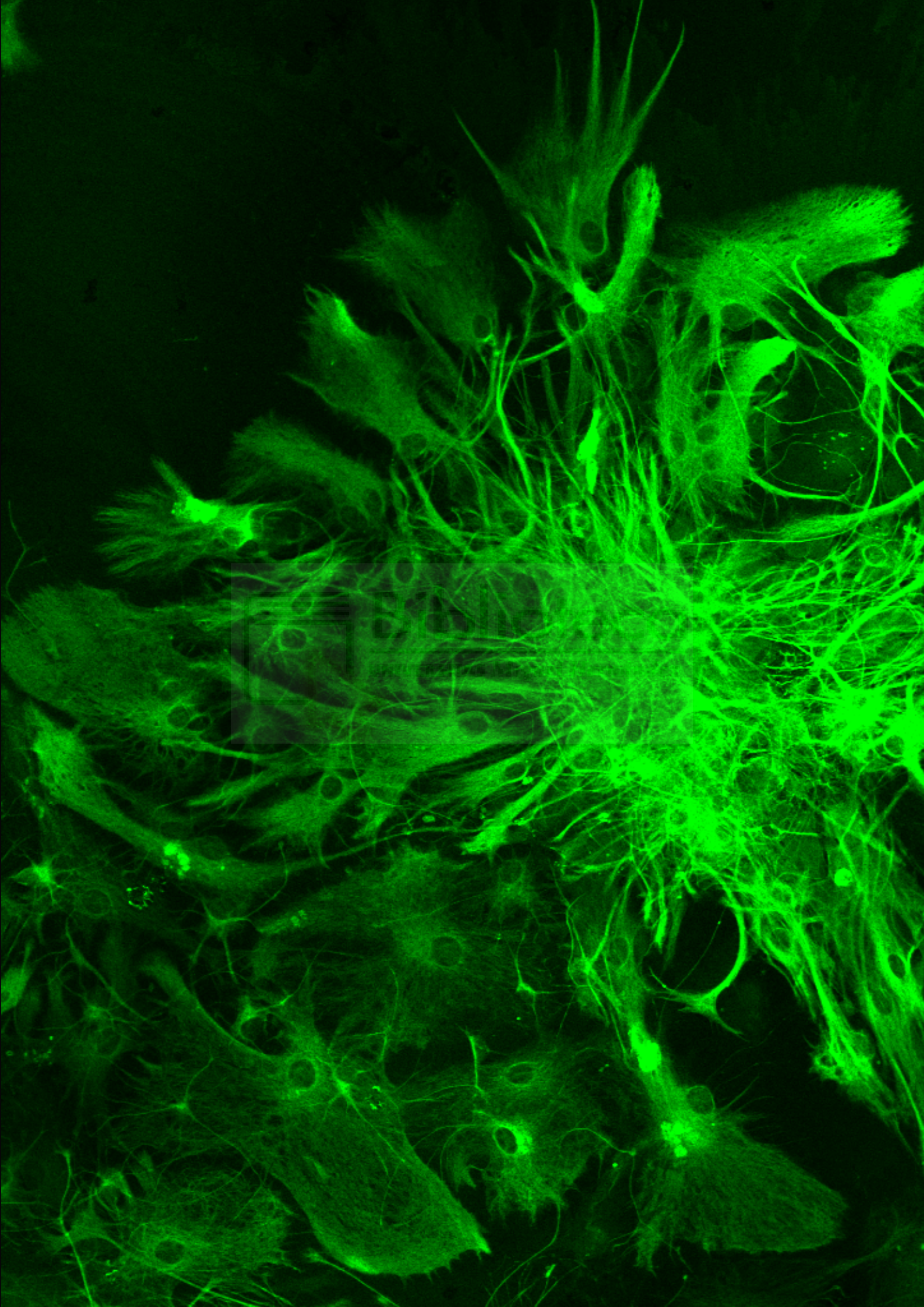
Going towards the most important people in my life, I would like to thank here my family which has been unbelievably supportive during the entire process. Dziękuję Wam Mamo, Tato, Bartek i Justi. Bez Was nigdy by mi się nie udało.

Wielokrotnie myślałem, że nie dam rady. Jeden telefon i już wiedziałem, że jestem w błędzie. Dzięki.

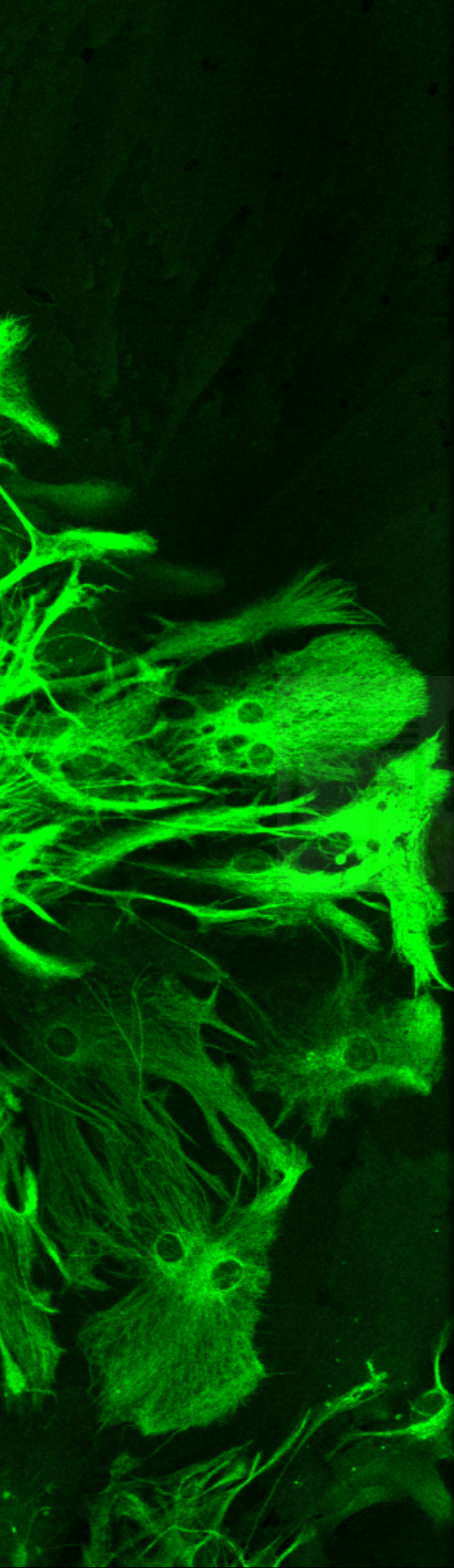
Y a mi familia nueva: Mari, Salvador, Salva, Mariló y Sergio (¡y Eloi!). Gracias por hacerme sentir querido y por hacer España mi nueva Casa. Me alegro mucho de formar parte de vuestra familia.

And most of all I need to thank my love, my best friend and my teammate - Noelia. Only you know how long and bumpy journey it has been and I know couldn't have done it without you. You have been absolutely amazing on every step of the way. You showed me the way. You know my strengths and my weaknesses and you know how to help me use them. Thank you for the most beautiful moments of my life, we will have more of those together. Gracias a la mejor compañera de viaje. Te quiero.





Index

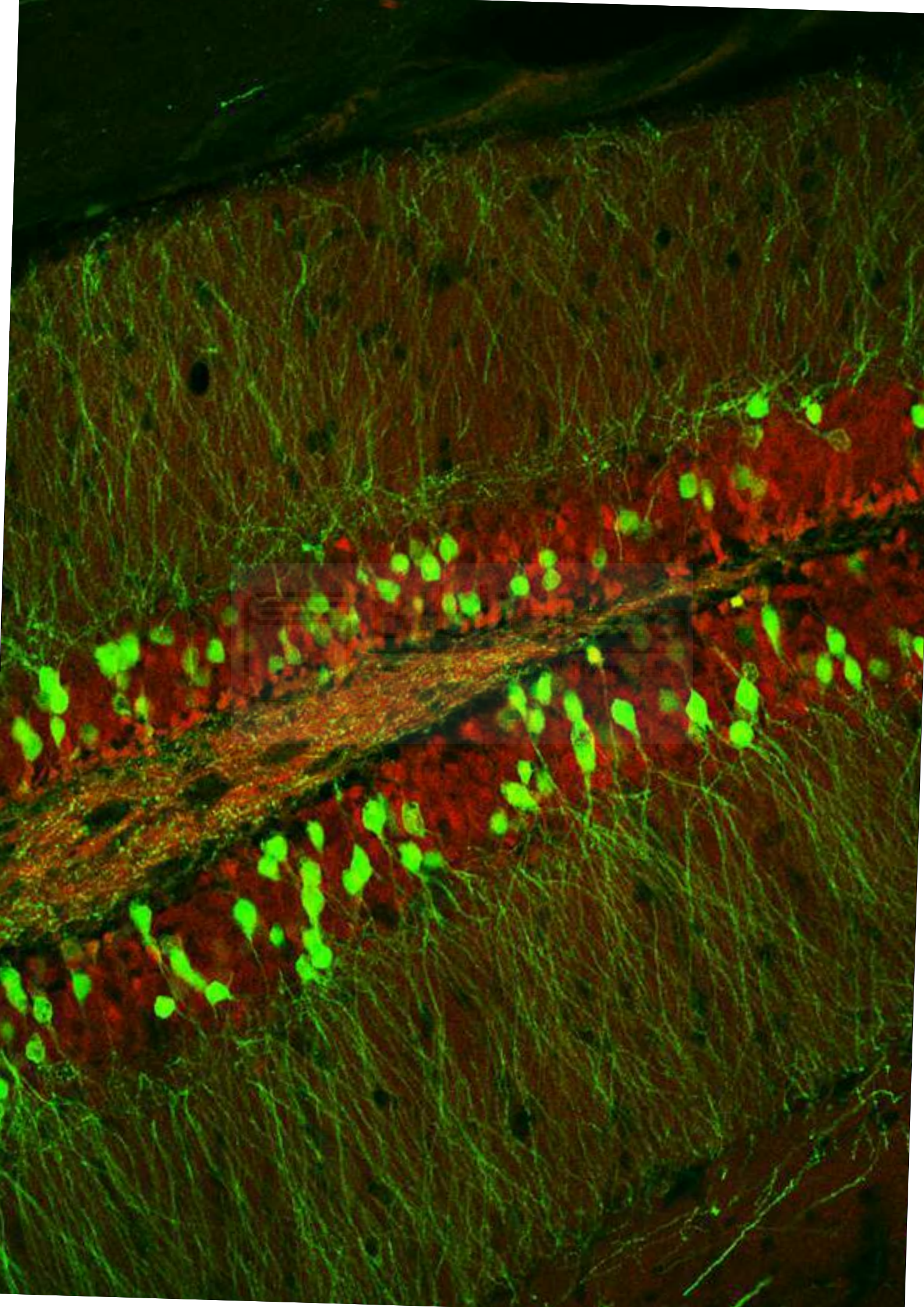


Biblioteca
UNIVERSITAS Miguel Hernández

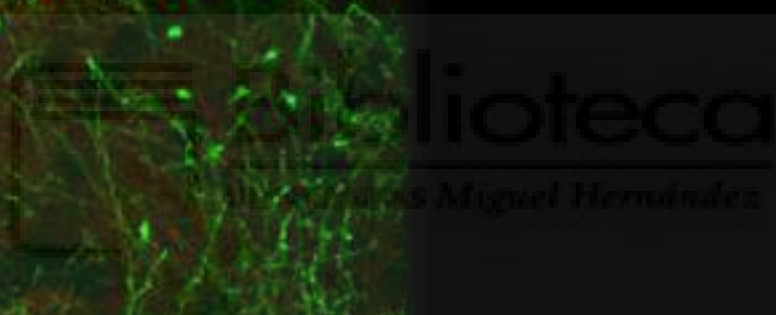
ABSTRACT	1
RESUMEN	3
TABLE OF ABBREVIATIONS	7
1. INTRODUCTION	13
1.1. Epigenetics and transcription	15
1.1.1. The Epigenetic landscape	15
1.1.2. The 3D structure of the interphasic chromatin	18
1.1.3. DNA methylation and other nucleic acids modifications	19
1.1.4. Posttranslational modifications	21
1.1.4.1. Histone acetylation.....	23
1.1.5. Chromatin regulation through protein binding	25
1.1.5.1. Epigenetic mark “readers”	25
1.1.5.2. Chromatin remodelers and transcription factors.....	27
1.1.6. Non-coding RNAs	28
1.2. Epigenetic regulation of neuronal function	32
1.2.1. Neuronal development – model of cellular reprogramming.....	32
1.2.1.1. Epigenetic basis of differentiation	32
1.2.1.2. Neuronal identity mechanisms.....	34
1.2.1.3. Dedifferentiation, transdifferentiation and reprogramming.....	37
1.2.2. Adult brain: plasticity and cognition.....	38
1.3. KAT3 proteins: CBP and P300	41
1.3.1. Shared complex protein structure	42
1.3.2. Two (not so) independent functions	44
1.3.2.1. Scaffolding.....	44
1.3.2.2. Lysine acetyltransferase.....	46

1.3.3. Functional difference between KAT3 proteins.....	49
1.3.4. KAT3 function in the CNS	51
1.3.4.1. Role in neural differentiation and maturation.....	52
1.3.4.2. Role in learning and memory.....	54
2. OBJECTIVES	61
3. MATERIALS AND METHODS	63
4. RESULTS	79
4.1. Chapter I – CBP and p300 jointly safeguard cellular identity by maintaining histone acetylation levels	79
4.1.1. The simultaneous, but not individual, loss of CBP and p300 in adult forebrain principal neurons causes severe neurological deficits	83
4.1.2. Neurons lacking both KAT3 proteins display massive synaptic loss and reduced electrical activity.....	86
4.1.3. The expression of neuronal-specific genes is greatly impaired when both CBP and p300 is missing.....	91
4.1.4. bHLH transcription factors drive the binding of KAT3 proteins to neuron-specific genes and regulatory regions	96
4.1.5. H3K27ac levels are strongly decreased in neuro-specific locations and correlate with the downregulation of transcription.....	101
4.1.6. Targeted histone acetylation increases the expression of the associated genes	105
4.2. Chapter II – Proper levels of CBP, but not p300, are essential for the establishment of experience-induced gene programs and neuroadaptation in adult excitatory neurons.	113
4.2.1. Excitatory neuron-specific elimination of CBP, but not p300, in the adult forebrain causes mild cognitive impairment.....	117
4.2.2. The loss of CBP in the forebrain excitatory neurons causes a moderate transcriptional impairment. The loss of p300 has virtually no effect on transcription.	119

4.2.3. Transcriptional changes in CBP can be linked to histone acetylation deficits	121
4.2.4. CBP excitatory neuron-specific knockout causes a dramatic failure in neuroadaptation	124
5. DISCUSSION	131
5.1. The comparison of KAT3 ifKOs reveals dose-dependent effect.....	133
5.2. Mechanism of CBP and p300 function at their shared targets.....	135
5.3. Unique and specific functions of CBP and p300	136
5.3.1. Differences in the enzymatic activity of the KAT domain	137
5.3.2. Specific interactions with transcription factors and other molecules ...	138
5.3.3. Differences in the level of expression.....	138
5.3.4. Functions and regulations unaccounted for	139
5.4. Role of CBP and p300 in cognition.....	139
5.5. CBP role in neuroadaptation	141
5.6. Role of histone acetylation in transcription.....	142
5.7. The recruitment of KAT3 by cell-specific TF regulates cell identity	143
5.8. Role of NeuroD and other bHLH proteins in cell identity	144
5.9. Mechanisms of KAT3 protection of cell identity	146
6. CONCLUSIONS	153
BIBLIOGRAPHY	161
ANNEX I - Top 100 DEGs in the hippocampus of dKAT3-ifKO mice.....	197
ANNEX II – Full publication list.....	200
ANNEX III – Authored article 1	201
ANNEX IV – Authored article 2.....	219



Abstract & Resumen



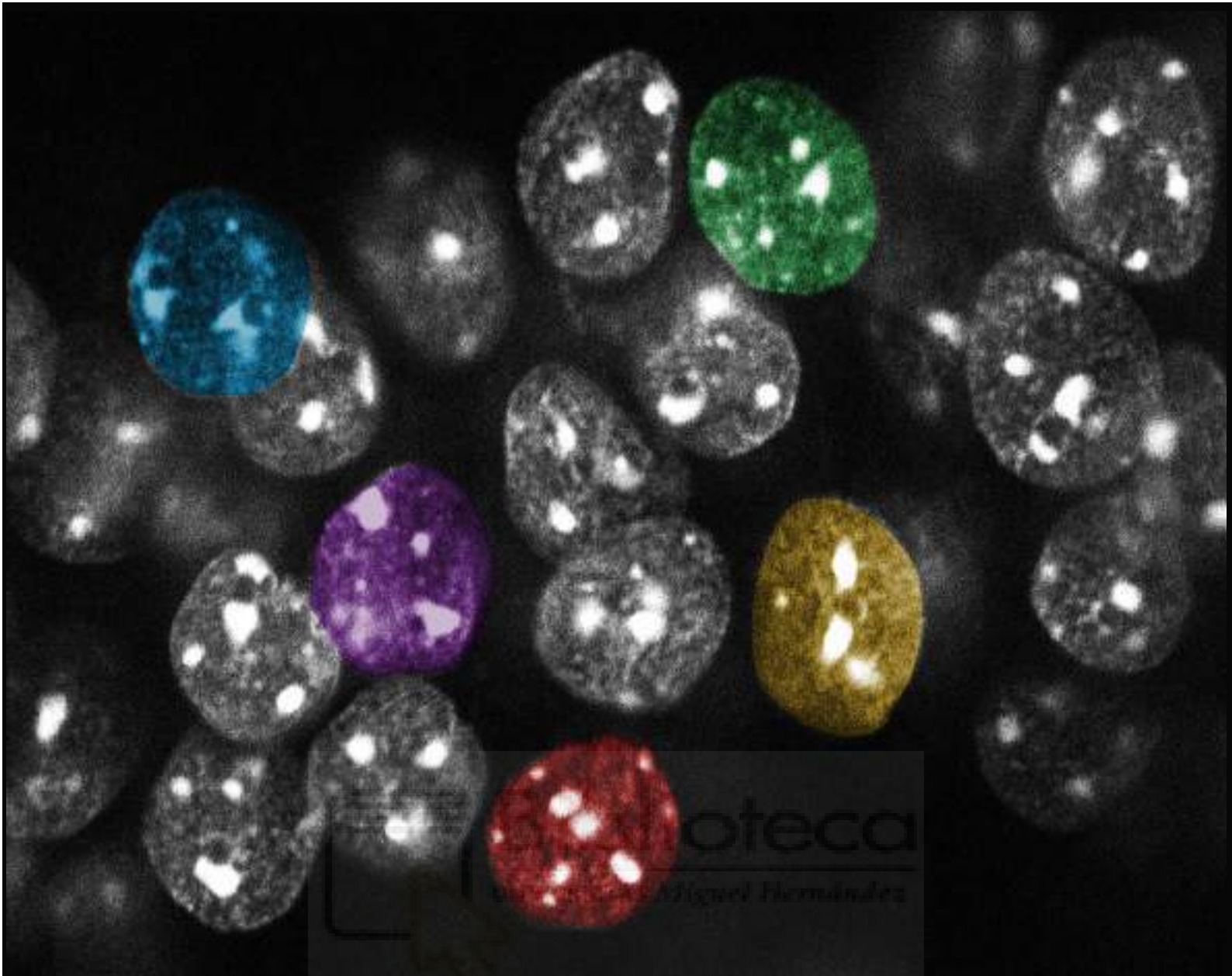
ABSTRACT

The paralog lysine acetyltransferases (KAT) CREB binding protein (CBP) and E1A binding protein (p300) are both essential for the normal development of the nervous system, but their specific function in post-mitotic neurons remain unclear. To investigate these functions, we produced inducible forebrain-specific knockout mice for either one or both proteins. When both KATs were knocked out simultaneously in the adult brain, but not after individual ablation, mice showed a rapid deterioration, severe neurological phenotypes and premature death. These phenotypes were associated with the reduction of once-acquired dendritic complexity and electrical activity in excitatory neurons, which correlates with the transcriptional shutdown of neuronal genes and a dramatic loss of H3K27 acetylation and occupancy by pro-neural transcription factors at neuronal enhancers. Targeted lysine acetylation using the CRISPR/dCas9 system restituted neuronal-specific gene expression. These experiments demonstrate that KAT3 proteins are necessary for maintaining neuronal identity and function in the adult brain by preserving correct chromatin acetylation levels. Further insight into the phenotype of a single-KAT3 induced forebrain knockouts showed that a homozygous loss of a CBP caused a highly specific phenotype in cognition, transcription and histone acetylation. Meanwhile, the modest changes in histone acetylation caused homozygous loss of p300 did not correlate with any changes in behavior or gene expression. Interestingly, the difference between CBP and p300 was highlighted when mice were exposed to a neuroadaptive paradigm like environmental enrichment or pro-epileptic drug sensitization. Whereas the p300 knockouts again did not show any difference from the control littermates, the CBP knockout mice were unable to adapt to the environmental change. This effect was paralleled by a failure in induction a specific gene expression programs induced in control mice as a result of the challenge. Therefore, CBP and p300 jointly maintain neuro-specific transcriptional programs in adult excitatory neurons, and CBP seems to be vital for shifting these programs in response to experiences or environmental changes.



RESUMEN

La proteína de unión a CREB (CBP) y la proteína de unión a E1A (p300) pertenecen a la familia de acetiltransferasas de lisinas (KAT), y son esenciales para el desarrollo del sistema nervioso, aunque su función específica en neuronas maduras se desconoce. Para investigar dichas funciones, hemos producido líneas de ratones donde uno de los genes, o los dos a la vez, pueden ser inactivados de manera inducible y específica en las neuronas excitadoras del telencéfalo (ifKO). Cuando inactivamos las dos KAT3 al mismo tiempo en el cerebro adulto, los ratones rápidamente muestran síntomas neurológicos severos que derivan en una muerte prematura, efectos que no fueron observados cuando las proteínas fueron inactivadas por separado. Este fenotipo está asociado a la reducción de la complejidad dendrítica y actividad eléctrica de las neuronas excitatorias. A nivel transcriptómico, este efecto está correlacionado con un bloqueo de la expresión de genes neuronales y una pérdida pronunciada tanto de la acetilación de H3K27 como de la presencia de factores de transcripción pro-neurales en *enhancers* neuronales. El reclutamiento mediado por el sistema CRISPR/dCas9 de la actividad KAT al locus *Neurod2*, catalogado como gen neuronal, es capaz de restituir la transcripción del gen. Estos experimentos demuestran que las proteínas KAT3 son necesarias para el mantenimiento de la identidad neuronal, salvaguardando el correcto nivel de acetilación. Por otra parte, a partir de un análisis más detallado de los fenotipos de los ifKOs específicos de cada una de las KAT3, se ha observado que la pérdida de CBP produce un fenotipo más restringido que afecta la capacidad cognitiva, y la transcripción y acetilación de genes relacionados con plasticidad. Dichos defectos no se observan en los ratones deficientes para p300. La diferencia entre CBP y p300 es incluso más evidente cuando los ratones se exponen a un paradigma neuro-adaptativo como es el caso del ambiente enriquecido o la sensibilización a una droga pro-epiléptica. Mientras que los ifKOs de p300 no presentan ninguna diferencia en comparación con los animales controles, el sistema nervioso de los ifKOs de CBP es incapaz de adaptarse a las nuevas condiciones. La neuro-adaptación en los controles implica cambios en la expresión génica neuronal que no fueron observados en estos ratones. Por lo tanto, CBP y p300 mantienen conjuntamente el programa específico de las neuronas excitadoras adultas, además CBP parece, por si mismo, ser una pieza imprescindible en la adaptación del transcriptoma neuronal a cambios inducidos experiencia o cambios en el entorno.



oteca

Díaz Hernández

Abbreviations

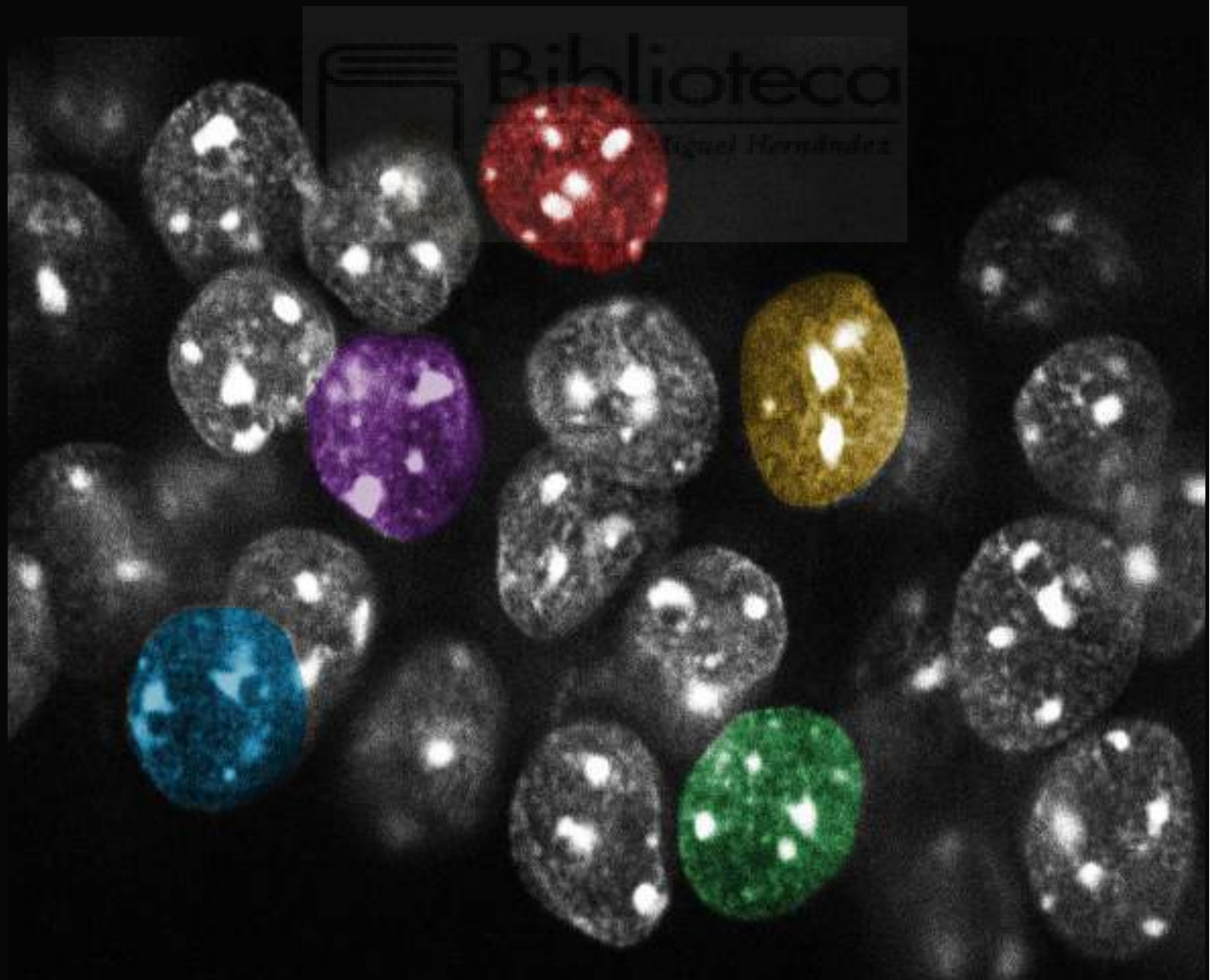




TABLE OF ABBREVIATIONS

3C	Chromatin Conformation Capture
3D	3 Dimensional
5mC	5-methylcytosine (DNA)
5hmC	5-hydroxycytosine (DNA)
5fC	5-formylcytosine (DNA)
5caC	5-carboxylcytosine (DNA)
ASD	Autism Spectrum Disorder
ATAC-seq	Assay for Transposase-Accessible Chromatin using sequencing
BDNF	Brain-Derived Neurotrophic Factor
bHLH	basic Helix-Loop-Helix
bp	base pairs
BrD	Bromodomain
Cas3	Caspase 3
Cas9	Caspase 9
CBP	CREB-binding protein
CBP-ifKO	CBP inducible forebrain knockout
ChIP	Chromatin Immunoprecipitation
ChIP-seq	Chromatin Immunoprecipitation followed by sequencing
CNS	Central Nervous System
CpG	Cytosine followed by Guanine
CpH	Cytosine followed by non-guanine nucleotide
CREBBP	CREB-binding protein
CRISPR	Clustered Regularly Interspaced Short Palindromic Repeats
CTCF	CCCTC-binding factor
DAR	Differentially Accessible Region
DHS	DNase I Hypersensitive Site
dKAT3-ifKO	double KAT3 inducible forebrain knockout
DNase I	Deoxyribonuclease I
DNase-seq	DNase I hypersensitive sites sequencing
E	Glutamic acid

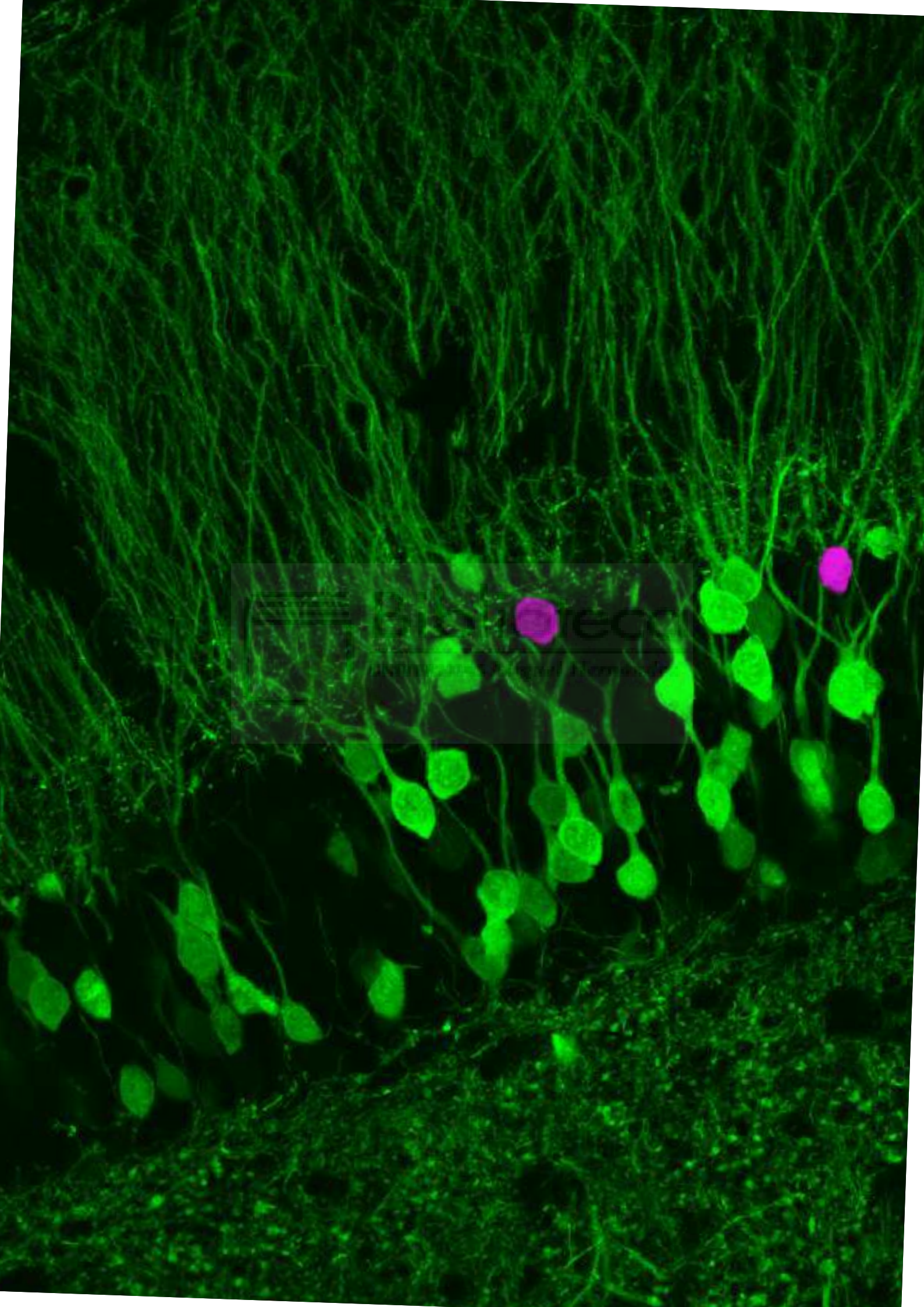
E1A	adenovirus early region 1A
EE	Environmental Enrichment
EM	Electron Microscopy
ENCODE	Encyclopedia of DNA Elements
EP300	E1A-associated protein p300
EPM	Elevated Plus Maze test
eRNA	enhancer RNA
ESC	Embryonic Stem Cell
FC	Fear Conditioning
FISH	Fluorescent <i>In-Situ</i> Hybridization
GO	Gene Ontology
GoF	Gain-of-Function
H	Histidine
HDAC	Histone deacetylase
HDACi	Histone deacetylase inhibitors
ICC	Immunocytochemistry
IDD	Intellectual Disability Disorder
IEG	Immediate-early gene
ifKO	Inducible forebrain knockout
IHC	Immunohistochemistry
IP	Intraperitoneal
iPSC	induced Pluripotent Stem Cell
K	Lysine
KAT	Lysine acetyltransferase
kb	kilobase
KO	Knockout
lncRNA	long non-coding RNA
LoF	Loss-of-Function
LFP	Local Field Potential
m⁶A	N ⁶ -methyladenosine (RNA)
m⁵C	5-methylcytosine (RNA)
MB	Marble Burying test
MBD	Methyl-CpG Binding Domain
mCA	methylated Cytosine followed by Adenine


mCG	methyated Cytosine followed by Guanine
mCH	methyated Cytosine followed by non-guanine nucleotide
MeCP2	Methyl-CpG binding Protein 2
MEF	Mouse Embryonic Fibroblasts
miRNA	microRNA
MWM	Morris Water Maze test
ncRNA	non-coding RNA
NGS	Next-Generation Sequencing
NOR	Novel Object Recognition
NPC	Neuronal Progenitor Cell
nt	nucleotides
OF	Open-Field test
P300-ifKO	P300 inducible forebrain knockout
PCA	Principal Component Analysis
PCAF	p300/CBP-Associated Factor
Pol2	RNA Polymerase 2
PRC2	Polycomb Repressive Complex 2
PTM	Posttranslational Modification
PTZ	Pentylene-tetrazol
qPCR	quantitative Polymerase Chain Reaction
R	Arginine
RA	Retinoic Acid
REST	Repressor element-1 silencing transcription factor
RNA-seq	RNA sequencing
RSTS	Rubinstein-Taybi Syndrome
RTT	Rett Syndrome
S	Serine
SYN1	Synapsin 1
T	Threonine
TAD	Topologically Associating Domain
TES	Transcription End Site
TF	Transcription Factor
TFBS	Transcription Factor Binding Site
TMX	Tamoxifen

TSS Transcription Start Site
WB Western blot
Y Tyrosine

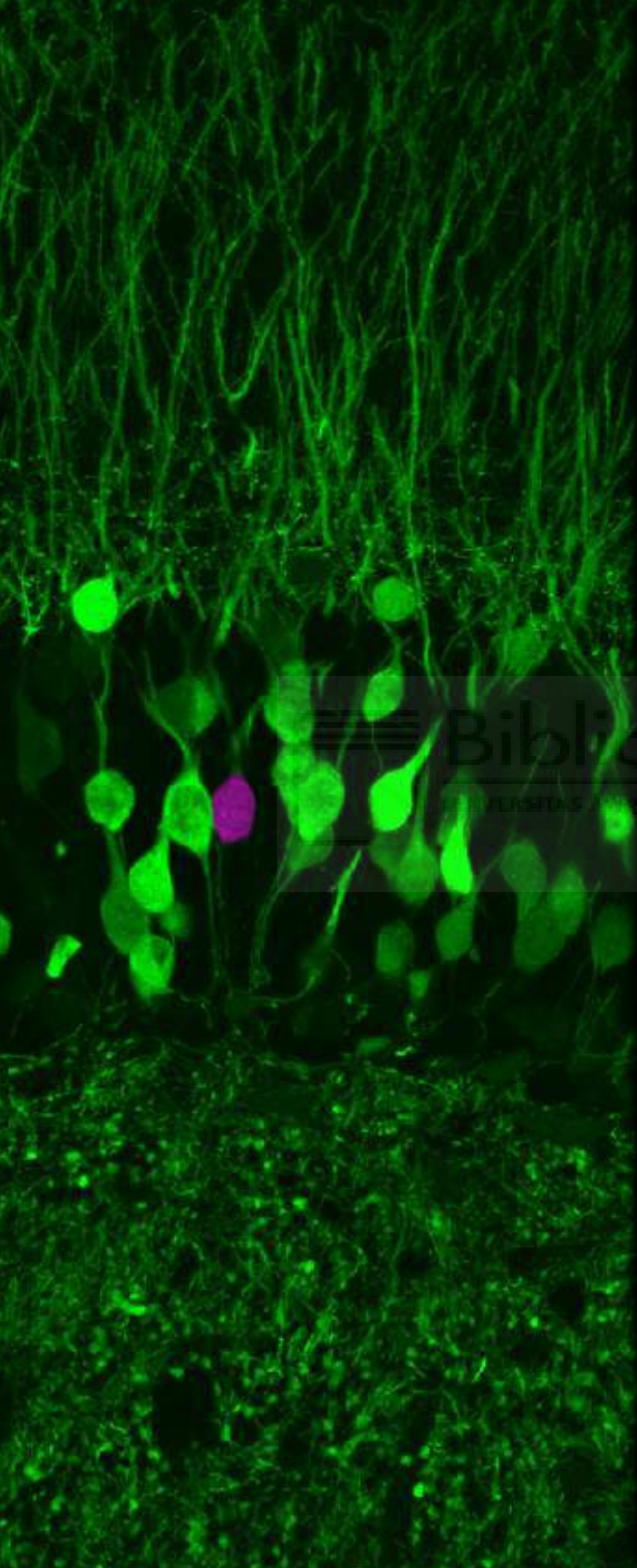






 **TECON**
TECHNOLOGY FOR NEURAL NETWORKS

Introduction



 **Biblioteca**
UNIVERSIDAD JOSÉ MARÍA HERNÁNDEZ



1.1. Epigenetics and transcription

1.1.1. The epigenetic landscape

Since ancient history, people tended to believe that the features acquired during the lifetime can be subsequently inherited. The inheritance of acquired characteristics (later also called *soft inheritance*), was accepted by many prominent philosophers and biologists, including Aristotle, Roger Bacon and Immanuel Kant (Zirkle 1935). In the early 1800s the idea was further popularized by Jean-Baptiste Lamarck in his “Philosophie Zoologique” (Lamarck 1809), which is why the hypothesis is subsequently referred to as *Lamarckism*. In the following years, the discovery of the basic laws of inheritance by Gregor Mendel (Mendel 1865) and Thomas Hunt Morgan (Morgan 1915) strongly contradicted the idea of soft inheritance. The experiments of Mendel and Morgan suggested that the information about the phenotype of the organism is hardwired into the organism, although it has not been clear how. The experiments of Mendel and Morgan suggested that the information about the phenotype of the organism is hardwired into the organism, although it has not been clear how. The development of this abstract concept led Wilhelm Johannsen to coin the term *gene* (Johannsen 1905) - an abstract inheritance vector with a fairly proven role, but which biological structure was deemed to be unknown for decades to come. With time, it became clear that a single gene mutation can cause different phenotypes in different cells, therefore the cell needs to somehow “know” what genes to turn on. In order to explain this phenomenon the terms *epigenetics* and *epigenotype* were first proposed by brilliant Conrad Hall Waddington in the early 1940’s (Waddington 1942, reprinted in Waddington 2012). In 1957 in “The strategy of the genes”, Waddington introduced a so-called *epigenetic landscape* - a metaphor for how different genes interact with the environment in order to create a particular cellular phenotype (Waddington 1957). The time has proven this analogy to be particularly solid.

Currently the word *epigenetic* is somewhat confusing. It has been widely used as some version of extragenetic regulation since 1990’s, when the genetic revolution started. However, only in 2009 some of the leading scientists in epigenetics forged a precise definition of the word as: “An epigenetic trait is a stably heritable phenotype resulting from changes in a chromosome without alterations in the DNA sequence.” (Berger et al. 2009). This definition however, especially the word “heritable”, seem to

create some controversy. Under this definition, some of the features widely recognized as “epigenetic”, for example most histone post-translation modifications (PTMs), would not enter in the field of epigenetics. In this work, I would like to follow the strategy undertaken by several newer large-scale projects. Roadmap Epigenomics Project for example define epigenetics as “both heritable changes in gene activity and expression (in the progeny of cells or of individuals) and also stable, long-term alterations in the transcriptional potential of a cell that are not necessarily heritable” (<http://www.roadmapepigenomics.org/overview>).

The definition of the word “epigenetic” proposed in 2009 suggests where we are supposed to look for the source of this “epigenetic” regulation - the chromosome. The chromosome, or rather more generally chromatin, is a structured organization of the DNA, highly packed with all the accompanying proteins. Curiously, the chromatin was discovered and named in 1882 by Walther Flemming as a “substance in the cell nucleus which is readily stained” (Flemming 1882, Olins and Olins 2003). Although definitively proven in 1997 (Luger et al. 1997, 2012), the chromatin structure was first proposed by Roger Kornberg in 1974 (Kornberg 1974). There, every 145-147 base pairs of the genomic DNA are wrapped around a nucleosome - octamer structure built of 2 copies of 4 core histone proteins: H2A, H2B, H3 and H4. The DNA fragment linking the nucleosomes (linker DNA, 20-80 bp) contains another histone, the linker histone H1 (Maeshima et al. 2014). This organization brings to mind “beads on the string” and is often referred to as 10-nm chromatin fiber (Olins and Olins 2003, Maeshima et al. 2014). Classically, based on the electron microscopy (EM) observations *in vitro*, this 10-nm fiber was proposed to fold into highly organized 30-nm fibers (Finch and Klug 1976). However, these 30-nm fibers seem to be quite elusive *in vivo* and some recent data put their entire existence *in vivo* into question (Luger et al. 2012, Maeshima et al. 2014). Instead, a more flexible, malleable form of irregular folding of the 10-nm fiber has been proposed to occur under physiological conditions (**Fig. I-1**). This new model might fit slightly better with what we know about the behavior of the chromatin so far (Maeshima et al. 2014). Independently of how the real secondary chromatin structure looks like, we know it is tightly packed in the nucleus, where it forms two possible states: “euchromatin” (fairly loose) and “heterochromatin” (compacted). The euchromatin is the genetic material which is either actively transcribed, or at least ready to be transcribed (the case of stimulus-induced genes such as the immediate-early genes, IEG). On the other hand, the heterochromatin is the silenced state of the chromatin and

can be further divided into “constitutive” (highly condensed) and “facultative” (less condensed). The constitutive heterochromatin forms in parts of the genome that are never transcribed, for example pericentromeres, telomeres and repetitive sequences. The fact that these regions generally do not contain genes and are likely the same in every single cell-type makes it very different from the facultative chromatin. Facultative chromatin forms in various places in the genome that contain genes that are silenced in specific cell types or developmental stages. The decision regarding silencing of a particular part of the genome might happen throughout the development and might differ between cell-types (Saksouk et al. 2015). Each of these states has its own characteristics and markers, which will be discussed further in the following chapters.

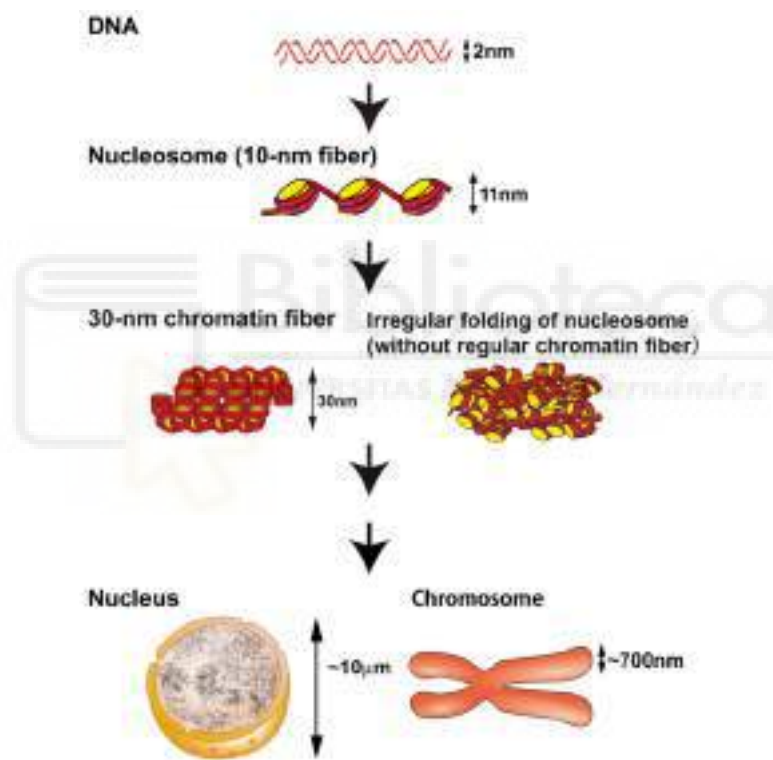


Figure I-1. Old and novel view on chromatin structure. Newer data (right) suggest that *in vivo* the chromatin might not be forming the long-accepted 30-nm fibers (left). Instead, it is likely creating irregular formations. Adapted from Maeshima et al. 2014.

The need for an exact verification of the state of chromatin opening (or more precisely – accessibility) has driven the scientific community to develop several methods for addressing this issue. In 1976 Weintraub and Groudine (Weintraub and Groudine 1976) discovered the existence of chromatin regions sensitive to the digestion by deoxyribonuclease I (DNase I). They hypothesized that these regions are likely bound by histones that are in alternative conformation, permitting the access of the

enzyme to the DNA. Not long after, these places were called DNase I hypersensitive sites (DHS) and started to be commonly used to define accessible chromatin regions in the DNA (Wu 1980, Keene et al. 1981, McGhee et al. 1981). During the genomic revolution in the early 2000s the application of next-generation sequencing (NGS) to this methodology (DNase-seq) resulted in a plentitude of genome-wide DHS accessibility profiles (Crawford et al. 2006, Boyle et al. 2008, Risca and Greenleaf 2015). This type of information was important enough to be the major object of study in massive multinational projects like Encyclopedia of DNA Elements (ENCODE 2007, 2012). In the recent years, multiple alternative techniques have been proposed (FAIRE-seq, MNase-seq, etc. summarized in Risca and Greenleaf 2015), with one recently gaining a particular interest of the scientific community. The Assay for Transposase-Accessible Chromatin using sequencing (ATAC-seq) arose as the favorite substitute thanks to its simplicity (Buenrostro et al. 2013) and requirement of very little chromatin input (most recently even single-cell; Buenrostro et al. 2015). This technique apart from delineating chromatin accessibility allows for mapping of the nucleosome positions and footprinting of transcription factor binding.

1.1.2. The 3D structure of the interphasic chromatin

It is important to say that the chromatin is not organized only in two dimensions: more loose or more condensed. In fact, its complex 3D structures have been suggested to play an important role in the regulation of transcription of the associated regions (Bickmore 2013). Light and electron microscopy-based experiments from the 1970s had already indicated that the chromatin in the nucleus is organized in some kind of loops (Chetverina et al. 2017). Since then, newer methodologies based on chromatin fluorescent *in-situ* hybridization (FISH) or chromatin conformation capture (3C) allowed for more and more accurate outlining of higher-order chromatin organization. Much research in the recent years have been also focused on the identification of the function of so-called Topologically Associating Domains (TADs). These regions are limited by binding of the architectural protein CTCF and seem to be somehow hardwired into the intrinsic properties of the genome sequence as they do not differ much between cells with a very different function (Bickmore 2013).

The function of chromatin structure in transcription is currently under debate (Bonev and Cavalli 2016). On one hand, multiple studies suggest a good correlation

between high-order chromatin structure and gene expression and engineering a chromatin loop in a gene locus is sufficient to induce transcription (Deng et al. 2012, Deng et al. 2014, Bonev and Cavalli 2016, Bonev et al. 2017). On the other hand, several other studies suggest a limited causal role of the 3D structure in gene expression. For example, translocation of some highly active gene loci to the transcriptionally inactive periphery does not affect the gene expression of these genes *in vitro* (Shachar et al. 2015). Moreover, a complete elimination of chromatin loops causes only a modest impact on transcription (Rao et al. 2017). On a similar note, our laboratory showed that fusing a GFP reporter to the histone H2B causes robust changes in the subnuclear structure. Interestingly, introducing these alterations in adult forebrain excitatory neurons caused very restricted transcriptional deregulation that affected serotonergic gene expression and triggered serotonin-related behavioral changes (Ito et al. 2014) (ANNEX IV). This observation is particularly important, as the manipulation affected directly and exclusively the chromatin 3D structure and this was sufficient to trigger a cognitive impairment. Whether genome 3D structure controls the transcription on genome-wide scale requires further validation.

1.1.3. DNA methylation and other nucleic acids modifications

The DNA methylation is one of the better-established models of epigenetic gene expression regulation. Classically, the DNA was thought to be methylated almost exclusively on the fifth position of the pyrimidine ring of a cytosine (5mC) followed by a guanine (5mCG or simply mCG). Although 80-90% of all these CG dinucleotides are methylated in the mammalian genome, the regions that are particularly highly enriched with CG dinucleotides (CpG islands) are mostly lacking the DNA methylation (Shin et al. 2014). The CpG methylation has been profoundly studied and its correlation with transcription regulation is well-established. Still, even though the mCG generally correlates with low expression or even active silencing, this regulation might be much more complex and depends on the precise genomic location or cell developmental state (Shin et al. 2014, He and Ecker 2015, Ciernia and LaSalle 2016).

In the pre-genomics era the analysis of the DNA methylation was purely focused on the study of the CpG islands. The introduction of the whole-genome approaches permitted for the discovery of non-CG methylation, namely CpC, CpA and CpT, jointly named CpH methylation (also 5mCH or mCH). It was a big surprise at the moment that

these modifications were actually so abundant in the mammalian genome (Lister et al. 2009, Ciernia and LaSalle 2016). The role of the CpH methylation is still not entirely clear. Its genomic enrichment pattern is plainly non-random, however it does not correlate directly with the level of gene expression of the corresponding gene (He and Ecker 2015). Interestingly, some recent research suggests that mCA might play a specific role in early-life fine-tuning of gene transcription in neurons (Stroud et al. 2017). As the mCA is the most abundant mCH in many tissues (especially the brain), it is likely playing a crucial role in precise adjustments of the transcription. Nevertheless, more work needs to be done in order to identify the roles of each CpH methylation in different cellular contexts.

The first enzyme managing the levels of 5mC to be discovered, was DNA methyltransferase 1 Dnmt1 (Bestor 1990), which was later followed by other two DNA methyltransferases expressed in the mammalian cells - Dnmt3a and Dnmt3b (Okano et al. 1998, Shin et al. 2014). All three enzymes add the methyl group to the mammalian DNA, however with various specificity towards the dinucleotide (mCG versus mCH) and towards the previous methylation state (Shin et al. 2014, Stroud et al. 2017). The demethylation pathway has not been discovered until much later, while first demethylating Ten-eleven translocation (Tet) proteins were identified. This finding also finally confirmed that the 5-hydroxymethylation (5hmC), long observed in the mammalian genome, is not solely DNA damage marker but the first step in the healthy cell DNA demethylation pathway (Tahiliani et al. 2009, He et al. 2011, Ito et al. 2011, Shin et al. 2014). Around the same time, further oxidized forms of DNA methylation like 5-formylcytosine (5fC) and 5-carboxylcytosine (5caC) were observed in the mammalian genome (Ito et al. 2011). Although the abundance of these demethylation products (especially 5hmC) has been proven *in vivo*, their exact role is still under debate (Shin et al. 2014).

As a final remark regarding nucleic acid modifications, I would like to mention that not only the DNA can be modified. RNA modifications have been described already the 1960s, but only till very recently they did not get that attention from the epigeneticists. In the year 2012 with the first applications of the NGS technologies to investigate the RNA modifications, the new field of *epitranscriptomics* emerged (Roundtree et al. 2017). Although it is pretty well established already that the modifications of mRNA like N⁶-methyladenosine (m⁶A), 5-methylcytosine (m⁵C), and pseudouridine (Ψ) play an important role in almost all the steps of mRNA regulation

(Gilbert et al. 2016, Roundtree et al. 2017), it is still too early to say what would be the extent of their relevance in gene expression.

1.1.4. Posttranslational modifications

The other highly studied chromatin regulation mechanism goes through the covalent PTM of proteins. Indeed most, if not all proteins can be modified and modification of the transcriptional factors and chromatin regulators is an important mechanism of chromatin regulation. However, here I will focus mostly on the modifications of histones.

In 1962 the binding between DNA and histone molecules was shown to inhibit the transcription of the underlying sequence (Huang and Bonner 1962), which suggested a novel mechanism of gene expression regulation. Two years later Vincent Allfrey in his seminal study discovered that arginine-rich (H3 and H4) histone acetylation is able to reduce this inhibitory activity without affecting the DNA-binding efficiency of the histones (Allfrey et al. 1964). Of course, the 1960s technology did not allow the scientists to identify the specific residue of modification. Nowadays we know that each of the 5 histones can be modified by adding various chemical groups in multiple different residues. These modifiable sites can be found along the entire histone proteins, not only as primarily thought, on the N-terminals (Mersfelder and Parthun 2006, Kouzarides 2007, Bannister and Kouzarides 2011, Huang et al. 2014, Soshnev et al. 2016). It is true however, that thanks to their flexibility and exposure to the external influence, the N-terminal tails represent the majority of the modified residues. Hence, the histones tails can be modified on most lysines (K), arginines (R), threonines (T), serines (S) and some histidines (H), tyrosines (Y) and glutamic acids (E). The spectrum of different modifications is impressive and our knowledge about them seems to be growing by the day. Apart from the already mentioned acetylation histones can be methylated, phosphorylated, SUMOylated or citrullinated, just to name a few (Huang et al. 2014, Zhao and Garcia 2015, Vanzan et al. 2017). The highly studied methylation of lysine residues is special in a sense of creating mono-, bi- or trimethylation chains, each with its own property and regulation, depending on the specific residue (Kouzarides 2007, Bannister and Kouzarides 2011). Each of these histone marks will have a slightly different *modus operandi*. Some, like histone acetylation, have the potential to affect the biophysical properties of the chromatin itself, although likely this is not their main role

(discussed in the next chapter). It is also critical to understand that these histone modifications are not mutually exclusive. As a matter of fact, multiple marks are always present on a single histone tail and the cross-talk between them proves to be essential in the complex regulation of the genome (Soshnev et al. 2016; see for example **Fig. I-2**).

Till early 2000s it was thought that histone methylation, unlike phosphorylation or acetylation, is stable and generally irreversible. However, the discovery of histone methyltransferases (Rea et al. 2000) and, more importantly, histone demethylases (Shi et al. 2004), suggested that this regulation is much more dynamic. Therefore, it could play an active role in genome expression control. Indeed, it has been shown that there is a clear enrichment of histone H3 lysine 4 trimethylation (H3K4me3) and a depletion of H3K4 monomethylation (H3K4me1) in the promoters of actively transcribed genes. A reverse correlation could be observed in the gene enhancers (high H3K4me1 and low H3K4me3). At the same time H3K9me2 or H3K9me3 mark constitutive heterochromatin and the H3K27me3 facultative heterochromatin, both of which usually show low H3K4me3 (with the exception of bivalent promoters presenting both H3K27me3 and H3K4me3; Calo and Wysocka 2013, Voigt et al. 2013, Vanzan et al. 2017). However, some obvious ambiguities observed in genome-wide studies suggest that there are no fixed rules regarding the correlation between histone marks, genomic location and transcription. For example, H3K9me3 - a mark that univocally should label the transcriptionally silent regions of the genome - can be found in some transcribed regions as well (Vakoc et al. 2005, Blahnik et al. 2011). Although several general principles can still apply (H3K4me3 will mark active promoters rather well), it is clear that the relationship of histone marks with gene expression is very complex and depends strictly on the specific genomic location and its local environment (Rando 2012).

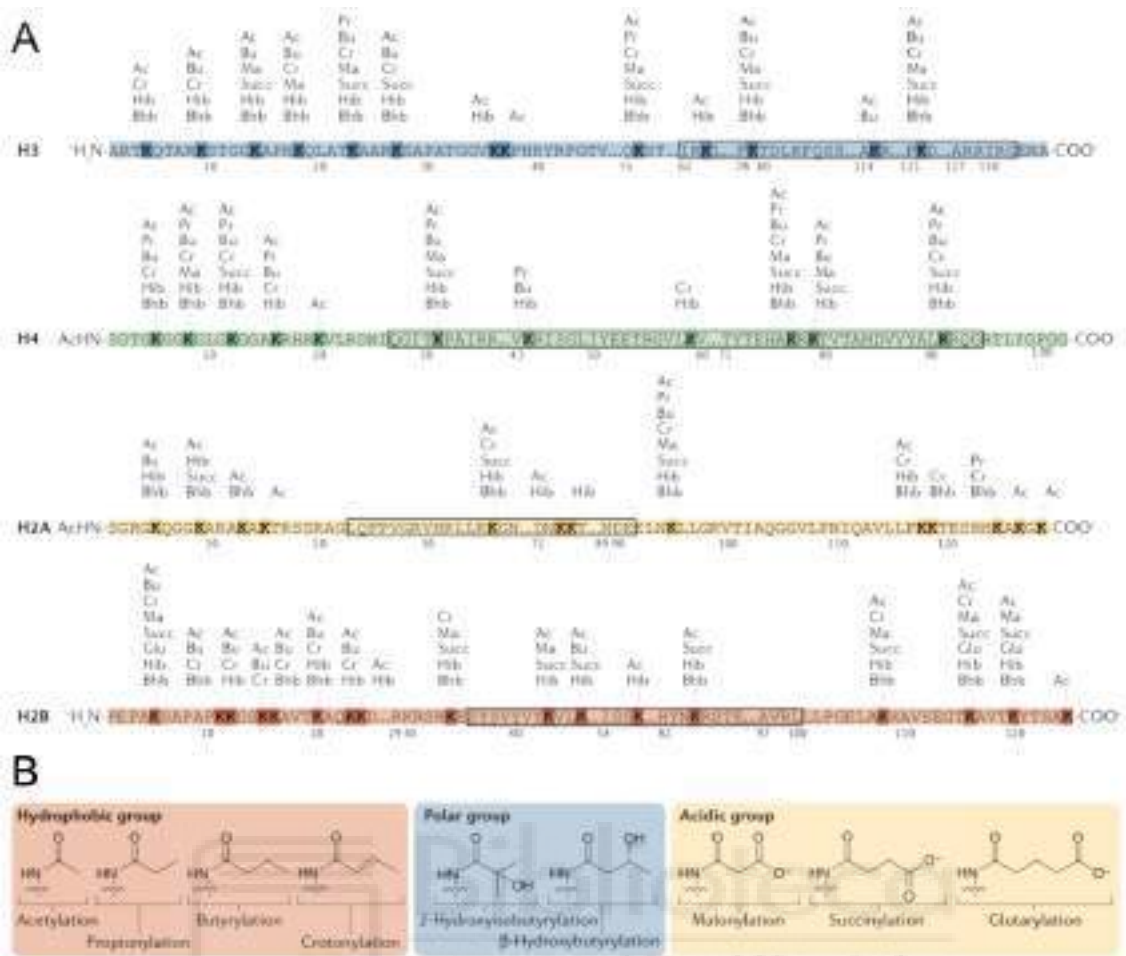


Figure I-2. Core histones and their possible acylation residues **A.** Lysine residues on all four core histones modified by acylations. **B.** Chemical structures of different acylation PTMs. Adapted from Sabari et al. 2017. For a more complete list go to Zhao and Garcia 2015.

1.1.4.1. Histone acetylation

Among all twenty amino acids encoded by the genetic code, the one presenting the biggest variety of modifications is the lysine (K) (Azevedo and Saiardi 2016). Likely the major source of lysine's regulatory potential is the presence of chemically reactive terminal ϵ -amino group. Indeed, over 25 different modifications of lysine have been identified to date (for a comprehensive and updated list see Protein Lysine Modification Database <http://plmd.biocuckoo.org/> from Xu et al. 2017; Azevedo and Saiardi 2016). As many as 14 of them have been found on histones (Zhao and Garcia 2015, Huang et al. 2018b). Some of them are fairly new and unfamiliar, like different forms of histone acylation: succinylation, propionylation, crotonylation, malonylation, butyrylation and β -hydroxyisobutyrylation (Zhao and Garcia 2015, Sabari et al. 2017). Others, like methylation and acetylation, are very heavily studied and can be observed

on multiple residues of every histone protein (Kouzarides 2007, Bannister and Kouzarides 2011, Zhao and Garcia 2015, Vanzan et al. 2017). In this section I will focus on histone acetylation, which will be one of the major subjects of this dissertation.

Already in the first study reporting histone acetylation, a clear direct correlation between this histone mark and transcription was observed (Allfrey et al. 1964). In the physiological conditions the ϵ -amino group of the lysine occurs in a positively charged form $-\text{NH}_3^+$ (Azevedo and Saiardi 2016). This positive charge creates an electrostatic affinity between the amino acid and the negatively charged DNA. Adding the electrostatically neutral acetyl group in this position neutralizes the positive charge of the lysine and theoretically by itself could loosen the binding between the histone and the DNA (Struhl 1998). However, experiments from the 1990's showed that the DNA-histone binding is not weakened by histone acetylation (Mutskov et al. 1998). Subsequent discovery of lysine acetylation-binding proteins (Dhalluin et al. 1999) and the general abundance of different acetylation sites, made it almost certain that the change in the nucleosome net charge is not the principal mechanism of transcriptional regulation through histone acetylation (Eberharter and Becker 2002).

Although almost every known histone acetylation residue correlates to some extent to active transcription, they have different regulations and genomic localizations. Histone H3 is the most highly modified conventional histone with at least 9 lysines (and likely 14) that can be acetylated (**Fig. I-2**; Zhao and Garcia 2015). For example, H3K9ac, H3K14ac and the double mark H3K9,14ac tend to localize in sharp peaks close to transcriptionally active promoters, and to lesser extend close to enhancers. Moreover, the level of the H3K9,14ac correlates very well with the expression of the corresponding gene (Wang et al. 2008, Karmodiya et al. 2012, Lopez-Atalaya et al. 2013, Rajagopal et al. 2014). Another histone mark – acetylation of K27 on histone H3 - is a major indicator of enhancer activity (Heintzman et al. 2009, Creyghton et al. 2010, Rada-Iglesias et al. 2011, Nord et al. 2013). H3K27ac has been very recently shown to directly influence the expression of genes proximal to the enhancers (Raisner et al. 2018), though the precise mechanism of its regulation remains unknown. The scientific community is still largely divided in their support for either the causative or simply permissive role of histone acetylation in gene expression (for the discussion on the subject see Lopez-Atalaya and Barco 2014). On one hand, some evidence suggests that a complete lack of activating histone marks, among them histone acetylation, does not prohibit the transcription to happen (Perez-Lluch et al. 2015). On the other hand, recent

advances in CRISPR (Clustered Regularly Interspaced Short Palindromic Repeats) - based technology allowed for a locus-specific increase in histone acetylation (so-called “epi-editing”, **Fig. I-3**). In the presence of all necessary transcription factors, increasing the level of H3K27ac either in a gene enhancer or promoter leads to activation of the gene expression (Hilton et al. 2015). This result indicate that histone acetylation might play a causative role in gene expression. Further studies should address the exact order of events during acetylation-dependent activation of transcription and its dependence on transcription factors.

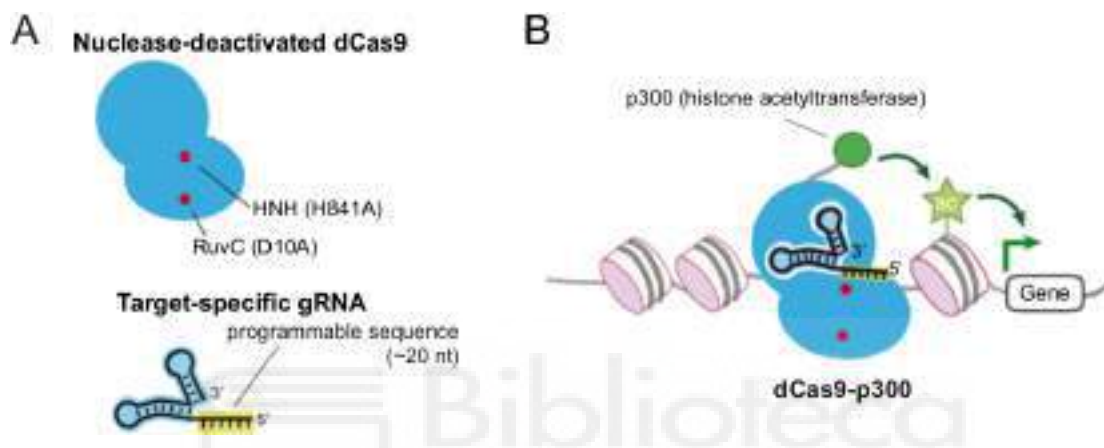


Figure I-3. Epi-editing system used for hyperacetylation of a specific genomic locus
A. CRISPR-dCas9 modified system with two point mutations inactivating the endonuclease activity of the Cas9 enzyme (top) and a programmable gRNA (bottom). **B.** Epi-editing tool for driving the acetyltransferase activity to a specific DNA sequence encoded by the gRNA. Adapted from Lo and Qi 2017

1.1.5. Chromatin regulation through protein binding

1.1.5.1. Epigenetic mark “readers”

A possible mechanism by which the acetylation and other histone marks can affect transcription is through their specific binding proteins, sometime referred to as *readers* (Yun et al. 2011). The existence of this kind of proteins could explain how the cell makes use of such an enormous variety of histone modifications of the same type, as discussed in the previous section (Allis and Jenuwein 2016). The discovery of the first *reader* protein, PCAF, in 1999 (Dhalluin et al. 1999) led in fact to the creation of a prominent theory of the *histone code*. According to this theory every combination of histone modifications would have its specific function in the control of transcription – a code deciphered in part by specific *readers* (Strahl and Allis 2000, Jenuwein and Allis

2001). Although the theory has been widely challenged and evolved ever since (Rando 2012), the body of proof for the importance of readers in the epigenetic regulation has been only growing (Andrews et al. 2016).

The histone acetylation binding bromodomain present on the p300/CBP-associated factor (PCAF) has been the first to be identified (Dhalluin et al. 1999). Since then, a multitude of protein domains recognizing histone acetylation (i.e. bromodomain and double plant homeodomain or DPD), methylation (i.e. chromodomain, Tudor domain, plant homeodomain or PHD), phosphorylation (14-3-3) and other histone modifications, have been identified (Yun et al. 2011, Musselman et al. 2012). The proteins carrying these modules can trigger a cascade of transcriptional regulation, drive the remodeling of the chromatin, or work as an anchor for enzyme that either places or eliminates another histone mark (respectively “writers” or “erasers”). The role of the histone-binding protein will depend on an individual case, however they have the potential to both activate and repress gene expression (Yun et al. 2011, Musselman et al. 2012, Marmorstein and Zhou 2014, Patel 2016). Just to give a particular example of a histone binding protein, I would like to mention the Polycomb Repressive Complex 2 (PRC2). The PRC2 is an evolutionarily conserved complex of proteins crucial for cell proliferation, differentiation and maintenance of cellular identity (Schuettengruber et al. 2017). This complex can catalyze the trimethylation of the H3K27 residue through its EZH2 subunit. However, this enzymatic activity requires the presence of subunits SUZ12 and EED, the latter of which can bind the catalytic product of PRC2 – H3K27me3 (Holoch and Margueron 2017). The PRC2 provides a great model of how a collective partnership between histone mark “writer” and “reader” activity of a single protein complex provide a control of its own function.

It is also important to say, that not only histone modifications can attract the binding of proteins. Distinct methyl-CpG binding domain (MBD) and methyl-CpG binding zinc-finger proteins of the Kaiso family are able to recognize DNA methylation (Bogdanović and Veenstra 2009). These proteins play mostly a role in gene repression, although their function might be much more complex. Probably the most studied DNA methylation-binding protein is the Methyl-CpG binding Protein 2 (MeCP2). This protein plays a very important function in brain development/maturation and its mutations cause an autism spectrum disorder (ASD) called Rett syndrome. It is still not clear what is the major mechanism through which MeCP2 regulates neuronal function but it seems to regulate more than one DNA methylation-related process, for example

gene repression and higher-order chromatin structure (reviewed by Ausió et al. 2014, Bedogni et al. 2014, Ip et al. 2018). Recently it has been reported that MeCP2 (Mellen et al. 2012) and a number of other proteins (Spruijt et al. 2013) can bind the oxidated forms of DNA methylation as well. In the newest update on the subject, the MeCP2 has been shown to be bound to the mCA as well (Gabel et al. 2015). Further investigation is required to verify how common the non-CpG binding is and if MeCP2 is somehow special in this sense.

1.1.5.2. Chromatin remodelers and transcription factors

Some of the epigenetic mark-binding proteins play an important role in chromatin 3D structure control, by directly affecting nucleosome positioning. Chromatin remodelers, as they are usually called, utilize the energy stored in the ATP molecules to directly disrupt the contacts between histones and the DNA. These proteins are classified in 4 groups: SWI/SNF (switch/sucrose-non-fermenting), ISWI (imitation switch), CHD (chromodomain-helicase-DNA binding) and INO80 (inositol requiring 80). All four classes contain a broad ATPase domain allowing for the hydrolyzation of the ATP and displacement of the nucleosomes from the DNA, but not separating the DNA strands like regular helicases (Tyagi et al. 2016).

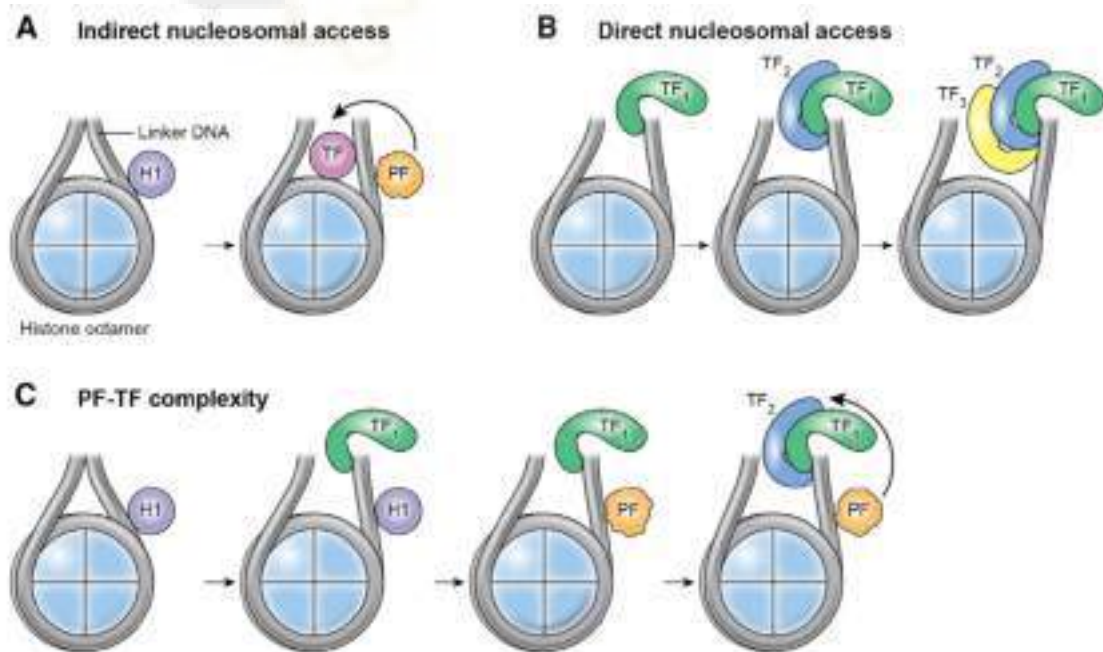


Figure I-4. Three different mechanisms through which a new active place is introduced in the chromatin. A. Pioneer factor (PF) like FoXA1 uses its similarity to the linker histone H1 to provide the access of a transcription factor (TF) to the otherwise closed chromatin. **B.** Multiple

transcription factors cooperate to provide an increasing accessibility of the locus. C. PF and TF reciprocally work together. Adapted from Sartorelli and Puri 2018.

Chromatin remodelers coordinate their function with transcription factors (TF) by recognizing the current chromatin state (Längst and Manelyte 2015) and acting upon it by either changing the composition of the nucleosomes (i.e. alternative histone variant exchange) or by exposing the DNA binding site for a specific TF (Clapier and Cairns 2009). So-called pioneer transcription factors, have the ability to scan the facultative chromatin for their partially exposed binding sites and engage the chromatin remodelers to the specific genomic locations (Soufi et al. 2015, Iwafuchi-Doi and Zaret 2016). The chromatin remodelers will “make space” for the non-pioneer transcription factors to perform their action and engage the RNA Polymerase (**Fig. I-4**; Sartorelli and Puri 2018). Interestingly, these “spaces” remain highly accessible even after the pioneer factor is evicted and exchanged by a different TF (Lilja et al. 2017, Sartorelli and Puri 2018). Therefore, DNA binding motif analysis of the genome regions with high relative accessibility (accessibility peaks) can help to predict the TF bound in these places (Buenrostro et al. 2013). Different interactions between transcription factors and their function in neurons will be discussed in the next chapters.

1.1.6. Non-coding RNAs

If one considers *epigenetics* as extragenetic control of transcription, another biological phenomenon fitting the category of *epigenetic regulators* would be non-coding RNAs (ncRNAs)(Allis and Jenuwein 2016). The difference between the coding RNA (classically mRNA) and non-coding RNA is that the non-coding RNA does not get translated into proteins (Uszczynska-Ratajczak et al. 2018). Some ncRNAs like tRNAs (transfer RNA) and rRNAs (ribosomal RNA) entered the canon of cell biology already in the 1950s. The discovery of the first enzymatically active RNA in 1983 opened new possibilities for extending the RNA role in the cell metabolism (Kruger et al. 1982). Subsequent years brought the finding of X-inactive-specific transcript RNA (*Xist* RNA, Brown et al. 1991) and micro RNAs (Lee et al. 1993), but the real ncRNA research explosion started at the beginning of years 2000 with the mapping of the human genome (Green et al. 2015).

The genomic revolution allowed the scientists to verify that 80% of the human genome, is somehow biochemically active (ENCODE 2012, Pennisi 2012). This

observation created some controversy, since the evolutionary statistical methods inferring the sequence conservation suggested that the majority of the genome is likely redundant (Parenteau et al. 2008). Additionally, the fact that a genome sequence is transcribing, by itself does not imply that the transcript has any relevant function. However, at the same time, many seemingly purposeless transcripts have indeed been shown to play a role in cell biology (see the examples in the next paragraph and Cech and Steitz 2014). In the most recent example, two 2019 Nature publications show that the accumulation of intron RNA in yeast plays an important role for their survival in nutrient-poor condition (Edwards and Johnson 2019, Morgan et al. 2019, Parenteau et al. 2019). Although previously apparently proven to be redundant in basal condition, these two examples show that this particular type of genetic material has a previously secluded role. Therefore, even if we cannot identify the function of some biological entities right now, it does not mean they do not have one. Similarly, it is quite possible that we are still blind to some functionality of the vast “database” that is human genome.

The NGS era, with the ENCODE project as the leading international initiative, provided us with a number of tools to identify the ncRNA elements in the genome. The usual RNA sequencing protocol (also called mRNA-seq) uses the polyA tails of the mRNA to specifically enrich the sequencing library in protein-coding RNAs (and to some extent lncRNAs as well) (Mortazavi et al. 2008). In the recent years other methods have been invented to enrich other RNA species. For example, depleting the rRNA from the RNA pool (total RNA-seq, also called Ribo-Zero or rRNA-depleted RNA-seq) allows for a general amplification of smaller categories of RNA (Cui et al. 2010). Interestingly, the newest improvements in molecular biology allow for a targeted sequencing of a specific class of RNA (like miRNA-seq in Alon et al. 2011, or eRNA-seq in Tyssowski et al. 2018). The identification of active transcription sites by CHIP-seq for polymerase 2 (Pol2) and active histone marks (e.g. H3K4me3), can be also used describe the locations of ncRNA genes in the genome (Rinn and Chang 2012, Scandaglia et al. 2017).

Nowadays we are aware of a staggering number of different ncRNA regulatory mechanisms (Cech and Steitz 2014). The sequences of RNA vary greatly in length. Except for the tRNA and rRNA, probably the most studied ncRNA species are miRNA. After a few rounds of processing in the nucleus, these short sequences bind in the cytoplasm to the Dicer cleavage complex and posttranscriptionally inhibit expression of

specific genes (Fiorenza and Barco 2016). Curiously, miRNAs in its fully processed form is just 22 nucleotides (nt) on average (Cech and Steitz 2014, Fiorenza and Barco 2016). RNA sequences that exceed 200 nt fall into a bigger category called long non-coding RNAs (lncRNA), a category which comprises multiple classes of regulatory RNAs. There are 4 models likely explaining most of the mechanisms of transcriptional regulation by lncRNA (**Fig. I-5**, Rinn and Chang 2012): by recruiting different chromatin-regulating complexes to a DNA template (“guide”, **Fig. I-5A**), sequestering specific transcription factors by imitating their DNA binding regions (“decoy”, **Fig. I-5B**), bringing multiple proteins to create a functional complex (“scaffold”, **Fig. I-5C**), and enhancing the transcription factor activity (“enhancer”, **Fig. I-5D**).

A special type of ncRNAs called enhancer RNAs (eRNAs) are transcribed directly from the enhancer regulatory elements (Kim et al. 2010, Ørom et al. 2010). They have RNA molecules of various length (some spanning from 200 to 2000 nt) and are different from other lncRNAs as they are expressed bidirectionally, at lower levels and most often are not polyadenylated (Kim et al. 2010, Kim et al. 2015b). Multiple studies have shown, that the expression of eRNAs correlates with the expression of nearby genes, which initially led to the conclusion that they were a by-product of these gene’s transcription (Rinn and Chang 2012). While some recent studies suggest the eRNAs are crucial for the induction of mRNA transcription (Schaukowitch et al. 2014, Joo et al. 2016, Carullo et al. 2018), their causative role is still under debate. It is however pretty well documented that the eRNA play a role in promoter-enhancer loop building (Mousavi et al. 2013, Hsieh et al. 2014, Schaukowitch et al. 2014) and activation of crucial transcriptional regulators, like CREB-binding protein (CBP; Bose et al. 2017), which is the main actor in this thesis.

An interesting type of lncRNA is long intronic non-coding RNA (lincRNA). It has been recently shown, that although they do not produce structured proteins, they are able to produce short peptides. This in fact raises a question, whether we can still call these RNA species “non-coding” (Ransohoff et al. 2018). More interesting examples like this are still to be discovered as the field of non-coding RNA investigation is just gaining momentum.

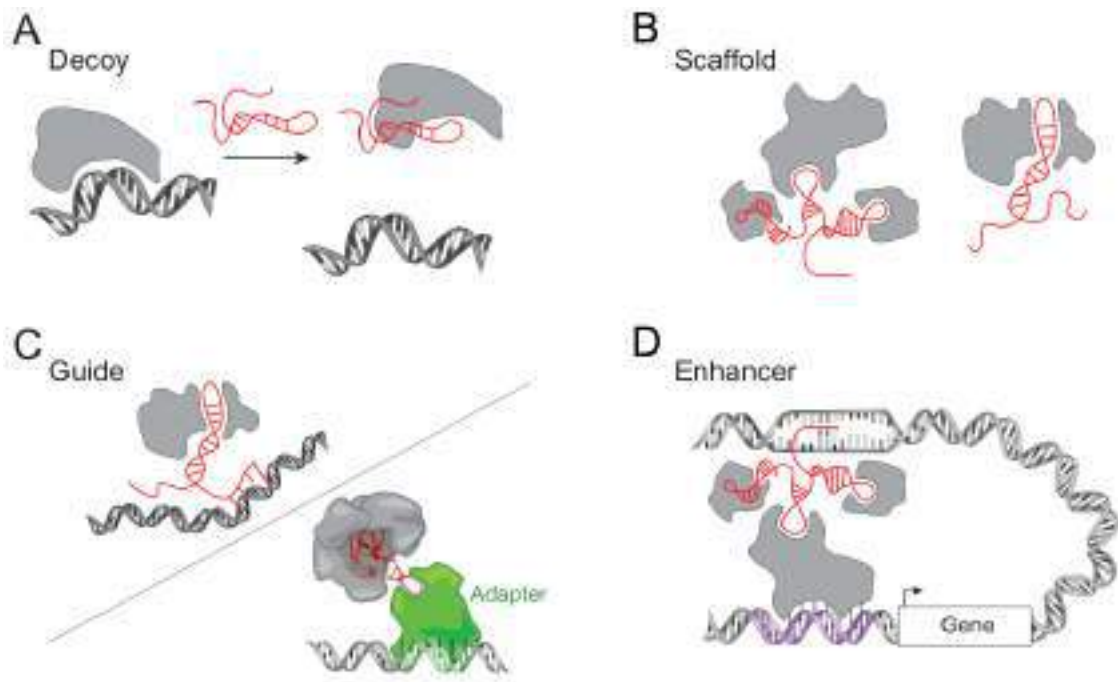


Figure I-5. Four ways through which the lncRNA can regulate the transcription.
 Description in the text. Adapted from Rinn and Chang 2012.



1.2. Epigenetic regulation of neuronal function

Very often diseases caused by the mutations in genes encoding epigenetic proteins have a neurological dysfunction component, which indicates that proper chromatin states are necessary for neuronal function (Fahrner and Bjornsson 2014, Bjornsson 2015). For example, mutations in chromatin remodelers SWI/SNF remodeler ATRX cause the Alpha-thalassemia X-linked intellectual disability and CHD7 mutations cause the CHARGE syndrome (Bjornsson 2015, Hota and Bruneau 2016, Tyagi et al. 2016). Another chromatin remodeler - CHD8 - has also received some attention recently, as it is one of the highest-confidence ASD risk genes (Stessman et al. 2017). If we consider just the proteins that directly interact with the chromatin, 41 out of 44 diseases caused by their mutations include some kind of neurological dysfunction (Bjornsson 2015). In the following chapters I will summarize the role of epigenetics in different stages of neuronal life, concentrating on the central nervous system (CNS).

1.2.1. Neuronal development – model of cellular reprogramming

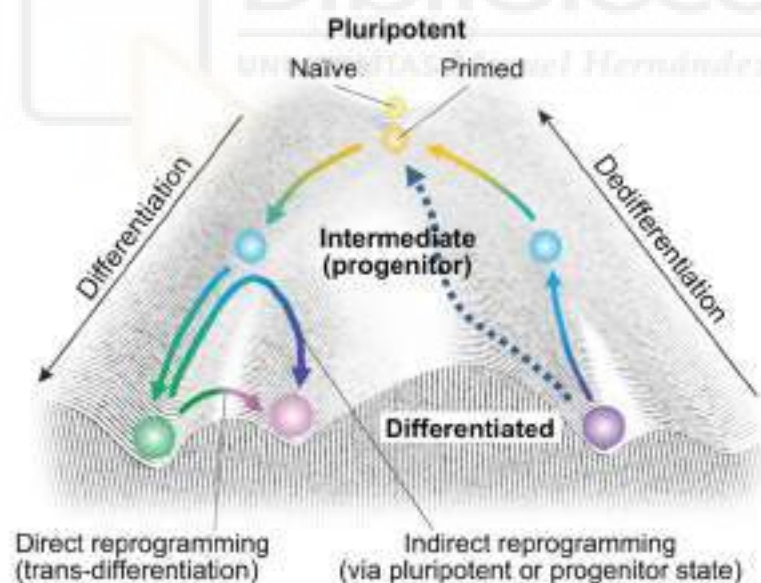


Figure I-6. Waddington's epigenetic landscape updated for the current knowledge on different cell state transitions. Adapted from Takahashi and Yamanaka 2015

1.2.1.1. Epigenetic basis of differentiation

Waddington in his epigenetic landscape (**Fig. I-6**) presented in a very elegant way how a multipotent cell through a series of decisions becomes more and more

specialized, until it reaches its final fate of a fully differentiated cell. Throughout this process the cell acquires its specific epigenome. Even the early embryo undergoes multiple rounds of epigenetic reprogramming (Monk et al. 2019). The chromatin, highly accessible at the beginning, becomes progressively more and more restricted. This process likely happens through the establishment of a new pattern of DNA methylation, first permissive for stemness and developmental genes, later methylated and silenced during subsequent stages of differentiation (Atlasi and Stunnenberg 2017). Deposition of some repressive histone modifications like H3K9me2 (constitutive heterochromatin associated with nuclear lamina) highly correlates with the DNA methylation (Smith and Meissner 2013, Atlasi and Stunnenberg 2017). Other repressive histone mark H3K27me3 show a reverse correlation with DNA methylation and seem to play a very specific role in temporal silencing of genes important during differentiation. H3K27me3 is deposited and later bound by the PRC2, which protects the pluripotent cell from spontaneous differentiation (Boyer et al. 2006). The same mechanism subsequently assures the implementation of the correct transcriptional program as depleting PRC2 and H3K27me3 impairs the differentiation process (Ezhkova et al. 2009, Xie et al. 2014).

Simultaneously with silencing of the chromatin, incremental activation of more specialized, neuronal genes takes place. In neurons, transcription factors like basic helix-loop-helix (bHLH) Ascl1 (Wapinski et al. 2013) and likely Neurod1 (Pataskar et al. 2016, Brulet et al. 2017) work as pioneers and together with supporting TFs (Brn2, Myt11, etc.) access the previously heterochromatinized neuronal-specific genomic sites (Morris 2016, Atlasi and Stunnenberg 2017, Ninkovic and Gotz 2018). Although we cannot discard the role of TSS-proximal promoters, the distal gene enhancers seem to be the major drivers of cell-type specific expression (Atlasi and Stunnenberg 2017, Catarino and Stark 2018). Currently it is thought that after activating a set of enhancers, the transcription factors will recruit a number of epigenetic enzymes able to lock the sites in the activated state (**Fig. I-7**, Atlasi and Stunnenberg 2017). It has been proposed that often the enhancer will be first “primed” by placing the H3K4me mono- or dimethylation (H3K4me1/2) by an enzyme from the MLL family (Wang et al. 2016, Atlasi and Stunnenberg 2017). This process is likely necessary to prepare the enhancer for activation through acetylation of histone H3 in lysine K27 (Wang et al. 2015). The process of depositing H3K27ac and enhancer activation is likely regulated by acetyltransferases CBP and its paralog p300, as they both catalyze this mark and

localize at active enhancers (Visel et al. 2009, Creyghton et al. 2010, Nord et al. 2013; more on CBP/p300 and its role in neuronal function in the chapter 1.3). As the set of epigenetic marks and TFs are instituted in their definitive locations (neuronal *epigenetic landscape*) the neuronal gene expression program is being established. In this process, known as neurogenesis, the cell progresses from stem cell to neuronal progenitor, immature neuron, until it reaches its final fate of mature neuron (Mehler and Kessler 1997, Urban and Guillemot 2014).

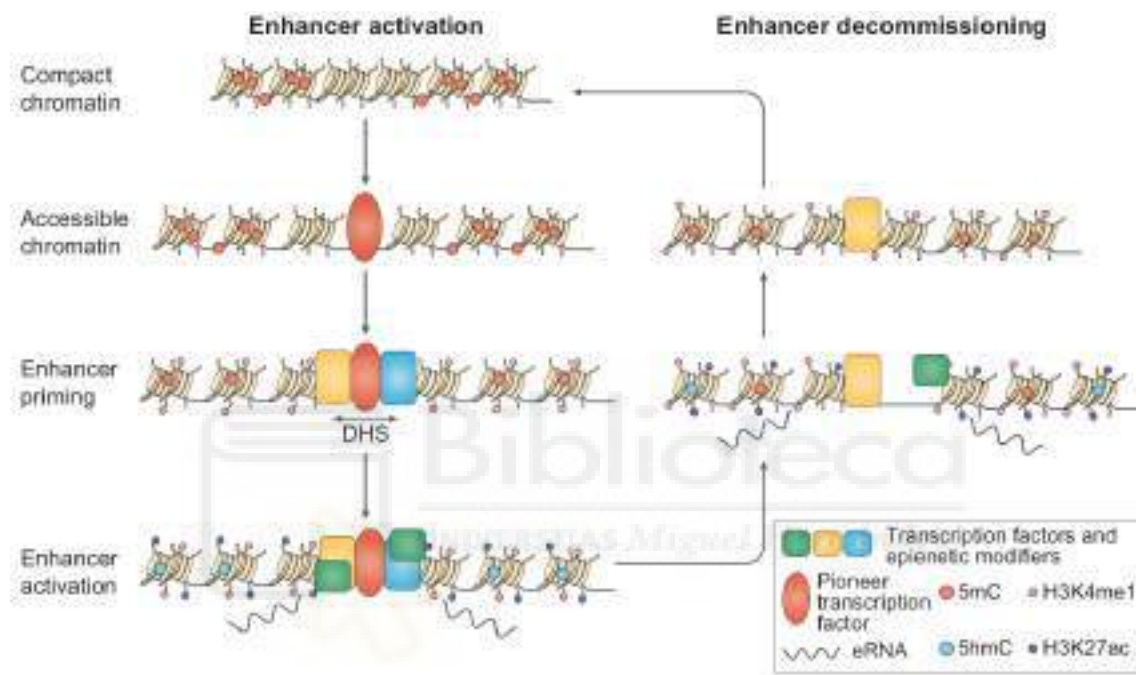


Figure I-7. Scheme representing the process of enhancer activation (left) and elimination, also called “decommissioning” (right). Adapted from Atlasi and Stunnenberg 2017

1.2.1.2. Neuronal identity mechanisms

In the 1880s Santiago Ramon y Cajal used his mastered Golgi stain and a simple microscope to report an impressive variety in neuronal morphology (Ramón y Cajal 1909). This was likely the first mention of multiple neuronal types (classes) ever reported. Zeng and Sanes in their recent review cautiously define a neuronal type as “a population of neurons with properties that are homogeneous within the population but differ from those of other neurons” (Zeng and Sanes 2017). These crucial “properties” used for defining neuronal types are morphological, physiological and molecular (genetic). In other words, a neuron type has a very specific morphology (axon, dendrite, etc.), electrophysiological properties (firing pattern) and expresses a unique set of

markers (**Fig. I-8**). In theory, different types of neurons will present properties common for each subtype and at the same time deviate from the rule in specific details. As the neurons show an exceptional diversity, looking for the commonalities might prove to be more difficult than looking for the differences. The identification of a theoretical pan-neuronal gene expression program is a non-trivial goal some laboratories are currently trying to achieve (Stefanakis et al. 2015).

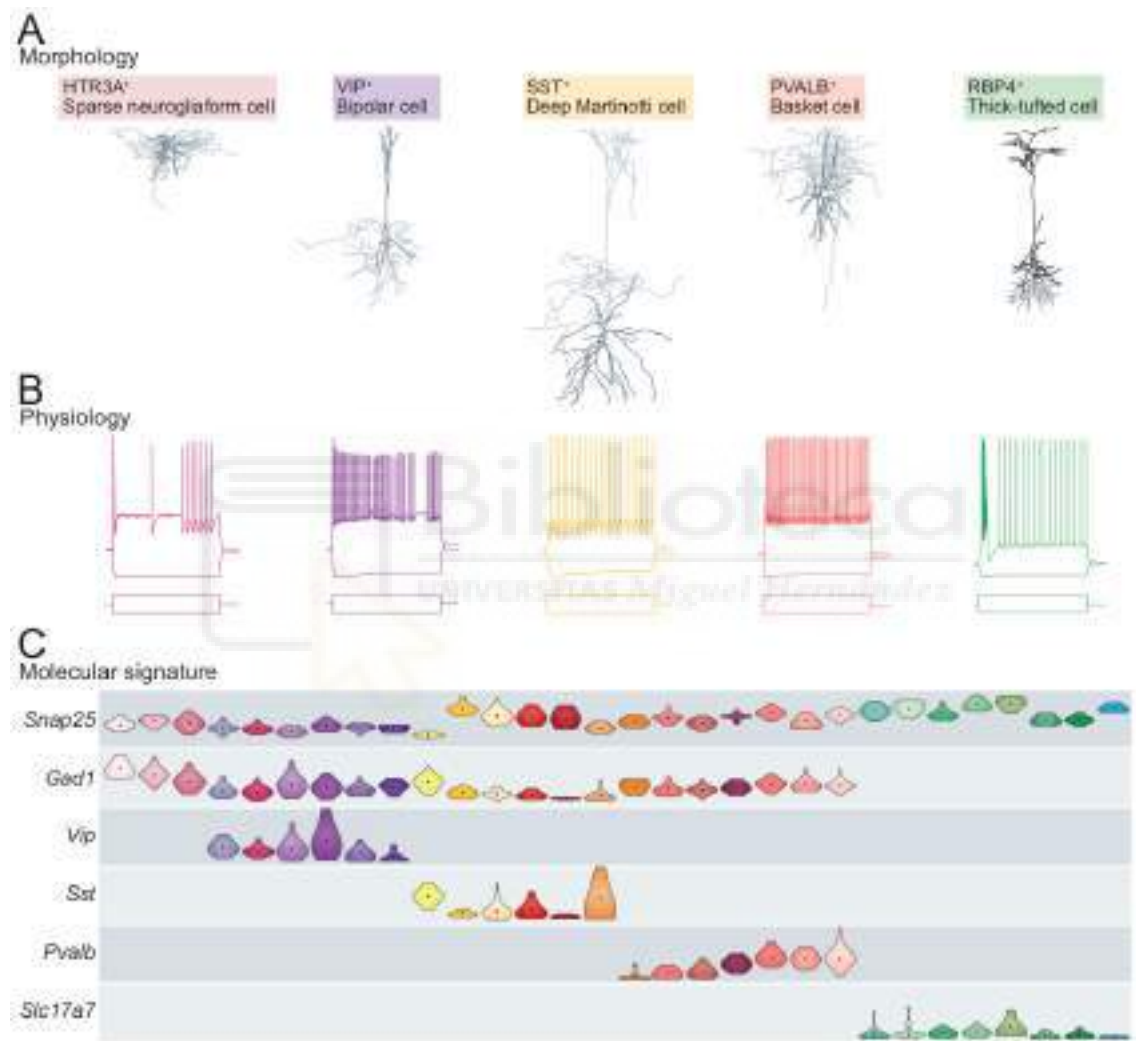


Figure I-8. Three different properties defining a neuronal (cellular) type. A. Morphology B. Physiology C. Gene expression. Examples are presented with corresponding colors. Adapted from Zeng and Sanes 2017.

Where to draw the line between specific cellular subtypes is a matter of discussion right now. In some cases, this seems easy. The pyramidal neuron of the cortical layer V (Thick-tufted cell in **Fig. I-8**), is a glutamatergic, far-projecting excitatory cell that expresses Calcium/calmodulin-dependent protein kinase type II alpha chain (*CaMKII α*). On the other hand, the inhibitory GABAergic basket cell,

innervates locally and expresses parvalbumin, but not *CaMKII α* (Zeisel et al. 2015, Tasic et al. 2016, Zeng and Sanes 2017). The unbiased single-cell sequencing technology provided us with means to identify an array or continuum of new neuronal subtypes (Wagner et al. 2016). Using this technology in 2015 Sten Linnarsson's laboratory was able to classify 16 different subtypes of interneurons in the cortex (Zeisel et al. 2015). In 2016, a collaborative work between Cepko, Regev and Sanes labs singled out 15 retinal bipolar cells, two of which had never been reported (Shekhar et al. 2016).

Neurons are very long-living cells, able to survive, almost without any replacement, for decades in an adult human nervous system. An important question to ask at this point is what keeps the neuron from changing its type during its post-mitotic existence. What keeps its "neuronal identity"? It has been shown that specific neuronal subtypes have specific DNA methylation profiles (Mo et al. 2015). Proper distribution of 5hmC and H3K9me3 have been shown to block the alternative cell fates (Colquitt et al. 2013, Becker et al. 2017). An important role for cell identity has been also shown for so-called "super-enhancers". These large (median 8667 kb) genomic features are in fact densely clustered active enhancers, i.e., marked with large domains of H3K27ac enrichment (Hnisz et al. 2013, Whyte et al. 2013, Pott and Lieb 2015, Thakurela et al. 2015). All this suggests that the neuronal identity maintenance at least to some degree is a passive process, protected by developmentally established epigenetic marks. Notwithstanding, growing body of evidence suggests that the presence of specific transcription factors, is crucial for the neuron to keep its transcriptional program (Holmberg and Perlmann 2012, Deneris and Hobert 2014, Hobert 2016, Mall et al. 2017). As mentioned earlier, in the process of differentiation, some transcription factors initiate activation of cell-type specific sites, but in the mature excitatory neurons the expression of these factors (*Ascl1* and *Neurod1*) is minimal (Zeisel et al. 2015). It has been proposed that in the last steps of the differentiation, transcription factors known as "terminal selectors" will regulate and maintain the expression of the gene expression characterizing the cell type, for example synaptic proteins in neurons (Flames and Hobert 2011, Deneris and Hobert 2014). The mechanism, through which these transcription factors maintain the transcription, and largely the transcription factors themselves, are still mostly unknown.

1.2.1.3. *Dedifferentiation, transdifferentiation and reprogramming*

It is important to point out that the final cell fate is not final (see **Fig. I-6**). Several non-mammalian vertebrates can reverse the specialization of a fully differentiated cell in a process called dedifferentiation. The dedifferentiating cells usually become pluripotent and start dividing again (Jopling et al. 2011). Animals like amphibians, fish and reptilians use this method to fully regenerate damaged organs (e.g. heart in zebrafish) (Jopling et al. 2010), or entire limbs in the example of axolotl (Gerber et al. 2018). Axolotls have been reported to show a similar regenerative ability in the CNS, being able to reproduce an entire cellular diversity upon cortical injury (Amamoto et al. 2016). In the mammalian CNS, Schwann cells have been shown to have the ability to dedifferentiate and proliferate, an important process for nerve regeneration (Mirsky et al. 2008). In 2006, Yamanaka's group revolutionized the scientific world by discovering a combination of four TFs (Oct4, Sox2, Klf4 and Myc), also known as *Yamanaka factors* or *Yamanaka cocktail*, capable to dedifferentiate any specialized cell. Since then, a combination of two or three of these factors is widely used to generate so-called induced pluripotent stem cells (iPSC). Using this method, any cell, including those from accessible tissue of patients (i.e. skin or blood), can be dedifferentiated and subsequently re-differentiated into neuronal cells (Takahashi and Yamanaka 2006, Takahashi et al. 2007, Chatterjee et al. 2016, Hamazaki et al. 2017). This process is the most widely used method for cellular reprogramming in human biomedicine. As one of the latest advances, a self-organizing, three-dimensional culture called "organoids" can be made of the iPSC cells, increasing the comparability of this experimental model to an actual organ (Arlotta 2018).

Interestingly, the cells can also change their final fate from one cell-type to another without entering into the proliferative stem cell phase (Jopling et al. 2011). The process is known as "transdifferentiation", and although very rare, it also occurs in nature, for example lens reparation (in the amphibian newt) (Tsonis et al. 2004). The first reports for induced transdifferentiation preceded by far the discovery of the Yamanaka factors. The protein MyoD1 was found to reprogram fibroblasts to myoblasts as soon as in 1987 (Davis et al. 1987). Now, dozens of different transcription factors have been found to reprogram various cell types to others (Jopling et al. 2011, Morris 2016). Many of them, like Ngn2, which changes astrocytes to neurons (Heinrich et al. 2010), or MyoD1 itself,

are bHLH proteins. The molecular basis of the transdifferentiation process is currently under intense research.

1.2.2. Adult brain: plasticity and cognition

As mentioned earlier in section 1.2, the majority of disorders caused by mutations in chromatin-related proteins have a neurological component (Bjornsson 2015). It is very well established in the field of cognitive research, that transcriptional regulation is crucial for learning and memory (Flavell and Greenberg 2008, Alberini and Kandel 2014, Benito and Barco 2015). Thus, in many of the “epigenetic” diseases a certain part of the etiology is most probably caused by a faulty neuronal development and the other part, by protein malfunction or deficiency in the mature nervous system. An excellent example of such situation is the intellectual disability disorder (IDD) called Claes-Jensen syndrome. Claes-Jensen is caused by mutations in KDM5C, a lysine demethylase protein able to demethylate active chromatin mark H3K4me3. Recent publication from our group has shown that during the neuronal differentiation and maturation KDM5C restricts the transcription of genes that are required to be silenced. This function is however no longer necessary in the adult brain, where these genes are “permanently” inhibited by established DNA methylation and the role of KDM5C is limited to protection from spurious transcription (Scandaglia et al. 2017). In the case of another epigenetics-related disorder, the Rett syndrome, the data suggest that most of the disease’s etiology is caused by the MeCP2 role in mature neurons. The IDD symptoms of the Rett start between 6 and 18 months after birth ([OMIM #312750](#)). Before that age, the child develops normally. Additionally, in the Rett syndrome mouse model of MeCP2 deletion, recovered expression of the protein almost completely rescues the phenotype (Guy et al. 2007, Tillotson et al. 2017).

The idea of connecting epigenetic changes with brain higher function is not new. The first description of a link between the learning process and the DNA methylation was reported in mid 1970s (in Soviet scientific literature) by Boris Fedorovich Vanyushin (Vanyushin et al. 1974, Vanyushin and Ashapkin 2017). Likely sparked by the discovery in 1999 of a link between MeCP2 and Rett syndrome (Amir et al. 1999), David Sweatt and his team proposed for the first time in 2001 that histone modifications can also play a crucial role in memory formation (Swank and Sweatt 2001). Since then, numerous studies correlated changes in histone modifications and DNA methylation

with cognitive processes (Day and Sweatt 2011). Arguably the most reported epigenetic mark associated with cognition is histone acetylation (Peixoto and Abel 2012, Gräff and Tsai 2013). To some extent, the acetylation of each core histone has been linked with the long-term memory formation or synaptic plasticity (Peixoto and Abel 2012). Yet, the evidence for histone acetylation to be the cause of transcription-regulated neuronal plasticity and contribute to nuclear memory storage (Day and Sweatt 2011) are scarce (Lopez-Atalaya and Barco 2014). Bonn and colleagues recently found, that although many histone marks (including acetylation) indeed change in neurons after a learning paradigm, none of them show a real genome-wide correlation with the observed transcriptional changes (Halder et al. 2016). The only epigenetic mark that seems to be an exception to this rule is DNA methylation (Halder et al. 2016).

Histone deacetylase (HDAC) inhibitors (HDACi) – drugs nonspecifically increasing histone acetylation by shifting the balance between acetyltransferase and deacetylase activity (Valor et al. 2013b, Lopez-Atalaya and Barco 2014) – have allowed for some important findings regarding the subject. The use of these drugs, have proven to be efficient in ameliorating many cognitive dysfunctions (Alarcon et al. 2004, Kazantsev and Thompson 2008, Graff and Tsai 2013). Healthy function of central nervous system requires a proper balance of histone acetylation (**Fig. I-9**). Changes in this histone PTM can be observed in diseases like Huntington disease (Valor et al. 2013a), Alzheimer disease and aging (Stilling and Fischer 2011). Interestingly, in a recent study, orally administered clinically approved HDACi vorinostat was able to recover the transcriptional and behavioral decline observed in aging mice (Benito et al. 2015). However, using genome-wide approaches our laboratory showed that the restricted transcriptional alterations caused by HDACi Trichostatin A (TSA) cannot be directly linked with the broad increase in histone acetylation (Lopez-Atalaya et al. 2013). One reason for it might be, that the HDACi increases the acetylation of many other proteins than just histones, among them prominent transcription factors (Lopez-Atalaya and Barco 2014, further discussed in the Chapter 1.3).

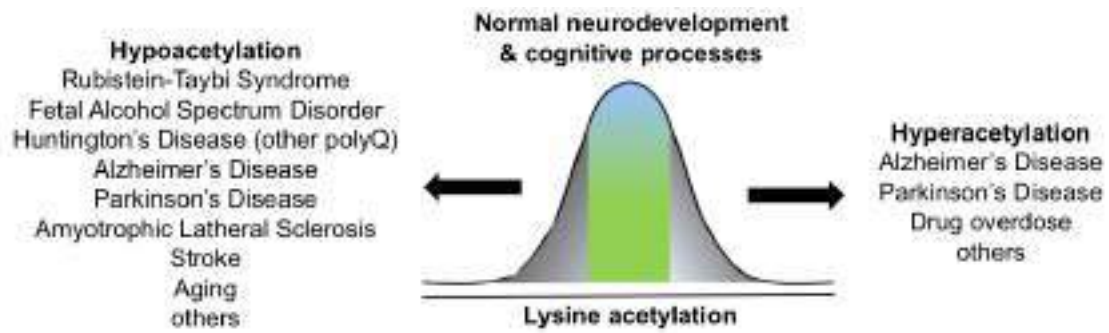


Figure I-9. Proper balance in lysine acetylation correlates with a healthy nervous system function. Both hypoacetylation (left) and hyperacetylation (right) are correlated with a number of neurological disfunctions. A proper level of lysine acetylation (green zone) allows for a correct function of the nervous system. Adapted from Valor et al. 2013b.



1.3. KAT3 proteins: CBP and P300

A total of 37 different mammalian proteins have the ability to catalyze the reaction of adding acetylation to a lysine. In the past, it was believed that these enzymes acetylate almost exclusively histones, which is why they were called histone acetyltransferases (HAT). Since then, a wide range of non-histone lysine targets of these acetyltransferases have been described and therefore the official name has been changed to *lysine acetyltransferases* (KAT) (Allis et al. 2007). Similarly, enzymes eliminating lysine acetylation should be called KDAC, instead of HDAC, although this nomenclature is less commonly used (Sheikh and Akhtar 2018).

KAT proteins, depending on their sequence homology can be categorized into four families: CBP/p300, GNAT (enzymes Gcn5, Pcaf and Atat1), MYST (among others: MOZ/Morf, Ybf2/Sas3, Sas2, Tip60) and a heterogenous group containing other enzymes (TAF, NCOA1-3, CLOCK, etc.) (Bishopric 2016, Tapias and Wang 2017). Most of these enzymes will have a specific name according to the new nomenclature, for example Gcn5 is also called KAT2A and Pcaf is called KAT2B. Additionally, based on their cellular localization, KATs can be divided in Type A and Type B – Type A localizing in the nucleus and Type B in the cytoplasm (Sheikh and Akhtar 2018). In this study, I will almost exclusively focus in a specific family of Type A KATs – the ubiquitously expressed KAT3 proteins CBP and p300 (**Fig. I-10**).

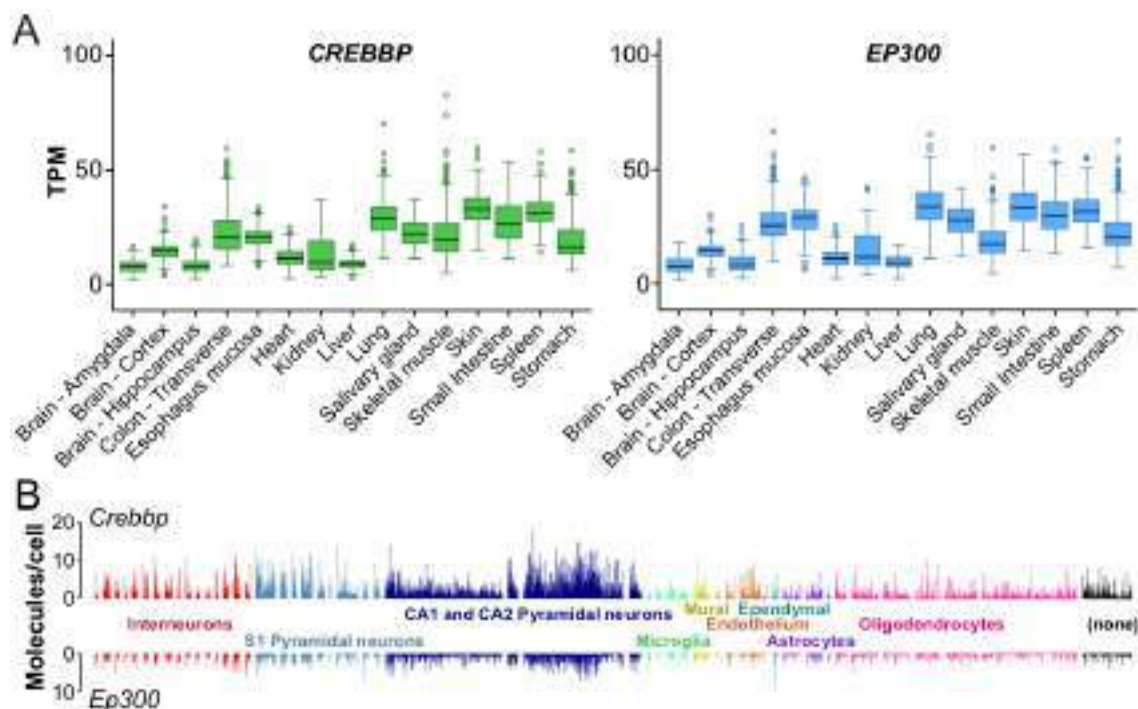


Figure I-10. *Crebbp* and *Ep300* are ubiquitously expressed genes in mammals. **A.** GTEx gene expression data show that both *CREBBP* and *EP300* are expressed in every analyzed human tissue. Representative tissues were selected from the available data (<https://gtexportal.org>). TPM – Transcripts per million. **B.** Precise single-cell RNA-seq data suggest that in the mouse cortex although *Crebbp* and *Ep300* are both ubiquitously expressed, the *Crebbp* expression is generally higher than *Ep300* (supplementary data from Zeisel et al. 2015, adapted from Lipinski et al. 2019).

1.3.1. Shared complex protein structure

KAT3A (CBP) and KAT3B (p300), in humans encoded by the genes *CREBBP* and *EP300*, are the only two members of the KAT3 family (**Fig. I-11**). In most of the unicellular organisms, including a well-established model organism *Saccharomyces cerevisiae*, there is no ortholog of KAT3. The structurally closest protein in *S. cerevisiae* is one called *Rtt109* (Dancy and Cole 2015). Interestingly, some of the unicellular marine organisms, including green algae *Ostreococcus tauri* (<https://www.ebi.ac.uk/interpro/protein/A0A1Y5IIZ0>) and very primitive diatoms like *Thalassiosira oceanica* (<http://www.ebi.ac.uk/interpro/protein/K0SP97>), do have a protein very similar to the KAT3. As much as it is an exception in the unicellular world, having at least one KAT3 ortholog seems to be a rule among the multicellular species (Dancy and Cole 2015, Lipinski et al. 2019). In the kingdom of animals, a single KAT3-like protein can be found in every genome from cnidaria to the more primitive chordates. Two copies of KAT3 are likely present in all the vertebrate animals, although some papers report certain animals to deviate from that rule (Dancy and Cole 2015). Interestingly, the genomic region surrounding the KAT3 genes in humans and mice contain eight other paralogue pairs, clearly suggesting that the entire chromosome region (16p and 22q) was duplicated in the course of recent vertebrate evolution (Giles et al. 1998), which is consistent with the 1970's theory of evolution by gene duplication of Susumu Ohno (Ohno 1970). Similar event, or rather a series of events, happened during the evolution of some plants. *Arabidopsis thaliana* for example, have as many as five KAT3 paralogs (Pandey et al. 2002, Lipinski et al. 2019). The evolutionally conserved multiplication of this gene together with the ubiquitous expression of these proteins, indicates a crucial role of KAT3 in more complex organisms. It also raises a question about the difference in their function, especially considering the ubiquitous expression of KAT3 in mammalian tissues (**Fig I-10**).

The hypothesis of vertebrate KAT3 gene duplication might explain their exceptional level of homology – as much as 57% of similarity at the amino acid level considering the entire human proteins. Both KAT3 are also very large, 2442 amino acids in the human *CREBBP* and 2414 amino acids in the human *EP300*. Depending on the classification, up to 10 different functional domains can be identified in their structure (see **Fig. I-12** in the next chapter; Dancy and Cole 2015, Dyson and Wright 2016, Lipinski et al. 2019). These functional domains represent even higher likeness between the KAT3 proteins, ranging from 66% up to 93%, with the KAT domain itself being 88% identical (Valor et al. 2013b, Lipinski et al. 2019).

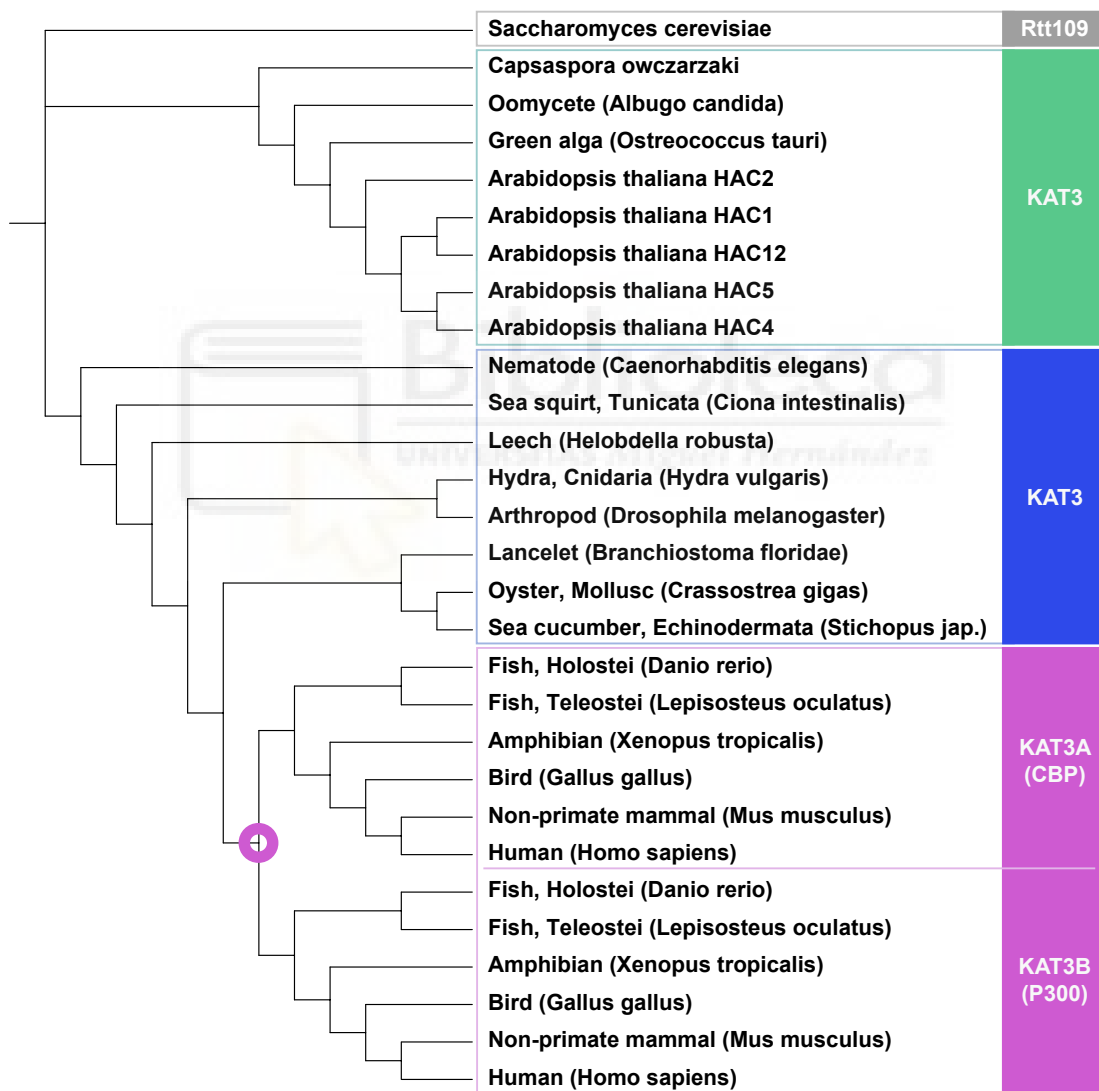


Figure I-11. KAT3 evolution Phylogenetic tree for KAT3 and KAT3-like proteins in different organisms throughout the evolution. Gray: the protein closest to KAT3 common ancestor; green: KAT3 genes, non-Animalia; blue: single KAT3 gene, Animalia; magenta: two KAT3 paralog genes, Animalia. Hypothetical KAT3 duplication in vertebrates is marked with a magenta circle. Reproduced from Lipinski et al. 2019

1.3.2. Two (not so) independent functions

1.3.2.1. *Scaffolding*

Excluding the KAT domain, all KAT3 function domains present an important protein-binding potential, resulting in CBP/p300 being able to bind more than 410 proteins (**Fig. I-12**, Dancy and Cole 2015). Among those proteins you can find kinases, structural proteins, chromatin remodelers, other acetylation-regulating factors (like PCAF, HDAC1 and HDAC6) and most importantly transcription factors (Bedford et al. 2010, Dancy and Cole 2015). Historically the most important CBP partner is CREB, from which the coactivator takes its name. CBP can bind to the phosphorylated CREB through the KIX domain (Chrivia et al. 1993, Giordano and Avantaggiati 1999), and it is still thought to be the major pathway through which PKA-dependent CREB phosphorylation activates transcription. Other prominent KAT3 partners are Fos, Jun, p53, p65, Sp3, Stat1 and 2, Gli3, Foxo family, Elk-1, Hif-1a and basic helix-loop-helix proteins like MyoD, Ngn1 or NeuroD1 (Giordano and Avantaggiati 1999, Bedford et al. 2010, Dancy and Cole 2015). Interestingly, several studies reported that CBP and p300 are in limited amount in the cell and that different transcription factors compete for their availability (Giordano and Avantaggiati 1999, Sun et al. 2001, Vo and Goodman 2001, Dancy and Cole 2015, Dyson and Wright 2016). This competition has been shown for proteins binding the same KAT3 region, like Stat2 and p65 (Hottiger et al. 1998), and binding different KAT3 regions, like AP1 and nuclear receptors (Kamei et al. 1996). This suggests that KAT3 expression in the cell is under a very strict control and the precise amount of CBP and p300 in the cell might be used to regulate the expression of downstream genes.

The extraordinary ability of CBP and p300 to bind different proteins is reflected by more than just a large abundance of their targets. KAT3 proteins can bind multiple proteins at the same time as well (Bedford et al. 2010, Yi et al. 2015), and that binding might in fact change its coactivator activity (Yi et al. 2017). For many years, X-ray crystallography was used to discover the molecular structure of various CBP and p300 domains (Wang et al. 2013a, Dyson and Wright 2016, Contreras-Martos et al. 2017). Only recently the structure of the entire p300 protein, both alone and in a complex, was described using Cryo-Electron Microscopy. Confirming some previous reports, this study showed a high intrinsic flexibility of p300, especially when in complex with some

other proteins (Yi et al. 2015). The protein-binding domains and the KAT domain of KAT3 are in fact separated by intrinsically disordered linker domains (Dyson and Wright 2016, Contreras-Martos et al. 2017). This allows for enough structural flexibility to bind at least two different proteins simultaneously, participating in formation of a sort of a scaffold (Shikama et al. 1997, Wang et al. 2013a). It has been proposed that this scaffold allows for a synergistic function of multiple CBP/p300 binding partners (Merika et al. 1998) as in the so-called enhanceosome (for more on the subject see Panne 2008). As some early studies showed that CBP can bind simultaneously to RNA Pol2 and to phosphorylated CREB (Kee et al. 1996), some scientists went even further and proposed that KAT3 can form a “bridge” between the Pol2 and TFs (Shikama et al. 1997). Indeed, using 3C experiments, Fang and colleagues showed that CBP participates in creation of multi-kilobase-spanning complexes (Fang et al. 2014). The causal role of these complexes in KAT3-dependent regulation of transcription is still under a debate.

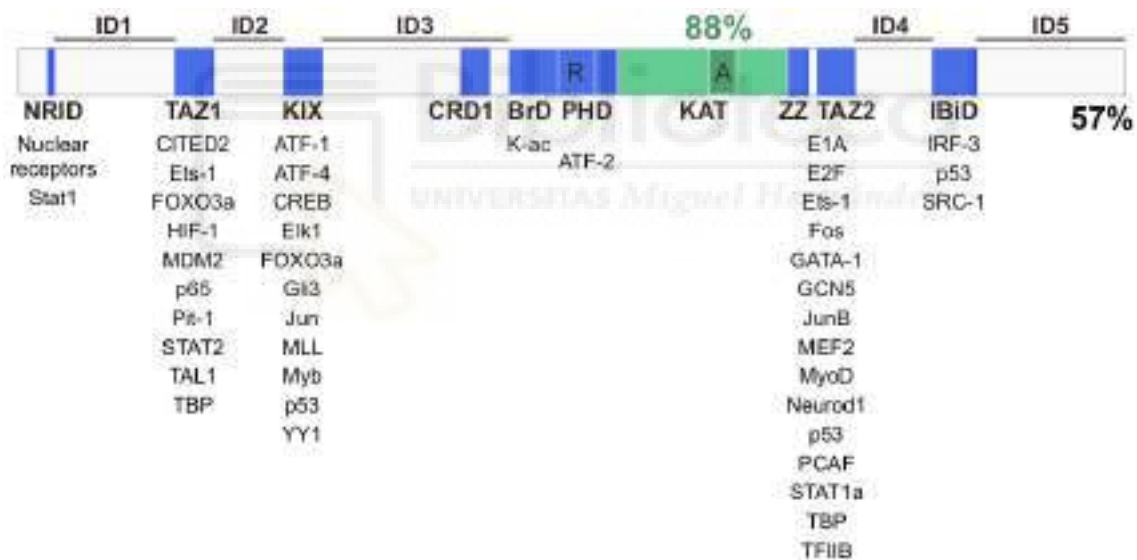


Figure I-12. KAT3 structure The structure of the human CREBBP gene: NRID: nuclear receptor interaction domain; TAZ1-2: transcriptional adapter zinc-binding motifs 1 and 2; KIX: kinase-inducible domain for interaction with CREB; CRD1: cyclin-dependent kinase inhibitor-reactive domain; BrD: bromodomain; PHD domain is discontinued by the RING finger domain (R); KAT: lysine acetyltransferase domain; A: autoinhibitory loop; ZZ: dystrophin-like small zinc-binding domain; IBiD: interferon-binding domain; ID1-5: intrinsically disordered regions 1-5. Names on the bottom represent the transcription regulators that bind to each domain. Percentage values represent the identity between KAT3 proteins for the entire protein and the KAT domain alone. Adapted from Lipinski et al. 2019 updated with information from Goodman and Smolik 2000, Chen and Li 2011, Wang et al. 2013a

1.3.2.2. *Lysine acetyltransferase*

Soon after CBP and p300 discovery, their intrinsic KAT activity was uncovered (Bannister and Kouzarides 1996, Ogryzko et al. 1996). As indicated before, this catalytic activity is mediated through a large KAT domain, that occupies almost the entire center of the protein (Lipinski et al. 2019). Unlike the other KAT proteins, KAT3 most likely acetylate their K targets through a relatively rare “hit-and-run” (Theorell-Chance) catalytic mechanism (Liu et al. 2008, Montgomery et al. 2015). In this model, KAT3 stably pre-bind the acetyl-CoA and later rapidly transfers the acetyl group to the lysine. During the second step, the KAT3 do not form a firm complex with the lysine and do not change its ternary structure (Liu et al. 2008, Karukurichi and Cole 2011, Maksimoska et al. 2014). The use of this mechanism by CBP and p300 is likely the reason why they can acetylate an impressive variety of targets (Dancy and Cole 2015). Very recent developments in the mass-spectrometry technology and the discovery specific acetyltransferase domain inhibitors allowed for a precise identification 11000 to 21000 lysine targets. This is between 3500 and 5300 proteins acetylated by CBP/p300 in cell lines (Weinert et al. 2018). Among them, one can find all kind of nuclear proteins (the database can be explored in <http://choudharylab.org/p300>). Just to mention a few: p53 (Gu and Roeder 1997, Dornan et al. 2003), p65 (Saha et al. 2007), MyoD (Poleskaya et al. 2000), STAT1 (Krämer et al. 2006) and Pol2 (Schröder et al. 2013), have all been reported to be acetylated by KAT3. CBP and p300 themselves have been identified as targets of autoacetylation, a process that can be reversed by an environmentally regulated HDAC Sirt2 (Black et al. 2008). A highly disordered inhibitory loop is present within the KAT substrate-binding pocket and its acetylation increases KAT3 catalytic activity by physically displacing the loop (Thompson et al. 2004, Stiehl et al. 2007, Ortega et al. 2018). Of note, the autoacetylation has been proposed to happen mostly between molecules and not within them (Karanam et al. 2006). In a recent groundbreaking study, Ortega and colleagues (2017) showed that binding dimerized TFs brings two p300 molecules close to each other, allowing them to form unstable dimers. This results in an insertion of the autoinhibitory loop into the KAT domain of the neighboring p300, which there becomes acetylated and released (**Fig. I-13A**).

One of the major targets of KAT3 acetyltransferase activity are histones. Although CBP and p300 can acetylate multiple lysine residues on all four histones

(Bannister and Kouzarides 1996, Ogryzko et al. 1996, Weinert et al. 2018), some of these targets seem to be exclusive of the KAT3 proteins. Histone H2A and H2B N-tails and histone H3 residues K18 and K27, have been reported to be particularly sensitive to the changes of KAT3 level (Jin et al. 2011, Valor et al. 2011, Lopez-Atalaya et al. 2012, Kasper et al. 2014, Bose et al. 2017, Raisner et al. 2018, Sheikh and Akhtar 2018, Weinert et al. 2018). Especially H3K27 acetylation seems to be an important target, as it plays a crucial role for the function of developmentally established enhancers (Nord et al. 2013, Catarino and Stark 2018, Raisner et al. 2018). Indeed, CBP and p300 have been reported to mark both active and poised (ready to be activated) enhancers and therefore correlate with the presence of H3K27ac in the genome (Visel et al. 2009, Creighton et al. 2010, Nord et al. 2013). Active enhancers present stable expression of eRNAs, which very recently have been reported to bind to the CBP autoacetylation loop, displace it from its autoinhibitory state and consequently activate the enzymatic activity, similarly as what happens as a result of autoacetylation (**Fig. I-13B**, Bose et al. 2017). Thus, KAT3-dependent H3K27ac promotes the expression of eRNAs (Raisner et al. 2018), which in turn activates KAT3 ability to acetylate the H3K27 residue. Although the eRNA-driven CBP activation is still controversial (Ortega et al. 2018), this feedback loop could represent a key mechanism for the maintenance of enhancers during the years of cellular maturity in long-living cell-types like neurons. Interestingly, a recent genome-wide profile of KAT3 autoacetylation, reports this process to happen mostly in gene promoters (Kaypee et al. 2018), suggesting that autoacetylation and eRNAs binding might be two independent mechanisms for activating the enzymatic activity of KAT3 proteins dependent on their genomic location.

It is important to remember that CBP and p300 by themselves do not have a DNA-binding activity. Therefore, their genomic presence identified in ChIP-seq experiments represents KAT3 binding to different DNA-bound transcription factors (Ramos et al. 2010). It is likely that the wide range of proteins bound by KAT3, will drive the acetylation of the surrounding proteins (so called “acetyl-spray” proposed by Weinert et al. 2018), influencing the associated gene expression (Ortega et al. 2018). Considering that KAT3 are mostly found in tissue-specific enhancers (Visel et al. 2009, Creighton et al. 2010, Nord et al. 2013), their binding will likely depend on the context and be highly cell-type specific. Indeed, many of the transcription factors bound by KAT3, like MyoD (Lassar et al. 1986, Tapscott 2005) or NeuroD (Pataskar et al. 2016), are crucial for the differentiation of specific cell-type (myocytes and neurons,

respectively). Hence, it is possible that CBP and p300 will regulate in some way the expression of cell-type specific genes.

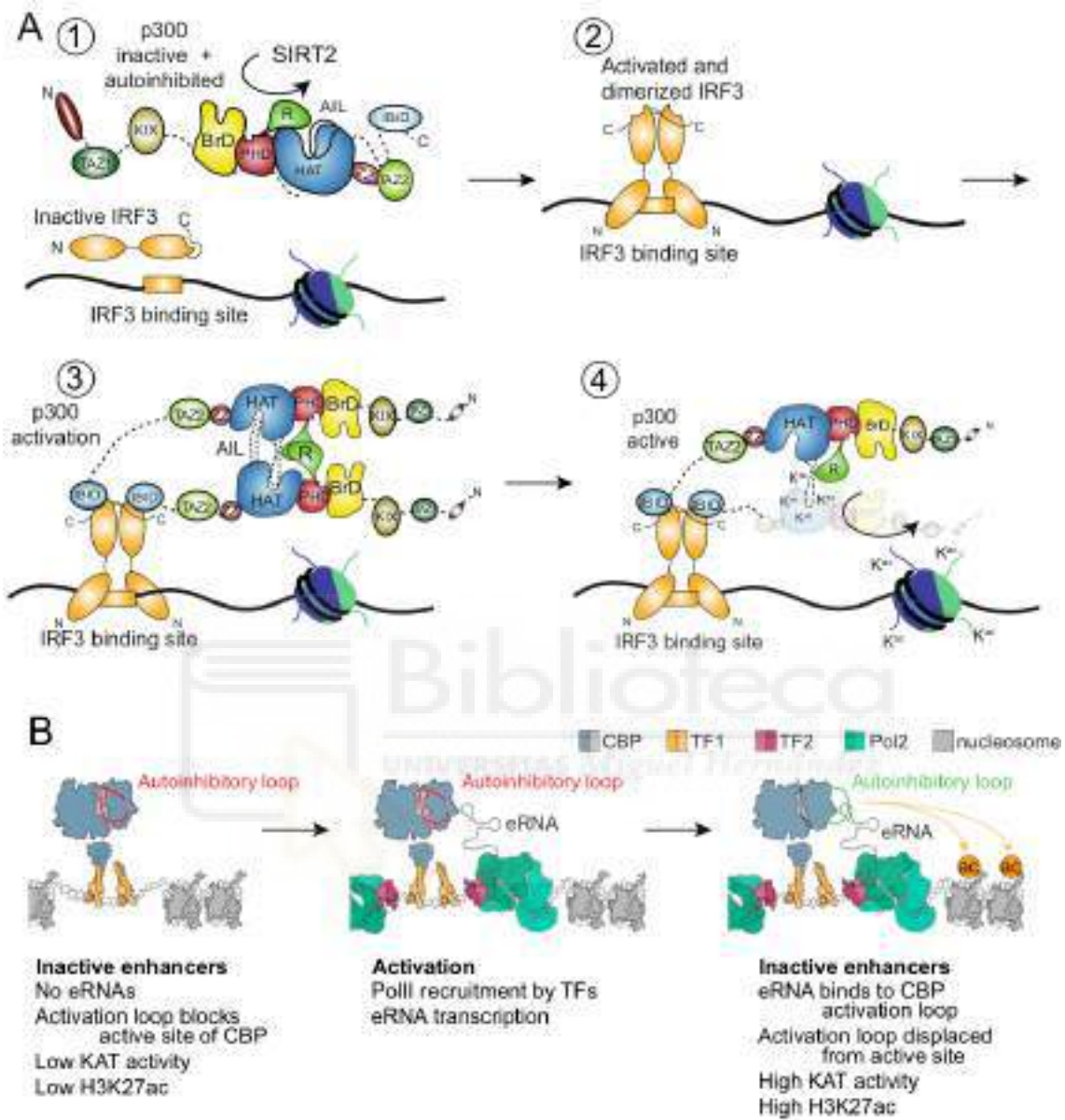


Figure I-13. KAT3 acetyltransferase regulation of transcription **A.** Model of autoacetylation-dependent p300 activation. AIL -autoinhibitory loop, the rest of the labels like in **Fig. I-12**. In the inactive state, p300 does not bind to IRF3 efficiently (1). As soon as IRF3 gets activated by phosphorylation, it dimerizes and binds to its specific DNA binding sites (2). Dimerized IRF3 binds two p300 molecules, allowing them to interact through their autoinhibitory loops (3). As a result, the AIL gets acetylated by the neighboring molecule and gets displaced from the KAT domain substrate pocket, exposing it to possible substrates (4). Modified from Ortega et al. 2018 **B.** Binding of eRNAs to the autoinhibitory loop allows for an activation of the KAT3 acetyltransferase activity of the CBP protein. Adapted from Bose et al. 2017.

1.3.3. Functional difference between KAT3 proteins

In the late 1990's the groups of Shunsuke Ishii and Richard Eckner published the first full mouse knockouts of CBP and p300 (Tanaka et al. 1997, Yao et al. 1998). Mice missing both CBP or both p300 alleles died between E9-E10.5 due to a failure in the neural tube closure (Tanaka et al. 1997, Yao et al. 1998, Oike et al. 1999b, Tanaka et al. 2000). With the exception of Mof and Tip60, full knockouts of all major KATs result in death from mid-gestation to around birth. No lethality in the early stages, suggests an important role in specialized development and differentiation rather than cell survival, metabolism or proliferation (Sheikh and Akhtar 2018, Voss and Thomas 2018). The heterozygous knockouts of CBP are mostly viable, however show bone malformations, electrophysiological and cognitive impairment (Tanaka et al. 1997, Yao et al. 1998, Oike et al. 1999a, Oike et al. 1999b, Tanaka et al. 2000, Alarcon et al. 2004). The elimination of a single p300 allele causes a similar effect to the $CBP^{+/-}$ regarding growth and bone malformations, however results in a milder cognitive phenotype (Viosca et al. 2010). This is reminiscent to the situation in human patients, where congenital heterozygous mutations in the *CREBBP* and *EP300* genes produce an intellectual disability disorder called Rubinstein-Taybi syndrome (RSTS1 OMIM #180849 for *CREBBP*, or RSTS2, OMIM #613684 for *EP300*). I will discuss the RSTS in more detail in the following sections. For now, I would like to point out that likely due to their structural similarity, the elimination of either one of the two KAT3 proteins causes a very similar (but not identical) phenotype. Remarkably, the CBP/p300 double heterozygous mouse dies around E10 with identical phenotype to $CBP^{-/-}$ and $p300^{-/-}$ (Yao et al. 1998). This might suggest that KAT3 not only play an analogous, but at least partially overlapping function.

It is very difficult to draw a line between the overlapping and specific biological functions of CBP and p300. The only three studies comparing the CBP and p300 genome-wide binding show that KAT3 protein binding in the basal cellular state mostly overlap (Wang et al. 2009, Ramos et al. 2010, Kasper et al. 2014). There are however several well documented functional differences between CBP and p300 (summarized in **Table I-1**). From the structural standpoint, CBP has at least two phosphorylation sites (S301 and S436) missing in p300, playing an important role in the coactivator activity of the protein (Zanger et al. 2001, Impey et al. 2002). Additionally, only CBP, but not p300 requires the intact PHD domain for its full catalytic activity (Bordoli et al. 2001),

which is critical, as some syndromic patients have been identified to have PHD domain mutations (Kalkhoven 2004). The literature suggests that some organs are also more sensitive to the elimination of one of the proteins than the other. P300 has been shown to be more important for the development of the heart, skeletal muscles, small intestine and lungs (Roth et al. 2003, Shikama et al. 2003). Mostly because of the deeper intellectual disability in the human RSTS patients (Fergelot et al. 2016) CBP has been generally considered to play a bigger role in neuronal function (Tanaka et al. 2000).

Table I-1. Summary of reported differences between CBP and p300

Difference	Publication	Type
CBP, but not p300, needs the PHD domain for full acetyltransferase activity	Bordoli et al. 2001	Biochemical
CBP-specific phosphorylation at S436 increases its ability to bind transcription factor Pit-1	Zanger et al. 2001	
CBP-specific phosphorylation at S301 increases its transcriptional activation ability	Impey et al. 2002	
<i>In vitro</i> retinoic acid enhances the binding of Ngn2 to CBP but not to p300	Lee et al. 2009	
Insulin suppresses hepatic glucose production by disassembling CBP-CREB, but not p300-CREB complexes due to a lack of S436 site on p300	He et al. 2012	
CBP and p300 have different enzymatic specificity <i>in vitro</i>	Henry et al. 2013	
CBP, but not p300, can be found bound to CRE elements in U2-OS cell extracts	Arany et al. 1995	Molecular
p300, but not CBP, has been shown to be part of the differentiation regulatory factor (DRF) complexes	Kitabayashi et al. 1995	
p300 and not CBP is the preferential partner of MyoD at its DNA binding sites	Puri et al. 1997	
Tax-2B mediated inhibition of p53 in lymphoid cells depends on CBP but not on p300	Meertens et al. 2004	
Mutant huntingtin represses CBP, but not p300	Cong et al. 2005	
AP1 and SRF motifs are more common in CBP specific peaks, whereas AP2 and SP1 are in p300 peaks	Ramos et al. 2010	
p300 reduces and CBP enhances Stra8 expression in mouse ESC	Chen et al. 2013	
Retinoic-acid-induced differentiation p21/Cip1 required only p300, and p27/Kip1 only CBP	Kawasaki et al. 1998	Physiological
CBP and p300 show a different subcellular localization in different tissues during organogenesis.	Partanen et al. 1999	

CBP and p300 have different function in differentiation of F9 cells	Ugai et al. 1999	
p300 but not CBP is important for apoptosis in response to ionizing radiation	Yuan et al. 1999	
Full dose of CBP, but not p300 is necessary for hematopoietic differentiation	Kung et al. 2000	
Full dose of CBP, but not p300, is crucial for hematopoietic stem cell self-renewal	Rebel et al. 2002	
p300, but not CBP, is essential for proper hematopoietic differentiation	Rebel et al. 2002	
p300 is necessary for a correct heart, lung and small intestine development; CBP either not or to lesser extent	Shikama et al. 2003	
p300 is necessary for a correct myogenesis; CBP either not or to lesser extent	Roth et al. 2003	
Conditional CBP ^{f/f} have impaired motor neuron production, migration and axonogenesis and p300 ^{f/f} doesn't (only together with CBP ^{f/+})	Lee et al. 2009	
CBP heterozygous loss results in a stronger ID than the loss of p300	Viosca et al. 2009 (mice), Fergelot et al. 2016 (humans)	Physiological
CBP-specific phosphorylation at S436 is crucial for its ability to bind promoters in neural lineage differentiation	Wang et al. 2010	
p300 but not CBP is crucial for cell survival and the invasive properties of prostate cancer cells	Santer et al. 2011	
CBP is expressed in higher levels in neurons than p300	Zeisel et al. 2015	
The use of p300 by β -catenin pathway promotes differentiation, the use of CBP promotes stemness	Thomas and Kahn 2016	
CBP and p300 regulate distinct gene sets during myogenic differentiation	Fauquier et al. 2018	

1.3.4. KAT3 function in the CNS

The Rubinstein-Taybi syndrome is a rare genetic disorder caused by CBP or p300 haploinsufficiency (Stevens 2002, Lopez-Atalaya et al. 2014). RSTS was first described in 1963 by Jack Rubinstein and Hooshang Taybi (Rubinstein and Taybi 1963) and it represents between 1 in 100000 to 1 in 125000 births (Hennekam 2006). The typical symptom of both RSTS1 and RSTS2 are exceptionally broad thumbs and big toes, which is where the alternative name of the disease, “broad thumb-hallux syndrome”, comes from (Tapias and Wang 2017). Other abnormalities present in the patients, like dysmorphic facial features, microcephaly, mental retardation and postnatal

growth deficiency (Hennekam 2006, Milani et al. 2015) are pretty common in genetic diseases caused by KATs and HDACs mutations (Tapias and Wang 2017). RSTS patients express a remarkable range of neurological symptoms including poor motor coordination, short attention and seizures. Although it is not a classic ASD, autistic traits can be a part of the phenotype (Milani et al. 2015). The intellectual disability itself is present from the birth and ranges from mild (IQ 50–69) to severe (IQ<35) (Daily et al. 2000, Alari et al. 2018). As mentioned before, *CREBBP* mutations, constituting approximately 50% of all the cases, generally cause a significantly stronger IDD than *EP300* mutations (5-8% of the cases) (Fergelot et al. 2016, Tapias and Wang 2017). The duplication of the chromosomal region 16p13.3, containing *CREBBP* has been also related to a mild to moderate IDD and accompanying skeletal deformation (Thienpont et al. 2010). IDD symptoms resembling RSTS have been also identified in patients carrying a duplication in 22q13.2 – a chromosomal region that contains *EP300* (Pramparo et al. 2008, Samanich et al. 2012).

It is very important to notice that mutations causing RSTS often causes structural changes of the brain (Milani et al. 2015). Some of them, like Chiari malformation (cerebellum descending to the spinal canal, [NCBI MedGen/196689](#)) or tethered spinal cord ([NCBI MedGen/36387](#)) might be secondary to the cranial malformations. Others however, for example the failure to correctly develop corpus callosum (Sener 1995) and possibly Dandy-Walker cerebellar malformation ([NCBI MedGen/4150](#)), result rather from an impairment of the neuronal development. At the same time, it becomes more and more clear that RSTS patient behavior might change in the early adulthood and keep declining with age (Hennekam 2006). This might indicate an important role of KAT3 during later postnatal periods and calls for a meticulous determination of CBP and p300 function in the adult versus developing brain. In the next sections I will summarize the research on KAT3 role in the central nervous system, performed using both time- and cell-type-specific genetic manipulations in animal models.

1.3.4.1. Role in neural differentiation and maturation

The first reports showing that KAT3 are important for cell differentiation were published in the 1990s (Mymryk et al. 1992, Kirshenbaum and Schneider 1995, Shi and Mello 1998). The failure in closing of the neural tube observed in the CBP and p300

null embryos (Yao et al. 1998, Tanaka et al. 2000) was in fact the first to indicate an important role of KAT3 in neural development. Very soon after, genetic manipulation of Xp300 protein (undefined KAT3 ortholog) in *Xenopus* confirmed the prominent role of KAT3 in vertebrate neural differentiation (Fujii et al. 1998). Similar to the mouse CBP (Partanen et al. 1999, Lee et al. 2009), the embryonic expression of Xp300 was reported to be ubiquitous, though enriched in the dorsal, neuronal regions of the *Xenopus* embryo. Also analogously to the mouse, the injection of truncated Xp300 RNA into the embryos resulted in early lethality and “loose neural plates” (Fujii et al. 1998). Later, more advanced studies showed that CBP is indispensable for the differentiation of: murine motor neurons (Lee et al. 2009), interneurons (Tsui et al. 2014, Medrano-Fernandez et al. 2018), cerebellar granule neurons (Merk et al. 2018), cortical (Wang et al. 2010) and hippocampal excitatory neurons (Del Blanco et al. 2019). Additionally, recent study showed that neurons derived from RSTS patients iPSCs have an impaired morphology and reduced excitability (Alari et al. 2018).

A recurring mechanism by which CBP seems to regulate neural differentiation is binding to transcription factors, that play an important role in neural development. *In vitro* studies have shown that during neurogenesis CBP-Smad1 complexes preferentially bind bHLH factor Ngn1 instead of Stat1 and Stat3 proteins. This way the cell drives the neuronal transcription and restricts the alternative, astrocytic fate enforced by the Stat proteins (Sun et al. 2001). Similar competition for CBP access has been shown between Stat3 and another bHLH protein Olig2 during oligodendrogenesis (Fukuda et al. 2004). CBP has been also shown to bind to Ngn2 and retinoic acid (RA) in motor neurons. Secreted by paraxial mesoderm, RA is an external factor crucial for motor neuron differentiation and spinal cord development (Lee et al. 2009). In contrast to bHLH-driven regulation, in primary hippocampal cultures CBP deficiency proved to downregulate SRF-dependent genes. This resulted in an impaired dendritic growth and spine maturation. Interestingly, the overexpression of constitutively active SRF variant was able to rescue both the gene expression and the morphological changes (Del Blanco et al. 2019). In summary, CBP seems to bind to distinct transcription factors in order to trigger the cell-type specific gene expression and regulate the specification of multiple cell-types within the neural lineage (**Fig. I-14**).

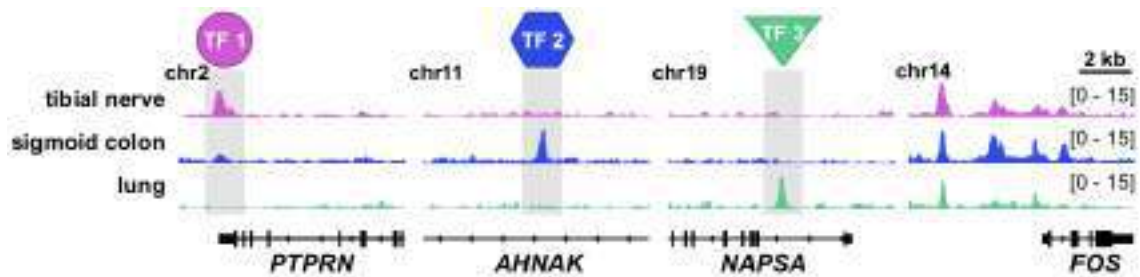


Figure I-14. KAT3 binding is highly specific for the tissue Snapshots from the ENCODE p300 ChIP-seq profiles show that p300 binding is specific for the tissue. This localization likely depends on the transcription factor (TF 1-3) interacting with the KAT3 in that tissue. Adapted from Lipinski et al. 2019.

One could also wonder how distinct are the roles of CBP and p300 in the neuronal specification process. In the only direct comparison published so far, CBP is significantly more important for the development of the motor neurons. The conditional knockouts of both CBP alleles caused significant problems in motoneuron differentiation and axon pathfinding, while the elimination of p300 did not. The elimination of both p300 alleles and one CBP allele had however a much more severe effect than the elimination of one CBP allele alone (Lee et al. 2009). The mechanism of this regulation is not clear, although it has been shown that CBP-Ngn2 complex binding to the chromatin is enhanced by RA, while it is not true for the p300-Ngn2 complexes (Lee et al. 2009). Consistently with the dominant role of CBP in neural fate establishment, the phosphorylation at the CBP-specific S436 has been shown to be critical for neurogenesis, astrogenesis and oligodendrogenesis (Wang et al. 2010). Altogether this suggests a CBP-p300 interprotein compensatory dosage effect, where CBP protein is more important for the neural differentiation. Further studies unequivocally explaining the asymmetric roles of KAT3 proteins in neural fate determination are pivotal.

1.3.4.2. Role in learning and memory

KAT3's partner CREB and transcription itself are known to be essential for memory formation and storage (Benito and Barco 2010, Alberini and Kandel 2014). Surely, neuronal activity, calcium- and synaptic signaling have all been shown to stimulate transcription through a CBP-dependent pathway (Hardingham et al. 1999, Hu et al. 1999, Guan et al. 2002, Impey et al. 2002). Thus, the intellectual impairment observed in the RSTS patients was suspected to be partially independent of the neural

development and caused by CBP and p300 role in coregulating gene expression (Korzus et al. 2004). As suggested before, mouse phenotype mimics very well the RSTS symptoms, therefore mice can serve as a great model to study the role of CBP and p300 in cognition (the following data have been summarized in the **Table I-2**).

Table I-2. Summary of different KAT3 knockouts and their role in cognition. Red cells label impaired performance in the indicated task while blue cells indicate a normal performance. White cells with grey text indicate that the strain has not been evaluated in that task. LTM – long-term memory; STM – short-term memory. CBP^{+/-} (Alarcon et al. 2004), CBP^{+/ Δ} (Oike et al. 1999a, Bourtchouladze et al. 2003), CaMK-CBP Δ 1 (Wood et al. 2005), CaMK-CBP[KAT-] (Korzus et al. 2004), CBP^{KIX/KIX} (Wood et al. 2006), CaMK-cre/CBP^{ff} (V) (Valor et al. 2011), AAV-cre/CBP^{ff} (Barrett et al. 2011), CaMK-cre/CBP^{ff} (C) (Chen et al. 2010), p300^{+/-} (Viosca et al. 2010), CaMK-p300[KAT-] (Oliveira et al. 2007), CaMK-cre/p300^{ff} (Oliveira et al. 2011)

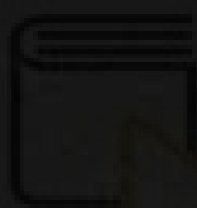
	CBP defects	p300 defects
Novel object recognition (LTM)	CBP ^{+/-}	CaMK-p300[KAT-]
	CBP ^{+/Δ}	CaMK-cre/p300 ^{ff}
	CBP ^{KIX/KIX}	p300 ^{+/-}
	CaMK-CBP[KAT-]	
	CaMK-cre/CBP ^{ff} (C)	
	CaMK-cre/CBP ^{ff} (V)	
	AAV-cre/CBP ^{ff}	
	CaMK-CBP Δ 1	
Fear conditioning (LTM)	CBP ^{+/-}	CaMK-p300[KAT-]
	CBP ^{+/Δ}	CaMK-cre/p300 ^{ff}
	CBP ^{KIX/KIX}	p300 ^{+/-}
	CaMK-CBP Δ 1	
	CaMK-cre/CBP ^{ff} (C)	
	AAV-cre/CBP ^{ff}	
	CaMK-CBP[KAT-]	
	CaMK-cre/CBP ^{ff} (V)	
Morris Water Maze (LTM)	CaMK-CBP Δ 1	p300 ^{+/-}
	CaMK-CBP[KAT-]	CaMK-p300[KAT-]
	CaMK-cre/CBP ^{ff} (C)	CaMK-cre/p300 ^{ff}
	CBP ^{+/-}	
	CaMK-cre/CBP ^{ff} (V)	
	CBP ^{+/Δ}	
	CBP ^{KIX/KIX}	
	AAV-cre/CBP ^{ff}	
Short-term Fear Memory (STM)	CaMK-cre/CBP ^{ff} (C)	CaMK-p300[KAT-]
	CBP ^{+/-}	CaMK-cre/p300 ^{ff}
	CBP ^{+/Δ}	p300 ^{+/-}
	CBP ^{KIX/KIX}	
	CaMK-CBP[KAT-]	
	CaMK-CBP Δ 1	
	CaMK-cre/CBP ^{ff} (V)	
	AAV-cre/CBP ^{ff}	

To address the issue of the role of KAT3 in learning and memory, multiple groups used *CaMKII α* promoter as the driver of a specific KAT3 gene manipulation in mature excitatory neurons of the forebrain (Tsien et al. 1996, Kojima et al. 1997, Wang et al. 2013c). Complete elimination of CBP using this promoter driving Cre recombinase expression resulted in an unequivocal failure of episodic memory, as determined using Novel Object Recognition (NOR) task (Chen et al. 2010, Valor et al. 2011). The long-term episodic memory loss is the only cognitive feature defective in almost every mouse model of impaired CBP function in the hippocampus (see also Bourtchouladze et al. 2003, Korzus et al. 2004, Wood et al. 2006, Barrett et al. 2011). The long-term spatial memory, as investigated using Morris Water Maze (MWM) has been impaired only in some of the reports (Korzus et al. 2004, Wood et al. 2005, Chen et al. 2010), but not in others (Alarcon et al. 2004, Valor et al. 2011). Similar discrepancies have been observed in fear memory, where some reports saw significant defects (Wood et al. 2006, Chen et al. 2010, Barrett et al. 2011) and others did not (Korzus et al. 2004, Valor et al. 2011). As for the case of cognitive deficits in the *CaMKII α* -driven p300 impairments, the laboratory of Ted Abel reported both declarative and fear memory loss (Oliveira et al. 2007, Oliveira et al. 2011). Although this data is not consistent with a very weak cognitive defect of the p300 heterozygous mice and RSTS2 patients (Viosca et al. 2010), it might be caused either by a complete loss of p300 expression in the conditional knockouts (Oliveira et al. 2011) or by a dominant negative effect (Oliveira et al. 2007).

An important point is that the regular *CaMKII α* -cre approach is not the cleanest way of describing the non-developmental function of KAT3. Some studies suggest that *CaMKII α* -driven expression is very weak though detectable at P0-P4, clearly detectable at P8-P10, and reaching stable levels at P12-P16 (Burgin et al. 1990, Kojima et al. 1997). Newer approaches report however that *CaMKII α* expression is widely detectable in the entire forebrain as soon as at P0 (Wang et al. 2013c) and likely earlier ([Allen Brain Atlas Camk2a expression](#)). Therefore, one cannot discard the cre protein to be present even at the perinatal stage in *CaMKII α* -cre mice. Simple *CaMKII α* promoter-based cre-system provides a model in which the role of KAT3 is investigated in mature excitatory neuron, though we cannot discard a possible confounding influence of the knockout during the postnatal forebrain development (Semple et al. 2013). Cleaner, doxycycline-based approach has been only used in the case of KAT-inactive CBP overexpression (Korzus et al. 2004). Full knockouts of CBP or p300, clearly restricted

to the adulthood, have never been published in the context of learning and memory. An improved approach should help to definitively address the role of KAT3 role in the adult brain.

Regarding the mechanism of described memory impairments, multiple studies observed a significant decrease in histone acetylation in KAT3-deficient mice. In some cases, the treatment of the CBP-impaired mice with the HDAC inhibitor TSA rescued, or partially rescued the behavioral deficits (Alarcon et al. 2004, Korzus et al. 2004). This indicates two things: 1) at least some part of cognitive impairment was indeed caused by CBP function in the adulthood; 2) at least some part of cognitive impairment might be caused by lysine acetylation problems. The TSA treatment was only successfully rescuing the behavioral phenotype in heterozygous mice, but not in conditional homozygous CBP knockouts, even despite a significant increase in H2B and H3 histone N-tail acetylation (Chen et al. 2010). This suggests, that at least one allele of CBP is necessary for the beneficial effect of TSA and that this effect is not mediated through an increase in bulk H2B and H3 acetylation. Interestingly, the double loss of CBP and p300 in excitatory neurons has not been reported so far. This kind of model could provide us a valuable information on the common and separate functions of KAT3 proteins in the adult brain.



Biblioteca

UNIVERSITAS *Michael Hernández*

Objectives

 **Biblioteca**
Universitaria Miguel Alemán



2. OBJECTIVES

Although the mutations in CBP and p300 have been known to cause serious developmental pathologies and human disease, not much is known regarding the specific and overlapping roles of these two paralog proteins in adult brain because the early embryonic lethality of the conventional KAT3 knockouts hindered such studies. Experiments in other tissues and in cell cultures suggest that CBP and p300 are important for gene expression and their action depend on a specific partner transcription factors. However, their precise role in the regulation of neuronal gene expression and the identity of their partners *in vivo* remain largely unknown. In the context of this thesis we defined the following objectives:

1. To develop a mouse model of CBP and p300 single and combinatorial elimination in the excitatory neurons of the forebrain, exclusively during adulthood.
2. To verify the role of CBP and p300 in animal well-being, behavior and cognition.
4. To investigate the transcriptional alterations caused by the loss of CBP and/or p300, with a particular interest in both the differences and commonalities.
5. To identify the genomic targets of KAT3-dependent histone acetylation.
6. To determine the relevance of KAT3-dependent lysine acetylation in the regulation of gene expression in excitatory neurons.



Biblioteca

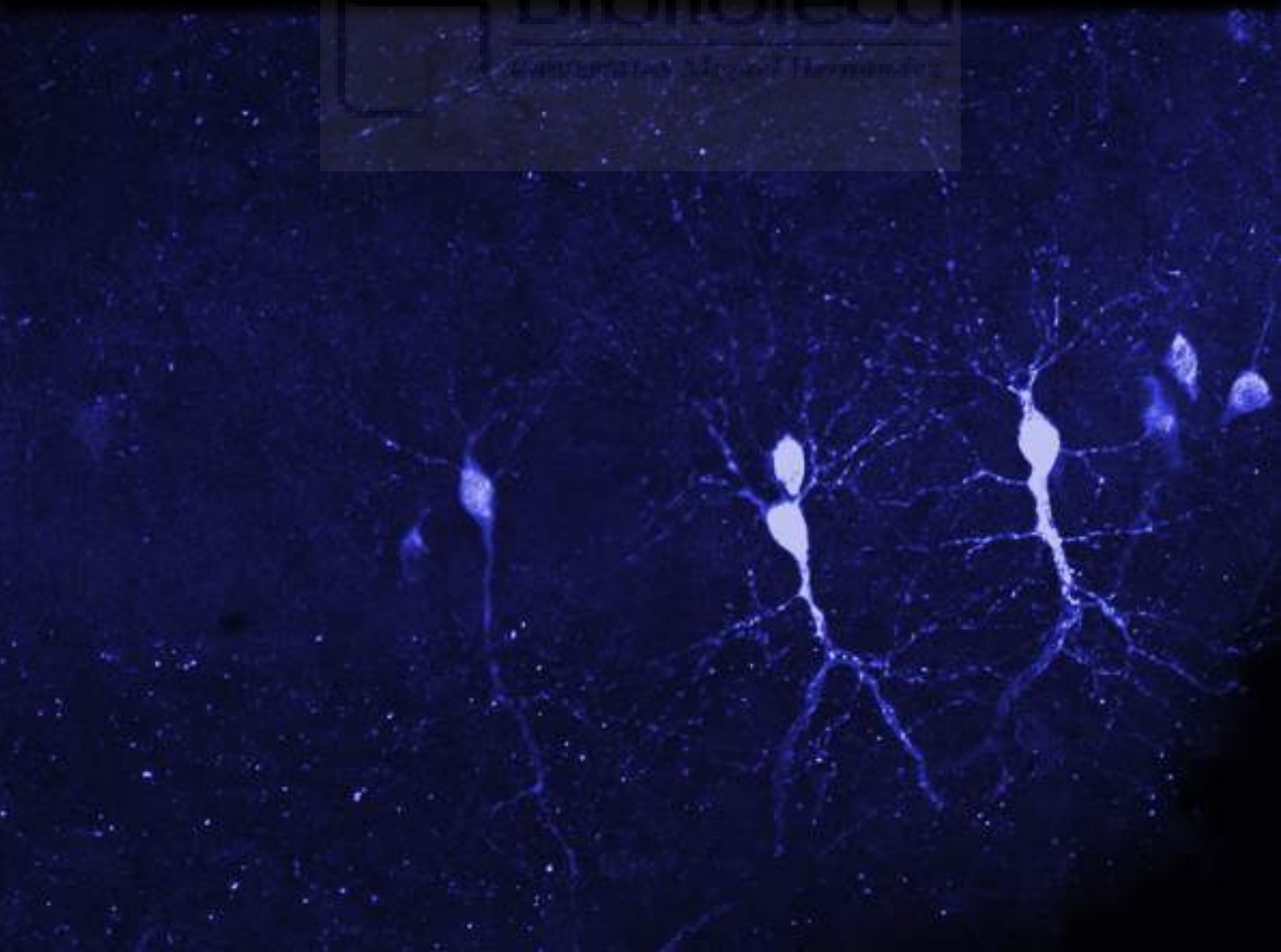
UNIVERSITAS Miguel Hernández

Materials & Methods



Biblioteca

Universitat de València





3.1. Animals and tamoxifen treatment

Previously described CaMKII α -creERT2 (Erdmann et al. 2007), *Ep300*^{ff} (Kasper et al. 2006) and *Crebbp*^{ff} (Zhang et al. 2004) mice were crossed for the purpose of obtaining double and triple conditional knockouts. Animals were housed according to the Spanish and European regulations and the experiments were approved by the Institutional Animal Care and Use Committee. Mice were caged in a 12-12 hour cycle (8:00-20:00) with the food and water available *ad libitum*. CaMKII α -creERT2-carrying mouse lines were maintained in their standard housing without interruption for 3-4 months in order for them to fully develop the central nervous system. Then they were treated with tamoxifen (TMX) as described before (Fiorenza et al. 2016) allowing for a complete elimination of either p300, CBP or both of these proteins. All dKAT3-ifKO experiments were performed at least 30 days after the first tamoxifen administration, unless explicitly stated otherwise. Mice heterozygous for the recombinase presented a complete elimination of the targeted protein (**Fig. 1B-D**) and their Cre⁻ littermates were used as controls. Animals in a very poor state or showing signs of pain were instantaneously sacrificed. To improve the well-being of the mice lacking both KAT3, we provided them with several high-protein food pellets (Teklad global 2919, Envigo) always available on the bedding. Environmental enrichment (EE) experiment was performed as reported in Lopez-Atalaya et al. 2011. Animals were kept in the EE for at least a month before starting the behavioral testing and housed inside the EE for the entire time of the testing. EE mice used for the biochemical studies were taken directly from the enriched environment housing.

3.1. Drug-induced seizures

Kindling drug sensitization protocol was done with modifications as in Yeghiazaryan et al. 2014. Animals were injected IP with a subthreshold dose (45 mg/kg for *Crebbp*^{ff} mice) of a pro-epileptic drug Pentylentetrazol (PTZ). After the treatment mice were observed for the first 30 min and scored for their maximal seizure response according to the modified scale from Yeghiazaryan et al. 2014 (**Table M-1**). The treatment was repeated every second day, which caused an incremental sensitization to the PTZ and increase in epileptic response. Mice continued with the treatments until

they reached the exclusion condition – 3 consecutive experimental days of seizure level 4 or 5.

Table M-1. Seizure scores for kindling PTZ drug sensitization protocol

Score	Kindling seizure
1	Immobility
2	Small body twitches with bringing the ears back
3	Rigid position, forelimb extension leading to abnormal body position
4	Clonic seizures of the forelimbs, head, neck and the trunk ("curling", "hitting the ground"), falling
5	Tonic-clonic seizures, falling and staying on the bedding, forelimb and hindlimb extension, violent jerks of the whole body, jumping. Often after the tonic-clonic convulsions absent seizures can be observed.
6	Death

3.2. Behavioral testing

All the behavioral testing has been performed using a mix of male and female mice. Animals survival and well-being were monitored daily starting with the first day after TMX administration (Day 1) for at least one month (Day 30). The SHIRPA, Open-field, Elevated Plus Maze, Novel Object Recognition, Morris Water Maze and Fear Conditioning were performed as presented previously in (Viosca et al. 2010). In each of the tests, the experimenter was blind to the animal genotype. Open-field, Elevated Plus Maze were recorded and analyzed using SMART software (Panlab S.L.). Fear conditioning was recorded and analyzed using Freezing software (Panlab S.L.). Novel Object Recognition was recorded using SMART and the videos were analyzed *a posteriori* by manually measuring the time spent interacting with each of the objects. For SHIRPA analysis, *CamKIIa-CreERT2::Crebbp^{ff}::Ep300^{ff}*, *CamKIIa-CreERT2::Crebbp^{ff}::Ep300^{ff/+}* and *CamKIIa-CreERT2::Crebbp^{ff/+}::Ep300^{ff}* mice were first tested two days before TMX treatment and again three days after the last TMX injection (Day 12).

3.3. Stereotaxic surgeries and virus administration

Mice were deeply anesthetized i.p. with a mixture of midazolam (5 mg/kg), medetomidine (1 mg/kg) and fentanyl (0.05 mg/kg) mixed in NaCl (0.9%) to a volume of 10-15 μ l/g of body weight. As soon as the total loss of reflexes was observed, the animals were positioned in a digital stereotaxic frame (Stoelting). At this point the body temperature was constantly monitored and maintained during the surgery at 37°C using electric blanket. Local anesthetic (EMLA 25%, lidocaine/prilocaine, AstraZeneca) was applied on the ear bars and the ophthalmologic gel (Viscotears, Bausch + Lomb) was administered on eyes to avoid the formation of ulcers. Once the cranium has been exposed, a hole was drilled in the calvaria in the location corresponding to the hippocampi. A glass capillary (World Precision Instruments) containing the adeno-associated virus (AAV) was placed slowly in the coordinates of the hippocampal hilus (-2.0, +/-1.35, -1.95; in mm relative to bregma) and left in place for five minutes. 500 nl of either AAVs rAAV5-hSyn-GFP-Cre or rAAV5-hSyn-mCherry-Cre was injected (Vector Core at the University of North Carolina at Chapel Hill). The capillary was then left in place for another five minutes and withdrawn. After the surgery, anesthesia was reversed with subcutaneous atipamezole (0.02 mg/kg). Buprenorphine in food pellet (1 mg/ml) was placed in the home cages to reduce post-surgery pain and mice were monitored daily until fully recovered.

3.4. In vivo electrophysiology

Mice were deeply anaesthetized with 4% isoflurane (Isoflo®, Esteve Veterinaria S.A.) in 0.8 L/min oxygen and fixed in a stereotaxic setup (NARISHIGE Group) over a heating pad at 37°C. Isoflurane was kept at 1-2%, 0.8 L/min oxygen to maintain the anaesthesia. After checking the lack of reflexes, mice were placed and fixed in a stereotaxic frame (NARISHIGE Group). The skin of the head was cut, the scalp and the periosteum were separated. Two 1.8 mm \varnothing holes were made in the skull using a milling cutter (FST 18004-18, Fine Science Tools) attached to a cordless micro drill (58610V, Stoelting Co.) in the appropriated coordinates to introduce the electrodes. Then one bipolar stimulating electrode (10-15 k Ω , 325 μ m \varnothing , TM53CCNON, World Precision Instruments) was introduced in the perforant pathway (from bregma, in mm: -4.3 AP, +2.5 ML, +1.4 DV, 12° angle), and one recording probe (single shank, 50 μ m contact

spacing, 32 channels; NeuroNexus Technologies) was targeted to the hippocampus CA1 and dentate gyrus regions (from bregma, in mm: -2 AP, +1.5 ML, -2 DV). Recording and stimulating electrodes were implanted following stereotaxic standard procedures and optimized based on the online recording to have the best quality of the signal in the dentate gyrus and CA1, especially taking into account the typical evoked potential in dentate gyrus (Andersen et al. 1966). A custom-made Ag/AgCl wire was placed in contact with the skin and used as a ground. After optimizing the final position, the tissue was allowed to rest for 30 minutes before acquiring electrophysiological data. The position of the electrodes was confirmed *post mortem*. The stimulating electrode was connected to a pulse generator and current source (STG2004, Multichannel Systems) controlled by MC_Stimulus software (Multichannel Systems). Electrophysiological data from the recording probes were filtered (0.1-3 kHz), amplified and digitalized (20 kHz sampling rate for evoked potentials and 32 kHz for spontaneous activity recordings) and analysed off-line using the Spike2 software (Cambridge Electronic Design Limited) or MATLAB (MathWorks) using ICAofLFPs package (Castellanos and Makarov 2006, Herreras et al. 2015). Stimulating and recording protocols entailed spontaneous recordings (5 minutes) and evoked potentials, that consisted of a classical Input-Output (IO) stimulation protocol (stimulation intensities of 0.05, 0.1, 0.2, 0.4, 0.6, 0.8, 1 and 1.2 mA). For evaluating the Excitatory Post-Synaptic Potential (EPSP) the deepest slope of the evoked potential in molecular layer (dentate gyrus) was measured. To reflect the Population Spike (PS) the amplitude of the spike recorded in hilus was measured. Data were averaged by animal, per stimulation intensity, and then by group. Spontaneous activity signals coming from representative channels in dentate gyrus were selected to analyse the power of the frequency bands and the wavelet spectrum. Briefly, after down-sampling of spontaneous recordings to 2.5 KHz, the signals were filtered (high pass at 0.5 Hz and notch at 50 and 100) and then analysed to extract: a) its power density by frequency bands; b) the wavelet spectrum, using the Fourier Transformation or the Wavelet spectrum analysis, respectively, implemented in the MATLAB package ICAofLFPs. Data extracted from the representative channels were averaged by group. Single Unit Activity (SUA), as local activity reflex (Perel et al. 2015), was analysed using a supervised tool integrated in Spike2 software. Briefly, after applying a band pass (0.3-3 KHz, Butterworth digital filter), the different waveforms were extracted with intensity threshold set at $\pm 3^{-4}$ mV (to avoid noise) for all the putative SUA-spikes recorded

nearby the recording electrode in the dentate gyrus or in CA1. After the complete scan of the electrophysiological signal, per area, we manually chose only those waveforms that clearly fit with the typical one reflecting neuronal activity (supervised procedure). The number of spikes was averaged by area, animal, and then by group to avoid an overestimation of the total n for the statistical comparisons.

3.5. Histology and image processing

Experimental and control animals were anesthetized using a mix of xylazine (Xilagesic, CALIER) and ketamine (Imalgene, Merial Laboratorios) and perfused transcardially, first with PBS (pH 7.4) to removed whole blood, then with a solution containing 4% paraformaldehyde in PBS. Brains were perfused and postfixed overnight (4% paraformaldehyde) were cut on vibratome into 50 μm sections. Sections were used for immunohistochemistry (fluorescent and diaminobenzidine) and Nissl staining as previously described in (Fiorenza et al. 2016). Some antibodies used for the fluorescent immunohistochemistry required a 30 min antigen retrieval in 80°C sodium citrate buffer (10mM Sodium Citrate, 0.05% Tween 20, pH 6.0). The TUNEL staining was performed using In Situ Cell Death Detection Kit (Roche REF:11684795910) where DNaseI-treated control brain sections were used as positive control of DNA damage. The Golgi-Cox impregnation has been performed using the FD Rapid GolgiStain™ Kit (FD NeuroTechnologies, Inc.). Experimental and control animals were anesthetized using a mix of xylazine and ketamine to prevent any head damage and sacrificed using cervical dislocation. The brains were instantly removed from the skull, rinsed very briefly with double distilled water in order to remove the excess of blood and placed in the impregnation solution in room temperature. The solution was changed to a fresh one after the first 24 hours. After 10 days in total the brains were immersed in solution C for 72 hours after which it was changed to a fresh solution C for the next 24 hours. Subsequently, the brains were carefully cut on vibratome in a 1:1 mix of PBS and solution C into 100 μm sections. These sections were next mounted on gelatin-coated slides, revealed using solutions D and E, dehydrated using ethanol and xylene and covered using Neo-Mount® (Merck). This protocol resulted in a sparsely marked neurons along the entire section of the brain, ideal for reconstructing the neuronal morphology. In light image quantifications and processing, samples marked using Golgi technique were visualized under a bright field microscope with a motorized

stage. Dentate gyrus granule neurons with mostly intact dendritic trees were traced and subsequently reconstructed using the NeuroLucida software (MBF Bioscience). The reconstructions were used to perform a Sholl analysis, where the number of intersections was calculated every 2 μm starting from 5 μm from the soma. The thickness of CA1 sub-regions was quantified based on the Nissl staining (sagittal cut) bright field images made with a 2.5x objective. In Fiji ImageJ four lines were drawn perpendicularly to the CA1 and the thickness of stratum pyramidale or stratum radiatum was measured along each of the lines (see **Fig. 3B**). The average value was the final measurement for each animal. The immunofluorescence images were made using either Leica fluorescent microscope or Olympus Confocal. Whole section images were made using Leica stereomicroscope.

For electron microscopy (EM) experiments, mice were anesthetized and perfused as described for the immunohistochemistry with the addition of 2.5% glutaraldehyde in the fixation solution. Then brains were then cut on vibratome to 100 μm thick slices. Selected slices with dorsal hippocampus were postfixed with 1% osmium tetroxide for 1 h at room temperature. Dehydration was performed by incubating the slices in increasing ethanol concentrations and in pure propylene oxide. During dehydration, tissue was stained with 1% uranyl acetate in 70% ethanol. Slices were embedded in the Epon resin between two Aclar sheets. After polymerization, Cornu Ammonis (CA1), stratum radiatum and dentate gyrus regions fragments were cut out and stick to an empty block of resin. Next, sixty-five nanometer sections were prepared and post stained with uranyl acetate and Reynold's lead citrate. Electron micrographs were taken with JEM 1400 transmission electron microscope at 80 kV (JEOL co., Tokyo, Japan, 2008). Quantification of synapses and heterochromatin clumps number were performed by Fiji ImageJ software with the Cell Counter plugin and macro based on the Analyze Particles function respectively.

3.6. Fluorescence-activated nuclear sorting (FANS)

The Fluorescence-Activated Nuclear Sorting (FANS) was performed as in Fernandez-Albert et al. 2019. Experimental mice were sacrificed by cervical dislocation and the hippocampal tissue was extracted from the brains. This tissue was subsequently homogenized using a douncer tissue grinder (KONTES® 2ml) in a buffer containing 0.5% IGEPAL and filtered on a 35 μm nylon mesh (Falcon #352235). The resulting

suspension of hippocampal nuclei was stained using mouse anti-NeuN antibody, anti-mouse Alexa 647 antibody and DAPI. At this point three independent samples were pooled to form a single replicate that was centrifuged in Optiprep (MERCK) gradient. Nuclei purified this way were sorted using BD FACS Aria II Flow Cytometer by their size (FSC), complexity (SSC), DAPI and NeuN-Alexa647. dKAT3-ifKO samples contained two populations of neuronal nuclei: (I) strongly immunofluorescent for NeuN, which did not undergo Cre recombination; and (II) weakly immunofluorescent for NeuN, which still expressed higher levels than non-neuronal cell-types (**Fig. M-1A**). Specific gate was set up in the flow cytometer to isolate only the second group of dKAT3-ifKO nuclei for the ATAC-seq experiments (**Fig. M-1B**).

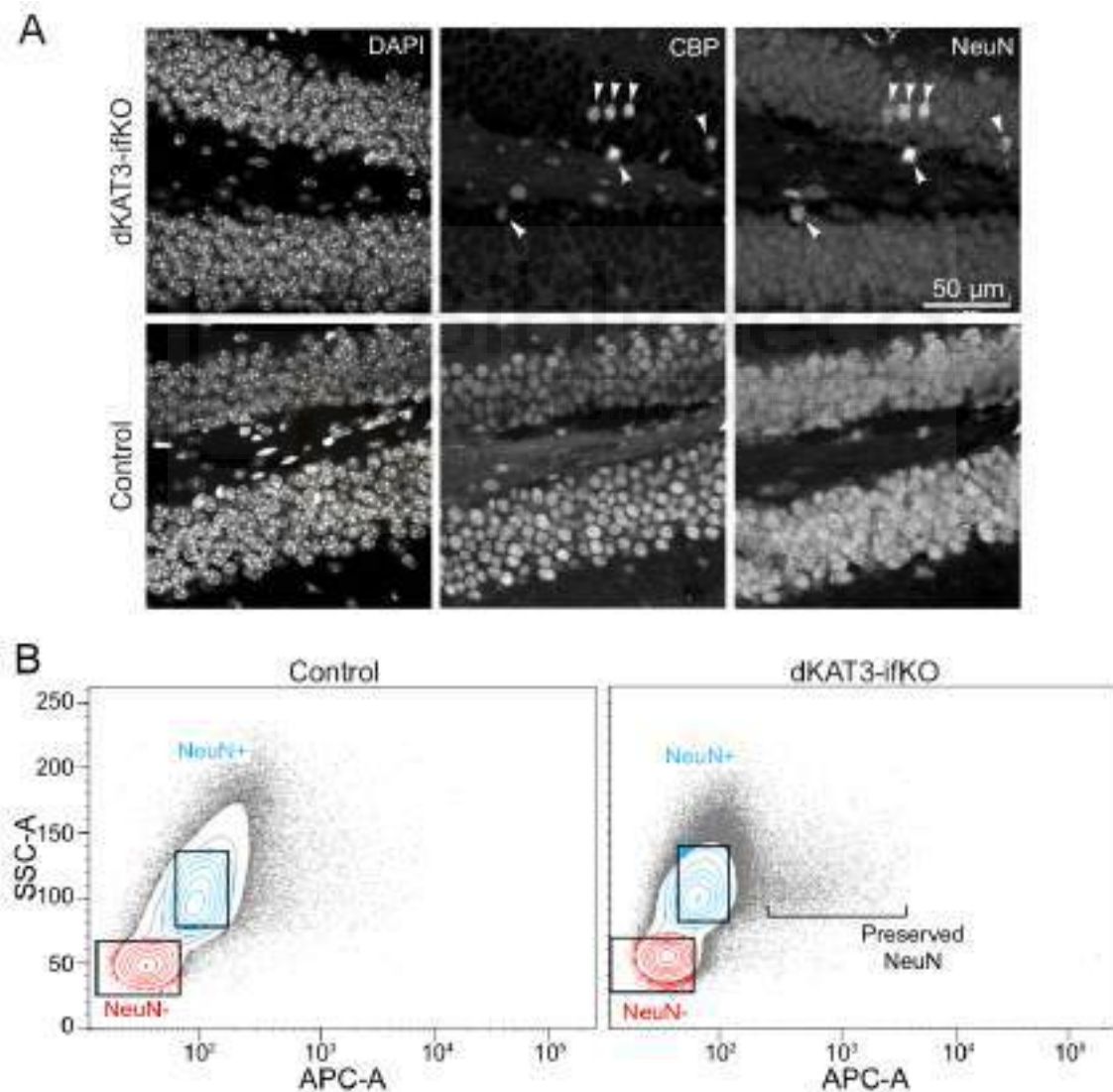


Figure M-1. dKAT3-ifKO neurons with a decrease in NeuN expression can still be differentiated in from the non-neuronal cell-types in the FANS A. Immunohistochemistry showing two subpopulations of neuronal cells: first those expressing CBP (and p300) and normal levels of NeuN protein (arrowheads); second, the cells that have lost CBP (and p300)

expression, thus diminished NeuN levels. The first group likely contains interneurons and granule cells born after the TMX treatment, as the recombination does not happen in the progenitor cells. **B.** FANS gating snapshot, showing that although the NeuN staining (APC-A) is diminished in dKAT3-ifKO, a clear cloud of points can be still easily distinguished if plotted by both NeuN expression and complexity (SSC-A). Notice that a group of nuclei had an increased NeuN expression in comparison to the main cloud in dKAT3-ifKO (marked). These nuclei correspond to the neurons marked with the arrowheads in the panel **A**, and were discarded during the selection/gating process. Only the nuclei marked in blue were subsequently used in the ATAC-seq experiment.

3.7. RT-PCR and RNA-seq analysis

Extraction of RNA from the hippocampal tissue was performed using TRI-reagent (MERCCK) as previously described (Scandaglia et al. 2017). Resulting total RNA was treated with DNase I (Qiagen) and its quality was confirmed using NanoDrop (Thermo Fisher) and Bioanalyzer (Agilent). Three or more independent samples were prepared for both control and ifKO mice. Each sample corresponded to a single mouse. RNA obtained this way was either analyzed using QuantStudio 3 Real-Time PCR System (Thermo Fisher) or sequenced using NGS technology. For most of the samples (dKAT3-ifKO, p300-ifKO), PolyA libraries were prepared. In the case of the CBP-ifKO experiments, either PolyA (**Fig. 17**) or Ribo-Zero (**Figs. 19 and 20**) libraries were prepared. The libraries were sequenced single-end using a HiSeq 2500 sequencer (Illumina, Inc). The output reads were mapped to the GRCm38 (mm10) *Mus musculus* genome assembly using HISAT2 algorithm (Kim et al. 2015a). Read counts were provided using HTSeq python package (Anders et al. 2015) and DESeq2 from R Bioconductor toolset (Love et al. 2014). R Bioconductor toolset was used to analyze data and provide the graphical representation.

3.8. ChIP-assay and ChIP-seq

Chromatin immunoprecipitation (ChIP) was performed as previously described (Lopez-Atalaya et al. 2011, Galvão-Ferreira et al. 2017). The CBP and p300 ChIP experiments required the following adjustments: Minced hippocampal tissue was fixed in 1% PFA for 30 min in 37°C (as suggested in Gasper et al. 2014), which allowed for crosslinking of the KAT3 cofactors to the DNA-binding proteins and to the DNA itself. As the KAT3 proteins were sensitive to a few rounds of sonication in 1% SDS (see **Fig. M-2**), the sonication buffer was changed to one containing 0.1% SDS, 1%

IGEPAL (Sigma-Aldrich) and 0.5% sodium deoxycholate. Additional 10 sonication cycles of 30''on/30''off were added to fragment the highly fixed DNA sufficiently for sequencing. Sequences of the primers used in the confirmatory ChIP-assay (**Fig. 9A**) can be found in **Table M-2**. The libraries were prepared with the immunoprecipitated DNA fragments and sequenced using HiSeq 2500 sequencer (Illumina, Inc). The output reads were mapped to the GRCm38 (mm10) *Mus musculus* genome assembly using Bowtie2 algorithm (Langmead and Salzberg 2012). The MACS algorithm was used to extract the chromatin regions enriched in given protein binding (Zhang et al. 2008). In order to avoid false positive results, the ChIP-seq Irreproducible Discovery Rate (IDR) recommendations of ENCODE were applied (Landt et al. 2012). R Bioconductor toolset was used to analyze the data and provide the graphical representation. Quantitative comparisons were made using DiffBind package (Stark and Brown 2011). Motif analysis was done using MEME-ChIP algorithm from the MEME-suite toolkit (meme-suite.org; more details regarding the methodology in Bailey 2002 and Bailey et al. 2015). Motif families were presented as given by the TOMTOM and CentriMo sub-algorithms. Only the results higher than E-value= 1×10^{-10} were represented in the graphs. Gene ontology analysis was performed using Panther (Thomas et al. 2003).

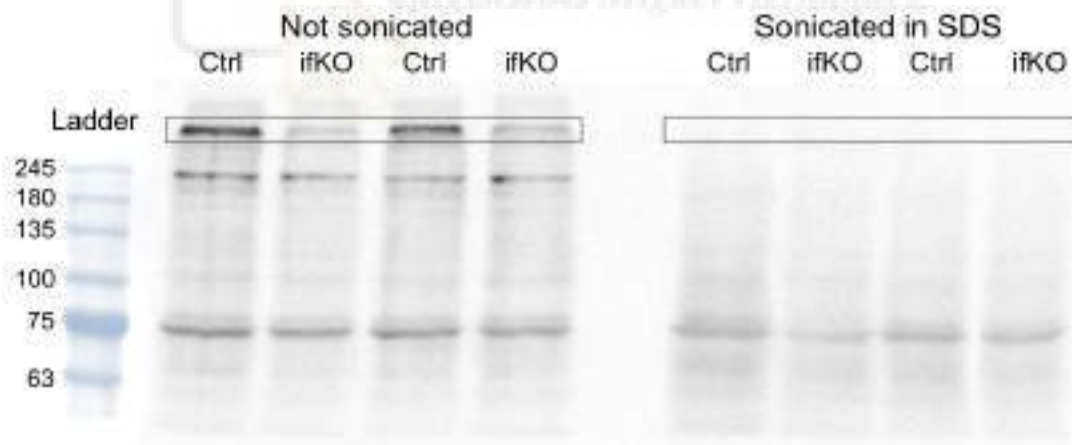


Figure M-2. CBP degrades completely when protein extracts were sonicated in high SDS. Anti-CBP Western-Blot made on hippocampal protein extracts from controls (Ctrl) and CBP-ifKO mice (ifKO). The extract was either left as it is (left), or sonicated in 2% SDS (right; 10 cycles 30s-30s). The boxes indicate the position of the band corresponding to the protein molecular weight of CBP. Notice an almost complete depletion of the signal in the ifKO extracts. The remaining blurry CBP band can be explained by the presence of CBP in cells other than excitatory neurons, such as glia. Of note, no truncated isoform was detected as a result of the recombination.

Table M-2. Oligonucleotides used in this study

Target name	Forward	Reverse	Use
<i>Gapdh</i>	CTTCACCACCATGGAGAAG GC	CATGGACTGTGGTCATGAGCC	RT-PCR
<i>Crebbp</i>	TCAGCTCTTCCAACCTCCTT GG	AAGGAGGCGCTGCTGTAGGT AT	RT-PCR
<i>Ep300</i>	AAAAGACCGACGGATGGAA AA	TTCTCGGCTAGGAGGTGATAG T	RT-PCR
<i>Bdnf</i> (all isoforms)	GAAGGTTTCGGCCCAACGA	CCAGCAGAAAGAGTAGAGGA GGC	RT-PCR
NeuN (<i>Rbfox3</i>)	GCAGTCGCGGTTGGAGTAGT	CGTTAAAAATGATCTCCACGT CTAAAAAT	RT-PCR
<i>Fos</i> promoter	CGCCCAGTGACGTAGGAAG T	GCAGTCGCGGTTGGAGTAGT	ChIP-assay
<i>Bdnf</i> promoter 3	GACCAATCGAAGCTCAACC G	GGCACTGGGGTCAGACATTA	ChIP-assay
Intergenic (upstr. <i>Bdnf</i>)	CTACCGAGTGTGATTGCCG T	TGATGCAAGTGTCAAGCTCAA TG	ChIP-assay
Neurod2 gRNA	CACCGAGATGCCACACTCGC TCCG	AAACCGGAGCGAGTGTGGCA TCTC	gRNA
<i>Hpca</i> gRNA A	CACCGAGACCCAGGGCGGT CGTTC	AAACGAACGACCGCCCTGGG TCTC	gRNA
<i>Hpca</i> gRNA B	CACCGCTGGCCCTGATTTTCG GGCC	AAACGGCCCCGAAATCAGGGC CAGC	gRNA
<i>Hpca</i> gRNA C	CACCGCACCCCTGGGCTCTGG TCCGG	AAACCCGGACCAGAGCCCAG GGTGC	gRNA

3.9. ATAC-seq

ATAC-seq was performed as described in (Buenrostro et al. 2013). Briefly, sorted neuronal nuclei were centrifuged and resuspended in the transposase reaction mix (TD buffer and Tn5 transposase, Illumina). The mix was placed in 37°C for 30 min and immediately after the DNA was extracted (Qiagen Minelute PCR Purification Kit). A DNA library was then prepared using Custom Nextera PCR primers 1 and 2. We monitored the saturation of the library using qPCR and afterwards extracted the DNA using kit. This final DNA extract was sequenced using HiSeq 2500 sequencer (Illumina, Inc). The reads were processed similarly to the ChIP-seq samples. The ATAC-seq motif analysis was performed as in the ChIP-seq analysis.

3.10. Primary hippocampal cultures and lentiviral vectors

Primary cultures were prepared as described in Benito et al. 2011. Briefly, *Crebbp^{ff}::Ep300^{ff}* pups were extracted from the pregnant mother at E17.5 and their brain and subsequently hippocampi isolated. The hippocampi were pooled, trypsinized and homogenated. Resulted cell isolate was seeded either on glass coverslips (for immunocytochemistry, ICC) or directly on a 24-well plate (QPCR). The surface for cell growth had been previously prepared by coating with poly-D-lysine. The day of plating is considered to be the day *in vitro* 1 (DIV1). On the DIV2, *Crebbp^{ff}::Ep300^{ff}* hippocampal cultures were infected with either a bicistronic lentivirus carrying GFP and Cre (LV PGK:Cre-Ubc:GFP) or with a GFP-only lentivirus (LV Syn:GFP), prepared as described before (Benito et al. 2011). For the morphological analysis the neurons were transfected with the pDsRed-Express2-C1 (Clontech) on the DIV9 using Lipofectamine 2000 (Invitrogen). On the next day, the cell red fluorescence was used to observe morphological changes using either a Leica or Olympus Confocal microscope. For the CRISPR experiments, infected cells were Lipofectamine-transfected on the DIV14 with a combination of two vectors: gRNA-mCherry plasmid carrying a specific gRNA (plus a mCherry reporter), and a vector carrying inactivated Cas9 fused with p300 KAT domain (dCas9-p300). Gene expression was analyzed the day after using ICC.

3.11. Antibodies

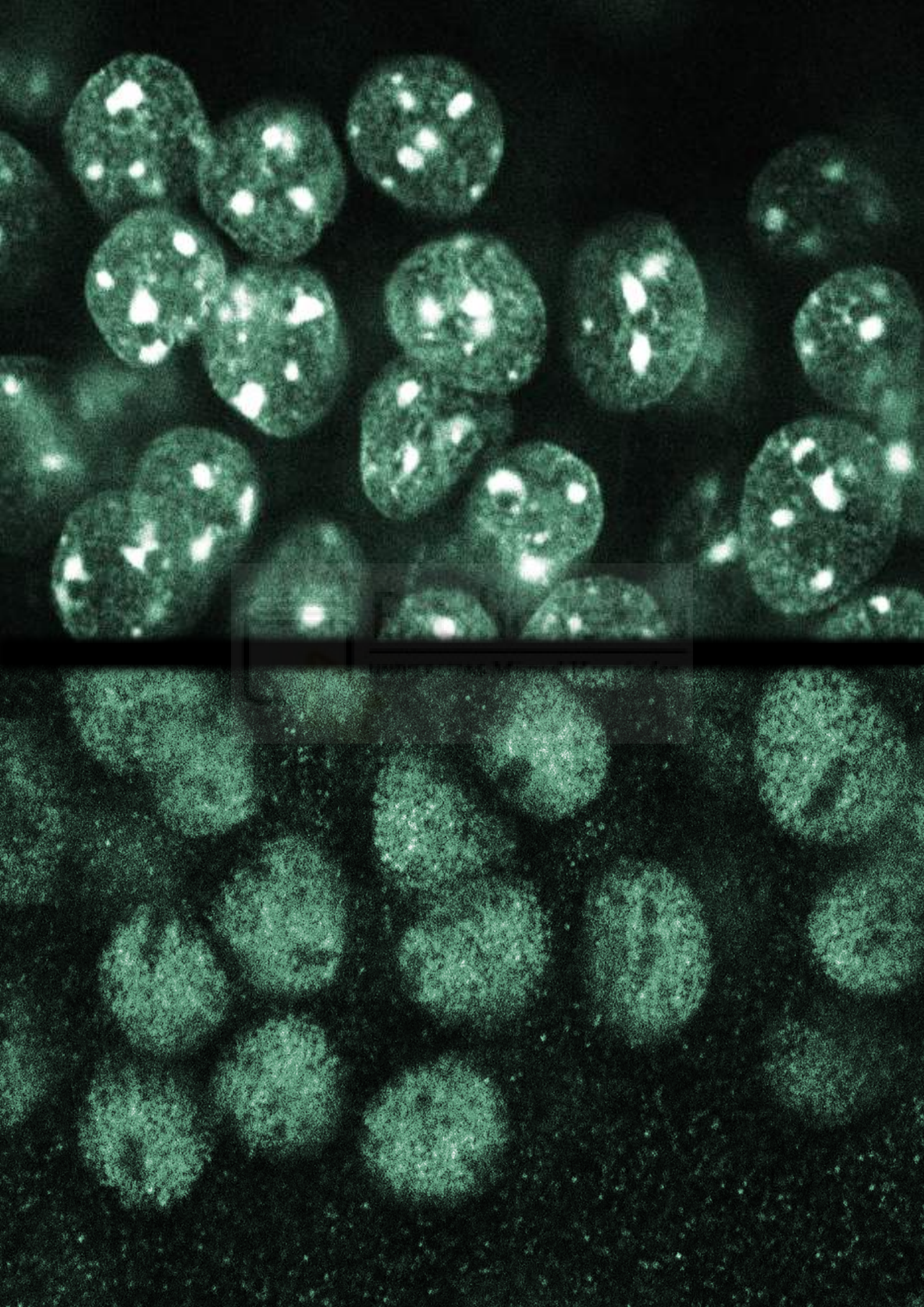
Antibodies used in this study: anti-CBP (Santa Cruz sc-583, sc-369, sc-7300), anti-p300 (Santa Cruz sc-585), anti-Neurod2 (Abcam ab109406), anti-acetylated histone N-tails H2A, H2B, H3 and H4 (homemade, described in Lopez-Atalaya et al. 2013), anti-H3K27ac (Abcam ab4729), anti-NeuN (Merck-Millipore MAB377), anti-hippocalcin (Abcam ab24560), anti-CaMKIV (BD Transduction Laboratories C28420), anti-Cleaved Caspase-3 Asp175 (Cell Signalling #9661), anti-mCherry/dsRed (Clontech 632496), anti-GFP (Aves Labs GFP-1020), anti-GFAP (Sigma G9269), anti-H2A.X gamma pS139 (Abcam ab2893).

3.12. Statistical analysis

All the statistics in the following work have been done using RStudio, GraphPad Prism or MATLAB, depending on the experiment. Statistical tests used in the study are indicated either in the Figure or in the corresponding legend. The performed statistical tests were all performed as two-sided. In all the bar plots the height represents the mean and the error bars represents the +/- standard error of mean. *ns*: non-significant, *: p-value < 0.05, **: p-value < 0.01 and ***: p-value < 0.001.



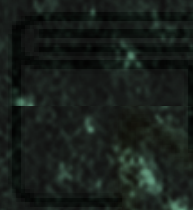




Results

Chapter I

CBP and p300 jointly safeguard cellular identity
by maintaining histone acetylation levels



Bibliotecas
Max Planck Society



The following study is highly multidisciplinary and was done in collaboration with several members of the laboratory of Prof. Angel Barco (Instituto de Neurociencias UMH-CSIC), and collaborators in the laboratories of Dr. Santiago Canals (Instituto de Neurociencias UMH-CSIC) and Prof. Grzegorz Wilczyński (Nencki Institute of Experimental Biology, Warsaw, Poland):

Dr. Rafael Muñoz Viana designed and performed the bioinformatic analysis of the sequencing data. Dr. Beatriz del Blanco provided the rescue culture experiments. Juan Medrano-Relinque helped with the AAV injections. Dr. Jose María Carames (Canals lab) made the *in vivo* electrophysiology experiments. Andrzej Szczepankiewicz (Wilczyński lab) provided the EM images and quantifications. Alejandro Medrano participated in the SHIRPA analysis and Jordi Fernandez-Albert in the FANS-ATAC-seq experiment.

I designed and performed all of the *in vivo* molecular, biochemical, histological, behavioral experiments and their statistical analysis. I have also performed some of the bioinformatic experiments and discussed the design of most of others. The project as a whole was designed and interpreted by me under the supervision of Prof. Angel Barco. The manuscript presented in this Chapter was written with important input from all the coauthors referred above.

I would also like to thank Roman Olivares, Nuria Cascales-Picó and Marián Llinares Granados for their technical help.



4.1.1. The simultaneous, but not individual, loss of CBP and p300 in adult forebrain principal neurons causes severe neurological deficits

In order to elucidate the neuronal roles of CBP and p300 in the adult brain, we selectively eliminated CBP, p300, or both KAT3 proteins in forebrain excitatory neurons of adult mice using the inducible Cre recombinase-driver *CaMKII α -CreERT2* (**Fig. 1A**). The three inducible forebrain-specific knockout strains (referred from now on as CBP-ifKO, p300-ifKO and dKAT3-ifKO, respectively) developed normally and did not show any neurological symptom before tamoxifen (TMX) administration triggered gene(s) ablation. As expected after TMX treatment, the loss of the corresponding proteins was restricted to pallial regions (i.e., cortex and hippocampus, **Fig. 1B**).

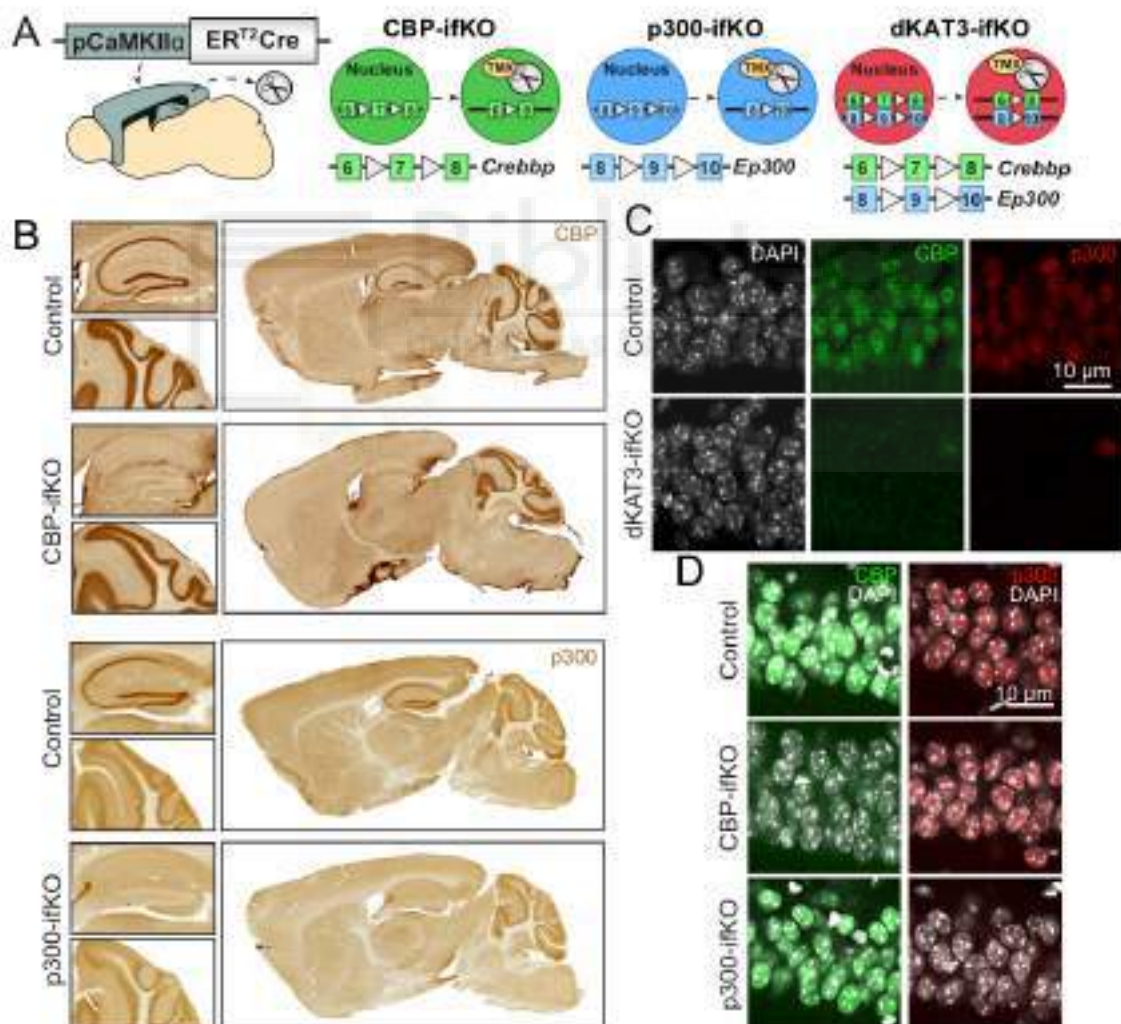


Figure 1. Genetic strategy to induce KAT3 loss in adult mouse forebrain. **A.** Scheme representing the genetic strategy for the production of inducible, forebrain-specific CBP (CBP-ifKO), p300 (p300-ifKO) and double KAT3 knockout (dKAT3-ifKO). Exon 7 was eliminated in the *Crebbp* gene and exon 9 was eliminated in *Ep300* gene. **B.** DAB immunohistochemistry images showing CBP/p300 loss in forebrain neurons of a corresponding

knockout 1 month after the TMX administration. Notice no change in the expression of the protein in the cerebella and a complete elimination of the protein the ifKO hippocampi (higher magnifications on the left). **C.** Double immunostaining against CBP and p300 in the CA1 region of dKAT3-ifKO and control littermates. A full ablation of both proteins can be observed in pyramidal and granular cells in the hippocampus. **D.** Immunohistochemistry against CBP and p300 in the CA1 region of wild type, CBP-ifKO and p300-ifKO mice. High specificity and no compensatory upregulation can be observed.

Gene ablation was very efficient and the loss of immunoreactivity was observed in virtually 100% of the pyramidal neurons in CA1 and cortex and granular neurons in the dentate gyrus (**Fig. 1B-D**) while brain regions such as the cerebellum and the basal ganglia in which the *CaMKII α* promoter is not active were spared (**Fig. 1B**). Importantly, the loss of either one of the paralog proteins did not affect the expression of the other (**Fig. 1D**).

Consistent with the characterization of other forebrain-specific KO strains for CBP or p300 (Chen et al. 2010, Oliveira et al. 2011, Valor et al. 2011) both CBP- and p300-ifKO mice had a normal lifespan and showed no overt neurological abnormalities in a general phenotyping screen called SHIRPA (**Fig. 2A**, blue and green). The situation was markedly different in dKAT3-ifKOs. The mice in which CBP and p300 were simultaneously removed in mature forebrain principal neurons presented a dramatic and rapidly progressing deteriorating phenotype (**Figs. 2B-C**, red). During the first week after TMX administration, mice showed hyperactivity, head bobbing and frequently froze in bizarre positions. Shortly after, the same mice showed a severe ataxia, loss of the righting reflex, escaping response after touching and tail-suspension-evoked stretching (**Fig. 2B**). Some animals also showed dry eyes and cataracts. The severity of their condition did not allow us to perform any cognitive testing. Although different animals reached the terminal phenotype at different times, virtually all mice died within the first weeks after TMX. However, the survival rate increased to around 30-50% (depending on the litter) within the first month by facilitating the access to food (**Fig. 2C**), which suggests that the high mortality is caused by problems in self-alimentation. Remarkably, mice carrying just one wild-type allele encoding CBP (*CaMKII α -CreERT2::Crebbp^{f/+}::Ep300^{f/f}*) or p300 (*CaMKII α -CreERT2::Crebbp^{f/f}::Ep300^{f/+}*) do not show these phenotypes, indicating that a single wild type allele of either one of the two KAT3 genes is enough to prevent the severe neurological symptoms and premature death (**Fig. 2**, violet and orange).

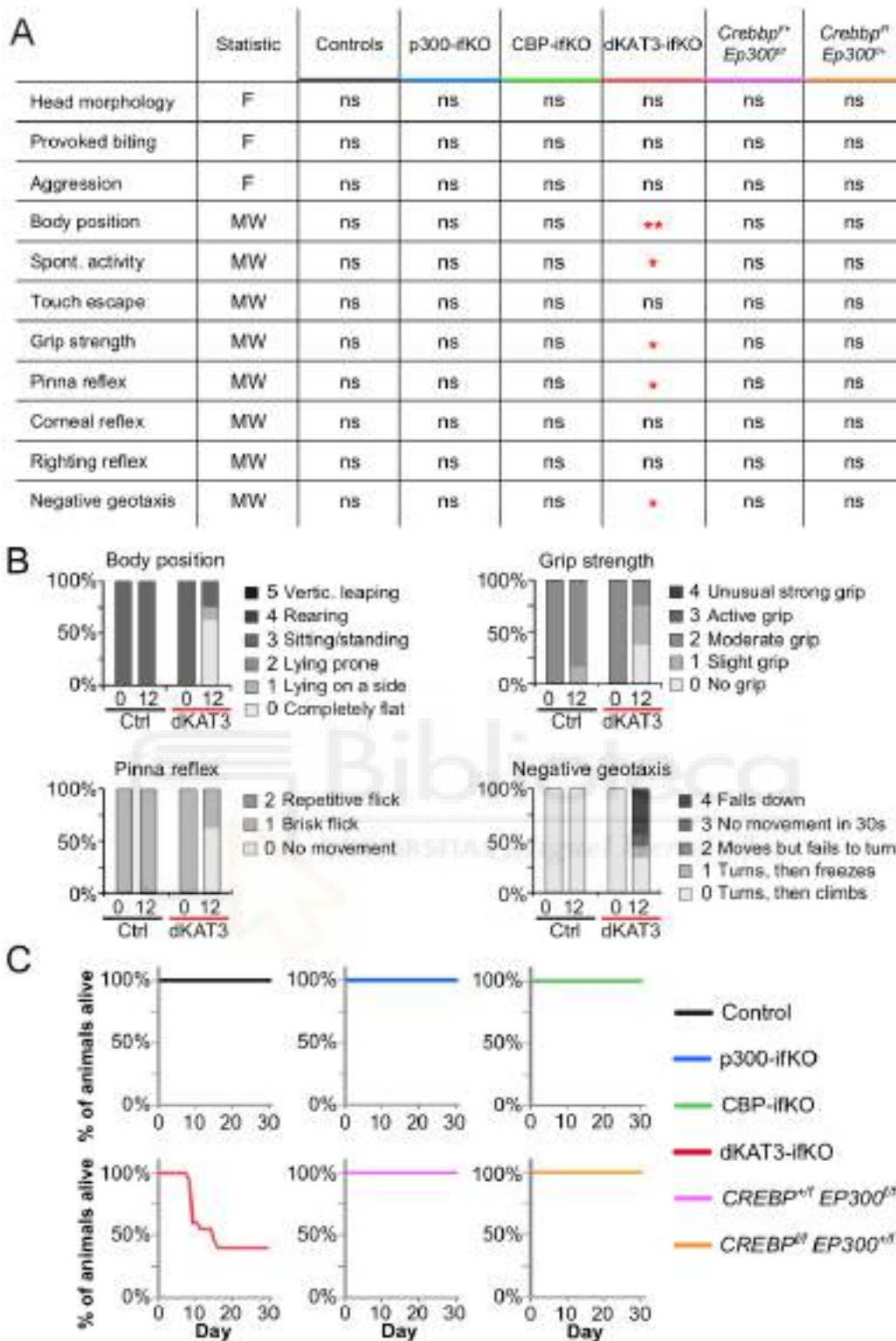


Figure 2. CBP and p300 play a redundant role in basic behavior and animal survival.

A. Score of various knockout mice and the control littermates in a number of SHIRPA categories. The remaining categories did not show any statistical difference. The dKAT3-*ifKO* animals were scored twice: first, right before starting the tamoxifen treatment (d0); second, 12 days from the first TMX administration (d12; control n=6, dKAT3-*ifKO* n=8). Each category is scored according to a specific scale. MW – Mann-Whitney U test, F – Fisher exact test.

B. Statistically significant categories represented as percentage bar charts. **C.** Survival of the

knockout mouse lines during the first 30 days, starting with the first TMX administration. (control n=20, dKAT3-ifKO n=27).

4.1.2. Neurons lacking both KAT3 proteins display massive synaptic loss and reduced electrical activity

Consistent with the severe neurological phenotype, the dKAT3-ifKO mice that survived for more than 2 months after TMX showed an obvious reduction of the entire cerebral cortex, whereas other brain regions non-targeted by gene deletion, such as the cerebellum, were unaffected (**Fig. 3**). Histological analyses indicated that this volume reduction was fundamentally caused by the loss of neuropili rather than neuronal cells.

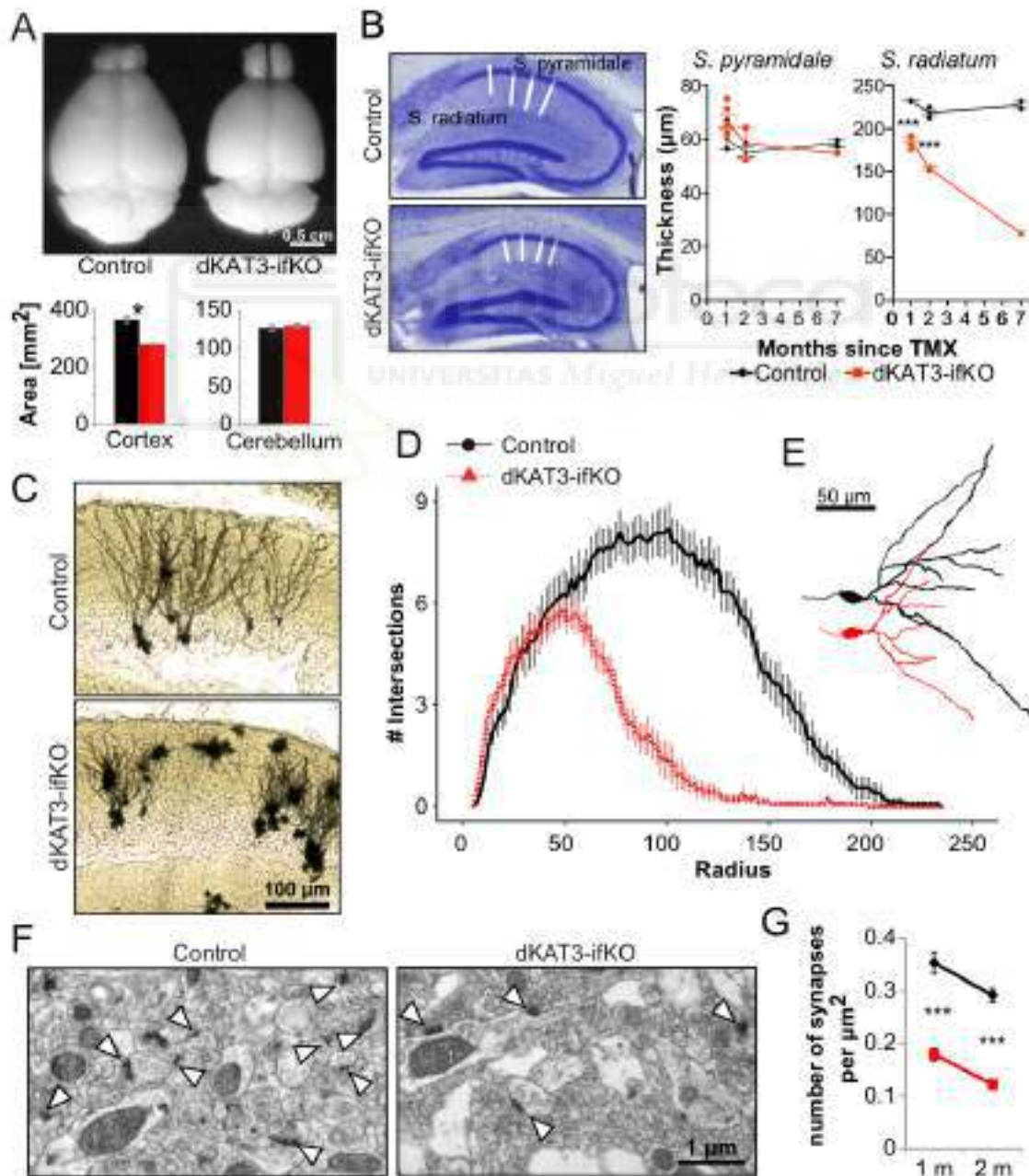


Figure 3. Ablation of both KAT3 proteins causes a retraction of the DG dendrites

A. Upper: Photo of control and dKAT3-ifKO brains 2 months after TMX. Bottom: Quantification of the cortical and cerebellar sizes (control in black, n=3; dKAT3-ifKO in red, n=2, t-test). **B.** Left: Scheme of CA1 sub-region quantification in control (upper) and dKAT3-ifKO (lower) animal 2 months after the TMX. Right: Thickness of the stratum pyramidale (S. pyr) and radiatum (S. rad) in control (1 month, n = 3; 2 months, n = 3; 7 months, n = 2) and dKAT3-ifKO (1 month, n = 6; 2 months, n = 2; 7 months, n = 1) mice at different time points after TMX. Two-way ANOVA. **C.** Dentate gyrus (DG) staining using Golgi method in controls and dKAT3-ifKOs (1 month after TMX). **D.** Dendrite Sholl analysis performed on the NeuroLucida-reconstructed DG neurons. (1 month after TMX; control: 32 neurons from 4 animals; dKAT3-ifKO: 38 neurons from 4 animals) **E.** Representative examples of the NeuroLucida-reconstructed neurons. **F.** Electron microscopy photo showing the stratum radiatum of the control and experimental mice (1 month after TMX). **G.** Quantification of the number of synapses per μm^2 in the stratum radiatum (average of 30 areas from 3 mice/condition, t-tests).

For instance, in the hippocampus of dKAT3-ifKOs, the *stratum pyramidale* - a layer in the CA1 subfield occupied by the somas of pyramidal neurons - had a normal thickness and did not show obvious signs of neurodegeneration even months after TMX treatment. In contrast, the *stratum radiatum* - a layer occupied by the basal dendrites of the CA1 neurons - was markedly thinner in dKAT3-ifKOs as soon as 1 month after TMX administration (**Fig. 3B**). In agreement with these quantifications, Golgi staining revealed a rapid retraction of dendrites in the dentate gyrus (**Fig. 3C-E**) and electron microscopy (EM) analyses confirmed the massive loss of synapses in dKAT3-ifKOs few weeks after TMX treatment (**Fig. 3F-G**).

EM images also show a largely normal *stratum pyramidale* in which neuronal nuclei did not present apoptotic bodies although the nucleoplasm appeared clearer in dKAT3-ifKOs than in control littermates (**Fig. 4A-B**). Further supporting the notion that cell death is not the main cause of forebrain shrinking and neurological defects, TUNEL staining (cell death, **Fig. 4C**), immunostaining against active caspase 3 (apoptosis, **Fig. 4D**) and the H2A.X variant (DNA damage, **Fig. 4E**), were all negative. Although we observed moderate active gliosis in a subset of dKAT3-ifKOs that had exhibited rare episodes of epilepsy, this was not a general feature of dKAT3-ifKO brains (**Fig. 4F**).

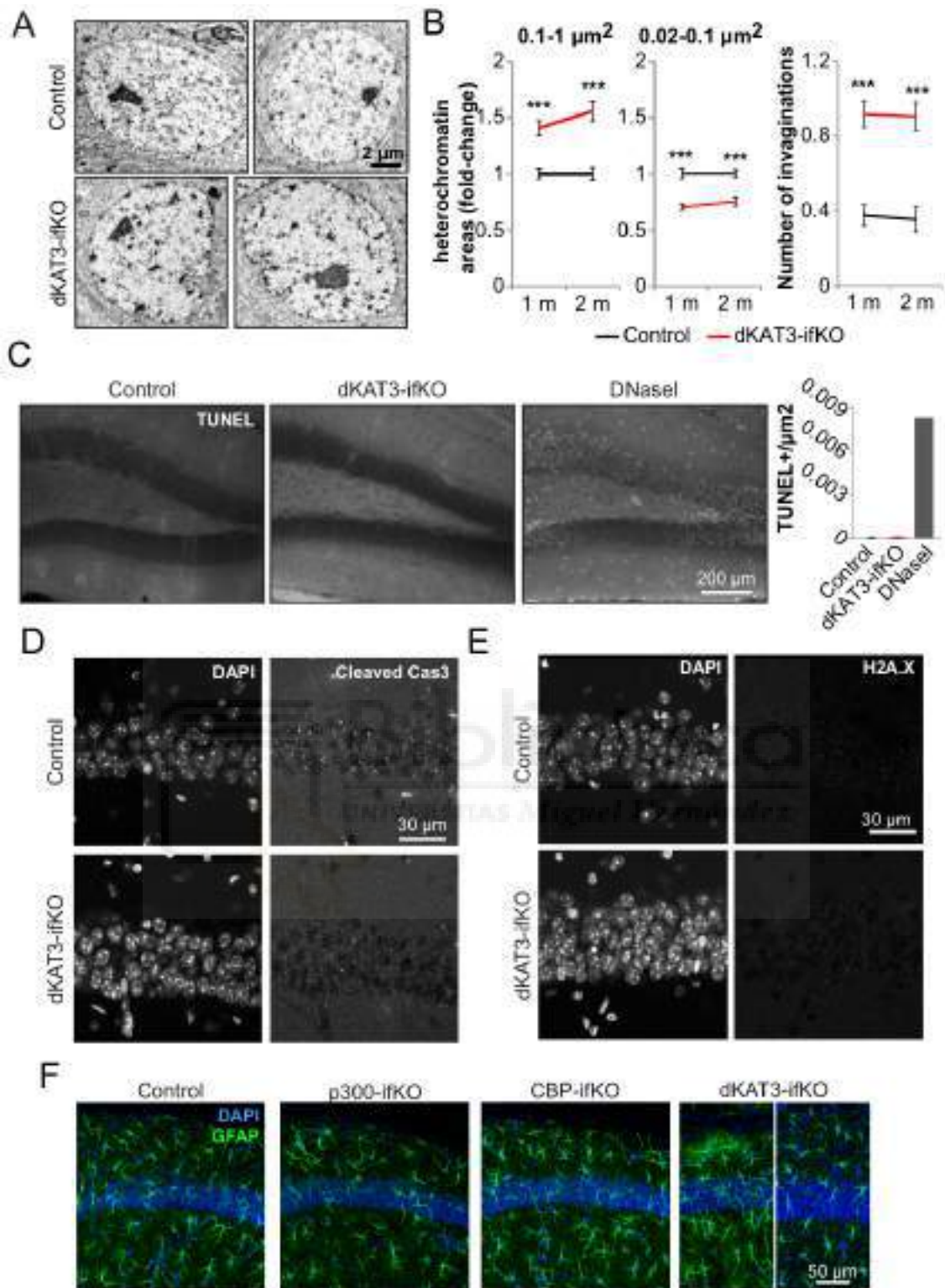


Figure 4. The KAT3 elimination is followed by chromatin changes but no apparent cell death **A.** Electron microscopy of CA1 nuclei in control and dKAT3-ifKO hippocampi 1 month after the TMX. **B.** Quantification of different nuclear features in electron microscopy images 1 and 2 months after TMX. Left panel represents the number of big chromatin granularities (0.1 - 1 μm), middle panel small granularities (0.02 - 0.1 μm) and the right panel the number of nuclear envelope invaginations per nucleus. T-tests. **C.** TUNEL staining images on the left and the quantification on the right show virtually no cell death either in the controls or in the

dKAT3-ifKO. A control brain section treated with DNase I was used to show a homogenous positive TUNEL staining. **D-E**. Immunohistochemistry for cleaved Cas3 (**D**) or phosphorylated H2A.X gamma (**E**) showing respectively no visible apoptosis or DNA damage in the CA1 of the dKAT3-ifKO mice 1 month after TMX. **E**. Immunostaining for GFAP reveals no gliosis in the CA1 subfield of CBP- and P300-ifKO mice. A subset of dKAT3-ifKO animals (roughly 2%) showed increased number of activated astrocytes likely due to observed epileptic episodes.

We next examined if dKAT3-KO forebrain neurons maintain correct electrophysiological activity. To this end, we implanted dKAT3-ifKO and control littermates with multichannel electrodes and performed electrophysiological recording in anesthetized animals. As soon as two weeks after genes ablation, dKAT3-ifKOs presented a dramatic reduction of spontaneous electrical activity, especially visible in the deeper layers corresponding to the hippocampus (**Figs. 5A-B**). This observation has been confirmed by a significantly decreased the number of single unit activity (SUA) spikes in 5 min (**Fig. 5C**). LFP measurements showed that the neuronal activity is decreased at every frequency band (**Fig. 5D**) Furthermore, stimulation of the hippocampal circuit by providing different currents to an electrode placed in the entorhinal cortex, revealed a strongly suppressed evoked electrical response (**Figs. 5E-F**). Overall, these data indicate that the simultaneous loss of both CBP and p300 alters neuronal morphology and impairs electrical responses leading to dramatic neurological defects.

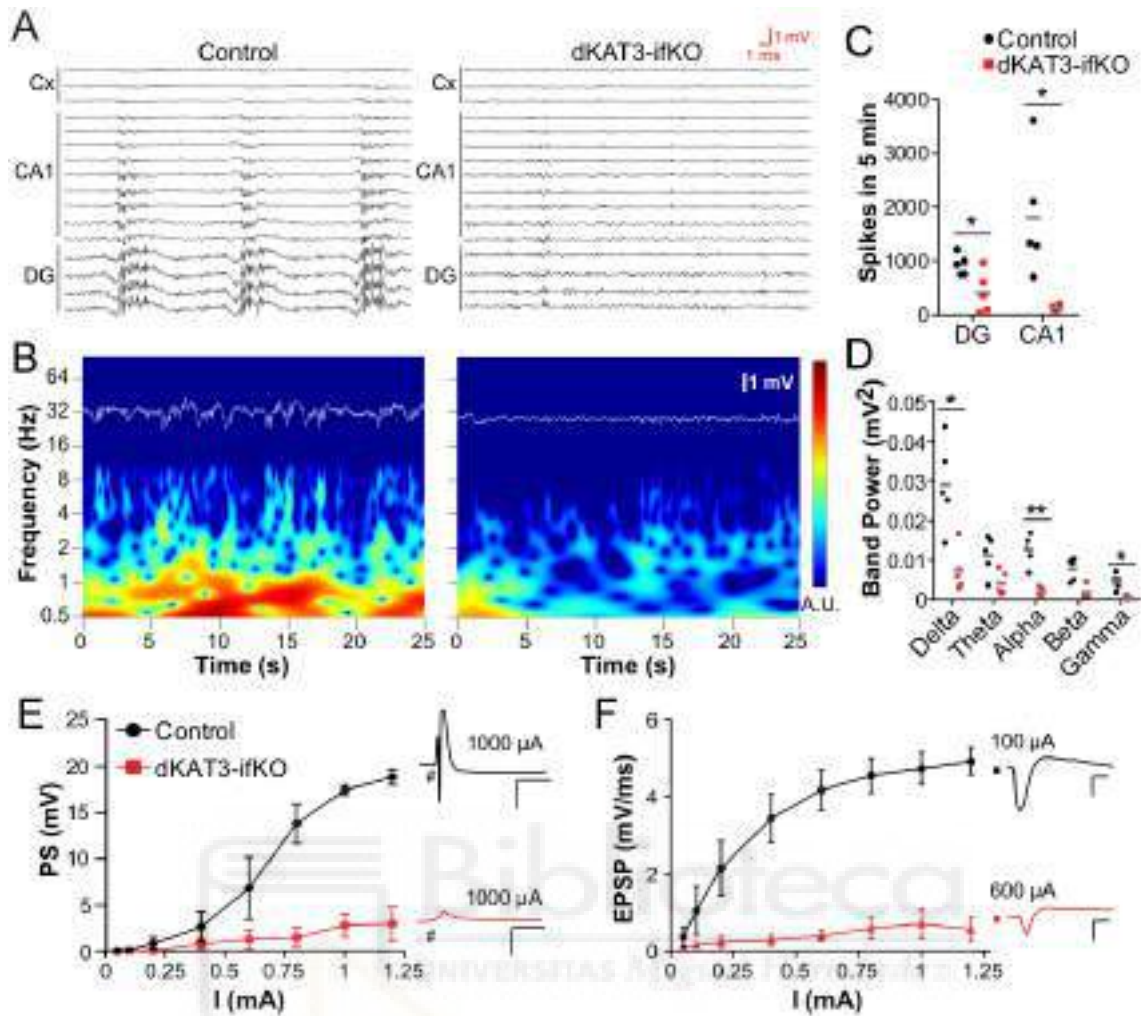


Figure 5. Electrophysiological properties of the dKAT3 neurons are severely impaired

A. Representative 50 s snapshots of *in vivo* electrophysiological recordings from a cortex-hippocampus column performed using multi-channel electrode. **B.** Wavelet spectra of dentate gyrus local field potentials (LFPs) from control (left) and dKAT3-ifKO (right) mice. Color scale in mV². Local field potential signal from the same channel is presented as a white line in the upper part of each panel. **C.** Number of spikes registered in different regions of the hippocampus within 5 minutes of the recording. Single unit activity (SUA), n=5, multiple t-tests corrected. **D.** Dentate gyrus LFPs band-power in the delta (0-4 Hz), theta (4-8 Hz), alpha (8-13 Hz), beta (13-30 Hz), and gamma (30-125 Hz) frequency bands. Multiples t-tests corrected. **E.** Population spike (PS) in the hippocampus after different stimulation intensities of the entorhinal cortex (n=5). The right graphs show representative response after 1 mA stimulation in control and dKAT3-ifKO mice. **F.** Quantification of EPSP slope of the stimulus-response curve recorded in dentate gyrus after perforant pathway stimulation for control (in black) and mutant (red) mice. Right: EPSPs evoked potentials. The horizontal scale both in **E** and **F** is 5 ms and the vertical scale 5 mV/ms. Note, that in **F** the stimulation intensity for mutant mice EPSP was 6-fold larger than in controls.

4.1.3. The expression of neuronal-specific genes is greatly impaired when both CBP and p300 is missing

In order to determine the molecular etiology of these phenotypes, we conducted an RNA-seq screen in the hippocampus of dKAT3-ifKOs and control littermates. Differential gene expression profiling revealed 1,955 differentially expressed genes (DEG) in dKAT3-ifKOs, with a clear preponderance both in number and magnitude of gene downregulations (**Figs. 6A**, see the top 100 DEG in the **ANNEX I**). Gene Ontology (GO) enrichment analysis indicates that these downregulations affect multiple neuronal functions (**Fig. 6B**). Hundreds of genes encoding channels and proteins important for synaptic transmission were downregulated in dKAT3-ifKOs (**Figs. 6C-E**), which explains the reduced neuronal firing and lack of electrical responses observed in the dKAT3-ifKO hippocampus (**Figs. 5A-F**). Gene upregulations were much more restricted and included genes related to inflammatory response (**Fig. 6B**) whereas typical genes related with the activation of cell death pathways were not upregulated (**Fig. 6F**). This is consistent with histological analyses (**Fig. 4D**) and clearly indicates a lack of cell death in the hippocampus of the dKAT3-ifKO. Of note, the housekeeping genes were largely unchanged by the genetic manipulation (**Fig. 6C**). Immunodetection experiments for neuronal proteins like CaMKIV, NeuN and hippocalcin (encoded by *Camk4*, *Rbfox3* and *Hpca*, respectively) confirmed the dramatic loss of expression of these neuronal proteins (**Fig. 6G**).

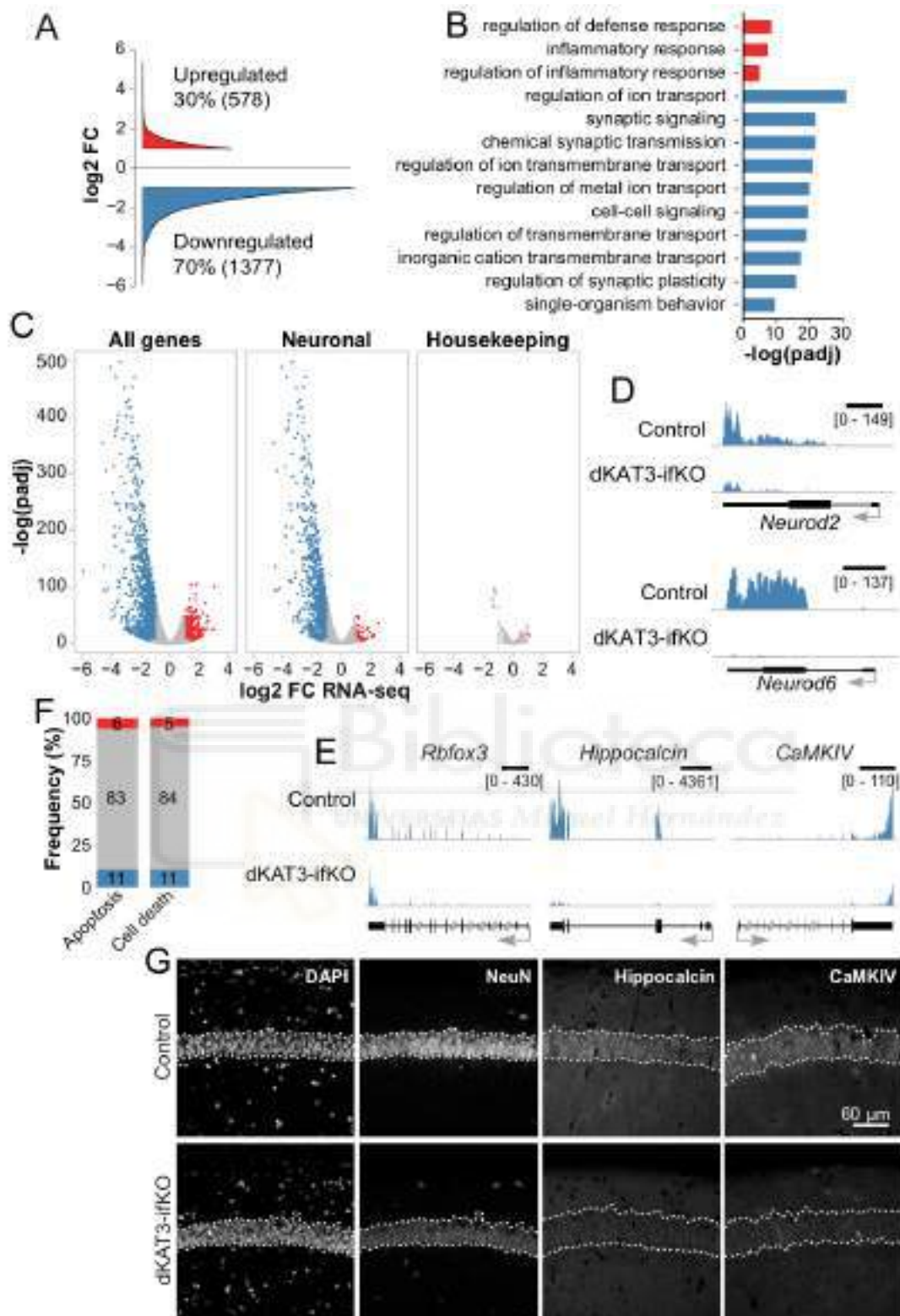


Figure 6. Hippocampal cells lacking KAT3 lose the ability to express neuronal-specific genes. **A.** Cumulative graph showing the log₂ fold-change value of the genes differentially expressed in dKAT3-ifKO. Significantly upregulated genes are presented in red and significantly downregulated genes in blue ($|\log_2FC| \geq 1$). **B.** Ten most significantly enriched categories identified by the Gene Ontology (GO) analysis performed on the genes that were upregulated (red) or downregulated (blue) with a $|\log_2FC| \geq 1$. Upregulated gene analysis resulted in just three categories. **C.** Volcano plot of the RNA-seq analysis. Each of the dots

represents a single gene. Grey dots represent the value for the genes that are not significantly deregulated. Red and blue as in the previous panels. **D.** Examples of RNA-seq profiles for the genes encoding the transcription factors NeuroD2 and NeuroD6. The scale is 1 kb. **E.** Top: Examples of RNA-seq profiles for three other neuronal-specific genes: *Rbfox3* (NeuN), *Hpca* and *Camk4*. The scale is 2 kb. Bottom: Immunohistochemistry for the same neuronal-specific genes in the CA1 region of the control or the dKAT3-ifKO hippocampus. Dashed line indicates the stratum pyramidale position based on the DAPI staining for each section. **F.** Percentage of genes related with apoptosis and cell death (from Gene Ontology) differentially expressed in the dKAT3-ifKO (colors as in **C**). No cell death transcriptional footprint can be observed.

The altered morphology, diminished electrophysiological properties and downregulation of neuronal genes suggest that the excitatory neurons of dKAT3-ifKOs mice rapidly lose their identity after the elimination of both KAT3. To validate this hypothesis, we compared the set of DEGs with transcriptome information for the different cell-types in the adult mouse brain using single-cell RNA-seq (scRNA-seq) data (Zeisel et al. 2015). Our analysis revealed that the genes enriched in CA1 and S1 pyramidal neurons were significantly downregulated in the hippocampus of dKAT3-ifKOs, whereas other cell-type transcriptional programs were unaffected except for a modest increase of microglia-specific genes related to inflammation (**Fig. 7A**). Importantly, although identity loss is often associated with dedifferentiation (the regression to an earlier stage of differentiation), we did not detect the upregulation of stemness genes (Ramalho-Santos et al. 2002, Boquest et al. 2005) (**Fig. 7B**). Furthermore, the comparison of DEGs in the hippocampus of dKAT3-ifKO mice with scRNA-seq data tracking the postnatal development of hippocampal neurons (Habib et al. 2016) revealed no changes in neuronal stem cell (NSC)- and neuroprogenitor (NPC)-specific gene expression. As a matter of fact, the overlap between the downregulated genes in dKAT3-ifKO and genes specific for subsequent differentiation stages grew with the progression of neuronal differentiation and maturation (**Fig. 7C**). The dKAT3 knockout neurons did not transdifferentiate to other cell types either, as we did not detect the expression signature of other brain cell-types (Zeisel et al. 2015) (**Fig. 7A**). Taken together, these results indicate that the dKAT3-KO cells lose their neuronal identity, but do not dedifferentiate or transdifferentiate to other cell types. Instead, the neurons of dKAT3-ifKO seem to be trapped in a non-functional interstate after simultaneous dKAT3 loss.

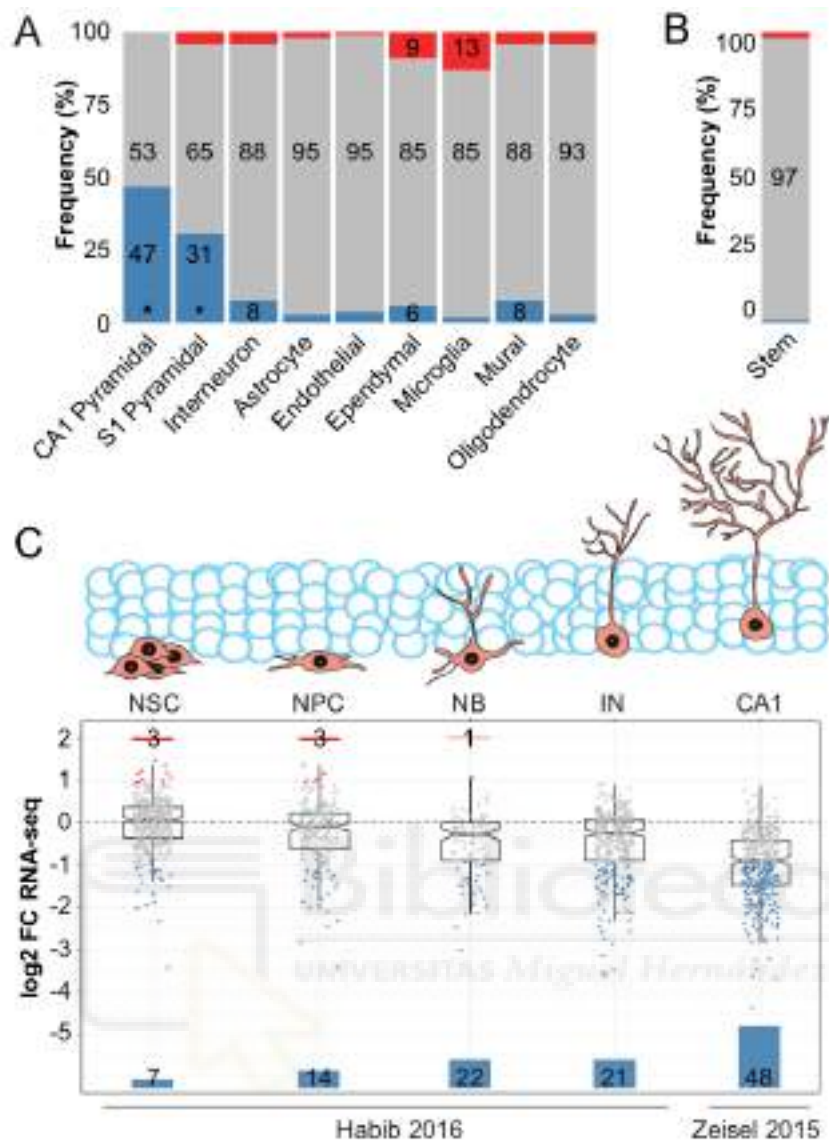


Figure 7. Loss of neuronal transcription program does not cause transdifferentiation or dedifferentiation. **A.** Change in the expression of specific markers of different cell-types (Zeisel et al. 2015). Marked in grey is a subset of unchanged genes, red is upregulated, blue is downregulated in dKAT3-ifKO. The percentage of up- or downregulated genes among all the genes in the category is presented respectively above or below each column. Asterisk indicates a statistically significant difference. **B.** Percentage of stemness markers (Ramalho-Santos et al. 2002) changing in dKAT3-ifKO. **C.** Change in expression of markers of specific neuronal differentiation stages: Neural Stem Cell (NSC), Neural Progenitor Cell (NPC), Neuroblast (NB), Immature Neuron (IN) from Habib et al. 2016 and mature excitatory neuron of CA1 (CA1) from Zeisel et al. 2015. Percentages of up- and downregulated genes are given above and below the dotplots. Colors as in the previous panels. Each of the dots represents a single gene.

To confirm that the loss of identity was a cell autonomous process, we infected the CA1 of the *Crebbp^{ff}::Ep300^{ff}* mice with adeno-associated virus (AAV) expressing cre recombinase under human synapsin promoter (**Fig. 8A**). Immunostainings confirmed the efficient and complete elimination of CBP and p300 in hippocampal

neurons (**Fig. 8B-C**). Consistent with the data in dKAT3-ifKOs the loss of these proteins correlated with a strong downregulation of neuronal markers such as NeuN (**Fig. 8D**). Again, we did not observe an increase in the number of apoptotic nuclei in the stratum pyramidale nor labeling for the cell death marker cleaved Cas3 (**Fig. 8E**). Altogether, the data show that KAT3 proteins play a redundant and cell-autonomous role preserving neuronal identity.

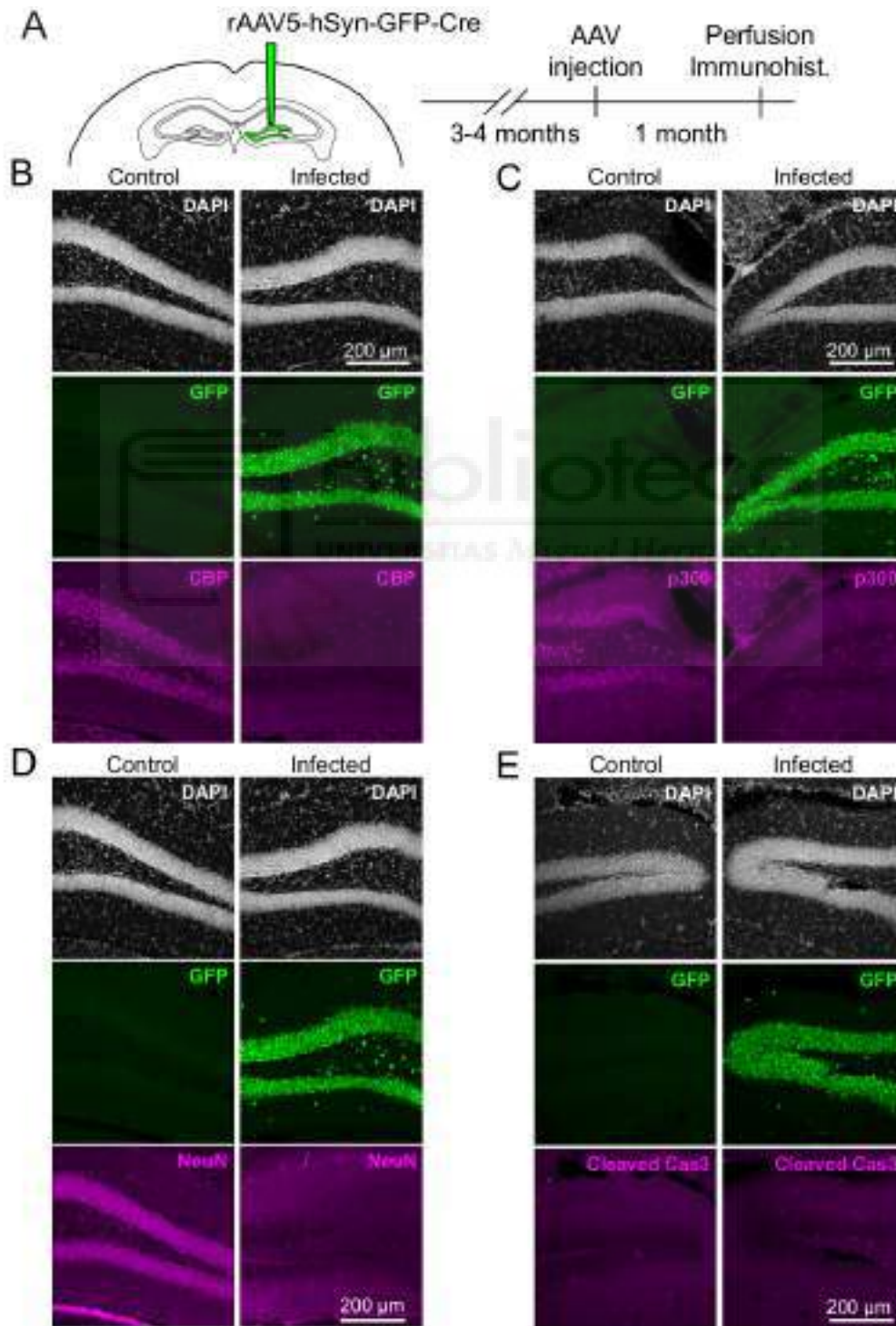


Figure 8. Adeno-associated virus injection demonstrates the cell-autonomous role of KAT3 in preserving neuronal identity. **A.** AAV-Cre-GFP stereotaxic injection experiment. The virus was injected unilaterally into the DG of adult *Crebbp^{ff}::Ep300^{ff}::Cre^{-/-}* mice. **B-E.** GFP expression can be seen only in the infected side. AAV-driven recombination causes loss of CBP (**B**) and p300 (**C**) protein, which goes together with specific loss of NeuN expression (**D**), but without visible apoptosis (**E**).

4.1.4. bHLH transcription factors drive the binding of KAT3 proteins to neuron-specific genes and regulatory regions

We next mapped the occupancy of hippocampal chromatin by CBP and p300 to determine the mechanism by which these epigenetic factors control the expression of neuronal-specific genes. Chromatin immunoprecipitation followed by whole-genome sequencing (ChIP-seq) using antibodies that differentiate between these two highly similar paralog proteins (**Fig. 1D**, **Fig. 9A**) retrieved 37,359 KAT3 peaks in the chromatin of wild type mice (**Fig. 9**). The overlap between CBP and p300 was remarkably high and may reach 100% of the peaks if we correct for the different efficiency of the two antibodies (**Figs. 9B-D**). These profiles demonstrate for the first time in neurons the virtual co-localization of both KAT3 proteins through the whole genome, which suggests a large functional redundancy.

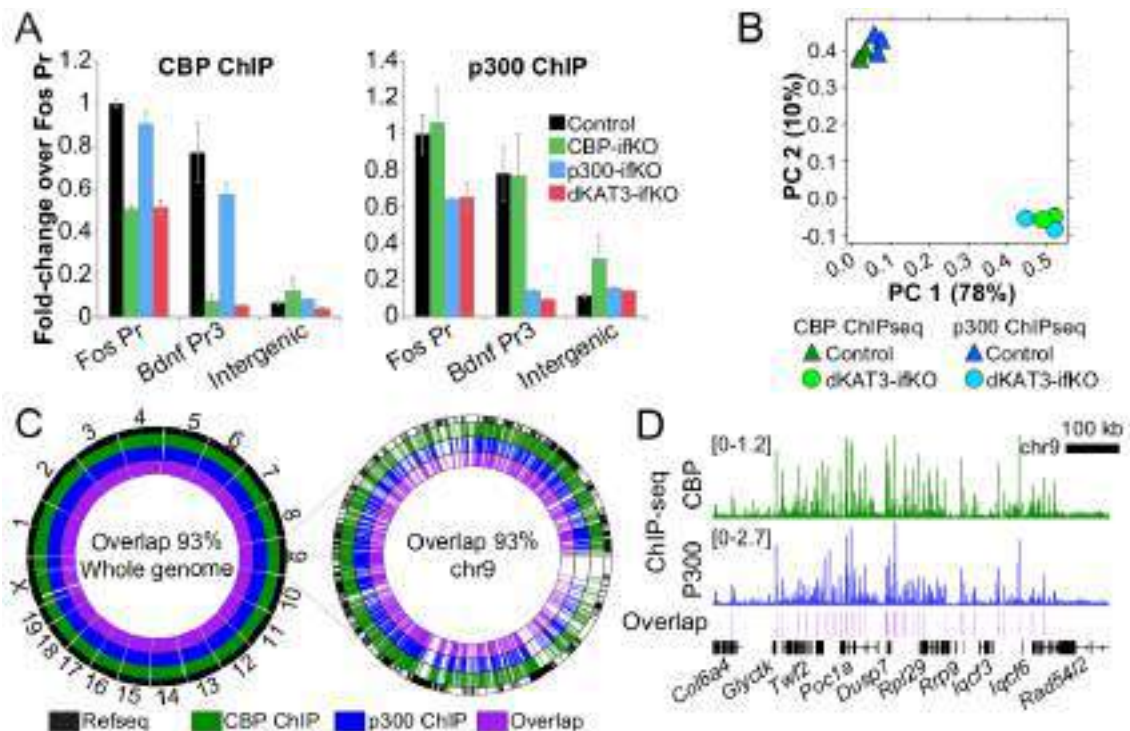


Figure 9. CBP and p300 localize virtually in the same genomic locations **A.** ChIP assays demonstrating the specificity of the CBP and p300 antibodies. **B.** Principal component analysis (PCA) of CBP and p300 ChIP-seqs from control and dKAT3-ifKO. CBP and p300 ChIP-seq samples cluster perfectly depending on the genetic background, indicating that they are nearly identical. **C-D.** Circos plots of entire genome (**C**) and chromosome 9 (**D**) showing ChIP-seq binding regions for CBP, p300, and their overlapping regions in control.

Note that since both proteins are ubiquitously expressed (**Fig. I-10**) but we eliminate them exclusively in excitatory neurons, the signal detected in the hippocampal chromatin of ifKOs (**Fig. 10A**) corresponds to CBP/p300 binding in other cell types. To investigate the changes in chromatin occupancy specifically associated with the loss of both KAT3 proteins in excitatory neurons, we sorted NeuN⁺ hippocampal nuclei from dKAT3-ifKOs and control littermates and prepared assay for transposase-accessibility chromatin (ATAC)-seq libraries (**Fig. 10B**). This technique requires lower input than ChIP-seq and presents a significant overlap with the occupancy profiles for CBP and p300 (**Fig. 10C**). Therefore, combining these two types of profiles allowed us to discriminate between different KAT3 binding peaks: neuronal-specific (present in control ATAC-seq, lost in dKAT3-ifKO), present in multiple hippocampal cell types, including neurons (present in control ATAC-seq, present in dKAT3-ifKO; from now on referred to as “pancellular”) and non-neuronal (not present in control ATAC-seq) (**Figs. 10A and 10D**). The KAT3 signal in the non-neuronal peak locations was very low and these locations were not analyzed further. Pancellular KAT3 peaks (around 4000) were mostly found in the promoter (**Figs. 10E-F**) of annotated genes involved in basic cellular functions, such as RNA processing and metabolism (**Fig. 10G**). In contrast, neuron-specific peaks (around 17,000) primarily locate at introns and intergenic regions with enhancer features, (**Fig. 10E-F**) and were associated almost exclusively with typical neuronal functions (**Fig. 10G**). We used binding and expression target analysis (BETA) to integrate ChIP-seq and RNA-seq data (Wang et al. 2013b) and found that the loss of KAT3 binding is an excellent predictor of transcriptional downregulation ($p = 4.41 \times 10^{-44}$, **Fig. 10H**). Up to 74% of the gene downregulations in ifKO-dKAT3 are linked to the loss of KAT3, while gene upregulations do not show that correlation.

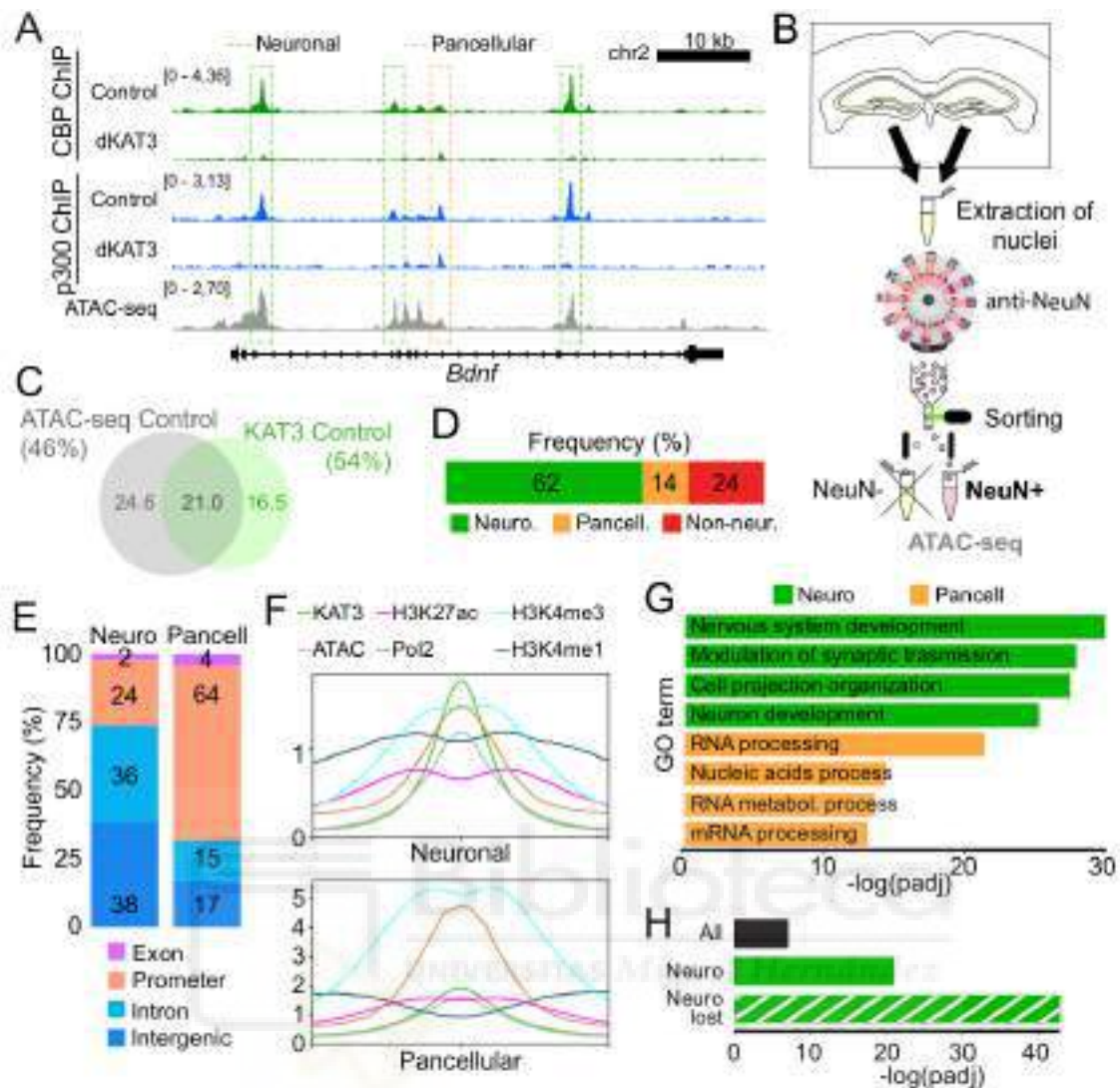


Figure 10. ATAC-seq from isolated neuronal nuclei allows for an isolation of neuronal-specific KAT3 enrichment peaks **A.** FANS-ATAC-seq experiment scheme. **B.** Snapshot for the *Bdnf* locus illustrating the coincidence of CBP and p300 ChIP-seq signal with ATAC-seq signal. KAT3 peaks recognized as neuronal or pancellular are marked with a green or orange dashed line, respectively. **C.** Overlap between ATAC and KAT3 (CBP + P300) peaks. Numbers in thousands. **D.** Classification of KAT3 peaks according to cell specificity. **E.** Distribution of neuronal and pancellular peaks by genomic feature. **F.** Metaplots showing signal of ATAC-seq and multiple protein binding along neuronal and pancellular KAT3 peak locations. **G.** GO enrichment analysis performed on the neuronal (green) and pancellular (yellow) KAT3 peaks. **G.** BETA analysis of all (black), neuronal (green) and neuronal KAT3 peaks lost in dKAT3-ifKO (green, dashed) shows a greatly significant correlation between the last two groups and the change in gene expression in dKAT3-ifKO.

Since KAT3 proteins do not bind to DNA directly, the KAT3 ChIP-seq peaks represent the recruitment of CBP and p300 by other DNA-binding proteins. In order to identify these proteins, we used binding motif analysis using MEME-suite. This technique revealed remarkable differences between pancellular and neuronal-specific

peaks: binding to pancellular locations seem to be primarily driven by transcription factors such as Sp, Egr, Fox, and Sox, all of which had been previously reported to bind to CBP or p300 (Bedford et al. 2010). In contrast, neuronal KAT3 peaks presented a very large enrichment for the DNA binding motif of basic helix-loop-helix (bHLH) proteins (**Fig. 11A-B**). These proteins are often referred to as pro-neural TFs (Bertrand et al. 2002) and many of them are critically involved in neuronal development (e.g., *Ascl1*, *Neurod1-6*, *Neurogenin1-3*, *Atoh1*).

We next compared ATAC-seq accessibility profiles in control and dKAT3-ifKO neuronal nuclei. This screen retrieved 6,598 differentially accessible regions (DARs), most of which (~97%) presented a severe reduction of accessibility in dKAT3-ifKO neurons that coincided with the downregulation of the most proximal gene (**Fig. 11C**). Consistent with the previous analyses, these DARs are located at enhancers (**Fig. 11C**) and enriched for bHLH motifs (**Fig. 11D**), which suggests that the change in accessibility is possibly a consequence of both the elimination of KAT3 and the resulting loss of these TFs themselves. Interestingly, our differential expression analysis retrieved 16 bHLH genes downregulated in the hippocampus of dKAT3-ifKOs (**Fig. 11E**), which could by itself explain the loss of neuron-specific gene expression. Interestingly, the regions of increased accessibility show enrichment for the CTCF motif (**Fig. 11F**), suggesting that the loss of neuronal identity may be associated with changes in chromatin architecture. Overall, these experiments indicate that CBP and p300 interact with bHLH proneural TFs in neuronal-specific genomic locations to maintain neuron-specific transcription.

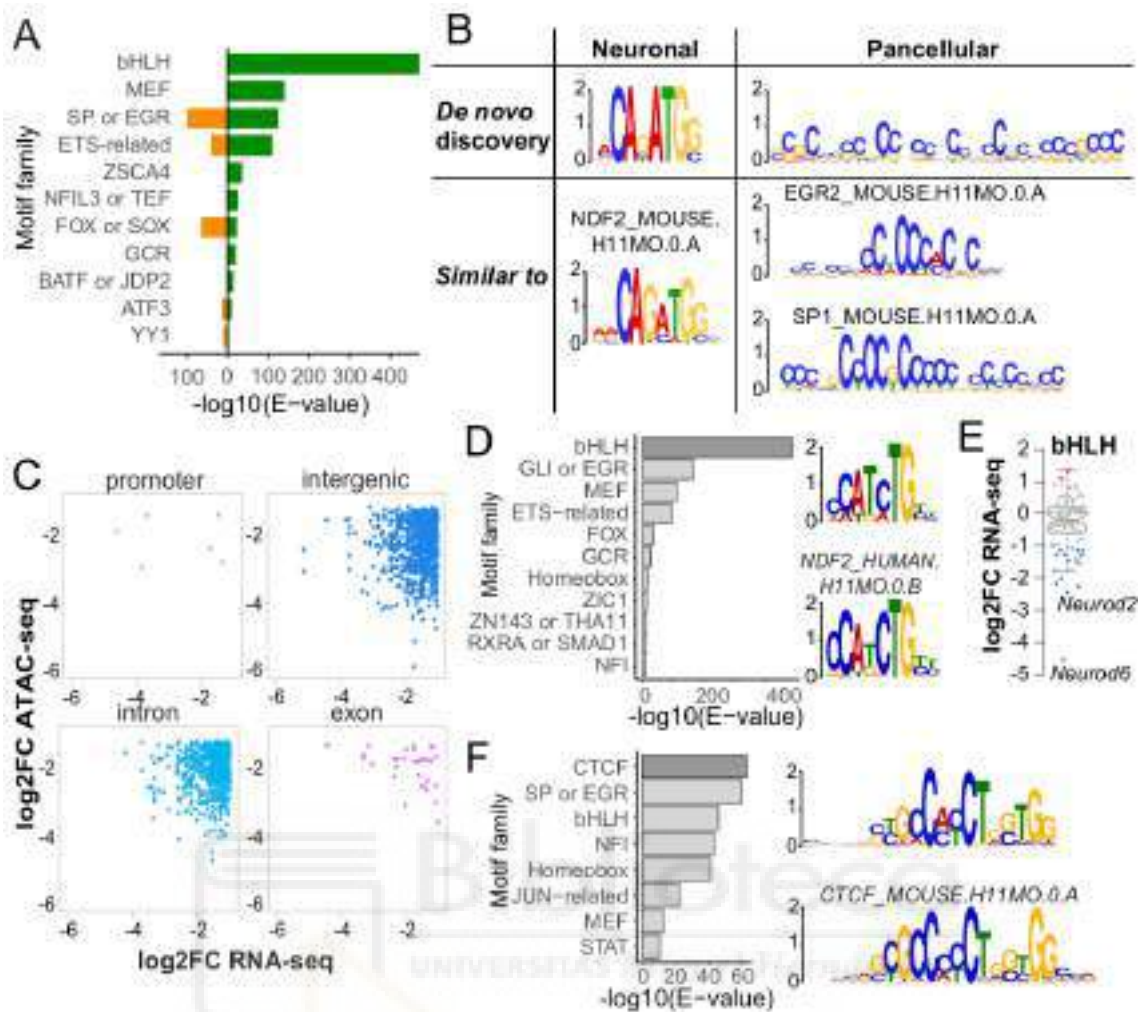


Figure 11. KAT3 in neuron-specific locations regulate predominantly the bHLH (proneural) transcription factors. **A.** Transcription factor binding site (TFBS) motif analysis performed on the neuronal (green) and pancellular (yellow) KAT3 peaks. Each motif family name is a user-curated approximation of the results provided by the MEME-suite algorithm. The scale for all the motif logo representation is in bits. **B.** Neuronal KAT3 peaks reveal a signature indistinguishable from the DNA binding sites of bHLH TFs like Neurod2 (NDF2). The TFBS motif most enriched in the pancellular peaks is relatively ambiguous therefore in the panel A this family is called “SP or EGR”. **C.** Relationship between loss of accessibility and gene expression in dKAT3-ifKO genetic background. Peaks were divided by genomic feature. Both ATAC-seq and RNA-seq signal decrease occur almost exclusively in intergenic and intron locations. **D.** TFBS motif analysis of genes showing lesser accessibility in the dKAT3-ifKO. The comparison between the most enriched *de novo* identified binding motif (up) and the Neurod2 motif (down) is presented on the right panels. **E.** Boxplot showing gene expression of bHLHs. **F.** TFBS motif analysis of genes showing higher accessibility in the dKAT3-ifKO. The comparison between the most enriched *de novo* identified binding motif (up) and the CTCF motif (down) is presented on the right.

4.1.5. H3K27ac levels are strongly decreased in neuro-specific locations and correlate with the downregulation of transcription

The acetylation of histone H3 at lysine 27 (H3K27ac) is a strong candidate to mediate KAT3 role maintaining neuronal identity because this histone PTM is a known target of CBP and p300. Additionally, it is enriched in active enhancers and its level correlates with tissue specification (Nord et al. 2013). Immunological analysis in dKAT3-ifKOs confirmed the variable dependence of the acetylation of different lysine residues on the KAT activity of CBP/p300. H3K27ac shows a dramatic reduction in the chromatin of hippocampal neurons, especially when both CBP and p300 are eliminated (**Fig. 12A**). Therefore, we investigated the genomic distribution of H3K27ac changes in the chromatin of dKAT3-ifKOs and control littermates. We retrieved 46,410 H3K27ac enriched-regions in the hippocampal chromatin of control mice. Consistent with its postulated regulatory role, this histone PTM primarily maps into introns, promoters and intergenic regions (**Fig. 12B**). As expected, H3K27ac-enriched regions showed an extensive overlap with KAT3 peaks, both neuronal and pancellular (**Figs. 12C-D**). ChIP-seq analysis confirmed the dramatic dKAT3-ifKO decrease of H3K27ac observed in the immunostaining. In total, we observed that 35% (16,161 out of 46,410) of all the H3K27ac peaks were strongly reduced in dKAT3-ifKOs (**Figs. 12D-G**), however mainly neuronal KAT3 peaks correlated with H3K27 hypoacetylation (**Fig. 12F**: 58% of neuronal and 3.8% of pancellular H3K27ac-enriched regions were lost in dKAT3-ifKOs). The loss of acetylation is primarily observed in introns and intergenic regions coinciding with the location of neuro-KAT3 peaks in these regions. (**Fig. 12E**). We then used H3K4me1/H3K4me3 presence to identify all enhancer regions in the genome (H3K4me1+/H3K4me3-; profiles available at the Barco's lab). The signal for H3K27ac is particularly decreased in enhancers, while the changes are mild in TSSs (**Fig. 12G**).

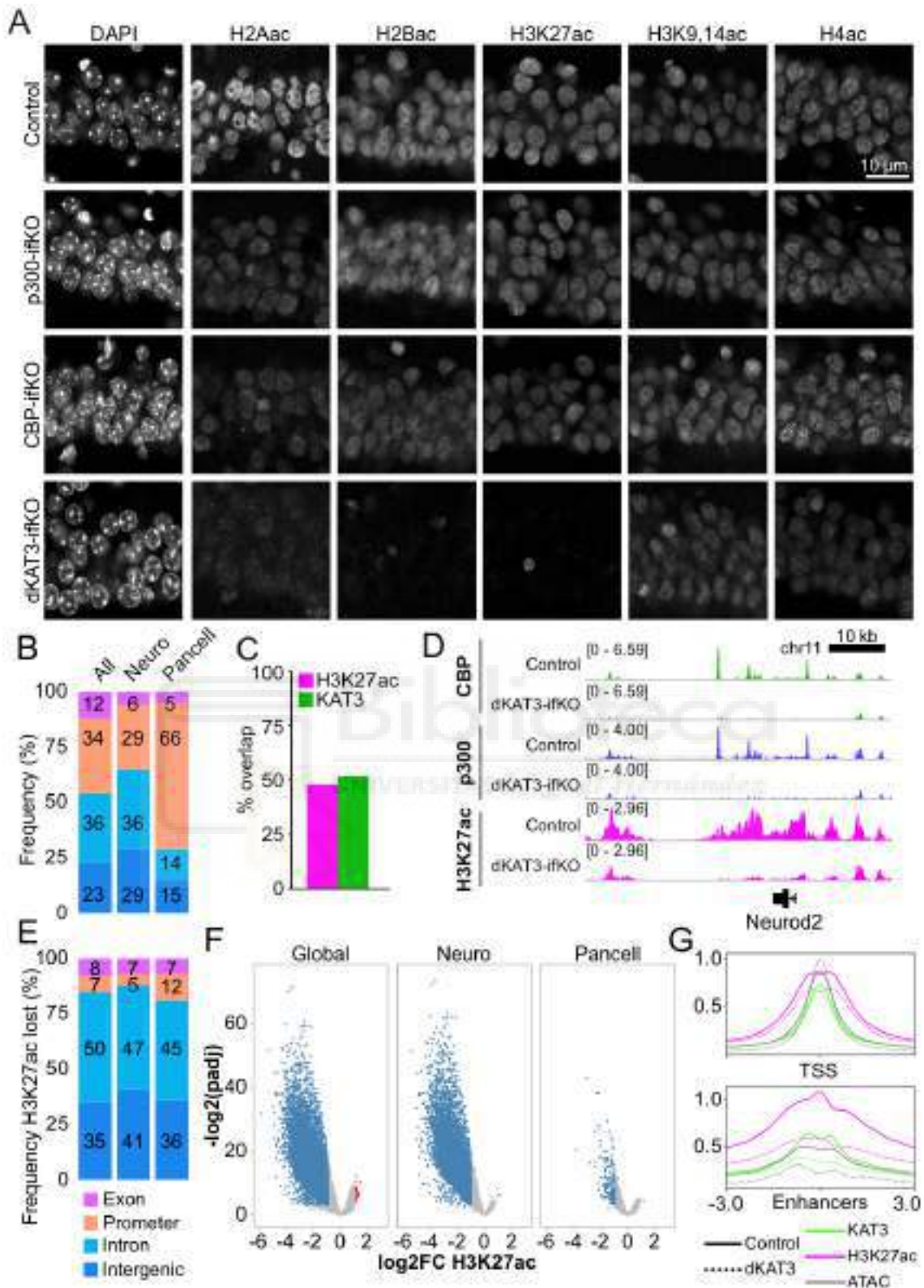


Figure 12. H3K27ac levels are strongly decreased in neuro-specific locations and correlate with the downregulation of transcription. **A.** Immunohistochemistry staining for different histone N-tail acetylations in controls and different KAT3 knockout lines. Images represent the CA1 region of the hippocampus. Significant decrease in signal for H2A and H2B acetylation was observed for all three knockouts. H3K27ac signal was dramatically reduced only as a result of the double KAT3 elimination. **B-C.** In **B**, the graph represents the genomic distribution of

H3K27ac peaks in the control genetic background categorized by genomic features (numbers represent percentages). As the H3K27ac peaks overlap significantly with the KAT3 peaks (shown in **C**, the peaks distribution was plotted for the locations overlapping with neuronal and pancellular KAT3 peaks. **D**. Snapshot of CBP, p300 and H3K27ac ChIP-seq in a representative gene region strongly losing the histone acetylation signal. **E**. Distribution of H3K27Ac lost peaks categorized by genomic feature. Lost H3K27ac peaks overlapping with neuronal (middle graph) and pancellular (right graph) locations are also represented. Colors like in panel **B**. **F**. Changes of H3K27ac in dKAT3-difKO were observed in both neuronal and pancellular peak locations. **G**. Metaplots of ATAC-seq, KAT3 and H3K27ac ChIP-seqs in enhancers and TSSs in controls (full lines) and dKAT3-ifKOs (dashed lines).

We also observe a strong correlation between the loss of H3K27ac and transcript downregulation (78% of the dKAT3-ifKO downregulated genes (1,073 out of 1,376) present a strong reduction of H3K27ac in dKAT3-ifKO). Furthermore, 74% (692 out of 937) of the genes with reduction in acetylation and expression are neuronal genes, which supports a role for H3K27ac in KAT3 regulation of neuronal-specific gene expression. The loss of H3K27ac in neuronal genes primarily occurs in introns and intergenic regions. On the other hand, H3K27ac loss in exons and promoters seems to have lesser influence in expression (**Fig. 13A**). Similarly, the downregulation is stronger in genes that show reduced H3K27ac in enhancers than in TSSs, as identified by H3K4me1/H3K4me3 enrichment (**Fig. 13B**). Then, we used BETA (Wang et al. 2013b) to correlate the presence of these enhancers and gene expression. Again, we found that enhancer regions that lose acetylation are exceptionally highly associated with downregulated genes (p-value = 3.13×10^{-35}) (**Fig. 13C**). The Phenotype analysis performed on the genes related with lost enhancers revealed enrichment in terms related to brain morphology, synaptic transmission, cognition, learning and memory (**Fig. 13D**).

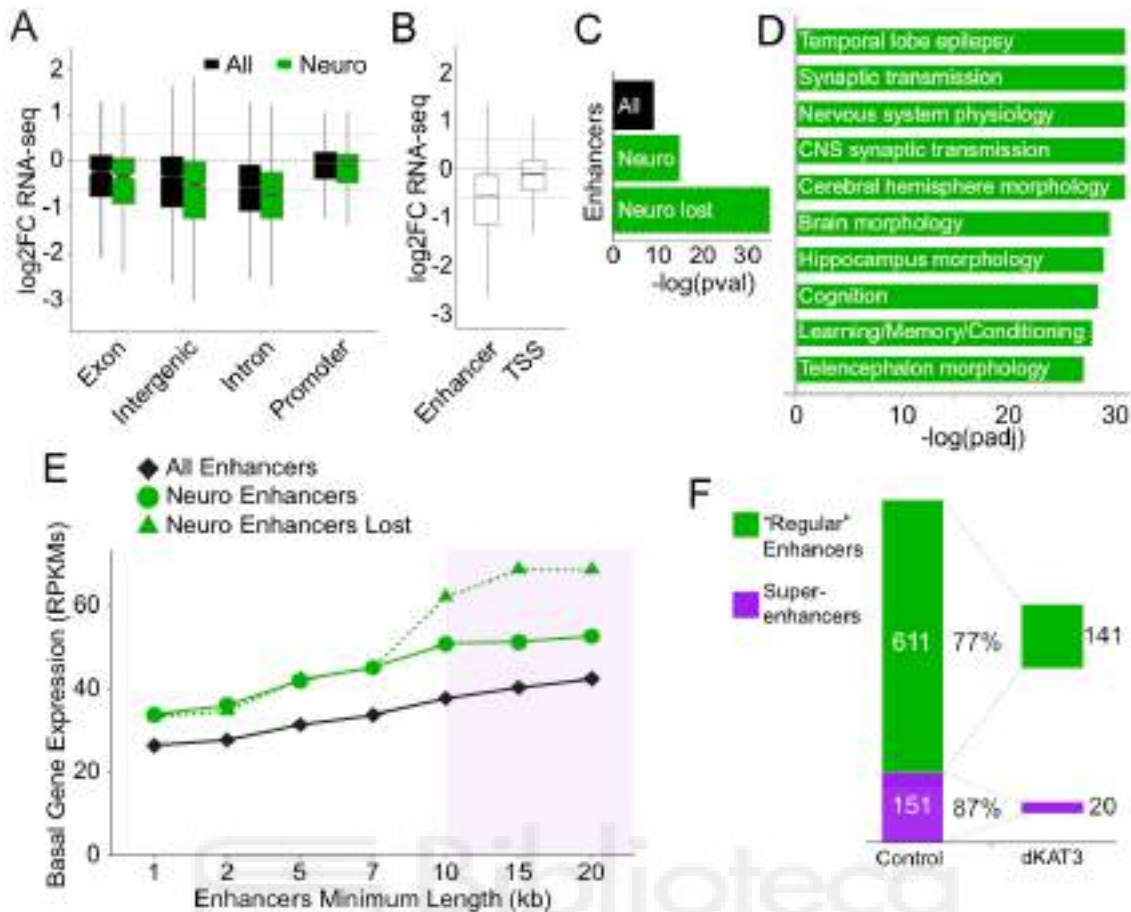


Figure 13. Downregulation of transcription correlates robustly with the loss of acetylation of enhancers and super-enhancers **A.** Changes in the expression of genes in dKAT3-ifKO hippocampus. Genes were separated by the position of the related H3K27ac peak (exon, intergenic, intron, promoter) and represented as well for the neuronal-specific locations. Intergenic and intron neuronal locations show a particular downregulation. **B.** Changes of gene expression in dKAT3-ifKO genetic background for genes associated with H3K27ac in the position of an enhancer or TSS. Similarly to **A**, boxplots suggest a greater downregulation of genes related with H3K27ac in enhancers. **C.** Association of enhancer regions to gene downregulation using BETA algorithm (one-tail Kolmogorov-Smirnov test). Also represented for the neuronal-specific enhancers and neuronal-specific enhancers with a lost H3K27ac. **D.** Top 10 enriched categories of the Phenotype analysis performed for genes harboring neuronal enhancers. **E.** Correlation of enhancer region size to the basal expression of their annotated genes. **F.** Number of downregulated genes that contain H3K27ac signal in the enhancer or super-enhancer in control mice.

As indicated in the introduction, it has been reported that a subset of enhancers called super-enhancers play a particular role in the control of cell identity. The conspicuous features of super-enhancers include the association of highly transcribed genes, broad domains of H3K27ac and a high density of TFBSs (Whyte et al. 2013). To identify putative neural super-enhancers, we generated a list of regions stitching previously identified enhancers that lie closer than 5 kb from each other. Highly

expressed genes that display strong downregulation in dKAT3-ifKOs were often associated with large enhancers (> 10 kb, i.e., super-enhancers) (**Fig. 13E**). From the 1,300 downregulated genes, we identified 611 associated with neuronal enhancers (i.e. presenting neuronal KAT3 peak) and 151 with neuronal super-enhancers, of which 77% and 87% were hypoacetylated in dKAT3-ifKOs, respectively (**Fig. 13F**). Amongst these super-enhancers harboring downregulated genes that lose acetylation, one can find *bona fide* neural regulators like *Camk2a*, *Arc*, *Egr1*, *Hpca*, *Nptx1*, *Nr4a1*, *Nrgn*, etc. The bHLH factors Neurod2 and Neurod6 also belong to that group (**Fig. 12D**). These findings are consistent with the abundant literature supporting a role for enhancers in cell-type specific gene expression (Bulger and Groudine 2010, Thakurela et al. 2015, Catarino and Stark 2018).

4.1.6. Targeted histone acetylation increases the expression of the associated genes

We turned to primary neuronal cultures (PNCs) to tackle the importance of bHLH TF binding and H3K27 acetylation in the loss of neuronal-specific gene expression in neurons lacking both KAT3. In agreement with our experiments in dKAT3-ifKOs, KAT3-depleted PNCs produced from *Crebbp^{ff}::Ep300^{ff}* embryos and infected with a Cre-recombinase expressing lentivirus (**Figs. 14A-B**) show impaired neuronal morphology in the absence of apparent neuronal death (**Fig. 14C**). The dKAT3-KO PNCs, like the ifKO mice, also show a severe downregulation of neuron-specific transcripts (**Fig. 14D**) and proteins (**Fig. 14E**), and H3K27ac levels (**Fig. 14F**). This system thereby allows a thorough investigation of underlying molecular mechanisms through rescue experiments.

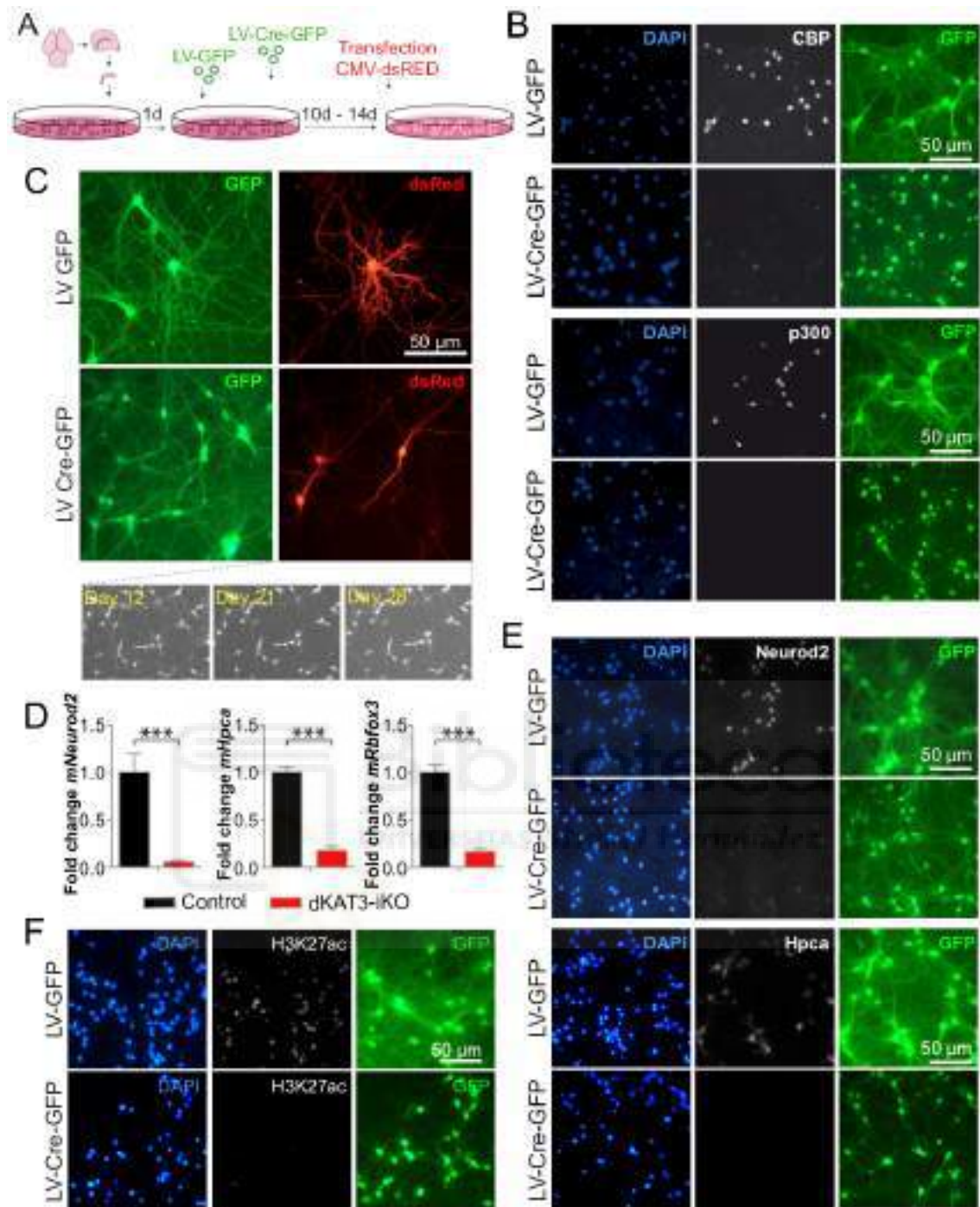


Figure 14. Hippocampal cell culture model recapitulates the results of induced forebrain KAT3 knockout. **A.** Design of the primary hippocampal neuron culture experiments. In this case, specifically the morphology analysis. **B.** Immunocytochemistry staining images showing a robust elimination of CBP and p300 in the GFP-positive neurons of the dKAT3-cKO cultures. **C.** Morphology is visibly impaired in the dKAT3-cKO neurons. Lower panels show no visible cell loss even after 28 days of culture. **D-E.** The neuronal markers are downregulated in the dKAT3-cKO cultures as shown by a qPCR (**D**) and immunocytochemistry (**E**). T-tests. **F.** Also as in the mouse model, dKAT3-cKO neurons have a strongly decreased H3K27ac level.

We first examined the consequences of overexpressing *Neurod2*, a bHLH TF highly expressed in mature excitatory neurons and strongly downregulated in the hippocampus of dKAT3-ifKO, in dKAT3-KO hippocampal cultures (**Fig. 6D**, **ANNEX I** and **Fig. 14E**). The overexpression of this TF alone can differentiate a pluripotent cells to neurons (Farah et al. 2000, Sugimoto et al. 2009, Matsushita et al. 2017) and combined with another specific TF can reprogram fibroblasts to induced neurons (Yang et al. 2011, Tsunemoto et al. 2018). Importantly, *Neurod2* regulates its own expression and fits with the features of a terminal selector TF maintaining neuronal identity (Deneris and Hobert 2014). Moreover, the profile of *Neurod2* binding in cortical chromatin (Bayam et al. 2015) show a large overlap with DARs in dKAT3-ifKOs (**Fig. 15A**). However, we found that h*Neurod2* overexpression did not increase the expression of any of the examined downstream neuronal-specific genes (**Fig. 15B**). This indicates that bHLH TF binding by itself is not enough to re-establish neuronal-specific transcription in dKAT3-KO cells.

Next, we examined whether increasing H3K27 acetylation was sufficient to rescue the transcriptional deficit. To this end, we took advantage of recently developed tools for epi-editing based on the expression of an inactive Cas9 enzyme (dCas9) fused to the KAT domain of p300 (Hilton et al. 2015). This system allows targeting specific genomic regions for p300-dependent acetylation using adequate guide RNAs (gRNA). We selected the *Neurod2* gene as a target, because this gene is both severely downregulated and deacetylated (H3K27ac) in the dKAT3-ifKO. gRNAs were designed to drive the binding of dCas9-p300 to the most proximal KAT3 peak of *Neurod2* (**Fig. 15A left**). As expected, the overexpression of the *Neurod2* (ND2) gRNA alone did not cause any change in NeuroD2 protein levels (**Fig. 15C**). Meanwhile, the co-transfection of plasmids carrying dCas9-p300 and the *Neurod2* gRNA caused a significant upregulation of NeuroD2 in around 60% of transfected neurons (**Fig. 15C**), while the use of an off-target gRNA (targeting *Hpca*) caused an upregulation of NeuroD2 in less than 20% of cells (**Fig. 15C**). The fact that the dCas9-based epi-editing system affects off-target locations more than regular Cas9 has been previously observed by other groups and seems to be a normal caveat of these tools (Galonska et al. 2018).

Next, we decided to investigate if the hyperacetylation alone is enough to induce the expression of a gene associated with a missing transcription factor binding. To this end, we chose the *Hpca* gene, whose most proximal upstream enhancer shows a dramatic loss of H3K27ac and a missing ATAC-seq peak in the position of the

NeuroD2 binding (**Fig. 15A right**). Interestingly, the use of dCas9-p300 targeting this location was not enough to rescue the expression of the Hippocalcin protein (**Fig. 15E**) and the preliminary data suggest that neither was the use of the NeuroD2 gRNA (data not shown). This suggests a crucial cooperation between the transcription factors and histone acetylation in driving the gene expression. Overall, these experiments demonstrate that the local increase on acetylation restore locus functionality although it requires the presence of accessible chromatin.



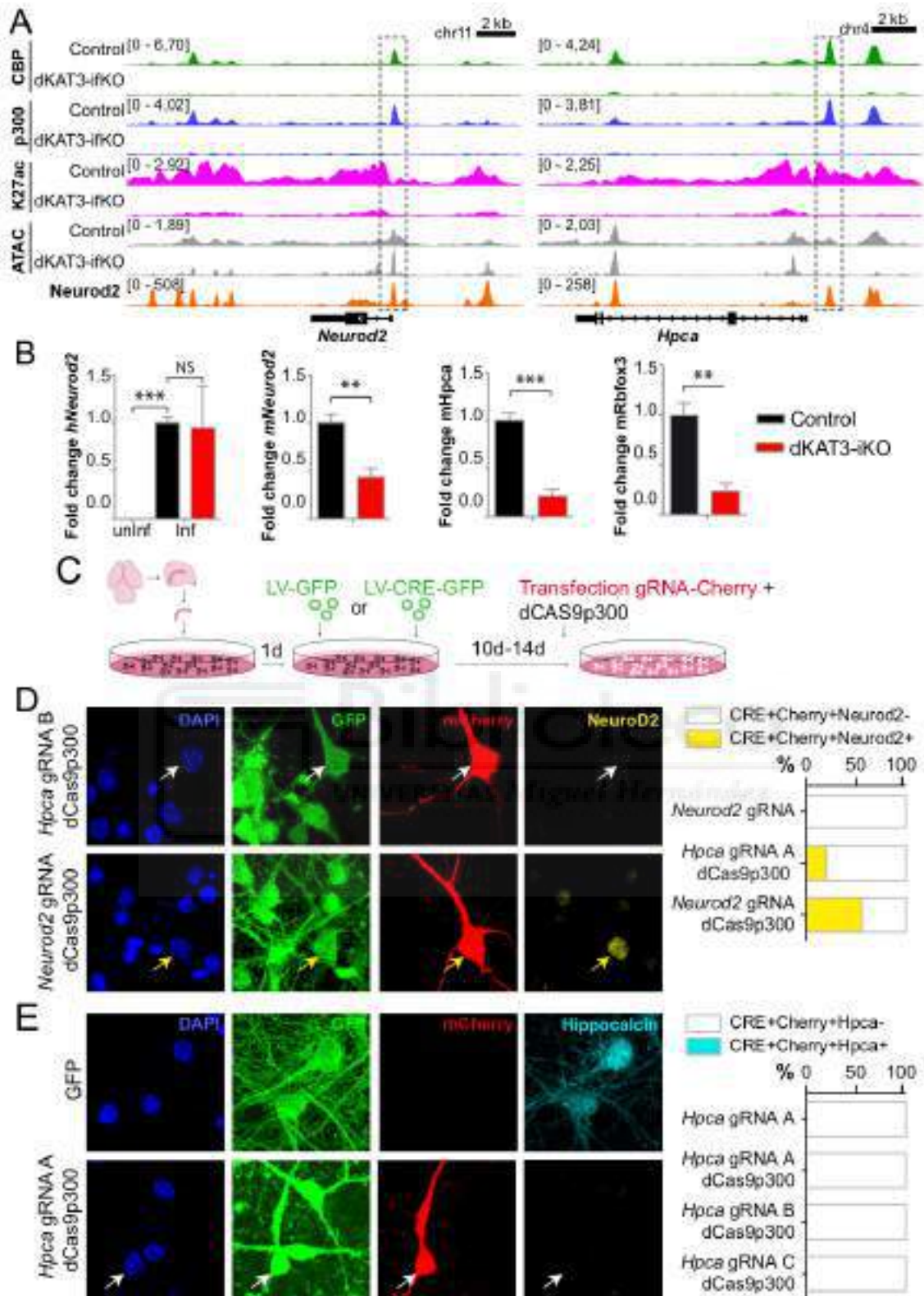
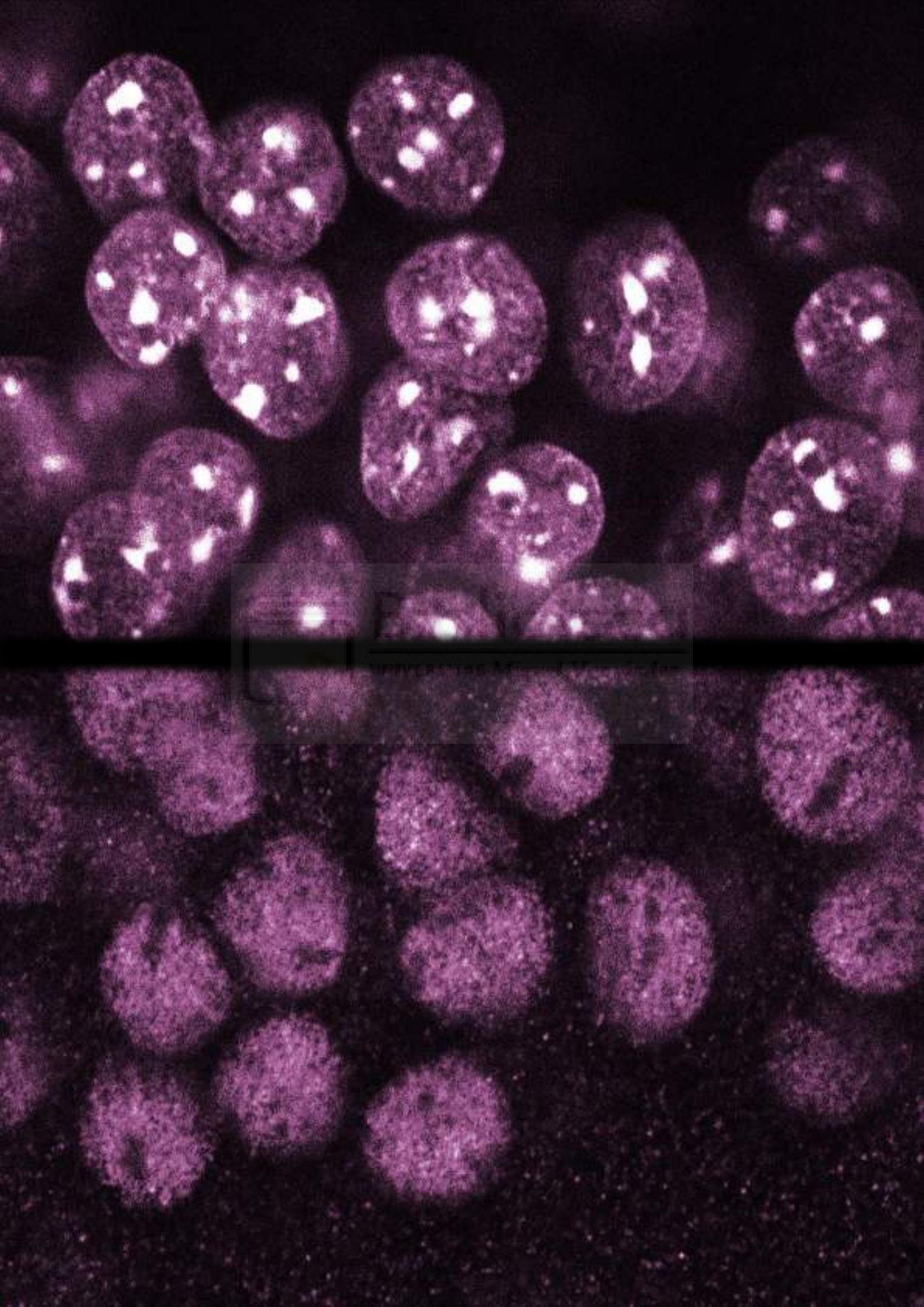


Figure 15. Targeted histone acetylation rescues the neuronal gene expression when transcription factor binding is present **A.** IGV snapshots of the genes targeted by the dCas9-p300 in our rescue experiments. Specific targeted regions are marked with the black dashed line. In the bottom profile (orange) you can see a *Neurod2* ChIP-seq from E15 cortex (Bayam et al. 2015). **B.** The overexpression of human *NEUROD2* (*hNeurod2*) is not sufficient to rescue the expression of neuronal genes in dKAT3-IFKO cultures. No endogenous neuronal marker

(*mNeurod2* - mouse *Neurod2*, *mHpc* - mouse *hippocalcin*, *mRbfox3* - mouse *Rbfox3*) expression was rescued, while the ectopic expression of *hNeurod2* is clearly detectable. Plots represent qPCR data. **C.** Scheme representing the design of the CRISPR rescue experiments. **D.** Co-transfection of dCas9-p300 construct and a vector carrying mCherry and *Neurod2* promoter-targeting gRNA (see panel **A** left) rescues the *Neurod2* expression (arrowhead) in a bigger percentage of cells than the control gRNA (*Hpc* targeting). Quantifications of the gRNA⁺/NeuroD2⁺ cells on the right. n=3 **E.** Co-transfection of dCas9-p300 with different gRNAs targeting the most proximal *Hpc* upstream regulatory locus (panel **A** right) does not rescue the Hippocalcin protein expression. It is likely because this region misses a TF binding (see ATAC-seq for dKAT3-ifKO in the panel **A**). n=3



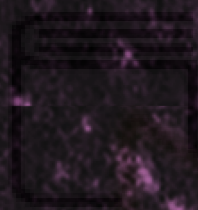




Results

Chapter II

Proper levels of CBP, but not p300, are essential for the establishment of experience-induced gene programs and neuroadaptation in adult excitatory neurons



Biblioteca
Universitat de València



The work described in the following Chapter is still in progress. The presented work was performed in collaboration with several members of the laboratory of Prof. Angel Barco under the co-supervision of Dr. Jose Pascual López-Atalaya.

Dr. Rafael Muñoz Viana and Dr. Jose Pascual López-Atalaya designed and performed the bioinformatic analysis of the sequencing data. Alejandro Medrano-Fernandez provided the behavioral data.

I designed and performed the *in vivo* molecular, biochemical and histological experiments and their statistical analysis. I have also performed the kindling experiment, and collaborated in the design of most bioinformatic analyses. The project as a whole was designed and interpreted by me, Prof. Angel Barco and Dr. Jose Pascual López-Atalaya, with important input from other coauthors of the work.

I would also like to thank Roman Olivares for the supervision of the mouse colony and technical support.





4.2.1. Excitatory neuron-specific elimination of CBP, but not p300, in the adult forebrain causes mild cognitive impairment

In **Chapter I**, I reported that the elimination of p300 or CBP in excitatory adult neurons does not decrease cell survival nor causes apparent neurological phenotypes (**Fig. 1**). However, previous literature suggests that KAT3 proteins might be necessary for correct memory formation (see **Introduction 1.3.4.2**). Therefore, I assessed here in greater detail the cognitive phenotype of our single KAT3 knockout mice. Both CBP-ifKOs and p300-ifKOs are apparently indistinguishable from their control littermates (SHIRPA, **Fig. 1A**). To investigate their phenotype in greater detail, we performed a battery of tests assessing multiple behavioral features like locomotion in an open field (OF task), anxiety (Elevated Plus Maze, EPM), depressive-like behaviors (Forced Swim Test, Porsolt), species-typical behaviors (Marble Burying, MB), object memory (Novel Object Recognition, NOR), spatial navigation (Morris water maze, MWM task) and fear memory (Fear Conditioning, FC). We kept the ifKO mice together with their CreERT2⁻ littermates until they were 3-4 months old. Then, TMX was administered and one month later the animals were subjected to a battery of behavioral tests. CBP-ifKO mice, did not show any differences in the OF, EPM or Porsolt tests (**Figs. 16B-D**), but we did observe a significantly less marbles buried by the CBP-ifKO mice in comparison to their wild-type littermates (**Fig. 16E**). Interestingly, loss of CBP in the excitatory forebrain neurons caused a strong impairment in object recognition memory (**Fig. 16F**), while leaving the context and cued fear memory completely unaffected (**Fig. 16G**). This result fully confirms the observations of the previous study from our lab, where CBP was eliminated in the CaMKIIa-positive neurons in a non-inducible manner (Valor et al. 2011) and suggest that CBP is necessary in adult excitatory neurons for optimal performance in some behavioral tasks. In contrast, the p300-ifKO mice did not show any significant difference in locomotion, anxiety, depression or species-typical behaviors (**Figs. 16H-J**) or memory tasks (**Figs. 16K-M**).

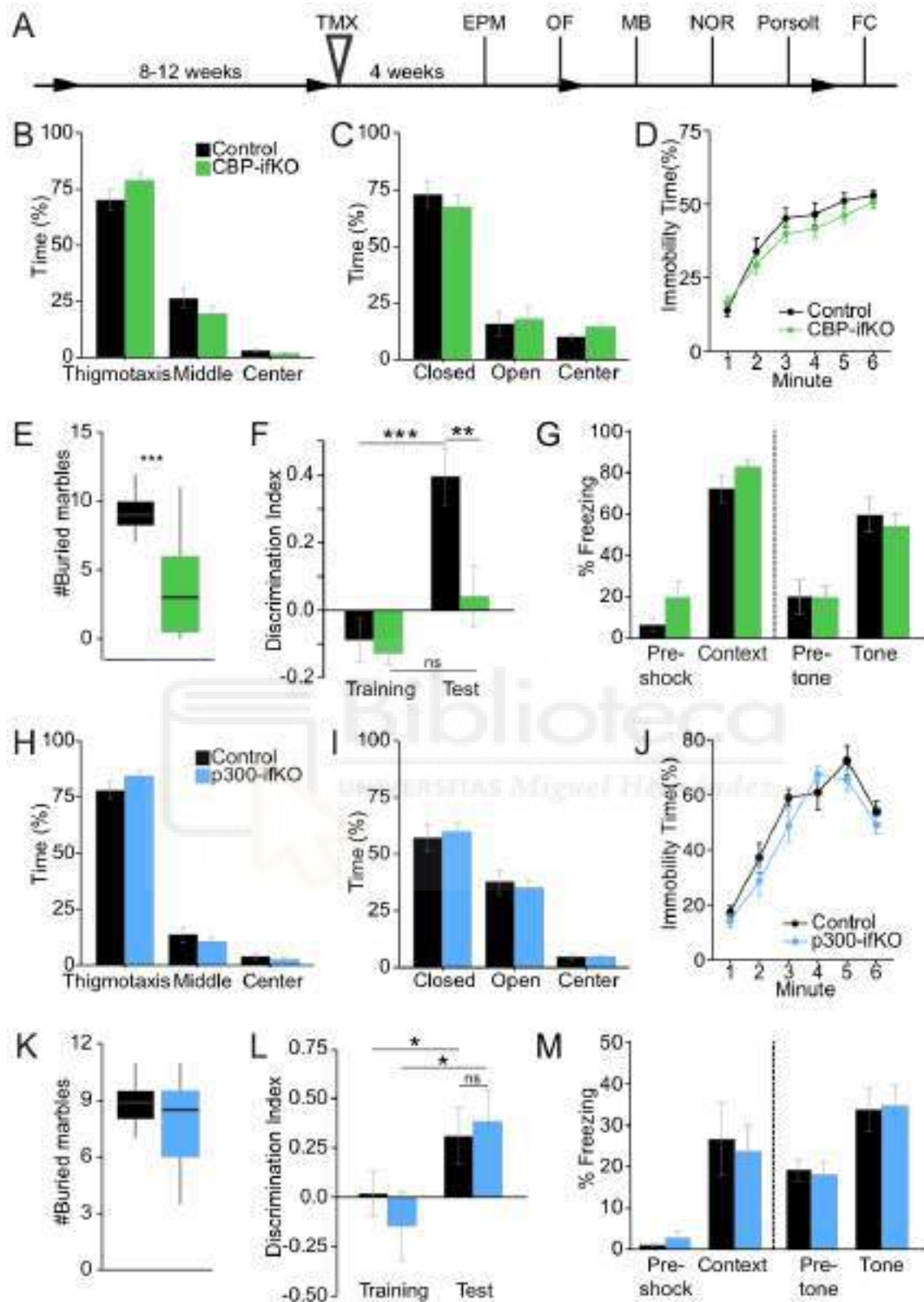


Figure 16. CBP-ifKO mice display a specific behavioral impairment, but the p300-ifKO mice appear to be completely normal A. Scheme representing the experimental design of the behavioral screening including open-field (B, H), elevated-plus maze (C, I), Porsolt forced swimming (D, J), marble burying (E, K), novel object recognition (F, L) and fear conditioning (G, M). Panels H-M show a completely normal behavior of the p300-ifKO mice (controls n=10 and ifKOs n=12). Meanwhile CBP-ifKOs (controls n=13 and ifKOs n=17) display normal

results in the open-field, elevated-plus maze and Porsolt, but impaired marble burying (**E**, hippocampal-dependent species-typical behavior) and novel object recognition (**F**, object memory). Interestingly, at the same time the fear memory results were completely normal (**G**). Statistical tests: t-test: **E** and **K**; two-way ANOVA: **A-D**, **F-J**, **L-M**.

4.2.2. The loss of CBP in the forebrain excitatory neurons causes a moderate transcriptional impairment. The loss of p300 has virtually no effect on transcription.

Next, we were interested in examining whether the single loss of p300 or CBP had any consequences in gene expression as we saw in the case of double KAT3 deletion (**Fig. 6**). Following the same approach as in the case of dKAT3-ifKO, we performed an RNA-seq analysis of the hippocampal transcriptome 1 month after the TMX administration. we observed 253 downregulated and 42 significantly upregulated genes (adjusted p-val >0.05, **Fig. 17A**) in the hippocampus of CBP-ifKOs. These changes were however relatively weak, as only 28 downregulated and 4 upregulated genes passed the low stringency cutoff of $\log_2FC \geq 0.6$ (50% of change). This number proved to be too small to identify any enriched categories in the GO analysis, therefore we have chosen to use a lower cutoff and evaluate the genes changing with $\log_2FC \geq 0.32$ (25% of change). While there were no GO results for the upregulated genes (38), the downregulated genes (200) showed a strong enrichment of chemical synaptic transmission, learning/ memory and neuronal differentiation (**Fig. 17B**). This group of genes included well-known memory-related proteins like *Bdnf*, *Htr2a*, *Calb2*, or *CaMKV*, which suggests that these gene expression changes might explain the changes in the cognitive traits we observed in CBP-ifKOs. To our great surprise, though consistent with the behavioral data, lack of p300 in the mature hippocampal neurons did not cause any significant gene expression changes (adjusted p-val >0.05, **Fig. 17C**). The only two significantly upregulated genes, *Arsi* and *Esr1*, are derived from the genetic approach used to generate ifKOs (*Arsi* is located next to the *CaMKIIa* promoter in the BAC used to create the Cre-driver strain, whereas the upregulation of *Esr1* is limited to the exons fused to the *Cre* recombinase gene to encode the CreERT2 chimeric protein). As the GO footprint of the CBP-ifKO DEG is somehow reminiscent of the dKAT3-ifKOs (**Fig. 6B**), we decided to compare the DEG identified for both genotypes. As expected, this comparison showed that virtually all (188/200, 94%) the genes downregulated in CBP-ifKO hippocampus were also downregulated in the

dKAT3-ifKO (**Fig. 17D**). The same comparison between the upregulated genes in both genotypes showed almost half (18/38, 47.4%) of the genes upregulated in CBP-ifKO to be found among genes upregulated in the dKAT3-ifKO (**Fig. 17E**). Genes both specifically down- or up-regulated in the CBP-ifKO mice (12/200 and 20/38 respectively) formed a very heterogenous group without any specific GO trace. Thus, while the loss of p300 does not cause practically any transcriptional alteration in the mouse hippocampus, the loss of CBP alone causes a modest but significant change in plasticity-related gene expression. Interestingly, while for most of the neuronal genes affected in dKAT3-ifKOs p300 alone is enough to maintain the correct transcription (3313 down. and 2734 up in dKAT3-ifKOs), this new screen identifies a specific subset of genes that seem to unconditionally require CBP (188 down. and 18 up in CBP-ifKOs). These transcripts are predominantly downregulated and show a behavior-related footprint.

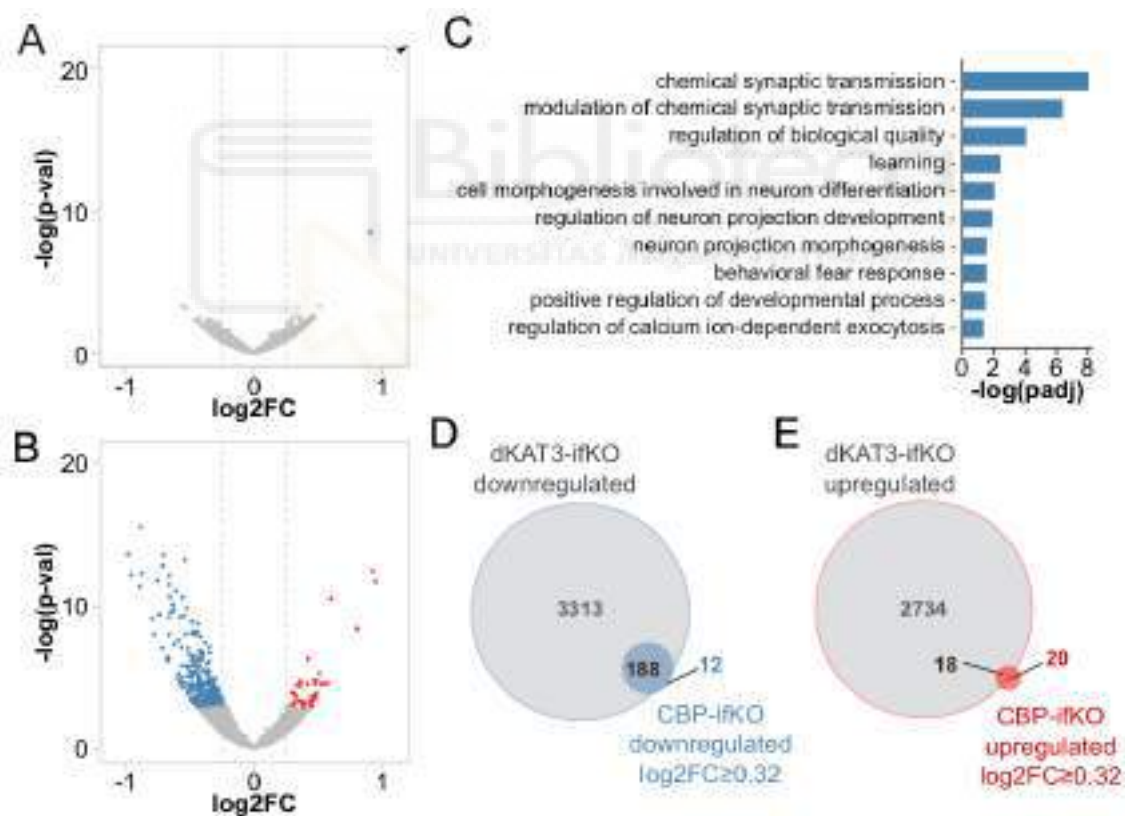


Figure 17. While the p300-ifKO mice show almost no transcriptional changes, the CBP-ifKO display a specific gene expression disfunction with a neuronal footprint **A-B**. Volcano plots displaying an RNA-seq differential expression in the p300-ifKO (**A**) and CBP-ifKO (**B**) hippocampal extract. All the significantly downregulated genes are marked in blue and all the significantly upregulated genes in red ($p\text{-adj}<0.05$, $\log_2FC\geq 0.32$). The arrowhead in **A** indicates the position of *Arsi*, which is out of scale. **C**. GO analysis of the genes downregulated in CBP-ifKOs. **D**. Comparison between the downregulated genes in dKAT3-ifKOs ($p\text{-adj}<0.05$, no cutoff) and CBP-ifKOs shows that all the genes downregulated

in CBP-ifKOs are also affected in dKAT3-ifKOs. **E.** Comparison between the upregulated genes in dKAT3-ifKO ($p\text{-adj}<0.05$, no cutoff) and CBP-ifKO show a significant, but not complete overlap.

4.2.3. Transcriptional changes in CBP can be linked to histone acetylation deficits

We next investigated if changes in lysine acetylation can be associated with the changes in histone acetylation. As it can be observed in the **Fig. 12A**, both CBP and p300 elimination seems to decrease the levels of H2A histone N-terminal tail acetylation (H2A-ac). CBP elimination resulted in an additional decrease of H2B N-tail acetylation (H2B-ac) and H3K27ac, but apparently not of H3K9,14ac or H4 histone N-tail (H4-ac). In order to confirm our initial observations in a semi-quantitative way, we performed Western-blotting on CBP-ifKO hippocampal protein extract (**Fig. 18A**). This experiment confirmed the previous results, pointing to H2B-ac and H3K27ac a prominent substrate of CBP. These observations are also fully consistent with the recently published CBP/p300-dependent acetylome, obtained through quantitative mass spectrometry (Weinert et al. 2018). In this *in vitro* study, H3K27ac and all the H2B N-terminal residues are among the sites most tightly regulated by KAT3. To see if the acetylation of any specific H2B N-tail residue is particularly sensitive to CBP elimination *in-vivo*, we performed Western-blotting (**Fig. 18B**) and IHC (**Fig. 18C**) against 4 different H2B N-terminal lysine residues (K5, K12, K15 and K20, see also **Fig. I-2**). In agreement with the published proteomic data, all 4 residues showed a significant decrease in acetylation level, as visualized by the Western-blot (**Fig. 18B**). Although, IHC was not sensitive enough to robustly show a change in acetylation level, a slight decrease in signal of every H2B target could be observed in the CBP-ifKO neuronal nuclei (**Fig. 18C**). Therefore, the acetylation of the N-tail of H2B is uniquely regulated by KAT3 *in vivo*.

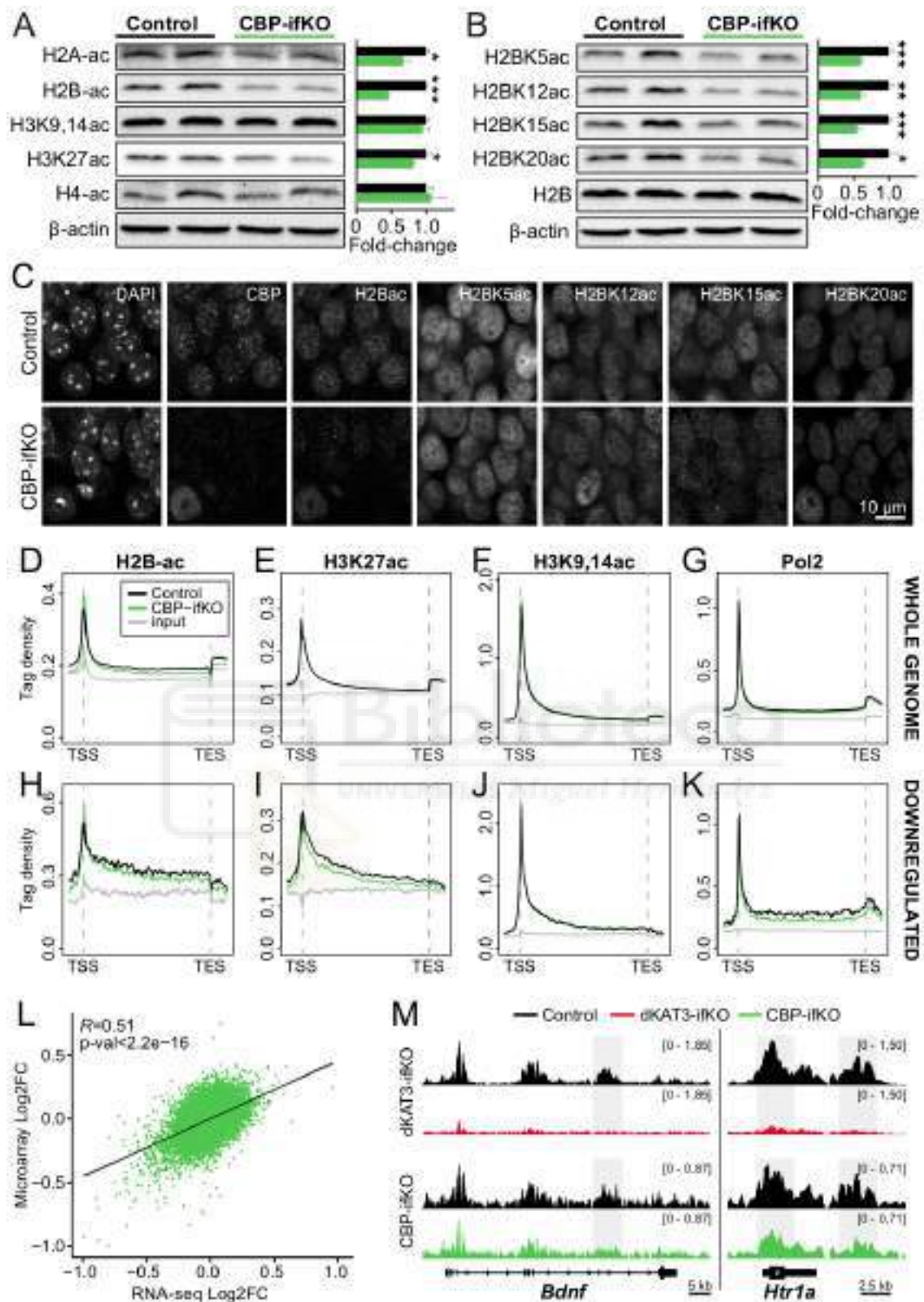


Figure 18. CBP-ifKO mice show a very strongly decreased histone acetylation. **A.** Western-blotting against different core histone acetylations made on the CBP-ifKO hippocampal protein extract. Quantification of the signal on the right. A significant decrease in the H2A-ac, H2B-ac and H3K27ac could be observed. H3K9,14ac and H4-ac were unaffected by the elimination of CBP. T-tests. **B.** Acetylation of different H2B N-tail lysine residues. All the investigated acetylations were significantly decreased in the WB. **C.** Immunohistochemistry for acetylation

of different H2B N-tail lysine residues. **D-G.** Genome-wide metagene signal representation of ChIP-seq against H2B-ac (**D**), H3K27ac (**E**), H3K9,14ac (**F**) and Pol2 (**G**). Notice no change in signal on the genome scale for **E-G** and a paradoxical H2B-ac increase in the **D**. This was however an artifact of the NGS, as the ChIP-assay on the same chromatin extract (**H**) show a significant decrease in the CBP-ifKO in all the regions. **I-K.** Metagene of the ChIP-seq matching the **E-G**, however with only the gene regions downregulated in the CBP-ifKO plotted (expression microarray). **L.** Correlation between microarray and RNA-seq expression data. **M.** IGV snapshots of the H3K27ac ChIP-seq in dKAT3-ifKO and CBP-ifKO. Two genes downregulated in CBP-ifKO are represented. Different scales between the CBP- and dKAT3-ifKO experiments is a result of a batch effect.

In order to link the deficient lysine acetylation with transcriptional changes, we extracted hippocampal chromatin from CBP-ifKO mice and performed ChIP-seq against H2B-ac and H3K27ac. The same method was used in parallel to validate the driver of transcription Pol2 and the bi-acetylation of H3K9 and K14, which is not targeted by KAT3 (**Figs. 12, 18A** and Weinert et al. 2018). H2B-ac ChIP-seq revealed a prominent reduction in acetylation along the entire genome (**Fig. 18D**). Note that this global decrease initially manifested as a paradoxical increase in promoter regions consistent with previous reports of HPTM changes occurring on the genome-scale (Bonhoure et al. 2014, Orlando et al. 2014, Egan et al. 2016, Guertin et al. 2018). The other three ChIP-seq experiments revealed milder differences, either did not show any change (H3K27ac and H3K9,14ac, **Figs. 18E and 18F**, respectively) or showed a negligible decrease when analyzed genome-wide (Pol2, **Fig. 18G**).

With the purpose of identifying the correlation between histone acetylation and transcription, we plotted the H2Bac, H3K27ac, H3K9,14 and Pol2 ChIP-seq signal within genes showing downregulation (**Figs. 18H-K**). Note that this analysis precedes the more recent CBP-ifKO RNA-seq screen presented in **Fig. 17** and was prepared using an earlier list of DEGs retrieved with *Affymetrix* expression microarrays (514 downregulated transcripts, corresponding to 462 genes). The microarray experiments show a good correlation with the RNA-seq data (Pearson correlation $R=0.51$, $p<2.2e-16$, **Fig. 18L**) and provide valid information on gene expression. As expected, we observed a strongly diminished H2Bac signal within the downregulated genes (**Fig. 18H**), similarly to observed along the entire genome (**Fig. 18D**). In contrast to this observation, a strong decrease in H3K27ac was visible only in the downregulated genes (**Fig. 18I**), which correlated with a decrease in Pol2 (**Fig. 18K**). It is crucial to emphasize that such effect cannot be seen at the genome-wide level (**Fig. 18E**). The H3K9,14ac levels in the downregulated locations were apparently unaffected (**Fig. 18J**),

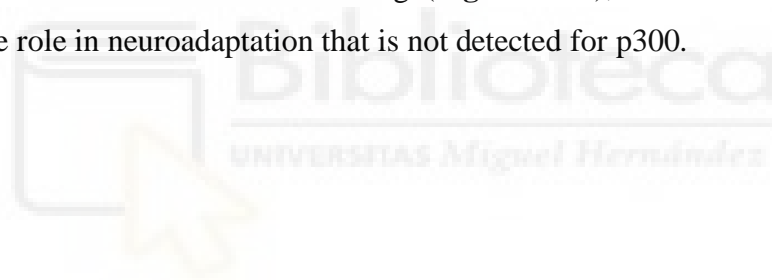
suggesting that CBP might be regulating the transcription through the maintenance of correct H3K27ac levels. These results are consistent with the observations made in dKAT3-ifKOs and indicate that CBP plays the same role in the genome regardless of the presence of p300. However, the H3K27ac changes observed in CBP-ifKOs were substantially smaller than in dKAT3-ifKOs (**Fig. 18M**). While we observed a complete disappearance of a number of peaks in dKAT3-ifKO chromatin these areas were only marginally hypoacetylated in CBP-ifKOs according to preliminary observation of H3K27ac profiles. This suggests that although H3K27ac is distinctly dependent on CBP (**Fig. 12A**), p300 alone is enough to maintain this hPTM in most locations. Future analyses should expand these initial observations (e.g., by peak calling and DiffBind statistics) and further meta-analyze CBP-ifKO acetylation profiles with dKAT3-ifKO ChIP-seq and transcriptomic data (with a particular focus on gene enhancers).

4.2.4. CBP excitatory neuron-specific knockout causes a dramatic failure in neuroadaptation

The “regular” neuronal transcriptome can be altered in adult brains as a result of various environmental or physiological events (drug abuse, epilepsy, etc.), resulting in persisting transcriptional changes (Delorenzo and Morris 1999, Robison and Nestler 2011, Zhou et al. 2014, Mirza et al. 2017). CBP can regulate this process thanks to its role regulating transcription and enhancers. Therefore, we decided to validate the hypothesis about the role of CBP in the process of transcriptional adjustment, to which we will refer to as “neuroadaptation”.

In order to do so, we subjected the CBP-ifKO mice to a paradigm of neuroadaptation called environmental enrichment (EE). It is well-established in the literature, that the EE paradigm not only improves the cognitive performance of mice, but also changes the transcriptome of the hippocampal neurons (Fischer 2016, Grégoire et al. 2018, Zhang et al. 2018). To evaluate the cognitive capacities of the mice, we performed a Morris water maze – a challenging test of hippocampus-dependent spatial memory (**Fig. 19A**). On the other hand, CBP-ifKO, although behaved like the control littermates in the standard cage (SC), they did not benefit from the EE (**Figs. 19D-E**). This result suggests that CBP is uniquely important for the CNS adjustment to the changes in the environment. Thus, we extracted the RNA from the hippocampus of the CBP-ifKO mice exposed to the EE and used the NGS platform to obtain the genome-

wide gene expression overview (**Fig. 19A**). The RNA-seq analysis revealed 98 genes displaying a significant change across both genotypes as a result of the EE treatment ($p\text{-adj}<0.1$, Main effect of EE, **Fig. 19F**). The EE exposure of the control mice evoked both an upregulation and a downregulation of a number of genes (**Fig. 19F, top and bottom lines**). However, the same transcriptional program was not induced in the CBP-ifKO mice (**Fig. 19F, two middle lines**). This suggests, that the lack of behavioral improvement as a result of the EE housing in the CBP-ifKO might be resulting from the inability to adjust gene expression. Furthermore, preliminary ChIP-assay experiment suggests that at least in the case of *Bdnf* promoter 3, control mice in EE seem to experience an increase in H3K27ac (**Fig. 19G**), which does not happen in the CBP-ifKO (**Fig. 19G**). Importantly, although we did not observe any significant changes in the p300-ifKO so far, we decided to add these animals to the analysis as well. Confirming the previous observations, the p300-ifKO mice acted as controls - did not show any impairments in the spatial memory and received a significant behavioral improvement as a result of the EE housing (**Figs. 19B-C**), which indicate that CBP plays a unique role in neuroadaptation that is not detected for p300.



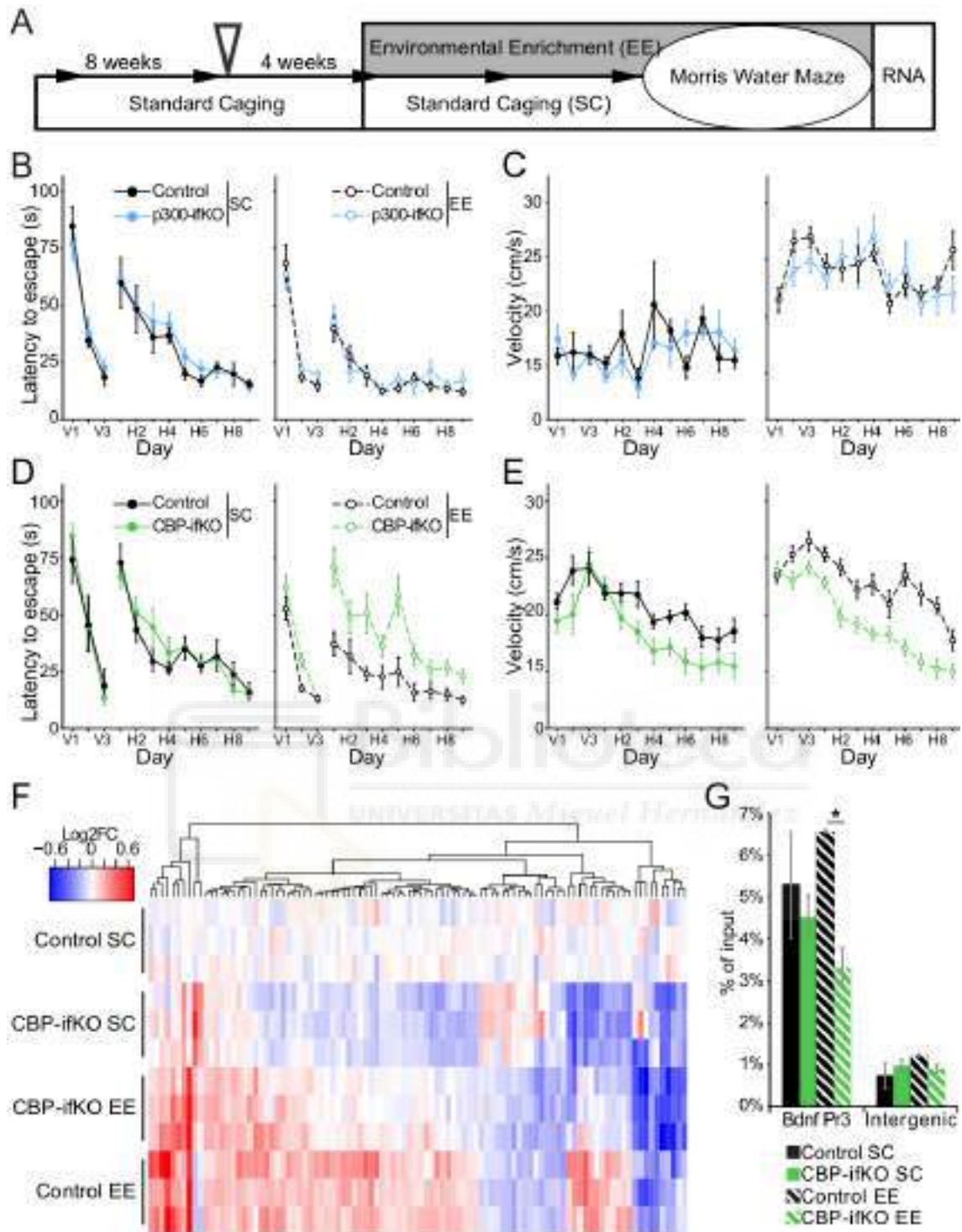


Figure 19. CBP is necessary for the transcriptional neuroadaptation after the EE
A. Scheme of the EE experiment. **B-C.** Morris Water Maze results of the control and p300-ifKO mice housed in the standard cage and EE. Graphs represent the time to find the platform **B** and the velocity of swimming **C**. No differences in p300-ifKO performance was observed either in the SC or the EE. **D-E.** Morris Water Maze results matching **B-C** however performed in CBP-ifKO mice. Notice that the EE-housed CBP-ifKO mice do not benefit from the paradigm as the controls (and p300-ifKO) do. **F.** RNA-seq analysis from the four conditions in the CBP-ifKO mice EE experiment. Heatmap represents 98 genes showing the main effect of the EE. **G.** Preliminary H3K27ac ChIP-assay analysis of *Bdnf* - one of the 98 genes identified in **F**. This

gene is upregulated in the EE in controls, but it is not in the CBP-ifKO. Similar observation can be made regarding its acetylation status (n=3, two-way ANOVA).

In order to further confirm the hypothesis regarding the role of CBP in establishing new transcriptional programs, we decided to use another paradigm that trigger a transcriptional response in excitatory neurons. The model of sensitization to a pro-epileptic drug pentylenetetrazol (PTZ) has been long used in the studies of epilepsy. In this protocol an initially sub-convulsive dose of PTZ, when repeatedly administrated, starts to induce more and more pronounced seizures. Although apparently there are no studies of kindling effects on gene expression using RNA-seq, earlier studies suggest long-lasting transcriptional consequences (Perlin et al. 1993, Liang and Seyfried 2001). Therefore, we used the PTZ kindling protocol on the CBP-ifKO mice to confirm that CBP is necessary for transcriptional neuroadaptation (**Fig. 20A**). The control mice reacted to the treatment as expected, with an initial latent non-convulsive period, followed by an incremental appearance of seizures. To our surprise, none of the CBP-ifKO mice entered the progressive seizure stage within more than 20 days of the experiment. (**Fig. 20B**). Next, we validated what are the transcriptional outcomes of the kindling protocol in each group. One week after the end of the experiment, mice were treated with the same dose of the PTZ once again and 30 min later their hippocampi were extracted for RNA (**Fig. 20A**). The RNA-seq analysis revealed a strongly affected transcriptome of PTZ-treated wild type mice. The effects of PTZ in CBP-ifKOs were much more limited (**Figs. 20C-D**). The RNA-seq analysis revealed 405 genes significantly changing across both genotypes as a result of the PTZ treatment (p-adj<0.1, Main effect of PTZ, **Fig. 20D**). We observed a virtual absence of upregulated genes, but a clear effect upon a selected group of genes that were significantly downregulated (indicating anomalous response to PTZ). A strong genotype-condition interaction affecting 34 genes was observed. Together, these results show that CBP plays a key role in the process of transcriptional adjustment of the CNS to the changing environment. Future experiments should explore the link between CBP binding, histone acetylation and both neuroadaptation protocols.

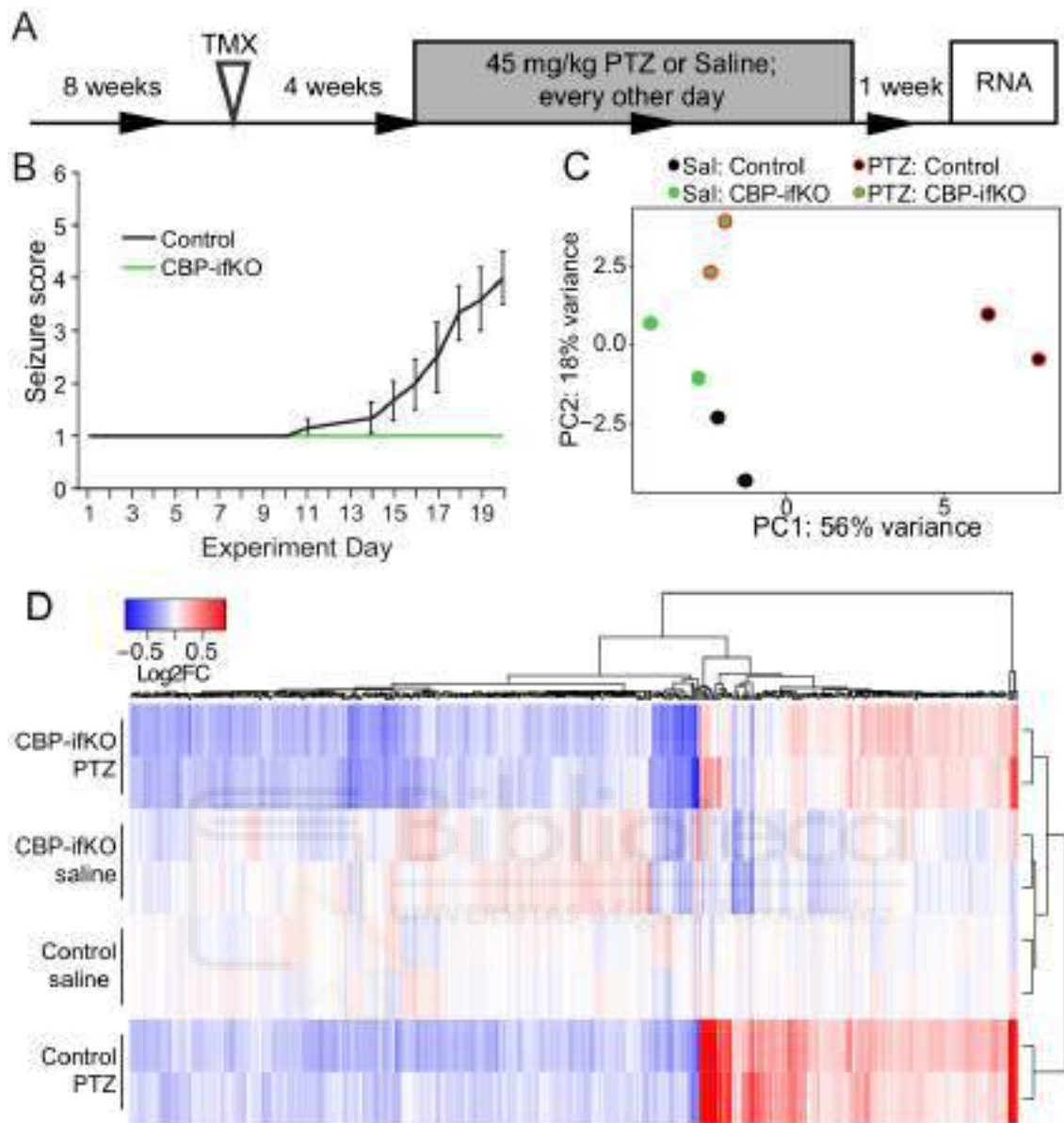
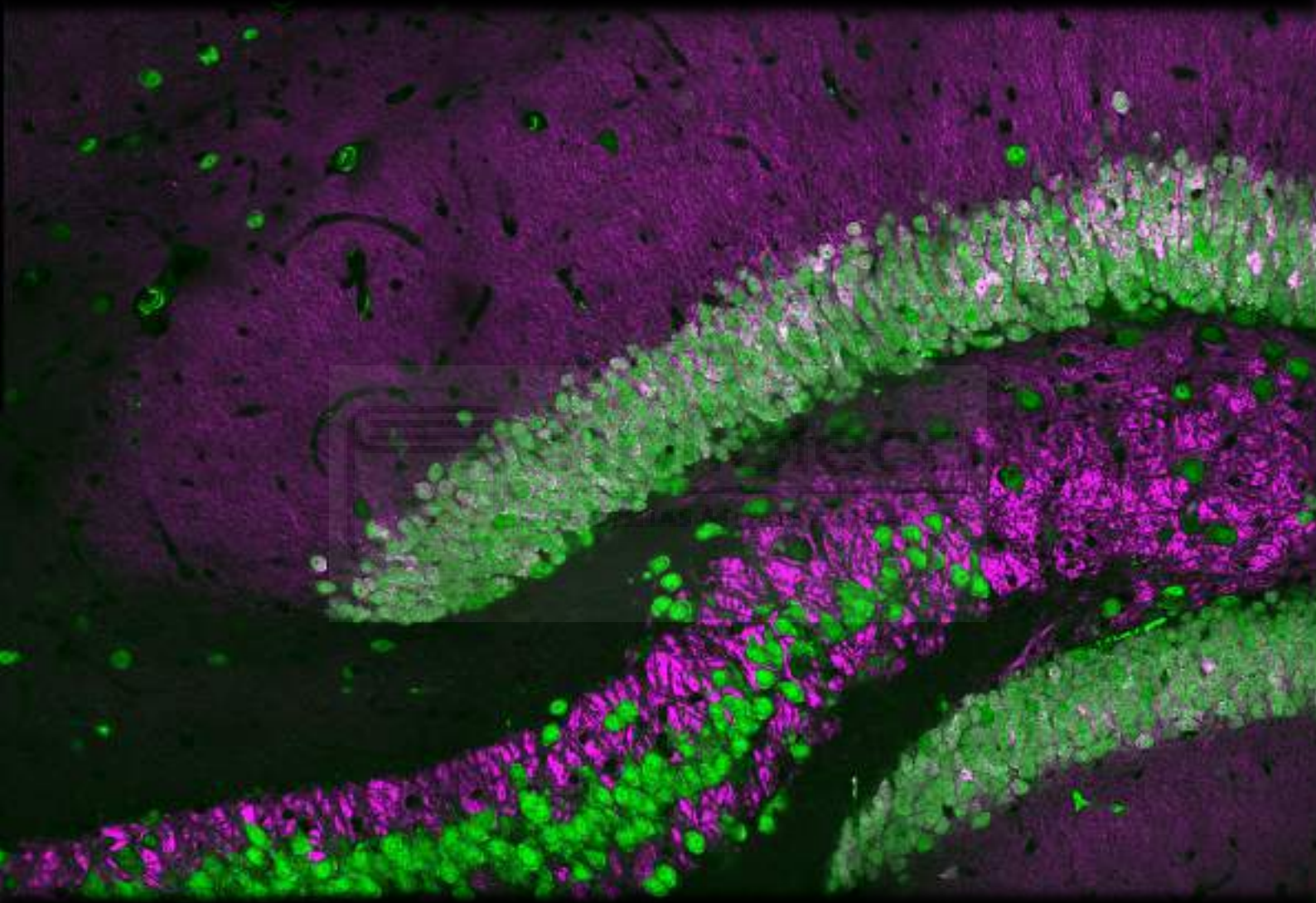


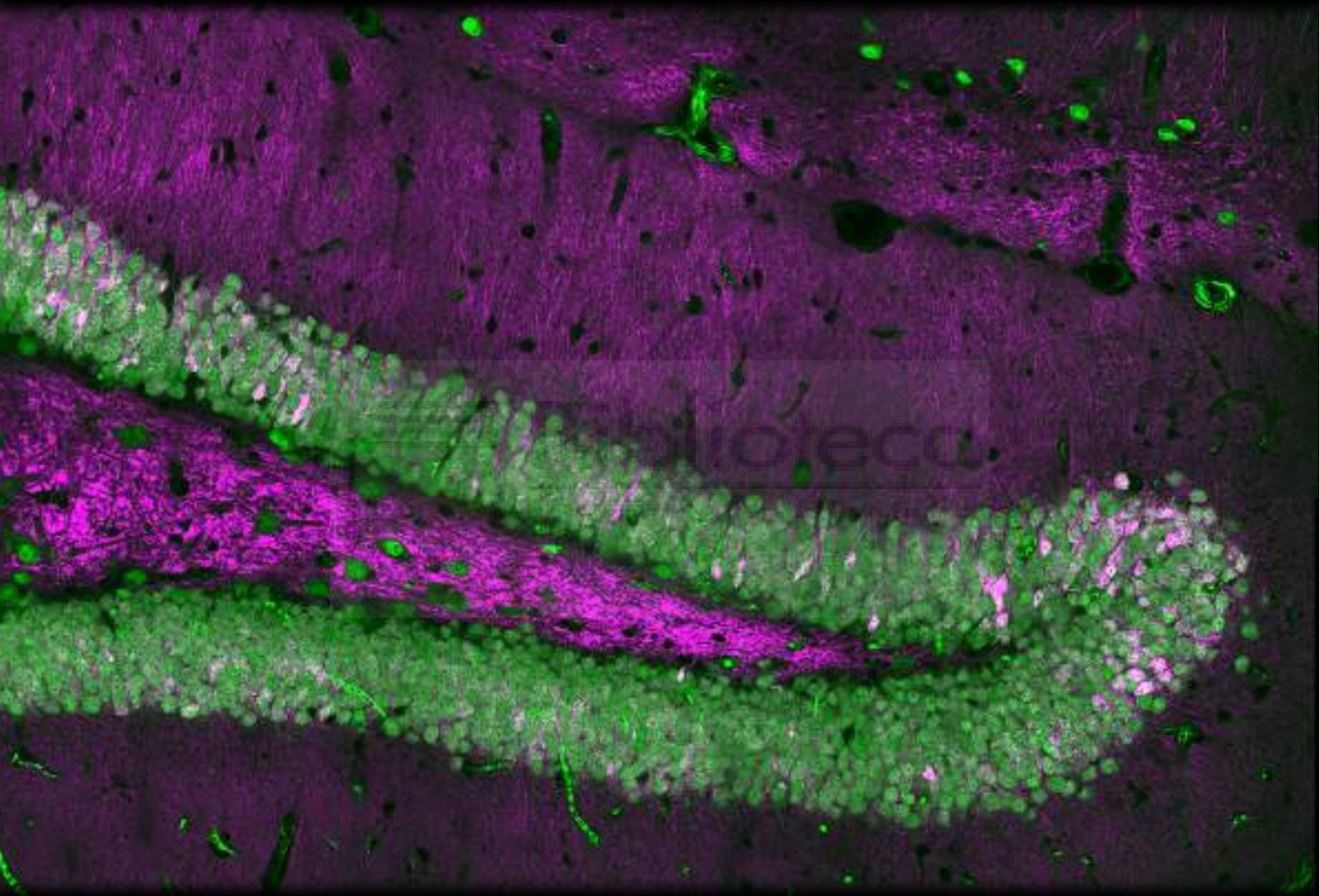
Figure 20. CBP is necessary for the transcriptional neuroadaptation after the kindling

A. Scheme of the kindling experiment. **B.** Seizure score during the kindling experiment. More details on the scoring can be found in the **Materials and Methods** section. Two data points are missing between the day 12 and 13 when the animals were treated with the PTZ, however not observed for the development of the seizures. **C.** Analysis of the RNA-seq performed on the hippocampal extracts from four conditions. “Sal” corresponds to the non-kindled animals treated with Saline on the day of the RNA extraction. “PTZ” corresponds to the kindled animals treated with the PTZ on the day of the experiment (red ring). **D.** Heatmap representing the 405 genes showing a main effect of the PTZ treatment among both genotypes. Notice a strong move towards the downregulation in the PTZ-treated CBP-ifKO.





Discussion





5.1. The comparison of KAT3 ifKOs reveals dose-dependent effect

Since the late 1990's, when the genes encoding CBP and p300 were identified and the proteins described for the first time, there is a stable inflow of publications describing some truly stunning aspects of the KAT3 protein biology. In the last 10 years, the technological jump regarding high-throughput sequencing, proteomics and new drug design provided answers regarding the substrate specificity, binding ligands, and the vast regulation that CBP and p300 might potentially be involved in (Lipinski et al. 2019). Nevertheless, many aspects of their biology like the overlap in their function or their specific role in neuron transcriptional regulation, remain either relatively unexplored or inconclusive. In this thesis, I undertook the goal of addressing several of these questions (listed in Objectives) to the best of my ability.

In order to unambiguously study the role of CBP and p300 in mature neuron biology, we designed a genetic strategy to eliminate either one or both proteins simultaneously in CaMKII α -positive neurons. As the recombination is triggered by an administration of tamoxifen, the genetic ablation is cell-type- (mature excitatory neuron), region- (forebrain) and time-specific (adult mice). Although this strategy has been used several times in previous projects of the laboratory of Angel Barco (Fiorenza et al. 2016, Scandaglia et al. 2017), this is the first time such approach is applied to investigate the role of KAT3 proteins in cognition (more regarding this in the next sections). The system is extremely efficient, resulting in an almost complete elimination of the KAT3 proteins in the specified pool of neurons. Surprisingly, the elimination of p300 alone did not cause any apparent change, apart from a small decrease in bulk H2A-ac. Every investigated aspect of the biology of these animals, including survival, behavior, transcription and neuroadaptation was completely normal. This was not the case of CBP conditional knockouts. CBP-ifKO showed a restricted, but neuro-specific phenotype in transcription and histone acetylation, which correlated with specific impairments in the NOR and MB tasks. A stronger phenotype was observed in these mice upon challenge, in paradigms in which the neuronal transcriptome needs to adjust to experience or changing environmental conditions. Both in the case of the EE housing and the pro-epileptic drug sensitization protocol, the CBP knockout mice were unable to adapt their behavioral and transcriptional response like the control littermates did.

The lack of changes in survival or overt behavioral abnormalities is a typical observation for any model of CBP or p300 adult knockout (Valor et al. 2013b). Although the single heterozygous CBP or p300 knockouts result in a slightly increased embryonic mortality (Tanaka et al. 1997, Yao et al. 1998, Viosca et al. 2010), the heterozygous animals that survive to birth, as well as every model of CBP or p300 deficit triggered in the postnatal periods, do not present any abnormal mortality levels (Alarcon et al. 2004, Viosca et al. 2010, Valor et al. 2013b). At the same time, both the homozygous knockout of either of the KAT3 proteins and the double heterozygous KAT3 knockout mice show embryonic lethality around E10 (Yao et al. 1998). This limiting phenotype has stopped the scientists from investigating the effects of a combined CBP and p300 elimination in the CNS *in vivo*. In this work, I am presenting the first brain-specific full knockout of both KAT3 proteins. Interestingly, although the complete loss of CBP or p300 does not cause any changes in survival, the simultaneous loss of both proteins in the mature forebrain caused a mortality reaching 100% within 1 month if standard housing conditions are maintained and access to food and water was not facilitated. After the initial phase of hyperexcitability (mostly until day 10-12), the dKAT3-ifKO animals show a very strong neurological phenotype including a low reactivity to the external stimulus and an impairment of reflexes. In parallel, we observed that the forebrain neurons targeted by the elimination lose their once acquired morphology and electrophysiological properties, which is likely the reason for the behavioral deterioration. We believe that these changes are caused by an ample dysregulation of neuro-specific transcription caused by KAT3 elimination. Consistently with the previous findings in other cell types (Hennig et al. 2013, Kasper et al. 2014) the expression of housekeeping genes was mostly intact, which suggests a clear role of KAT3 especially in cell-type specific transcription.

Therefore, our data clearly indicate that CBP and p300 play a common role in the maintenance of neuronal-specific transcription. If just one of them is missing, the other can almost completely take over the function of the neuronal identity caretaker. The survival curve and SHIRPA observations show that a single intact allele of *Crebbp* or *Ep300* in the forebrain neurons is enough to protect the animals from neuronal deterioration and death.

5.2. Mechanism of CBP and p300 function at their shared targets

In order to get a mechanistic insight into the observed transcriptional changes, we performed the first ever parallel CBP ChIP-seq and p300 ChIP-seq in the brain tissue. These experiments showed that the KAT3 proteins bind *in vivo* in almost exactly the same genomic locations. Interestingly, the neuro-specific peak locations correlate very well with the dKAT3-ifKO changes in transcription and show a powerful enrichment in the binding of bHLH (likely NeuroD) transcription factors. The neuronal-specific KAT3 binding also correlates with a depletion in H3K27 acetylation, as determined by the ChIP-seq analysis. Although it remains to be compared quantitatively, the decrease in the level of H3K27ac observed in the dKAT3-ifKO condition seems to be exponentially higher than when CBP alone is missing. This reproduces the transcriptional observations and suggests a mechanistic relationship between these two molecular changes. Indeed, the dKAT3-induced changes in expression gene correlated very well with the changes in H3K27ac in the most proximal enhancers. We observed that the H3K27ac was often depleted from the dKAT3-ifKO genome in multi-kilobase spanning domains, likely the so-called super-enhancers, which correlated closely with the transcriptional changes. CRISPR-targeted specific increase in histone acetylation in dKAT3 PNCs allowed for a rescue of the NeuroD2 expression. However, the same strategy did not correct Hippocalcin levels, which in dKAT3-ifKO lacks a bHLH TF binding in the enhancer, as determined by the ATAC-seq profile. Interestingly, an overexpression of the downregulated bHLH factor NeuroD2 alone does not rescue the expression of either of the investigated targets.

Therefore, CBP and p300 alone play an important, although mostly mutually redundant role for the function of mature excitatory neuronal system. CBP seems slightly more important for neurons, and actually essential to shift the neuronal transcription when needed. Even if neurons lack the apparently more important KAT3 protein in that cellular type - CBP, the decrease observed in neuronal-specific gene expression and H3K27ac is slim when compared with the changes observed in the combined CBP and p300 loss. Jointly, CBP and p300 play an irreplaceable role in safeguarding the neuronal identity in the mature excitatory neurons. The data indicates

that both KAT3 preferentially bind the bHLH transcription factors in the neuronal-specific locations, where they maintain the activity of enhancers and superenhancers.

5.3. Unique and specific functions of CBP and p300

Following the previous discussion, one could pose a question: are CBP and p300 playing in fact exactly the same role? The answer emerging from our study is that in some extent they are, and the previously published experiments would also suggest so. Even in the early seminal investigation of KAT3 KOs, the scientists observed that the *Crebbp*^{-/-} embryos had practically the same phenotype as *Ep300*^{-/-} embryos. Moreover, that was also the case for *Crebbp*^{+/-} *p300*^{+/-} (Yao et al. 1998). This suggests that the KAT3 proteins play at least a similar role in the mid-embryonic development. In the study published by Lee and colleagues (2009), *Crebbp*^{ff} *Ep300*^{+/+} and *Ep300*^{ff} *Crebbp*^{+/+} both had a severe deficit in motor neuron differentiation. However, neither of the conditions showed a complete halt in the specification, as 30-40% of the knockout cells were still able to reach their final cell fate. This likely means that the remaining KAT3 activity (two *Ep300* alleles or one *Crebbp* allele respectively) was enough to drive the differentiation. This again confirms that CBP and p300 can drive the neuronal-specific transcription in a kind of dose-dependent manner. Analogously to our case, elimination of both CBP and p300 in other cell-types has severely detrimental effects, while either of the proteins alone is enough to uphold the correct functionality of the cell (further discussed in the **Chapter 5.7**). Let us also remember, that the KAT3 proteins are almost identical in the structure and likely come from a single ancestor gene. This kind of evolutionary duplication in cell biology usually means that the gene plays a crucial function and the existence of a “backup” copy is highly beneficial and selected for. The most extreme example would be of the genes encoding histones, each presenting not one, but multiple copies in the mammalian genome (Henikoff and Smith 2015, Draizen et al. 2016).

What is worth mentioning, this evolutionary backup in the case of the KAT3 proteins comes with a little twist. Although they overlap very strongly in their function, they do seem to be more or less important depending on the tissue. It is very well documented for example, that p300 is absolutely crucial for the development of tissues like lung, small intestine and heart (Roth et al. 2003, Shikama et al. 2003). At the same time, p300 is typically less important for the correct function of the central nervous

system (Viosca et al. 2010). The results presented here are consistent with this view, as the p300-*if*KO mice do not show any apparent neurological phenotype. It is however surprising that the lack of a transcriptional coactivator p300 during months does not cause any transcriptional changes in the mature neurons. The fact that the elimination of CBP in the mature excitatory neurons causes a more robust (although still mild) change in histone acetylation and gene expression, is in accord with the previous findings of other groups. In contrast to p300, CBP is redundant for heart development (Roth et al. 2003, Shikama et al. 2003), but it plays a far more important role in neuronal function (Alarcon et al. 2004). Aforementioned Lee et al. 2009 study on motor neurons, also suggested that while the elimination of both *Ep300* alleles does not cause any handicap for the differentiation, the complete elimination of CBP decreases the efficiency of motor neuron production by 60-70%. According to our own data, CBP (but not p300) is crucial for correct levels of acetylation of lysine residues in various proteins, transcription, specific behaviors and neuroadaptation.

We are still unsure where does this functional difference come from. One should not forget that based on our data, CBP and p300 virtually bind to the same genomic locations. The previous reports on the genome-wide binding of both proteins in other cell-types, suggested a presence of peaks specific for one or the other KAT3 (Wang et al. 2009, Ramos et al. 2010, Kasper et al. 2014). These experiments however had a very low signal-to-noise ratio and it is highly likely that they missed a number of peaks. Of note, our ChIP-seq analysis provides the information on the KAT3 binding with unprecedented detail and quality. Although the p300 antibody has lower efficiency than the CBP antibody and, consequently, its ChIP-seq shows slightly lower quality, literally almost every p300 peak has a corresponding CBP peak in the same location. Therefore, considering the same genomic locations are regulated by both KAT3 proteins, the difference in their specific role might be caused by other factors, such as differences in their enzymatic activity and interactions with transcription factors, and distinct levels of expression and other modes of regulations.

5.3.1. Differences in the enzymatic activity of the KAT domain

In 2013 it has been reported using biochemical assays, that CBP and p300 show a slightly different specificities towards the H3 and H4 peptides (Henry et al. 2013). Although since then it has been observed that blocking both proteins limits the

acetylation in a very discrete pool of sites on these histones (Weinert et al. 2018), it is undeniable that at the biochemical level these two proteins might differ. In our experiments, the individual loss of CBP causes more substantial deficits in histone acetylation than the loss of p300. These changes include H2B-ac and H3K27ac. As I show in the **Chapter I** of the **Results**, especially the H3K27ac is an appealing culprit when looking for causes of the transcriptional changes. However, it is still to be determined if the relatively modest changes observed in the CBP-ifKO explain the transcriptional downregulation.

5.3.2. Specific interactions with transcription factors and other molecules

It has been widely reported, that KAT3 proteins bind a wide range of different transcription factors (Bedford et al. 2010, Dancy and Cole 2015, Lipinski et al. 2019). Several studies indicate that some of these interactions might differ in CBP and p300. For example, in motor neuron cell cultures both CBP and p300 bind Ngn2 bHLH TF, however only the binding of CBP, but not p300, is enhanced by RA. Most probably as an effect of this interaction, the RA induces the expression of neuronal genes like *Neurod1* or *Nefm* (Lee et al. 2009). In another recent example, the use of novel CBP/p300 inhibitors (ICG-001 and YH249/250) allowed for the identification of a different modification of the β -catenin pathway by each KAT3. The use of CBP by the β -catenin pathway drives the maintenance of cell division and self-renewal, while the use of p300 drives the differentiation (Thomas and Kahn 2016). The discovery of new KAT3 inhibitors specific for either CBP or p300 should help to further discriminate between these mechanisms (Breen and Mapp 2018), and eventually explains the KAT3-specific regulation that underlie the differences between p300 and CBP importance in various tissues.

5.3.3. Differences in the level of expression

Another mechanism explaining the difference between the KAT3-dependence of distinct tissues could be a simple difference in KAT3 expression. It has been shown over 20 years ago, that CBP and p300 proteins are present in the cell in limiting amount and multiple TFs compete for their co-activator activity (Kamei et al. 1996, Hottiger et

al. 1998, Giordano and Avantaggiati 1999). Since CBP is highly expressed than p300 in the CNS (**Fig. I-10B**), neurons likely depend more on the CBP levels. This is, however, an untested hypothesis that needs to be experimentally evaluated.

5.3.4. Functions and regulations unaccounted for

As the last aspect driving the difference between CBP and p300, I should mention that multiple aspects of KAT3 biology remain obscure and were not accounted for in this study. In the last few years, a number of so-called “orphan functions” have been reported for KAT3 proteins (Montgomery et al. 2015, Sabari et al. 2017). For example, KAT3 can act as E4 polyubiquitin ligases in the cytoplasm (Shi et al. 2009) or drive different acylations of histones (Sabari et al. 2015) and non-histone proteins (Huang et al. 2018a). Albeit it is a completely speculative discussion, it is tempting to hypothesize that some of these functions may be unique to one of the two KAT3 proteins and not to the other.

Finally, letting the reins of imagination even further, one could picture some kind of cascade of interactions between the two KAT3 proteins, where the CBP is upstream, thus the function of both KAT3 proteins depends on CBP. Recently, a very interesting study from Ortega and colleagues (2018) suggested that two p300 proteins not only transiently dimerize, but also their activity depends on the interactions formed through those dimers. Even though the existence of CBP/p300 heterodimers has not been described to my knowledge, it is somehow supported by our data, as we observe both CBP and p300 binding in the same genomic locations. It is therefore not impossible that CBP-dominant heterodimers could exist and specifically influence the behavior of some of the CBP-dependent genes.

5.4. Role of CBP and p300 in cognition

In this work, we evaluated the performance of CBP and/or p300-deficient mice in strains in which gene ablation was clearly limited to the mature excitatory neurons. Thanks to this genetic strategy, the elimination of the gene/s happen irrefutably when the neurons and the circuit are completely mature. The earlier works based on time-unrestricted CaMKIIa-Cre (Chen et al. 2010, Oliveira et al. 2011, Valor et al. 2011), the

proteins are eliminated in the postnatal forebrain, however this most likely happened in the early postnatal days when the cortex and hippocampal circuits are still undergoing changes and maturation. These late changes include, but are not limited to morphological and electrophysiological refinement, synaptogenesis and subsequent pruning (Sauer and Bartos 2010, Semple et al. 2013, Son et al. 2019). Based on some recent studies in our laboratory, we know that CBP plays a crucial role in the neuronal maturation (Del Blanco et al. 2019), and these processes may be thereby affected in CaMKIIa-cre cKOs.

Here, the data undeniably shows that the KAT3 proteins are eliminated in the hippocampi of their corresponding knockouts at the time of the behavioral experiments. There is also no question of developmental influences thanks to the tamoxifen-regulated system. Consequently, animals effectively missing either CBP or p300 in the mature excitatory neurons (CBP-ifKO and p300-ifKO), express normal context and spatial memory even a couple of months after the recombination. Although it does not mean, that the KAT3 proteins are not important for hippocampal memory, it clearly shows that in the conditional KOs long-term memory can function perfectly fine without CBP or p300. In fact, as much as the p300's role in cognition is proven false, it is not false to say that CBP is important for memory in general. We have clearly shown that CBP-ifKOs show an impairment in NOR memory paradigm and the NOR is consistently impaired in all in CBP knockouts published to date (**Table I-2**).

One could ask why one type of forebrain-dependent memory is impaired and another is not. A very interesting explanation was proposed by the group of Mark Mayford in their 2004 Neuron paper making a similar observation using CBP^{KAT}- mice: *“The visual-paired comparison task [NOR] recruits an innate behavioral preference for novelty and does not involve an exogenous reinforcer such as a swim stress (water maze) or an electric shock (fear conditioning). It is possible that these stressful reinforcers activate alternative synaptic and nuclear mechanisms for the stabilization of long-term memories.”* (Korzus et al. 2004). Another possibility to consider is that in contrast to the context fear conditioning, the NOR depends in fact on a pretty complex circuit involving various parts of the cortex, thalamus, subiculum and the hippocampus (Warburton and Brown 2015). Thus, this task requires all these different brain regions (many affected in the CBP-ifKO) to function correctly and may, therefore, be comparatively more demanding than the other examined tasks.

5.5. CBP role in neuroadaptation

Apart from particular CBP-ifKO changes observed in mice housed in the standard conditions, these animals show a very dramatic deficits when the CNS needs to adjust to the environmental changes (EE and kindling). As I already mentioned in the **Results**, the differentiation process could also be considered a type of transcriptional adjustment, and both CBP and p300 have been reported to play an important role in neuronal (Lee et al. 2009, Wang et al. 2010, Tsui et al. 2014, Del Blanco and Barco 2018, Medrano-Fernandez et al. 2018) and non-neuronal differentiation (Eckner et al. 1994, Kawasaki et al. 1998, Shi and Mello 1998, Ugai et al. 1999, Kung et al. 2000, Sun et al. 2001, Rebel et al. 2002, Victor et al. 2002, Roth et al. 2003, Fukuda et al. 2004, Fauquier et al. 2018). It is important to notice, that certain observations made in the past by different groups might indicate a similar CBP-dependence in other circumstances requiring neuroadaptation process in the adulthood. For instance in *Drosophila*, mutants of *nejire* fail to develop a typical long-lasting alcohol tolerance caused by a single alcohol exposure (Ghezzi et al. 2017). In a different example, dietary restriction increases the expression of CBP ortholog gene both in *C.elegans* (Zhang et al. 2009) and in mouse hypothalamus (Moreno et al. 2016). In *C.elegans*, this process correlates with an increase of the lifespan and protection from proteotoxicity, effects which are suppressed by the inhibition of *cbp-1* (Zhang et al. 2009). Last but not least, in examples from our own laboratory CBP seems to play a crucial role for two EE-induced enhancements: a) increase in hippocampal adult neurogenesis (Lopez-Atalaya et al. 2011) and b) improved axon regeneration after spinal cord injury (Hutson et al. 2019).

The mechanism behind the process of neuroadaptation certainly requires further rigorous investigation. As I indicate in the **Results** section, the ability to increase the histone acetylation levels might be playing a key role in the transcriptional reprogramming observed in the EE and kindling paradigms. The fact that H3K27ac is changing in CBP-ifKOs, but not in p300-ifKOs, paralleling the neuroadaptation phenotype, makes it a promising target. Even though this hypothesis seems to be supported by observations made by other experimenters (Ghezzi et al. 2017), the link between histone acetylation and transcription is not necessarily straight forward (Lopez-Atalaya and Barco 2014). Therefore, we should certainly consider other paths through which CBP might control the cellular adjustment as well, including regulating neuronal

metabolism by protein acetylation/acylation (Bedford et al. 2011, Guan and Xiong 2011, Mews et al. 2017, Huang et al. 2018a, Zaini et al. 2018)

5.6. Role of histone acetylation in transcription

As I mentioned a number of times in this work, the role of histone acetylation in controlling transcription is still debated. Our own data does not solve the current discussion but provide interesting novel insight. In accordance with recently published proteomic data (Weinert et al. 2018), H2A-ac and especially H2B-ac, are particularly sensitive to KAT3 manipulations. Histone H2A-ac is decreased regardless of which KAT3 is affected, with the remaining KAT3 only marginally rescuing the acetylation level of this histone PTM. Histone H2B-ac on the other hand, seems to be slightly more dependent on the CBP, as a small decrease can be observed already in the CBP-ifKO, but not in p300-ifKO. However, the effect becomes very dramatic when both proteins are eliminating, suggesting that p300 is a certain imperfect “backup” for CBP in the context of this histone mark. Although we have not investigated the specific genomic distribution of H2A-ac changes, we did perform a ChIP for H2B-ac that revealed a broad, almost genome-wide effect. This bulk decrease in H2A-ac and H2B-ac does not correlate with a very limited deficit in gene expression observed in the CBP-ifKO and no transcriptional change observed in the p300-ifKO. Even though the genes downregulated in CBP-ifKO will likely correlate with changes in both H2A-ac and H2B-ac, so do the number of genes unchanged in CBP-ifKO. This suggests that the acetylation of H2A-ac and H2B-ac is either unnecessary, or plays, at most, a secondary role for correct steady state transcription in the neurons. Again, this is consistent with the recent proteomic data in cultures, where a strong decrease especially in H2B-ac was paralleled by a limited transcriptional alteration (Weinert et al. 2018). Similar uncoupling of histone acetylation and transcription has been previously described at least in the case of the budding yeast genome, where a the heterochromatic gene expression can be induced with negligible levels of histone H3 and H4 acetylation (Zhang et al. 2014).

On the other side of the coin, we have our H3K27ac ChIP-seq and CRISPR-p300 experiments. Both in the dKAT3-ifKO and CBP-ifKO, the H3K27ac decrease seems to have a very good correlation with the downregulation of gene expression. This by itself does not imply a causal role of this histone PTM for the change in

transcription, since it might be an effect of lack of transcription (permissive model discussed in Lopez-Atalaya and Barco 2014). However, at the same time the CRISPR-p300 experiments show that when all the necessary TFs are present, the local increase in lysine acetyltransferase activity is enough to restore the correct transcription levels. Although I have not shown this explicitly in the current work, previous publications reported that dCas9-p300 system is able increase the H3K27ac level in the targeted locus (Hilton et al. 2015, Chen et al. 2019). Therefore, it is highly probable, that the increase of this histone PTM level is necessary for the transcription of an active locus.

5.7. The recruitment of KAT3 by cell-specific TF regulates cell identity

While interpreting the work presented here, it is fundamental to remember that the current consensus in the field is that KAT3 proteins do not have any DNA binding activity. Although it is theoretically possible that they interact or sequester the DNA in a similar way as they bind to the RNA (Bose et al. 2017), the biochemical data supporting this is extremely scarce (Song et al. 2002). Our KAT3 ChIP-seq data not only shows that the genomic presence of these proteins is highly specific to TF-bound promoters and enhancers, it also suggests that the most abundant binding motif in these locations, at least in neuronal cells, is the consensus E-box site CANNTG. This site is customarily bound by the HLH genes (Massari and Murre 2000, Amoutzias et al. 2008), as also identified by our TFBS analysis (further discussed in the next Chapter). Nonetheless, both in the neuronal-specific and the pancellular KAT3 positions, other TFs appear to be also implicated in KAT3 regulation. This is consistent with the numerous reports of CBP and p300 binding to a plethora of different TFs (see **Fig. I-12** and Bedford et al. 2010, Dancy and Cole 2015). Considering that KAT3 are ubiquitously present and a different pool of interacting TFs is expressed in every cell-type, their potential for facilitating the transcription is likely cell-type dependent.

Interestingly, none of our TFBS enrichment analyses identified the CREB motif, which is the classic binding partner of the CREB-Binding Protein (Chrivia et al. 1993). We have also observed just a small enrichment in AP1-like motifs (BATF/JPD2 and ATF3 in **Fig. 11A**), traditionally linked to the CBP function (Giordano and Avantaggiati 1999). Yet, the action of these TFs is usually linked to induced

transcription, thereby it is not that surprising that they are not enriched in the non-activated tissue. We might expect that after neuronal activation either new peaks corresponding to the AP1/CREB sites would emerge, or the existing AP1/CREB locations would be significantly enriched in KAT3 signal. This would illustrate either new sites bound by CBP/p300 or a bigger proportion of CBP/p300 molecules bound to the existing sites. As the archetypal AP1 binding locations surrounding the IEGs Fos or Npas4 already have a KAT3 peak in our KAT3 profiles (not shown), I would support the second hypothesis. In the future we plan to investigate the matter further by developing KAT3 profiles after neuronal activation.

5.8. Role of NeuroD and other bHLH proteins in cell identity

Our study identifies bHLH proteins as particularly important partners of KAT3 proteins. Depending on the method, the bHLH proteins can be classified into 6 (A-F, Jones 2004) or 7 (I-VII, Massari and Murre 2000), mostly overlapping, classes. Some of these proteins, promote cell proliferation like c-Myc (Class B/IV), or inhibit the differentiation like Id1 (D/V) or Hes1 (E/VI). Other groups however, are fundamental for the differentiation of various cell-types. The class A/II seems particularly interesting from our standpoint, as it includes TFs with tissue-restricted expression like MyoD (myogenesis) or Tal1 (hematopoiesis) (Massari and Murre 2000). Even considering that various bHLH play an important role in differentiation of other cell-types, the abundance of bHLH TFs crucial for the differentiation of various neural lineages, suggests their particularly important role in the CNS development. Just to mention a few: the Olig family plays an important role in oligodendrogenesis (Lu et al. 2000, Zhou et al. 2000, Fukuda et al. 2004) and motor neurons specification (Mizuguchi et al. 2001, Novitch et al. 2001, Zhou and Anderson 2002); *Ascl1* is a neurogenic pioneer factor (Wapinski et al. 2013, Raposo et al. 2015); *Atoh1* regulates cerebellar granule cell differentiation (Ben-Arie et al. 1997); *Twist1* is crucial for dorsal neural tube development (Chen and Behringer 1995, Soo et al. 2002, Barnes and Firulli 2009); Neurogenins regulate multiple aspects of forebrain neuron differentiation (Fode et al. 2000, Mattar et al. 2008, Dennis et al. 2019); and NeuroDs have been recently identified to be a convergence point of the transcriptional regulation during neuronal differentiation (*NeuroD2* in Telley et al. 2016 and *NeuroD4* in Schiebinger et al. 2019). These are however only a few examples from a wide literature describing the control of

cell differentiation and development directed by bHLH proteins (for more see Dennis et al. 2019).

Our KAT3 ChIP-seq peaks show a significant enrichment in bHLH binding motif. Although the identified motif seems most analogous with the sites bound by the NeuroD family (see HOCOMOCO database [NeuroD1](#) and [NeuroD2](#) binding motifs), conservatively speaking, we cannot be sure which bHLH protein is actually bound by the KAT3. Indeed CBP and p300 have been proven to interact with a number of bHLH TFs including MyoD (Puri et al. 1997), Ascl1 (Vojtek et al. 2003), Neurogenins (Sun et al. 2001, Vojtek et al. 2003, Lee et al. 2009), Twist (Hamamori et al. 1999) and NeuroD (Mutoh et al. 1998, Qiu et al. 1998). Therefore, it is reasonable to say that they likely bind multiple bHLH TFs expressed in neurons. Bearing in mind that bHLH proteins form dimers (Amoutzias et al. 2008, Dennis et al. 2019) and binding to a dimerized TF has been recently shown to be essential for the control of KAT3 activity (Ortega et al. 2018) makes them a perfect candidate to regulate KAT3 function.

If KAT3 proteins can indeed bind to a variety of bHLH factors and these proteins regulate cell-type specific transcription, an interesting possibility would be for KAT3 to regulate the cell-type specific transcription through lysine acetylation. Similarly, various bHLH TFs are differentially expressed throughout neuronal proliferation and specification. In a very simplified example of a cortical neuron (Ross et al. 2003, Ohtsuka and Kageyama 2010, Dennis et al. 2019), Hes1 and Hes5 promote NSC/NPC renewal and inhibit the specification, but are replaced by Ascl1 or Neurog2 to trigger the neural differentiation. These two are later succeeded (or accompanied) by other factors like NeuroD1, bringing more specific transcription; and the process is finished by the expression of TFs that are maintained throughout the lifetime of the neuron such as NeuroD2 or NeuroD6 (likely others as well). As CBP and p300 are important for neuronal differentiation, it is a deeply tempting idea that KAT3 binding is driven by each of these bHLH TFs at different stages of the development. The fact that *Crebbp*^{-/-} neural tube phenotype mimics the phenotype of Twist null knockout supports this hypothesis (Yao et al. 1998, Barnes and Firulli 2009). Further studies are necessary to verify this hypothesis.

In our dKAT3-ifKO some bHLH genes, including *Neurod2* and *Neurod6* are downregulated themselves and the accessibility peaks lost in the ATAC-seq of the dKAT3-ifKO also show a significant enrichment in E-box motif. In principle, the loss of these TFs could by itself cause a strong phenotype including a loss of neuronal-

specific transcription. However, not only *NEUROD2* expression does not rescue the neuronal-specific gene expression, the previously published data also does not support this idea. Although the full or early knockouts of *Neurod1*, *Twist1* and *Neurog2* are lethal at different developmental stages (Fode et al. 1998, Goebbels et al. 2005, Barnes and Firulli 2009), the knockouts of *Neurod2* and *Neurod6* are viable and can survive till adulthood. Full *Neurod6* knockout (Schwab et al. 1998) and heterozygous *Neurod2* knockouts (Olson et al. 2001) do not show any phenotype. Homozygous *Neurod2* knockouts do show an increased mortality in the adulthood (Olson et al. 2001), which however can be easily rescued by an outbreeding to a 129/SvJ background (Bormuth et al. 2013, Bormuth 2016). These mice also show an increase in the postnatal apoptosis, which we were unable to observe in dKAT3-ifKO (Olson et al. 2001). Considering that the acetylation itself is unable to recover the transcription in locations with a loss of bHLH ATAC-seq peaks, it is likely that both bHLH TFs and lysine acetylation are crucial for the activation of the genomic locus. Hence, the dKAT3-ifKO animal phenotype likely results from a combination of acetylation and bHLH TF loss.

5.9. Mechanisms of KAT3 protection of cell identity

If the bHLH factors actively expressed in the adulthood are indeed necessary to maintain the neuronal identity in this way or another, one could say that they fulfill all the requirements for a theoretical terminal selector gene (Deneris and Hobert 2014). *NeuroD2* starts being expressed in the last stages of the differentiation and keeps expressing throughout the life of the forebrain neuron (Zeisel et al. 2015, Telley et al. 2016), it can autoregulate by binding to its own regulatory features (see **Fig. 15**) and controls the transcription of multiple genes defining the forebrain neuronal identity (terminal effector genes). At least in the case of proneural TFs, they vastly localize in enhancers and in this manner they likely drive cell-type specific transcription (Seo et al. 2007, Wapinski et al. 2017). However, the bHLH factors apparently cannot work alone, and need lysine acetylation driven by one of the KAT3 proteins to maintain (and probably establish) the correct neuro-specific transcription. Indeed, the crucial role of H3K27-acetylated (active) enhancers and super-enhancers in cell-type specific transcription is pretty well established in the field of developmental epigenetics (Heintzman et al. 2009, Visel et al. 2009, Creighton et al. 2010, Bonn et al. 2012, Hnisz et al. 2013, Nord et al. 2013, Whyte et al. 2013, Arner et al. 2015, Heinz et al. 2015,

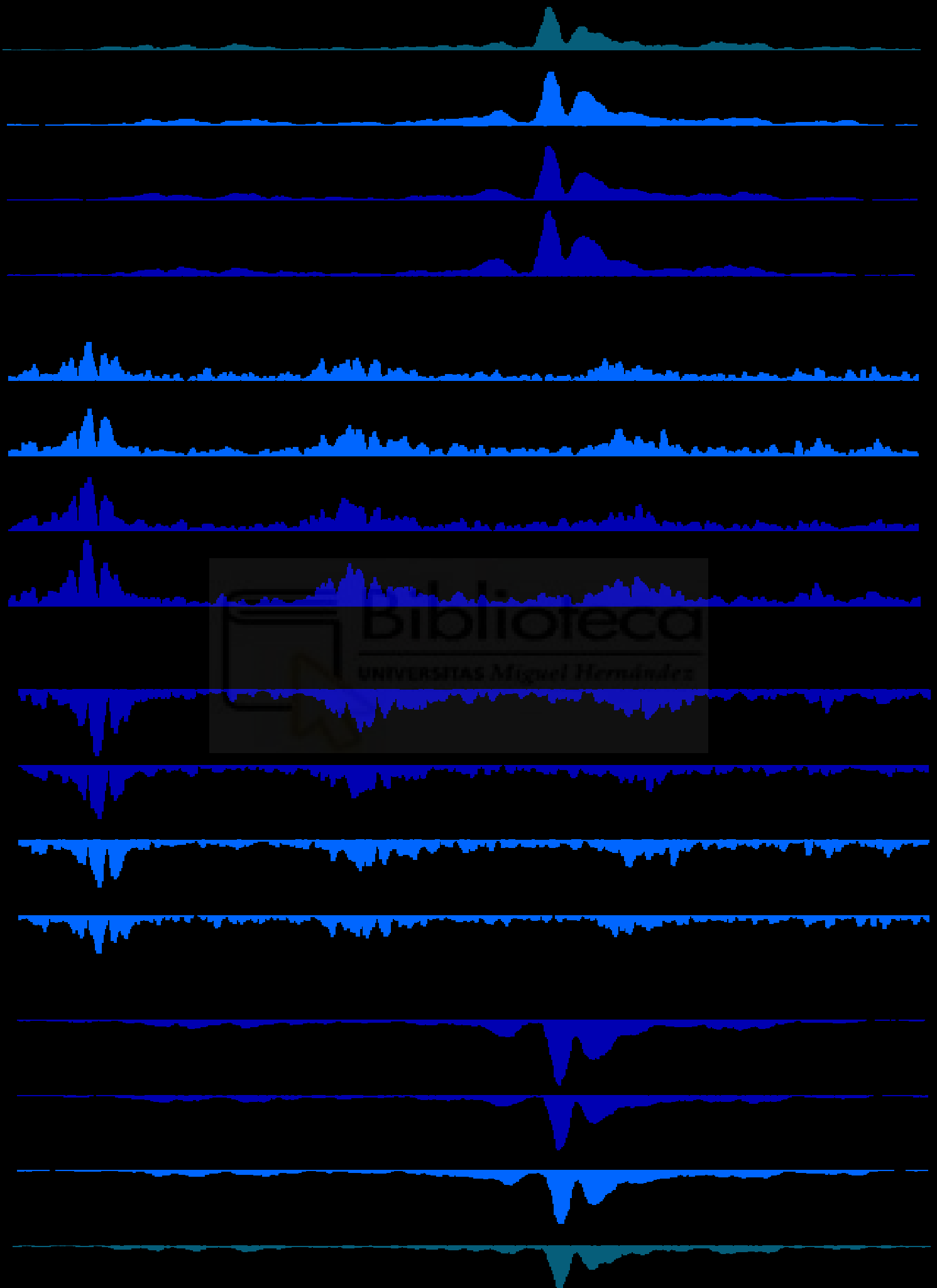
Thakurela et al. 2015). Although the specific relation of KAT3-bHLH-H3K27ac in cell-identity has not been reported before, there is a number of articles reporting that the elimination of both CBP and p300 causes a loss of cell-type specific gene expression in other tissues. Hence, the joint role of KAT3 in this kind of transcription has been described *in vivo* for the gonads (Carre et al. 2018), kidney juxtaglomerular cells (Gomez et al. 2009, Pentz et al. 2012), lymphocytes B (Xu et al. 2006), lens (Wolf et al. 2013), retina (Hennig et al. 2013), and a couple of *in vitro* cultured cells like primary myoblasts (Fauquier et al. 2018) and stem cells (Fang et al. 2014). This could mean that KAT3 proteins are universally implicated in the maintenance of cellular identity, in each cell collaborating with a terminal selector specific for the cell-type. I should note that in none of the mentioned publications the KAT3 proteins were eliminated in fully mature and established cells. Each of the *in vivo* studies was based on a non-inducible recombination strategy and the cre recombinase was expressed during cellular differentiation (Xu et al. 2006, Wolf et al. 2013, Carre et al. 2018) and maturation (Gomez et al. 2009, Pentz et al. 2012, Hennig et al. 2013). This gives an additional importance to our study, in which we make sure that the cellular identity of the affected neurons has been settled for several weeks and no developmental processes are affected. Therefore, there is an unprecedented unambiguity in our report of the joint KAT3 role in cellular identity maintenance.

An interesting conclusion that can be drawn from this work is that cell uses two separate, though conjunctive mechanisms of cell identity maintenance. Our study, together with the previous investigations of terminal selectors and enhancers/super-enhancers suggests a process of actively upholding the expression of cell-type specific genes (Deneris and Hobert 2014). On the other hand, the presence of heterochromatin epigenetic marks like 5hmC and H3K9me3 conserves the pro-proliferation and alternative gene loci silent (Colquitt et al. 2013, Becker et al. 2017, Scandaglia et al. 2017). In our dKAT3 model we miss one of the parts, but not the other, which is possibly why the cells do not dedifferentiate completely and do not start showing the features of progenitor or stem cells (genetic markers, proliferation). We could speculate, that if you eliminate the heterochromatin-based mechanism of identity conservation, for example by a treatment with DNA methylase inhibitors (Jopling et al. 2011), the dKAT3-ifKO cells could actually come back to the progenitor state. Although, it is not clear if the cell needs CBP and p300 to become a fully functioning neural progenitor, as

the dKAT3 KO cells are impaired in cell proliferation as well (Yao et al. 1998, Wong et al. 2018).

To finish, I would like to step back and contemplate the entire notion of cell identity. What is actually a cell identity? Is it fixed in fully differentiated cells or is it wavering or subjected to change? Can a cell be “partially a neuron”? Can we call a cell coming from the same neural lineage, like an astrocyte - “partially a neuron”? I do not have the answers to these questions as the scientific community itself is in the process of refining these concepts. Similarly, one question regarding my own work remains unanswered: What are the dKAT3 cells, if they have lost the neuronal identity? I can certainly say what they are not. They certainly do not transdifferentiate to another type of specified cells, as they do not express other cell-type markers or behave like another cell-type. They are not dedifferentiating to progenitors/stem cells, as they do not divide or show a transcriptional footprint of those either. They seem to be in some kind of functional limbo. Not under any active process of cell death like apoptosis or necrosis. Dormant, although metabolically active. As humans, we like to put things into drawers, call them by the names that we formulate. “What” are dKAT3 cells is only an issue if we consider the cell-types, or identities, as fixed categories. More and more studies using single-cell sequencing technologies prove that the specification borders are often blurry (Schiebinger et al. 2019). What is the limit between the cell-type and the current status of the cell, requiring a transcriptional change? Right now, and even more in the future, the number of identified cell types in the tissue will depend on where you decide to draw the line. Biology is entering an age of spectrums and nuances.





Conclusions & Conclusiones





6. CONCLUSIONS

1. The CaMKIIa-CreERT2 system provides an efficient and specific method to eliminate CBP and/or p300 in excitatory neurons of the adult forebrain.
2. Loss of p300 in the CaMKIIa⁺ neurons as far as we explored does not cause any significant consequences in gene expression, neuronal survival and animals' behavior.
3. Loss of CBP in the CaMKIIa⁺ neurons causes specific transcriptional and cognitive phenotypes that correlate with local histone acetylation deficits.
4. Neither the presence of CBP nor p300 (separately) in excitatory neurons of the forebrain is necessary for a correct spatial and contextual fear memory. Whether any KAT3 activity in these cells is necessary for this type of memory was not investigated because the severe neurological phenotype of the dKAT3-ifKO mice would inevitably skew the memory test results.
5. CBP, but not p300, is crucial for the implementation of novel transcriptional programs in hippocampal neurons as a response to experience and environmental changes.
6. While the individual loss of CBP or p300 in CaMKIIa⁺ neurons does not cause overt neurological problems, the combined loss of both proteins deteriorates the animal well-being and decreases the survival of the animals.
7. CBP and p300 are essential to maintain neuronal identity, as determined by gene marker expression, morphology and electrophysiological properties.
8. The presence of a single KAT3 allele, regardless of which, is sufficient to perform the KAT3 function as the protector of neuronal identity. This suggests a highly overlapping role of CBP and p300, although the neuroadaptation experiments suggest some essential aspects of CBP function for which it cannot be replaced by p300.

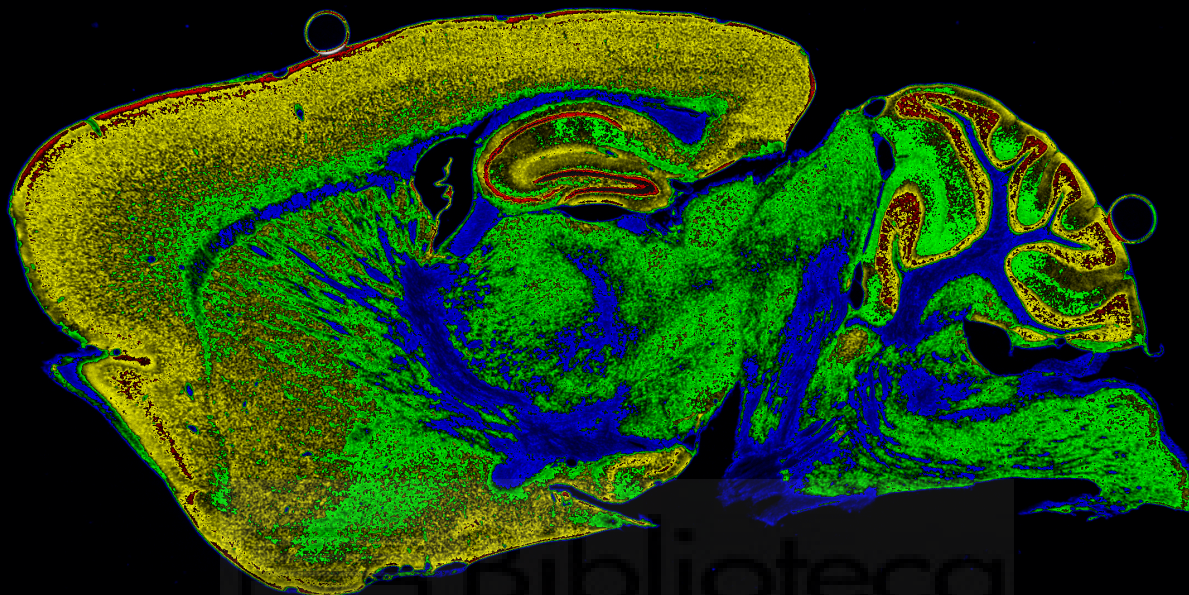
9. CBP and p300 bind to the same genomic locations, which likely explains their functional overlap.
10. The CBP and p300 location in the neuronal genome is mostly determined by the binding of their major neuronal partners – bHLH proteins.
11. The expression of a hypoacetylated gene can be increased by a CRIPSR-targeted binding p300 KAT domain. This effect could be achieved only in loci that have not lost chromatin accessibility.
12. KAT3 proteins jointly regulate the expression of neuronal genes by both conserving high levels of H3K27ac in neuronal enhancers and sustaining the expression of their own chromatin anchors – pro-neural bHLH TFs.
13. Overall, the findings reported in this thesis provide novel findings regarding the molecular role of CBP and p300 in mature excitatory neurons of the forebrain. Here, we provide evidence for the essential role of the KAT3 proteins in the establishment and maintenance of neuronal transcriptional programs, likely through their extensive role as lysine acetyltransferases.

CONCLUSIONES

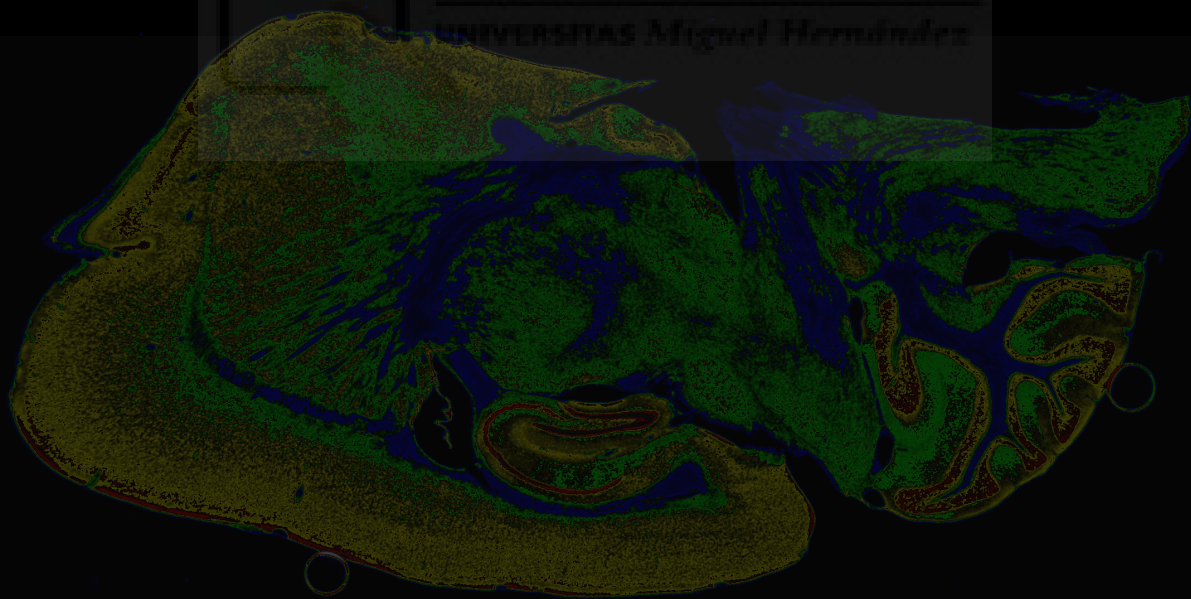
1. El sistema CaMKIIa-CreERT2 permite una eliminación eficiente y específica de CBP y/o p300 en las neuronas excitatorias del telencéfalo adulto.
2. Por lo que hemos podido comprobar, la pérdida de p300 en las neuronas CaMKIIa⁺ no genera cambios significativos en la expresión génica, supervivencia de las neuronas o el comportamiento de los animales ifKO.
3. La pérdida de CBP en las neuronas CaMKIIa⁺ genera cambios específicos en la expresión génica y un fenotipo cognitivo, ambos cambios se encuentran correlacionados con el déficit local de la acetilación de histonas.
4. La memoria contextual y espacial no requieren ni CBP ni p300 (por separado) en las neuronas excitadoras de telencéfalo. Los ratones dKAT3-ifKO presentan un fenotipo altamente grave, por lo que no nos ha permitido verificar si las proteínas KAT3 son necesarias para este tipo de memoria en general.
5. La implementación de nuevos programas transcripcionales en las neuronas de hipocampo inducida por experiencia y cambios ambientales, requiere CBP pero no p300.
6. Mientras que la pérdida individual de CBP o p300 en las neuronas CaMKIIa⁺ no genera problemas neurológicos evidentes. La pérdida conjunta de las dos proteínas deteriora el bienestar de los animales, así como la tasa de supervivencia.
7. La evaluación de las propiedades electrofisiológicas, morfología y expresión de los marcadores de neuronas en dKAT3-ifKO, demuestran que CBP y p300 son imprescindibles para mantener la identidad neuronal.
8. Solo un alelo de KAT3, independientemente cual, es suficiente para cumplir la funcionalidad de KAT3 como protectoras de la identidad de neuronas. De este modo, CBP y p300 tienen la misma función. Sin embargo, con los experimentos de neuroadaptación hemos observado que en algunas funciones esenciales p300 no puede sustituir a CBP.

9. CBP y p300 se unen a los mismos lugares en el genoma, lo que probablemente explica el solapamiento en sus funciones.
10. La unión con las proteínas bHLH, sus colaboradores principales en neuronas, determina el lugar de unión de CBP y p300 en el genoma.
11. La expresión de un gen hipoacetilado se puede incrementar a través de la unión del dominio KAT de p300, dirigida por el sistema CRISPR. Este efecto se puede producir solo en los *loci* que no habían perdido la accesibilidad de cromatina.
12. Las proteínas KAT3 juntas controlan la expresión de los genes neuronales, tanto conservando los niveles elevados de H3K27ac en los *enhancers* neuronales, como manteniendo la expresión de sus propias anclas – factores de transcripción pro-neuronales bHLH.
13. En conjunto, los descubrimientos descritos en esta tesis enseñan el rol molecular que juegan CBP y p300 en las neuronas excitadoras de telencéfalo. Nuestros resultados demuestran que las proteínas KAT3 tienen una función fundamental en el establecimiento y mantenimiento de los programas transcripcionales, probablemente a través de su rol como acetiltransferasas de lisina.





Biblioteca
UNIVERSITAS Miguel Hernández



Bibliography





BIBLIOGRAPHY

- Alarcon, J. M., Malleret, G., Touzani, K., Vronskaya, S., Ishii, S., Kandel, E. R. and Barco, A. (2004). "Chromatin acetylation, memory, and LTP are impaired in CBP^{+/-} mice: a model for the cognitive deficit in Rubinstein-Taybi syndrome and its amelioration." Neuron **42**(6): 947-959.
- Alari, V., Russo, S., Terragni, B., Ajmone, P. F., Sironi, A., Catusi, I., . . . Larizza, L. (2018). "iPSC-derived neurons of CREBBP- and EP300-mutated Rubinstein-Taybi syndrome patients show morphological alterations and hypoexcitability." Stem Cell Res **30**: 130-140.
- Alberini, C. M. and Kandel, E. R. (2014). "The regulation of transcription in memory consolidation." Cold Spring Harb Perspect Biol **7**(1): a021741.
- Allfrey, V. G., Faulkner, R. and Mirsky, A. E. (1964). "Acetylation and methylation of histones and their possible role in the regulation of RNA synthesis." Proc Natl Acad Sci U S A **51**: 786-794.
- Allis, C. D., Berger, S. L., Cote, J., Dent, S., Jenuwien, T., Kouzarides, T., . . . Zhang, Y. (2007). "New nomenclature for chromatin-modifying enzymes." Cell **131**(4): 633-636.
- Allis, C. D. and Jenuwein, T. (2016). "The molecular hallmarks of epigenetic control." Nat Rev Genet **17**(8): 487-500.
- Alon, S., Vigneault, F., Eminaga, S., Christodoulou, D. C., Seidman, J. G., Church, G. M. and Eisenberg, E. (2011). "Barcoding bias in high-throughput multiplex sequencing of miRNA." Genome Res **21**(9): 1506-1511.
- Amamoto, R., Huerta, V. G., Takahashi, E., Dai, G., Grant, A. K., Fu, Z. and Arlotta, P. (2016). "Adult axolotls can regenerate original neuronal diversity in response to brain injury." Elife **5**.
- Amir, R. E., Van den Veyver, I. B., Wan, M., Tran, C. Q., Francke, U. and Zoghbi, H. Y. (1999). "Rett syndrome is caused by mutations in X-linked MECP2, encoding methyl-CpG-binding protein 2." Nat Genet **23**(2): 185-188.
- Amoutzias, G. D., Robertson, D. L., Van de Peer, Y. and Oliver, S. G. (2008). "Choose your partners: dimerization in eukaryotic transcription factors." Trends Biochem Sci **33**(5): 220-229.
- Anders, S., Pyl, P. T. and Huber, W. (2015). "HTSeq--a Python framework to work with high-throughput sequencing data." Bioinformatics **31**(2): 166-169.
- Andersen, P., Holmqvist, B. and Voorhoeve, P. E. (1966). "Entorhinal Activation of Dentate Granule Cells." **66**(4): 448-460.

- Andrews, F. H., Strahl, B. D. and Kutateladze, T. G. (2016). "Insights into newly discovered marks and readers of epigenetic information." Nat Chem Biol **12**(9): 662-668.
- Arlotta, P. (2018). "Organoids required! A new path to understanding human brain development and disease." Nat Methods **15**(1): 27-29.
- Arner, E., Daub, C. O., Vitting-Seerup, K., Andersson, R., Lilje, B., Drablos, F., . . . Hayashizaki, Y. (2015). "Transcribed enhancers lead waves of coordinated transcription in transitioning mammalian cells." Science **347**(6225): 1010-1014.
- Atlasi, Y. and Stunnenberg, H. G. (2017). "The interplay of epigenetic marks during stem cell differentiation and development." Nat Rev Genet **18**(11): 643-658.
- Ausió, J., Martínez de Paz, A. and Esteller, M. (2014). "MeCP2: the long trip from a chromatin protein to neurological disorders." Trends Mol Med **20**(9): 487-498.
- Azevedo, C. and Saiardi, A. (2016). "Why always lysine? The ongoing tale of one of the most modified amino acids." Adv Biol Regul **60**: 144-150.
- Bailey, T. L. (2002). "Discovering novel sequence motifs with MEME." Curr Protoc Bioinformatics **Chapter 2**: Unit 2 4.
- Bailey, T. L., Johnson, J., Grant, C. E. and Noble, W. S. (2015). "The MEME Suite." Nucleic Acids Res **43**(W1): W39-49.
- Bannister, A. J. and Kouzarides, T. (1996). "The CBP co-activator is a histone acetyltransferase." Nature **384**(6610): 641-643.
- Bannister, A. J. and Kouzarides, T. (2011). "Regulation of chromatin by histone modifications." Cell Res **21**(3): 381-395.
- Barnes, R. M. and Firulli, A. B. (2009). "A twist of insight - the role of Twist-family bHLH factors in development." Int J Dev Biol **53**(7): 909-924.
- Barrett, R. M., Malvaez, M., Kramar, E., Matheos, D. P., Arrizon, A., Cabrera, S. M., . . . Wood, M. A. (2011). "Hippocampal focal knockout of CBP affects specific histone modifications, long-term potentiation, and long-term memory." Neuropsychopharmacology **36**(8): 1545-1556.
- Bayam, E., Sahin, G. S., Guzelsoy, G., Guner, G., Kabakcioglu, A. and Ince-Dunn, G. (2015). "Genome-wide target analysis of NEUROD2 provides new insights into regulation of cortical projection neuron migration and differentiation." BMC Genomics **16**: 681.
- Becker, J. S., McCarthy, R. L., Sidoli, S., Donahue, G., Kaeding, K. E., He, Z., . . . Zaret, K. S. (2017). "Genomic and Proteomic Resolution of Heterochromatin and Its Restriction of Alternate Fate Genes." Mol Cell **68**(6): 1023-1037 e1015.
- Bedford, D. C., Kasper, L. H., Fukuyama, T. and Brindle, P. K. (2010). "Target gene context influences the transcriptional requirement for the KAT3 family of CBP and p300 histone acetyltransferases." Epigenetics **5**(1): 9-15.

- Bedford, D. C., Kasper, L. H., Wang, R., Chang, Y., Green, D. R. and Brindle, P. K. (2011). "Disrupting the CH1 domain structure in the acetyltransferases CBP and p300 results in lean mice with increased metabolic control." Cell Metab **14**(2): 219-230.
- Bedogni, F., Rossi, R. L., Galli, F., Cobolli Gigli, C., Gandaglia, A., Kilstrup-Nielsen, C. and Landsberger, N. (2014). "Rett syndrome and the urge of novel approaches to study MeCP2 functions and mechanisms of action." Neurosci Biobehav Rev **46 Pt 2**: 187-201.
- Ben-Arie, N., Bellen, H. J., Armstrong, D. L., McCall, A. E., Gordadze, P. R., Guo, Q., . . . Zoghbi, H. Y. (1997). "Math1 is essential for genesis of cerebellar granule neurons." Nature **390**(6656): 169-172.
- Benito, E. and Barco, A. (2010). "CREB's control of intrinsic and synaptic plasticity: implications for CREB-dependent memory models." Trends Neurosci **33**(5): 230-240.
- Benito, E. and Barco, A. (2015). "The neuronal activity-driven transcriptome." Mol Neurobiol **51**(3): 1071-1088.
- Benito, E., Urbanke, H., Ramachandran, B., Barth, J., Halder, R., Awasthi, A., . . . Fischer, A. (2015). "HDAC inhibitor-dependent transcriptome and memory reinstatement in cognitive decline models." J Clin Invest **125**(9): 3572-3584.
- Benito, E., Valor, L. M., Jimenez-Minchan, M., Huber, W. and Barco, A. (2011). "cAMP response element-binding protein is a primary hub of activity-driven neuronal gene expression." J Neurosci **31**(50): 18237-18250.
- Berger, S. L., Kouzarides, T., Shiekhattar, R. and Shilatifard, A. (2009). "An operational definition of epigenetics." Genes Dev **23**(7): 781-783.
- Bertrand, N., Castro, D. S. and Guillemot, F. (2002). "Proneural genes and the specification of neural cell types." Nat Rev Neurosci **3**(7): 517-530.
- Bestor, T. H. (1990). "DNA methylation: evolution of a bacterial immune function into a regulator of gene expression and genome structure in higher eukaryotes." Philos Trans R Soc Lond B Biol Sci **326**(1235): 179-187.
- Bickmore, W. A. (2013). "The spatial organization of the human genome." Annu Rev Genomics Hum Genet **14**: 67-84.
- Bishopric, N. H. (2016). The Lysine Acetyltransferases in Cardiovascular Disease. Epigenetics in Cardiac Disease Backs J. and M. T., Springer, Cham: 147-190.
- Bjornsson, H. T. (2015). "The Mendelian disorders of the epigenetic machinery." Genome Res **25**(10): 1473-1481.
- Black, J. C., Mosley, A., Kitada, T., Washburn, M. and Carey, M. (2008). "The SIRT2 deacetylase regulates autoacetylation of p300." Mol Cell **32**(3): 449-455.
- Blahnik, K. R., Dou, L., Echipare, L., Iyengar, S., O'Geen, H., Sanchez, E., . . . Farnham, P. J. (2011). "Characterization of the contradictory chromatin signatures at the 3' exons of zinc finger genes." PLoS One **6**(2): e17121.

- Bogdanović, O. and Veenstra, G. J. (2009). "DNA methylation and methyl-CpG binding proteins: developmental requirements and function." Chromosoma **118**(5): 549-565.
- Bonev, B. and Cavalli, G. (2016). "Organization and function of the 3D genome." Nat Rev Genet **17**(11): 661-678.
- Bonev, B., Mendelson Cohen, N., Szabo, Q., Fritsch, L., Papadopoulos, G. L., Lubling, Y., . . . Cavalli, G. (2017). "Multiscale 3D Genome Rewiring during Mouse Neural Development." Cell **171**(3): 557-572 e524.
- Bonhoure, N., Bounova, G., Bernasconi, D., Praz, V., Lammers, F., Canella, D., . . . Cycli, X. C. (2014). "Quantifying ChIP-seq data: a spiking method providing an internal reference for sample-to-sample normalization." Genome Res **24**(7): 1157-1168.
- Bonn, S., Zinzen, R. P., Girardot, C., Gustafson, E. H., Perez-Gonzalez, A., Delhomme, N., . . . Furlong, E. E. (2012). "Tissue-specific analysis of chromatin state identifies temporal signatures of enhancer activity during embryonic development." Nat Genet **44**(2): 148-156.
- Boquest, A. C., Shahdadfar, A., Fronsdal, K., Sigurjonsson, O., Tunheim, S. H., Collas, P. and Brinchmann, J. E. (2005). "Isolation and transcription profiling of purified uncultured human stromal stem cells: alteration of gene expression after in vitro cell culture." Mol Biol Cell **16**(3): 1131-1141.
- Bordoli, L., Netsch, M., Luthi, U., Lutz, W. and Eckner, R. (2001). "Plant orthologs of p300/CBP: conservation of a core domain in metazoan p300/CBP acetyltransferase-related proteins." Nucleic Acids Res **29**(3): 589-597.
- Bormuth, I. (2016). Roles of bHLH Transcription Factors Neurod1, Neurod2 and Neurod6 in Cerebral Cortex Development and Commissure Formation. Human- und Zahnmedizin. <http://hdl.handle.net/11858/00-1735-0000-0028-8724-4>, University of Göttingen. **PhD**: 141.
- Bormuth, I., Yan, K., Yonemasu, T., Gummert, M., Zhang, M., Wichert, S., . . . Schwab, M. H. (2013). "Neuronal basic helix-loop-helix proteins Neurod2/6 regulate cortical commissure formation before midline interactions." J Neurosci **33**(2): 641-651.
- Bose, D. A., Donahue, G., Reinberg, D., Shiekhattar, R., Bonasio, R. and Berger, S. L. (2017). "RNA Binding to CBP Stimulates Histone Acetylation and Transcription." Cell **168**(1-2): 135-149 e122.
- Bourtchouladze, R., Lidge, R., Catapano, R., Stanley, J., Gossweiler, S., Romashko, D., . . . Tully, T. (2003). "A mouse model of Rubinstein-Taybi syndrome: defective long-term memory is ameliorated by inhibitors of phosphodiesterase 4." Proc Natl Acad Sci U S A **100**(18): 10518-10522.
- Boyer, L. A., Plath, K., Zeitlinger, J., Brambrink, T., Medeiros, L. A., Lee, T. I., . . . Jaenisch, R. (2006). "Polycomb complexes repress developmental regulators in murine embryonic stem cells." Nature **441**(7091): 349-353.

- Boyle, A. P., Davis, S., Shulha, H. P., Meltzer, P., Margulies, E. H., Weng, Z., . . . Crawford, G. E. (2008). "High-resolution mapping and characterization of open chromatin across the genome." Cell **132**(2): 311-322.
- Breen, M. E. and Mapp, A. K. (2018). "Modulating the masters: chemical tools to dissect CBP and p300 function." Curr Opin Chem Biol **45**: 195-203.
- Brown, C. J., Ballabio, A., Rupert, J. L., Lafreniere, R. G., Grompe, M., Tonlorenzi, R. and Willard, H. F. (1991). "A gene from the region of the human X inactivation centre is expressed exclusively from the inactive X chromosome." Nature **349**(6304): 38-44.
- Brulet, R., Matsuda, T., Zhang, L., Miranda, C., Giacca, M., Kaspar, B. K., . . . Hsieh, J. (2017). "NEUROD1 Instructs Neuronal Conversion in Non-Reactive Astrocytes." Stem Cell Reports **8**(6): 1506-1515.
- Buenrostro, J. D., Giresi, P. G., Zaba, L. C., Chang, H. Y. and Greenleaf, W. J. (2013). "Transposition of native chromatin for fast and sensitive epigenomic profiling of open chromatin, DNA-binding proteins and nucleosome position." Nat Methods **10**(12): 1213-1218.
- Buenrostro, J. D., Wu, B., Litzenburger, U. M., Ruff, D., Gonzales, M. L., Snyder, M. P., . . . Greenleaf, W. J. (2015). "Single-cell chromatin accessibility reveals principles of regulatory variation." Nature **523**(7561): 486-490.
- Bulger, M. and Groudine, M. (2010). "Enhancers: the abundance and function of regulatory sequences beyond promoters." Dev Biol **339**(2): 250-257.
- Burgin, K. E., Waxham, M. N., Rickling, S., Westgate, S. A., Mobley, W. C. and Kelly, P. T. (1990). "In situ hybridization histochemistry of Ca²⁺/calmodulin-dependent protein kinase in developing rat brain." J Neurosci **10**(6): 1788-1798.
- Calo, E. and Wysocka, J. (2013). "Modification of enhancer chromatin: what, how, and why?" Mol Cell **49**(5): 825-837.
- Carre, G. A., Siggers, P., Xipolita, M., Brindle, P., Lutz, B., Wells, S. and Greenfield, A. (2018). "Loss of p300 and CBP disrupts histone acetylation at the mouse Sry promoter and causes XY gonadal sex reversal." Hum Mol Genet **27**(1): 190-198.
- Carullo, N. V. N., Simon, R. C., Salisbury, A. J., Revanna, J. S., Bunner, K. D., Savell, K. E., . . . Day, J. J. (2018). "Enhancer RNAs are necessary and sufficient for activity-dependent neuronal gene transcription." bioRxiv(Preprint): 270967.
- Castellanos, N. P. and Makarov, V. A. (2006). "Recovering EEG brain signals: artifact suppression with wavelet enhanced independent component analysis." J Neurosci Methods **158**(2): 300-312.
- Catarino, R. R. and Stark, A. (2018). "Assessing sufficiency and necessity of enhancer activities for gene expression and the mechanisms of transcription activation." Genes Dev **32**(3-4): 202-223.
- Cech, T. R. and Steitz, J. A. (2014). "The noncoding RNA revolution-trashing old rules to forge new ones." Cell **157**(1): 77-94.

Chatterjee, I., Li, F., Kohler, E. E., Rehman, J., Malik, A. B. and Wary, K. K. (2016). "Induced Pluripotent Stem (iPS) Cell Culture Methods and Induction of Differentiation into Endothelial Cells." Methods Mol Biol **1357**: 311-327.

Chen, G., Zou, X., Watanabe, H., van Deursen, J. M. and Shen, J. (2010). "CREB binding protein is required for both short-term and long-term memory formation." J Neurosci **30**(39): 13066-13077.

Chen, J. and Li, Q. (2011). "Life and death of transcriptional co-activator p300." Epigenetics **6**(8): 957-961.

Chen, L. F., Lin, Y. T., Gallegos, D. A., Hazlett, M. F., Gomez-Schiavon, M., Yang, M. G., . . . West, A. E. (2019). "Enhancer Histone Acetylation Modulates Transcriptional Bursting Dynamics of Neuronal Activity-Inducible Genes." Cell Rep **26**(5): 1174-1188 e1175.

Chen, Z. F. and Behringer, R. R. (1995). "twist is required in head mesenchyme for cranial neural tube morphogenesis." Genes Dev **9**(6): 686-699.

Chetverina, D., Fujioka, M., Erokhin, M., Georgiev, P., Jaynes, J. B. and Schedl, P. (2017). "Boundaries of loop domains (insulators): Determinants of chromosome form and function in multicellular eukaryotes." Bioessays **39**(3).

Chrivia, J. C., Kwok, R. P., Lamb, N., Hagiwara, M., Montminy, M. R. and Goodman, R. H. (1993). "Phosphorylated CREB binds specifically to the nuclear protein CBP." Nature **365**(6449): 855-859.

Ciernia, A. V. and LaSalle, J. (2016). "The landscape of DNA methylation amid a perfect storm of autism aetiologies." Nat Rev Neurosci **17**(7): 411-423.

Clapier, C. R. and Cairns, B. R. (2009). "The biology of chromatin remodeling complexes." Annu Rev Biochem **78**: 273-304.

Colquitt, B. M., Allen, W. E., Barnea, G. and Lomvardas, S. (2013). "Alteration of genic 5-hydroxymethylcytosine patterning in olfactory neurons correlates with changes in gene expression and cell identity." Proc Natl Acad Sci U S A **110**(36): 14682-14687.

Consortium, E. P., Birney, E., Stamatoyannopoulos, J. A., Dutta, A., Guigo, R., Gingeras, T. R., . . . de Jong, P. J. (2007). "Identification and analysis of functional elements in 1% of the human genome by the ENCODE pilot project." Nature **447**(7146): 799-816.

Consortium, E. P., Dunham, I., Kundaje, A., Aldred, S. F., Collins, P. J., Davis, C. A., . . . Birney, E. (2012). "An integrated encyclopedia of DNA elements in the human genome." Nature **489**: 57.

Contreras-Martos, S., Piai, A., Kosol, S., Varadi, M., Bekesi, A., Lebrun, P., . . . Tompa, P. (2017). "Linking functions: an additional role for an intrinsically disordered linker domain in the transcriptional coactivator CBP." Sci Rep **7**(1): 4676.

- Crawford, G. E., Holt, I. E., Whittle, J., Webb, B. D., Tai, D., Davis, S., . . . Collins, F. S. (2006). "Genome-wide mapping of DNase hypersensitive sites using massively parallel signature sequencing (MPSS)." Genome Res **16**(1): 123-131.
- Creyghton, M. P., Cheng, A. W., Welstead, G. G., Kooistra, T., Carey, B. W., Steine, E. J., . . . Jaenisch, R. (2010). "Histone H3K27ac separates active from poised enhancers and predicts developmental state." Proc Natl Acad Sci U S A **107**(50): 21931-21936.
- Cui, P., Lin, Q., Ding, F., Xin, C., Gong, W., Zhang, L., . . . Yu, J. (2010). "A comparison between ribo-minus RNA-sequencing and polyA-selected RNA-sequencing." Genomics **96**(5): 259-265.
- Daily, D. K., Ardinger, H. H. and Holmes, G. E. (2000). "Identification and evaluation of mental retardation." Am Fam Physician **61**(4): 1059-1067, 1070.
- Dancy, B. M. and Cole, P. A. (2015). "Protein lysine acetylation by p300/CBP." Chem Rev **115**(6): 2419-2452.
- Davis, R. L., Weintraub, H. and Lassar, A. B. (1987). "Expression of a single transfected cDNA converts fibroblasts to myoblasts." Cell **51**(6): 987-1000.
- Day, J. J. and Sweatt, J. D. (2011). "Epigenetic mechanisms in cognition." Neuron **70**(5): 813-829.
- Del Blanco, B. and Barco, A. (2018). "Impact of environmental conditions and chemicals on the neuronal epigenome." Curr Opin Chem Biol **45**: 157-165.
- Del Blanco, B., Guiretti, D., Tomasoni, R., Lopez-Cascales, M. T., Muñoz-Viana, R., Lipinski, M., . . . Barco, A. (2019). "CBP and SRF co-regulate dendritic growth and synaptic maturation." Cell Death Differ.
- Delorenzo, R. J. and Morris, T. A. (1999). "Long-Term Modulation of Gene Expression in Epilepsy." The Neuroscientist **5**(2): 86-99.
- Deneris, E. S. and Hobert, O. (2014). "Maintenance of postmitotic neuronal cell identity." Nat Neurosci **17**(7): 899-907.
- Deng, W., Lee, J., Wang, H., Miller, J., Reik, A., Gregory, P. D., . . . Blobel, G. A. (2012). "Controlling long-range genomic interactions at a native locus by targeted tethering of a looping factor." Cell **149**(6): 1233-1244.
- Deng, W., Rupon, J. W., Krivega, I., Breda, L., Motta, I., Jahn, K. S., . . . Blobel, G. A. (2014). "Reactivation of developmentally silenced globin genes by forced chromatin looping." Cell **158**(4): 849-860.
- Dennis, D. J., Han, S. and Schuurmans, C. (2019). "bHLH transcription factors in neural development, disease, and reprogramming." Brain Res **1705**: 48-65.
- Dhalluin, C., Carlson, J. E., Zeng, L., He, C., Aggarwal, A. K. and Zhou, M. M. (1999). "Structure and ligand of a histone acetyltransferase bromodomain." Nature **399**(6735): 491-496.

- Dornan, D., Shimizu, H., Perkins, N. D. and Hupp, T. R. (2003). "DNA-dependent acetylation of p53 by the transcription coactivator p300." *J Biol Chem* **278**(15): 13431-13441.
- Draizen, E. J., Shaytan, A. K., Marino-Ramirez, L., Talbert, P. B., Landsman, D. and Panchenko, A. R. (2016). "HistoneDB 2.0: a histone database with variants--an integrated resource to explore histones and their variants." *Database (Oxford)* **2016**.
- Dyson, H. J. and Wright, P. E. (2016). "Role of Intrinsic Protein Disorder in the Function and Interactions of the Transcriptional Coactivators CREB-binding Protein (CBP) and p300." *J Biol Chem* **291**(13): 6714-6722.
- Eberharter, A. and Becker, P. B. (2002). "Histone acetylation: a switch between repressive and permissive chromatin. Second in review series on chromatin dynamics." *EMBO Rep* **3**(3): 224-229.
- Eckner, R., Ewen, M. E., Newsome, D., Gerdes, M., DeCaprio, J. A., Lawrence, J. B. and Livingston, D. M. (1994). "Molecular cloning and functional analysis of the adenovirus E1A-associated 300-kD protein (p300) reveals a protein with properties of a transcriptional adaptor." *Genes Dev* **8**(8): 869-884.
- Edwards, S. R. and Johnson, T. L. (2019). "Intron RNA sequences help yeast cells to survive starvation." *Nature* **565**(7741): 578-579.
- Egan, B., Yuan, C. C., Craske, M. L., Labhart, P., Guler, G. D., Arnott, D., . . . Trojer, P. (2016). "An Alternative Approach to ChIP-Seq Normalization Enables Detection of Genome-Wide Changes in Histone H3 Lysine 27 Trimethylation upon EZH2 Inhibition." *PLoS One* **11**(11): e0166438.
- Erdmann, G., Schutz, G. and Berger, S. (2007). "Inducible gene inactivation in neurons of the adult mouse forebrain." *BMC Neurosci* **8**: 63.
- Ezhkova, E., Pasolli, H. A., Parker, J. S., Stokes, N., Su, I. H., Hannon, G., . . . Fuchs, E. (2009). "Ezh2 orchestrates gene expression for the stepwise differentiation of tissue-specific stem cells." *Cell* **136**(6): 1122-1135.
- Fahrner, J. A. and Bjornsson, H. T. (2014). "Mendelian disorders of the epigenetic machinery: tipping the balance of chromatin states." *Annu Rev Genomics Hum Genet* **15**: 269-293.
- Fang, F., Xu, Y., Chew, K. K., Chen, X., Ng, H. H. and Matsudaira, P. (2014). "Coactivators p300 and CBP maintain the identity of mouse embryonic stem cells by mediating long-range chromatin structure." *Stem Cells* **32**(7): 1805-1816.
- Farah, M. H., Olson, J. M., Sucic, H. B., Hume, R. I., Tapscott, S. J. and Turner, D. L. (2000). "Generation of neurons by transient expression of neural bHLH proteins in mammalian cells." *Development* **127**(4): 693-702.
- Fauquier, L., Azzag, K., Parra, M. A. M., Quillien, A., Boulet, M., Diouf, S., . . . Vandell, L. (2018). "CBP and P300 regulate distinct gene networks required for human primary myoblast differentiation and muscle integrity." *Sci Rep* **8**(1): 12629.

- Fergelot, P., Van Belzen, M., Van Gils, J., Afenjar, A., Armour, C. M., Arveiler, B., . . . Hennekam, R. C. (2016). "Phenotype and genotype in 52 patients with Rubinstein-Taybi syndrome caused by EP300 mutations." Am J Med Genet A **170**(12): 3069-3082.
- Fernandez-Albert, J., Lipinski, M., Lopez-Cascales, M. T., Rowley, M. J., Martin-Gonzalez, A. M., Del Blanco, B., . . . Barco, A. (2019). "Integrative multi-omic analysis unveils the immediate and deferred epigenomic signature of neuronal activation." (Submitted).
- Finch, J. T. and Klug, A. (1976). "Solenoidal model for superstructure in chromatin." Proc Natl Acad Sci U S A **73**(6): 1897-1901.
- Fiorenza, A. and Barco, A. (2016). "Role of Dicer and the miRNA system in neuronal plasticity and brain function." Neurobiol Learn Mem **135**: 3-12.
- Fiorenza, A., Lopez-Atalaya, J. P., Rovira, V., Scandaglia, M., Geijo-Barrientos, E. and Barco, A. (2016). "Blocking miRNA Biogenesis in Adult Forebrain Neurons Enhances Seizure Susceptibility, Fear Memory, and Food Intake by Increasing Neuronal Responsiveness." Cereb Cortex **26**(4): 1619-1633.
- Fischer, A. (2016). "Environmental enrichment as a method to improve cognitive function. What can we learn from animal models?" Neuroimage **131**: 42-47.
- Flames, N. and Hobert, O. (2011). "Transcriptional control of the terminal fate of monoaminergic neurons." Annu Rev Neurosci **34**: 153-184.
- Flavell, S. W. and Greenberg, M. E. (2008). "Signaling mechanisms linking neuronal activity to gene expression and plasticity of the nervous system." Annu Rev Neurosci **31**: 563-590.
- Flemming, W. (1882). Zellsubstanz, Kern und Zelltheilung. Leipzig, F.C.W. Vogel.
- Fode, C., Gradwohl, G., Morin, X., Dierich, A., LeMeur, M., Golidis, C. and Guillemot, F. (1998). "The bHLH protein NEUROGENIN 2 is a determination factor for epibranchial placode-derived sensory neurons." Neuron **20**(3): 483-494.
- Fode, C., Ma, Q., Casarosa, S., Ang, S. L., Anderson, D. J. and Guillemot, F. (2000). "A role for neural determination genes in specifying the dorsoventral identity of telencephalic neurons." Genes Dev **14**(1): 67-80.
- Fujii, G., Tsuchiya, R., Itoh, Y., Tashiro, K. and Hirohashi, S. (1998). "Molecular cloning and expression of Xenopus p300/CBP." Biochim Biophys Acta **1443**(1-2): 41-54.
- Fukuda, S., Kondo, T., Takebayashi, H. and Taga, T. (2004). "Negative regulatory effect of an oligodendrocytic bHLH factor OLIG2 on the astrocytic differentiation pathway." Cell Death Differ **11**(2): 196-202.
- Gabel, H. W., Kinde, B., Stroud, H., Gilbert, C. S., Harmin, D. A., Kastan, N. R., . . . Greenberg, M. E. (2015). "Disruption of DNA-methylation-dependent long gene repression in Rett syndrome." Nature **522**(7554): 89-93.

- Galonska, C., Charlton, J., Mattei, A. L., Donaghey, J., Clement, K., Gu, H., . . . Meissner, A. (2018). "Genome-wide tracking of dCas9-methyltransferase footprints." *Nature Communications* **9**(1): 597.
- Galvão-Ferreira, P., Lipinski, M., Santos, F., Barco, A. and Costa, R. M. (2017). "Skill Learning Modulates RNA Pol II Poising at Immediate Early Genes in the Adult Striatum." *eNeuro* **4**(2).
- Gasper, W. C., Marinov, G. K., Pauli-Behn, F., Scott, M. T., Newberry, K., DeSalvo, G., . . . Wold, B. J. (2014). "Fully automated high-throughput chromatin immunoprecipitation for CHIP-seq: identifying CHIP-quality p300 monoclonal antibodies." *Sci Rep* **4**: 5152.
- Gerber, T., Murawala, P., Knapp, D., Masselink, W., Schuez, M., Hermann, S., . . . Treutlein, B. (2018). "Single-cell analysis uncovers convergence of cell identities during axolotl limb regeneration." *Science* **362**(6413).
- Ghezzi, A., Li, X., Lew, L. K., Wijesekera, T. P. and Atkinson, N. S. (2017). "Alcohol-Induced Neuroadaptation Is Orchestrated by the Histone Acetyltransferase CBP." *Front Mol Neurosci* **10**: 103.
- Gilbert, W. V., Bell, T. A. and Schaening, C. (2016). "Messenger RNA modifications: Form, distribution, and function." *Science* **352**(6292): 1408-1412.
- Giles, R. H., Dauwerse, H. G., van Ommen, G. J. and Breuning, M. H. (1998). "Do human chromosomal bands 16p13 and 22q11-13 share ancestral origins?" *Am J Hum Genet* **63**(4): 1240-1242.
- Giordano, A. and Avantaggiati, M. L. (1999). "p300 and CBP: partners for life and death." *J Cell Physiol* **181**(2): 218-230.
- Goebbels, S., Bode, U., Pieper, A., Funfschilling, U., Schwab, M. H. and Nave, K. A. (2005). "Cre/loxP-mediated inactivation of the bHLH transcription factor gene *NeuroD/BETA2*." *Genesis* **42**(4): 247-252.
- Gomez, R. A., Pentz, E. S., Jin, X., Cordaillat, M. and Sequeira Lopez, M. L. S. (2009). "CBP and p300 are essential for renin cell identity and morphological integrity of the kidney." *American Journal of Physiology-Heart and Circulatory Physiology* **296**(5): H1255-H1262.
- Goodman, R. H. and Smolik, S. (2000). "CBP/p300 in cell growth, transformation, and development." *Genes Dev* **14**(13): 1553-1577.
- Graff, J. and Tsai, L. H. (2013). "The potential of HDAC inhibitors as cognitive enhancers." *Annu Rev Pharmacol Toxicol* **53**: 311-330.
- Gräff, J. and Tsai, L. H. (2013). "Histone acetylation: molecular mnemonics on the chromatin." *Nat Rev Neurosci* **14**: 97.
- Green, E. D., Watson, J. D. and Collins, F. S. (2015). "Human Genome Project: Twenty-five years of big biology." *Nature* **526**(7571): 29-31.

- Grégoire, C.-A., Tobin, S., Goldenstein, B. L., Samarut, É., Leclerc, A., Aumont, A., . . . Fernandes, K. J. L. (2018). "RNA-Sequencing Reveals Unique Transcriptional Signatures of Running and Running-Independent Environmental Enrichment in the Adult Mouse Dentate Gyrus." Front Mol Neurosci **11**(126).
- Gu, W. and Roeder, R. G. (1997). "Activation of p53 sequence-specific DNA binding by acetylation of the p53 C-terminal domain." Cell **90**(4): 595-606.
- Guan, K. L. and Xiong, Y. (2011). "Regulation of intermediary metabolism by protein acetylation." Trends Biochem Sci **36**(2): 108-116.
- Guan, Z., Giustetto, M., Lomvardas, S., Kim, J. H., Miniaci, M. C., Schwartz, J. H., . . . Kandel, E. R. (2002). "Integration of long-term-memory-related synaptic plasticity involves bidirectional regulation of gene expression and chromatin structure." Cell **111**(4): 483-493.
- Guertin, M. J., Cullen, A. E., Markowetz, F. and Holding, A. N. (2018). "Parallel factor ChIP provides essential internal control for quantitative differential ChIP-seq." Nucleic Acids Res **46**(12): e75.
- Guy, J., Gan, J., Selfridge, J., Cobb, S. and Bird, A. (2007). "Reversal of neurological defects in a mouse model of Rett syndrome." Science **315**(5815): 1143-1147.
- Habib, N., Li, Y., Heidenreich, M., Swiech, L., Avraham-Davidi, I., Trombetta, J. J., . . . Regev, A. (2016). "Div-Seq: Single-nucleus RNA-Seq reveals dynamics of rare adult newborn neurons." Science **353**(6302): 925-928.
- Halder, R., Hennion, M., Vidal, R. O., Shomroni, O., Rahman, R. U., Rajput, A., . . . Bonn, S. (2016). "DNA methylation changes in plasticity genes accompany the formation and maintenance of memory." Nat Neurosci **19**(1): 102-110.
- Hamamori, Y., Sartorelli, V., Ogryzko, V., Puri, P. L., Wu, H. Y., Wang, J. Y., . . . Kedes, L. (1999). "Regulation of histone acetyltransferases p300 and PCAF by the bHLH protein twist and adenoviral oncoprotein E1A." Cell **96**(3): 405-413.
- Hamazaki, T., El Rouby, N., Fredette, N. C., Santostefano, K. E. and Terada, N. (2017). "Concise Review: Induced Pluripotent Stem Cell Research in the Era of Precision Medicine." Stem Cells **35**(3): 545-550.
- Hardingham, G. E., Chawla, S., Cruzalegui, F. H. and Bading, H. (1999). "Control of recruitment and transcription-activating function of CBP determines gene regulation by NMDA receptors and L-type calcium channels." Neuron **22**(4): 789-798.
- He, Y. and Ecker, J. R. (2015). "Non-CG Methylation in the Human Genome." Annu Rev Genomics Hum Genet **16**: 55-77.
- He, Y. F., Li, B. Z., Li, Z., Liu, P., Wang, Y., Tang, Q., . . . Xu, G. L. (2011). "Tet-mediated formation of 5-carboxylecytosine and its excision by TDG in mammalian DNA." Science **333**(6047): 1303-1307.

- Heinrich, C., Blum, R., Gascon, S., Masserdotti, G., Tripathi, P., Sanchez, R., . . . Berninger, B. (2010). "Directing astroglia from the cerebral cortex into subtype specific functional neurons." PLoS Biol **8**(5): e1000373.
- Heintzman, N. D., Hon, G. C., Hawkins, R. D., Kheradpour, P., Stark, A., Harp, L. F., . . . Ren, B. (2009). "Histone modifications at human enhancers reflect global cell-type-specific gene expression." Nature **459**(7243): 108-112.
- Heinz, S., Romanoski, C. E., Benner, C. and Glass, C. K. (2015). "The selection and function of cell type-specific enhancers." Nat Rev Mol Cell Biol **16**(3): 144-154.
- Henikoff, S. and Smith, M. M. (2015). "Histone variants and epigenetics." Cold Spring Harb Perspect Biol **7**(1): a019364.
- Hennekam, R. C. (2006). "Rubinstein-Taybi syndrome." Eur J Hum Genet **14**(9): 981-985.
- Hennig, A. K., Peng, G. H. and Chen, S. (2013). "Transcription coactivators p300 and CBP are necessary for photoreceptor-specific chromatin organization and gene expression." PLoS One **8**(7): e69721.
- Henry, R. A., Kuo, Y. M. and Andrews, A. J. (2013). "Differences in specificity and selectivity between CBP and p300 acetylation of histone H3 and H3/H4." Biochemistry **52**(34): 5746-5759.
- Herreras, O., Makarova, J. and Makarov, V. A. (2015). "New uses of LFPs: Pathway-specific threads obtained through spatial discrimination." Neuroscience **310**: 486-503.
- Hilton, I. B., D'Ippolito, A. M., Vockley, C. M., Thakore, P. I., Crawford, G. E., Reddy, T. E. and Gersbach, C. A. (2015). "Epigenome editing by a CRISPR-Cas9-based acetyltransferase activates genes from promoters and enhancers." Nature Biotechnology **33**(5): 510-517.
- Hnisz, D., Abraham, B. J., Lee, T. I., Lau, A., Saint-Andre, V., Sigova, A. A., . . . Young, R. A. (2013). "Super-enhancers in the control of cell identity and disease." Cell **155**(4): 934-947.
- Hobert, O. (2016). "Terminal Selectors of Neuronal Identity." Curr Top Dev Biol **116**: 455-475.
- Holmberg, J. and Perlmann, T. (2012). "Maintaining differentiated cellular identity." Nat Rev Genet **13**: 429.
- Holoch, D. and Margueron, R. (2017). "Mechanisms Regulating PRC2 Recruitment and Enzymatic Activity." Trends Biochem Sci **42**(7): 531-542.
- Hota, S. K. and Bruneau, B. G. (2016). "ATP-dependent chromatin remodeling during mammalian development." Development **143**(16): 2882-2897.
- Hottiger, M. O., Felzien, L. K. and Nabel, G. J. (1998). "Modulation of cytokine-induced HIV gene expression by competitive binding of transcription factors to the coactivator p300." Embo j **17**(11): 3124-3134.

- Hsieh, C. L., Fei, T., Chen, Y., Li, T., Gao, Y., Wang, X., . . . Kantoff, P. W. (2014). "Enhancer RNAs participate in androgen receptor-driven looping that selectively enhances gene activation." Proc Natl Acad Sci U S A **111**(20): 7319-7324.
- Hu, S. C., Chrivia, J. and Ghosh, A. (1999). "Regulation of CBP-mediated transcription by neuronal calcium signaling." Neuron **22**(4): 799-808.
- Huang, H., Sabari, B. R., Garcia, B. A., Allis, C. D. and Zhao, Y. (2014). "SnapShot: histone modifications." Cell **159**(2): 458-458 e451.
- Huang, H., Tang, S., Ji, M., Tang, Z., Shimada, M., Liu, X., . . . Li, X. (2018a). "EP300-Mediated Lysine 2-Hydroxyisobutyrylation Regulates Glycolysis." Mol Cell **70**(4): 663-678 e666.
- Huang, H., Zhang, D., Wang, Y., Perez-Neut, M., Han, Z., Zheng, Y. G., . . . Zhao, Y. (2018b). "Lysine benzoylation is a histone mark regulated by SIRT2." Nat Commun **9**(1): 3374.
- Huang, R. C. and Bonner, J. (1962). "Histone, a suppressor of chromosomal RNA synthesis." Proc Natl Acad Sci U S A **48**: 1216-1222.
- Hutson, T. H., Kathe, C., Palmisano, I., Bartholdi, K., Hervera, A., De Virgiliis, F., . . . Di Giovanni, S. (2019). "Cbp-dependent histone acetylation mediates axon regeneration induced by environmental enrichment in rodent spinal cord injury models." Sci Transl Med **11**(487).
- Impey, S., Fong, A. L., Wang, Y., Cardinaux, J. R., Fass, D. M., Obrietan, K., . . . Goodman, R. H. (2002). "Phosphorylation of CBP mediates transcriptional activation by neural activity and CaM kinase IV." Neuron **34**(2): 235-244.
- Ip, J. P. K., Mellios, N. and Sur, M. (2018). "Rett syndrome: insights into genetic, molecular and circuit mechanisms." Nat Rev Neurosci **19**(6): 368-382.
- Ito, S., Magalska, A., Alcaraz-Iborra, M., Lopez-Atalaya, J. P., Rovira, V., Contreras-Moreira, B., . . . Barco, A. (2014). "Loss of neuronal 3D chromatin organization causes transcriptional and behavioural deficits related to serotonergic dysfunction." Nat Commun **5**: 4450.
- Ito, S., Shen, L., Dai, Q., Wu, S. C., Collins, L. B., Swenberg, J. A., . . . Zhang, Y. (2011). "Tet proteins can convert 5-methylcytosine to 5-formylcytosine and 5-carboxylcytosine." Science **333**(6047): 1300-1303.
- Iwafuchi-Doi, M. and Zaret, K. S. (2016). "Cell fate control by pioneer transcription factors." Development **143**(11): 1833-1837.
- Jenuwein, T. and Allis, C. D. (2001). "Translating the histone code." Science **293**(5532): 1074-1080.
- Jin, Q., Yu, L. R., Wang, L., Zhang, Z., Kasper, L. H., Lee, J. E., . . . Ge, K. (2011). "Distinct roles of GCN5/PCAF-mediated H3K9ac and CBP/p300-mediated H3K18/27ac in nuclear receptor transactivation." Embo j **30**(2): 249-262.

- Johannsen, W. (1905). Arvelighedslærens Elementer, Kbh. : Gyldendal.
- Jones, S. (2004). "An overview of the basic helix-loop-helix proteins." Genome Biol **5**(6): 226.
- Joo, J. Y., Schaukowitch, K., Farbiak, L., Kilaru, G. and Kim, T. K. (2016). "Stimulus-specific combinatorial functionality of neuronal c-fos enhancers." Nat Neurosci **19**(1): 75-83.
- Jopling, C., Boue, S. and Izpisua Belmonte, J. C. (2011). "Dedifferentiation, transdifferentiation and reprogramming: three routes to regeneration." Nat Rev Mol Cell Biol **12**(2): 79-89.
- Jopling, C., Sleep, E., Raya, M., Marti, M., Raya, A. and Izpisua Belmonte, J. C. (2010). "Zebrafish heart regeneration occurs by cardiomyocyte dedifferentiation and proliferation." Nature **464**(7288): 606-609.
- Kaczmarek, Z., Ortega, E., Goudarzi, A., Huang, H., Kim, S., Marquez, J. A., . . . Panne, D. (2017). "Structure of p300 in complex with acyl-CoA variants." Nat Chem Biol **13**(1): 21-29.
- Kalkhoven, E. (2004). "CBP and p300: HATs for different occasions." Biochem Pharmacol **68**(6): 1145-1155.
- Kamei, Y., Xu, L., Heinzl, T., Torchia, J., Kurokawa, R., Gloss, B., . . . Rosenfeld, M. G. (1996). "A CBP integrator complex mediates transcriptional activation and AP-1 inhibition by nuclear receptors." Cell **85**(3): 403-414.
- Karanam, B., Jiang, L., Wang, L., Kelleher, N. L. and Cole, P. A. (2006). "Kinetic and mass spectrometric analysis of p300 histone acetyltransferase domain autoacetylation." J Biol Chem **281**(52): 40292-40301.
- Karmodiya, K., Krebs, A. R., Oulad-Abdelghani, M., Kimura, H. and Tora, L. (2012). "H3K9 and H3K14 acetylation co-occur at many gene regulatory elements, while H3K14ac marks a subset of inactive inducible promoters in mouse embryonic stem cells." BMC Genomics **13**: 424-424.
- Karukurichi, K. R. and Cole, P. A. (2011). "Probing the reaction coordinate of the p300/CBP histone acetyltransferase with bisubstrate analogs." Bioorg Chem **39**(1): 42-47.
- Kasper, L. H., Fukuyama, T., Biesen, M. A., Boussouar, F., Tong, C., de Pauw, A., . . . Brindle, P. K. (2006). "Conditional knockout mice reveal distinct functions for the global transcriptional coactivators CBP and p300 in T-cell development." Mol Cell Biol **26**(3): 789-809.
- Kasper, L. H., Qu, C., Obenaus, J. C., McGoldrick, D. J. and Brindle, P. K. (2014). "Genome-wide and single-cell analyses reveal a context dependent relationship between CBP recruitment and gene expression." Nucleic Acids Res **42**(18): 11363-11382.

- Kawasaki, H., Eckner, R., Yao, T. P., Taira, K., Chiu, R., Livingston, D. M. and Yokoyama, K. K. (1998). "Distinct roles of the co-activators p300 and CBP in retinoic-acid-induced F9-cell differentiation." Nature **393**(6682): 284-289.
- Kaypee, S., Sahadevan, S. A., Patil, S., Ghosh, P., Roy, N. S., Roy, S. and Kundu, T. K. (2018). "Mutant and Wild-Type Tumor Suppressor p53 Induces p300 Autoacetylation." iScience **4**: 260-272.
- Kazantsev, A. G. and Thompson, L. M. (2008). "Therapeutic application of histone deacetylase inhibitors for central nervous system disorders." Nat Rev Drug Discov **7**(10): 854-868.
- Kee, B. L., Arias, J. and Montminy, M. R. (1996). "Adaptor-mediated recruitment of RNA polymerase II to a signal-dependent activator." J Biol Chem **271**(5): 2373-2375.
- Keene, M. A., Corces, V., Lowenhaupt, K. and Elgin, S. C. (1981). "DNase I hypersensitive sites in Drosophila chromatin occur at the 5' ends of regions of transcription." Proc Natl Acad Sci U S A **78**(1): 143-146.
- Kim, D., Langmead, B. and Salzberg, S. L. (2015a). "HISAT: a fast spliced aligner with low memory requirements." Nat Methods **12**(4): 357-360.
- Kim, T. K., Hemberg, M. and Gray, J. M. (2015b). "Enhancer RNAs: a class of long noncoding RNAs synthesized at enhancers." Cold Spring Harb Perspect Biol **7**(1): a018622.
- Kim, T. K., Hemberg, M., Gray, J. M., Costa, A. M., Bear, D. M., Wu, J., . . . Greenberg, M. E. (2010). "Widespread transcription at neuronal activity-regulated enhancers." Nature **465**(7295): 182-187.
- Kirshenbaum, L. A. and Schneider, M. D. (1995). "Adenovirus E1A represses cardiac gene transcription and reactivates DNA synthesis in ventricular myocytes, via alternative pocket protein- and p300-binding domains." J Biol Chem **270**(14): 7791-7794.
- Kojima, N., Wang, J., Mansuy, I. M., Grant, S. G., Mayford, M. and Kandel, E. R. (1997). "Rescuing impairment of long-term potentiation in fyn-deficient mice by introducing Fyn transgene." Proc Natl Acad Sci U S A **94**(9): 4761-4765.
- Kornberg, R. D. (1974). "Chromatin structure: a repeating unit of histones and DNA." Science **184**(4139): 868-871.
- Korzus, E., Rosenfeld, M. G. and Mayford, M. (2004). "CBP Histone Acetyltransferase Activity Is a Critical Component of Memory Consolidation." Neuron **42**(6): 961-972.
- Kouzarides, T. (2007). "Chromatin modifications and their function." Cell **128**(4): 693-705.
- Krämer, O. H., Baus, D., Knauer, S. K., Stein, S., Jäger, E., Stauber, R. H., . . . Heinzl, T. (2006). "Acetylation of Stat1 modulates NF-kappaB activity." Genes Dev **20**(4): 473-485.

- Kruger, K., Grabowski, P. J., Zaug, A. J., Sands, J., Gottschling, D. E. and Cech, T. R. (1982). "Self-splicing RNA: autoexcision and autocyclization of the ribosomal RNA intervening sequence of Tetrahymena." Cell **31**(1): 147-157.
- Kung, A. L., Rebel, V. I., Bronson, R. T., Ch'ng, L. E., Sieff, C. A., Livingston, D. M. and Yao, T. P. (2000). "Gene dose-dependent control of hematopoiesis and hematologic tumor suppression by CBP." Genes Dev **14**(3): 272-277.
- Lamarck, J. B. (1809). Philosophie zoologique, ou exposition des considérations relatives à l'histoire naturelle des animaux., Musée d'Histoire Naturelle
- Landt, S. G., Marinov, G. K., Kundaje, A., Kheradpour, P., Pauli, F., Batzoglou, S., . . . Snyder, M. (2012). "ChIP-seq guidelines and practices of the ENCODE and modENCODE consortia." Genome Res **22**(9): 1813-1831.
- Langmead, B. and Salzberg, S. L. (2012). "Fast gapped-read alignment with Bowtie 2." Nat Methods **9**(4): 357-359.
- Längst, G. and Manelyte, L. (2015). "Chromatin Remodelers: From Function to Dysfunction." Genes (Basel) **6**(2): 299-324.
- Lassar, A. B., Paterson, B. M. and Weintraub, H. (1986). "Transfection of a DNA locus that mediates the conversion of 10T1/2 fibroblasts to myoblasts." Cell **47**(5): 649-656.
- Lee, R. C., Feinbaum, R. L. and Ambros, V. (1993). "The C. elegans heterochronic gene lin-4 encodes small RNAs with antisense complementarity to lin-14." Cell **75**(5): 843-854.
- Lee, S., Lee, B., Lee, J. W. and Lee, S. K. (2009). "Retinoid signaling and neurogenin2 function are coupled for the specification of spinal motor neurons through a chromatin modifier CBP." Neuron **62**(5): 641-654.
- Liang, D. and Seyfried, T. N. (2001). "Genes differentially expressed in the kindled mouse brain." Brain Res Mol Brain Res **96**(1-2): 94-102.
- Lilja, K. C., Zhang, N., Magli, A., Gunduz, V., Bowman, C. J., Arpke, R. W., . . . Dynlacht, B. D. (2017). "Pax7 remodels the chromatin landscape in skeletal muscle stem cells." PLoS One **12**(4).
- Lipinski, M., Del Blanco, B. and Barco, A. (2019). "CBP/p300 in brain development and plasticity: Disentangling the KAT's cradle." Curr Opin Neurobiol(Accepted).
- Lister, R., Pelizzola, M., Dowen, R. H., Hawkins, R. D., Hon, G., Tonti-Filippini, J., . . . Ecker, J. R. (2009). "Human DNA methylomes at base resolution show widespread epigenomic differences." Nature **462**(7271): 315-322.
- Liu, X., Wang, L., Zhao, K., Thompson, P. R., Hwang, Y., Marmorstein, R. and Cole, P. A. (2008). "The structural basis of protein acetylation by the p300/CBP transcriptional coactivator." Nature **451**(7180): 846-850.
- Lo, A. and Qi, L. (2017). "Genetic and epigenetic control of gene expression by CRISPR-Cas systems." F1000Res **6**.

- Lopez-Atalaya, J. P. and Barco, A. (2014). "Can changes in histone acetylation contribute to memory formation?" Trends Genet **30**(12): 529-539.
- Lopez-Atalaya, J. P., Ciccarelli, A., Viosca, J., Valor, L. M., Jimenez-Minchan, M., Canals, S., . . . Barco, A. (2011). "CBP is required for environmental enrichment-induced neurogenesis and cognitive enhancement." Embo j **30**(20): 4287-4298.
- Lopez-Atalaya, J. P., Gervasini, C., Mottadelli, F., Spena, S., Piccione, M., Scarano, G., . . . Larizza, L. (2012). "Histone acetylation deficits in lymphoblastoid cell lines from patients with Rubinstein-Taybi syndrome." J Med Genet **49**(1): 66-74.
- Lopez-Atalaya, J. P., Ito, S., Valor, L. M., Benito, E. and Barco, A. (2013). "Genomic targets, and histone acetylation and gene expression profiling of neural HDAC inhibition." Nucleic Acids Res **41**(17): 8072-8084.
- Lopez-Atalaya, J. P., Valor, L. M. and Barco, A. (2014). "Epigenetic factors in intellectual disability: the Rubinstein-Taybi syndrome as a paradigm of neurodevelopmental disorder with epigenetic origin." Prog Mol Biol Transl Sci **128**: 139-176.
- Love, M. I., Huber, W. and Anders, S. (2014). "Moderated estimation of fold change and dispersion for RNA-seq data with DESeq2." Genome Biol **15**(12): 550.
- Lu, Q. R., Yuk, D., Alberta, J. A., Zhu, Z., Pawlitzky, I., Chan, J., . . . Rowitch, D. H. (2000). "Sonic hedgehog--regulated oligodendrocyte lineage genes encoding bHLH proteins in the mammalian central nervous system." Neuron **25**(2): 317-329.
- Luger, K., Dechassa, M. L. and Tremethick, D. J. (2012). "New insights into nucleosome and chromatin structure: an ordered state or a disordered affair?" Nat Rev Mol Cell Biol **13**(7): 436-447.
- Luger, K., Mader, A. W., Richmond, R. K., Sargent, D. F. and Richmond, T. J. (1997). "Crystal structure of the nucleosome core particle at 2.8 Å resolution." Nature **389**(6648): 251-260.
- Maeshima, K., Imai, R., Tamura, S. and Nozaki, T. (2014). "Chromatin as dynamic 10-nm fibers." Chromosoma **123**(3): 225-237.
- Maksimovska, J., Segura-Pena, D., Cole, P. A. and Marmorstein, R. (2014). "Structure of the p300 histone acetyltransferase bound to acetyl-coenzyme A and its analogues." Biochemistry **53**(21): 3415-3422.
- Mall, M., Kareta, M. S., Chanda, S., Ahlenius, H., Perotti, N., Zhou, B., . . . Wernig, M. (2017). "Myt1l safeguards neuronal identity by actively repressing many non-neuronal fates." Nature **544**(7649): 245-249.
- Marmorstein, R. and Zhou, M. M. (2014). "Writers and readers of histone acetylation: structure, mechanism, and inhibition." Cold Spring Harb Perspect Biol **6**(7): a018762.
- Massari, M. E. and Murre, C. (2000). "Helix-loop-helix proteins: regulators of transcription in eucaryotic organisms." Mol Cell Biol **20**(2): 429-440.

- Matsushita, M., Nakatake, Y., Arai, I., Ibata, K., Kohda, K., Goparaju, S. K., . . . Ko, M. S. H. (2017). "Neural differentiation of human embryonic stem cells induced by the transgene-mediated overexpression of single transcription factors." Biochem Biophys Res Commun **490**(2): 296-301.
- Mattar, P., Langevin, L. M., Markham, K., Klenin, N., Shivji, S., Zinyk, D. and Schuurmans, C. (2008). "Basic helix-loop-helix transcription factors cooperate to specify a cortical projection neuron identity." Mol Cell Biol **28**(5): 1456-1469.
- McGhee, J. D., Wood, W. I., Dolan, M., Engel, J. D. and Felsenfeld, G. (1981). "A 200 base pair region at the 5' end of the chicken adult beta-globin gene is accessible to nuclease digestion." Cell **27**(1 Pt 2): 45-55.
- Medrano-Fernandez, A., Delgado-Garcia, J. M., Del Blanco, B., Llinares, M., Sanchez-Campusano, R., Olivares, R., . . . Barco, A. (2018). "The Epigenetic Factor CBP Is Required for the Differentiation and Function of Medial Ganglionic Eminence-Derived Interneurons." Mol Neurobiol.
- Mellen, M., Ayata, P., Dewell, S., Kriaucionis, S. and Heintz, N. (2012). "MeCP2 binds to 5hmC enriched within active genes and accessible chromatin in the nervous system." Cell **151**(7): 1417-1430.
- Mendel, G. (1865). Versuche über Pflanzenhybriden, Verhandlungen des naturforschenden Vereines in Brünn,.
- Merika, M., Williams, A. J., Chen, G., Collins, T. and Thanos, D. (1998). "Recruitment of CBP/p300 by the IFN beta enhanceosome is required for synergistic activation of transcription." Mol Cell **1**(2): 277-287.
- Merk, D. J., Ohli, J., Merk, N. D., Thatikonda, V., Morrissy, S., Schoof, M., . . . Schuller, U. (2018). "Opposing Effects of CREBBP Mutations Govern the Phenotype of Rubinstein-Taybi Syndrome and Adult SHH Medulloblastoma." Dev Cell **44**(6): 709-724 e706.
- Mersfelder, E. L. and Parthun, M. R. (2006). "The tale beyond the tail: histone core domain modifications and the regulation of chromatin structure." Nucleic Acids Res **34**(9): 2653-2662.
- Mews, P., Donahue, G., Drake, A. M., Luczak, V., Abel, T. and Berger, S. L. (2017). "Acetyl-CoA synthetase regulates histone acetylation and hippocampal memory." Nature **546**(7658): 381-386.
- Milani, D., Manzoni, F. M., Pezzani, L., Ajmone, P., Gervasini, C., Menni, F. and Esposito, S. (2015). "Rubinstein-Taybi syndrome: clinical features, genetic basis, diagnosis, and management." Ital J Pediatr **41**: 4.
- Mirsky, R., Woodhoo, A., Parkinson, D. B., Arthur-Farraj, P., Bhaskaran, A. and Jessen, K. R. (2008). "Novel signals controlling embryonic Schwann cell development, myelination and dedifferentiation." J Peripher Nerv Syst **13**(2): 122-135.

- Mirza, N., Appleton, R., Burn, S., du Plessis, D., Duncan, R., Farah, J. O., . . . Pirmohamed, M. (2017). "Genetic regulation of gene expression in the epileptic human hippocampus." Hum Mol Genet **26**(9): 1759-1769.
- Mizuguchi, R., Sugimori, M., Takebayashi, H., Kosako, H., Nagao, M., Yoshida, S., . . . Nakafuku, M. (2001). "Combinatorial roles of olig2 and neurogenin2 in the coordinated induction of pan-neuronal and subtype-specific properties of motoneurons." Neuron **31**(5): 757-771.
- Mo, A., Mukamel, E. A., Davis, F. P., Luo, C., Henry, G. L., Picard, S., . . . Nathans, J. (2015). "Epigenomic Signatures of Neuronal Diversity in the Mammalian Brain." Neuron **86**(6): 1369-1384.
- Monk, D., Mackay, D. J. G., Eggermann, T., Maher, E. R. and Riccio, A. (2019). "Genomic imprinting disorders: lessons on how genome, epigenome and environment interact." Nat Rev Genet.
- Montgomery, D. C., Sorum, A. W. and Meier, J. L. (2015). "Defining the orphan functions of lysine acetyltransferases." ACS Chem Biol **10**(1): 85-94.
- Moreno, C. L., Ehrlich, M. E. and Mobbs, C. V. (2016). "Protection by dietary restriction in the YAC128 mouse model of Huntington's disease: Relation to genes regulating histone acetylation and HTT." Neurobiol Dis **85**: 25-34.
- Morgan, J. T., Fink, G. R. and Bartel, D. P. (2019). "Excised linear introns regulate growth in yeast." Nature **565**(7741): 606-611.
- Morgan, T. H. (1915). The Mechanism of Mendelian Heredity, H. Holt.
- Morris, S. A. (2016). "Direct lineage reprogramming via pioneer factors; a detour through developmental gene regulatory networks." Development **143**(15): 2696-2705.
- Mortazavi, A., Williams, B. A., McCue, K., Schaeffer, L. and Wold, B. (2008). "Mapping and quantifying mammalian transcriptomes by RNA-Seq." Nat Methods **5**(7): 621-628.
- Mousavi, K., Zare, H., Dell'orso, S., Grontved, L., Gutierrez-Cruz, G., Derfoul, A., . . . Sartorelli, V. (2013). "eRNAs promote transcription by establishing chromatin accessibility at defined genomic loci." Mol Cell **51**(5): 606-617.
- Musselman, C. A., Lalonde, M. E., Cote, J. and Kutateladze, T. G. (2012). "Perceiving the epigenetic landscape through histone readers." Nat Struct Mol Biol **19**(12): 1218-1227.
- Mutoh, H., Naya, F. J., Tsai, M. J. and Leiter, A. B. (1998). "The basic helix-loop-helix protein BETA2 interacts with p300 to coordinate differentiation of secretin-expressing enteroendocrine cells." Genes Dev **12**(6): 820-830.
- Mutskov, V., Gerber, D., Angelov, D., Ausio, J., Workman, J. and Dimitrov, S. (1998). "Persistent interactions of core histone tails with nucleosomal DNA following acetylation and transcription factor binding." Mol Cell Biol **18**(11): 6293-6304.

Mymryk, J. S., Lee, R. W. and Bayley, S. T. (1992). "Ability of adenovirus 5 E1A proteins to suppress differentiation of BC3H1 myoblasts correlates with their binding to a 300 kDa cellular protein." Mol Biol Cell **3**(10): 1107-1115.

Ninkovic, J. and Gotz, M. (2018). "Understanding direct neuronal reprogramming-from pioneer factors to 3D chromatin." Curr Opin Genet Dev **52**: 65-69.

Nord, A. S., Blow, M. J., Attanasio, C., Akiyama, J. A., Holt, A., Hosseini, R., . . . Visel, A. (2013). "Rapid and pervasive changes in genome-wide enhancer usage during mammalian development." Cell **155**(7): 1521-1531.

Novitsch, B. G., Chen, A. I. and Jessell, T. M. (2001). "Coordinate regulation of motor neuron subtype identity and pan-neuronal properties by the bHLH repressor Olig2." Neuron **31**(5): 773-789.

Ogryzko, V. V., Schiltz, R. L., Russanova, V., Howard, B. H. and Nakatani, Y. (1996). "The transcriptional coactivators p300 and CBP are histone acetyltransferases." Cell **87**(5): 953-959.

Ohno, S. (1970). Evolution by Gene Duplication. New York, USA, Springer-Verlag New York Inc.

Ohtsuka, T. and Kageyama, R. (2010). The Basic Helix-Loop-Helix Transcription Factors in Neural Differentiation. Cell Cycle Regulation and Differentiation in Cardiovascular and Neural Systems: 15-34.

Oike, Y., Hata, A., Mamiya, T., Kaname, T., Noda, Y., Suzuki, M., . . . Yamamura, K. (1999a). "Truncated CBP protein leads to classical Rubinstein-Taybi syndrome phenotypes in mice: implications for a dominant-negative mechanism." Hum Mol Genet **8**(3): 387-396.

Oike, Y., Takakura, N., Hata, A., Kaname, T., Akizuki, M., Yamaguchi, Y., . . . Suda, T. (1999b). "Mice homozygous for a truncated form of CREB-binding protein exhibit defects in hematopoiesis and vasculo-angiogenesis." Blood **93**(9): 2771-2779.

Okano, M., Xie, S. and Li, E. (1998). "Cloning and characterization of a family of novel mammalian DNA (cytosine-5) methyltransferases." Nat Genet **19**: 219-220.

Olins, D. E. and Olins, A. L. (2003). "Chromatin history: our view from the bridge." Nat Rev Mol Cell Biol **4**(10): 809-814.

Oliveira, A. M., Estevez, M. A., Hawk, J. D., Grimes, S., Brindle, P. K. and Abel, T. (2011). "Subregion-specific p300 conditional knock-out mice exhibit long-term memory impairments." Learn Mem **18**(3): 161-169.

Oliveira, A. M., Wood, M. A., McDonough, C. B. and Abel, T. (2007). "Transgenic mice expressing an inhibitory truncated form of p300 exhibit long-term memory deficits." Learn Mem **14**(9): 564-572.

Olson, J. M., Asakura, A., Snider, L., Hawkes, R., Strand, A., Stoeck, J., . . . Tapscott, S. J. (2001). "NeuroD2 is necessary for development and survival of central nervous system neurons." Dev Biol **234**(1): 174-187.

- Orlando, D. A., Chen, M. W., Brown, V. E., Solanki, S., Choi, Y. J., Olson, E. R., . . . Guenther, M. G. (2014). "Quantitative ChIP-Seq normalization reveals global modulation of the epigenome." *Cell Rep* **9**(3): 1163-1170.
- Ørom, U. A., Derrien, T., Beringer, M., Gumireddy, K., Gardini, A., Bussotti, G., . . . Shiekhhattar, R. (2010). "Long noncoding RNAs with enhancer-like function in human cells." *Cell* **143**(1): 46-58.
- Ortega, E., Rengachari, S., Ibrahim, Z., Hoghoughi, N., Gaucher, J., Holehouse, A. S., . . . Panne, D. (2018). "Transcription factor dimerization activates the p300 acetyltransferase." *Nature* **562**(7728): 538-544.
- Pandey, R., Muller, A., Napoli, C. A., Selinger, D. A., Pikaard, C. S., Richards, E. J., . . . Jorgensen, R. A. (2002). "Analysis of histone acetyltransferase and histone deacetylase families of *Arabidopsis thaliana* suggests functional diversification of chromatin modification among multicellular eukaryotes." *Nucleic Acids Res* **30**(23): 5036-5055.
- Panne, D. (2008). "The enhanceosome." *Curr Opin Struct Biol* **18**(2): 236-242.
- Parenteau, J., Durand, M., Veronneau, S., Lacombe, A. A., Morin, G., Guerin, V., . . . Abou Elela, S. (2008). "Deletion of many yeast introns reveals a minority of genes that require splicing for function." *Mol Biol Cell* **19**(5): 1932-1941.
- Parenteau, J., Maignon, L., Berthoumieux, M., Catala, M., Gagnon, V. and Abou Elela, S. (2019). "Introns are mediators of cell response to starvation." *Nature* **565**(7741): 612-617.
- Partanen, A., Motoyama, J. and Hui, C. C. (1999). "Developmentally regulated expression of the transcriptional cofactors/histone acetyltransferases CBP and p300 during mouse embryogenesis." *Int J Dev Biol* **43**(6): 487-494.
- Pataskar, A., Jung, J., Smialowski, P., Noack, F., Calegari, F., Straub, T. and Tiwari, V. K. (2016). "NeuroD1 reprograms chromatin and transcription factor landscapes to induce the neuronal program." *Embo j* **35**(1): 24-45.
- Patel, D. J. (2016). "A Structural Perspective on Readout of Epigenetic Histone and DNA Methylation Marks." *Cold Spring Harb Perspect Biol* **8**(3): a018754.
- Peixoto, L. and Abel, T. (2012). "The Role of Histone Acetylation in Memory Formation and Cognitive Impairments." *Neuropsychopharmacology* **38**: 62.
- Pennisi, E. (2012). "ENCODE Project Writes Eulogy for Junk DNA." **337**(6099): 1159-1161.
- Pentz, E. S., Cordaillat, M., Carretero, O. A., Tucker, A. E., Sequeira Lopez, M. L. S. and Gomez, R. A. (2012). "Histone acetyl transferases CBP and p300 are necessary for maintenance of renin cell identity and transformation of smooth muscle cells to the renin phenotype." *American Journal of Physiology-Heart and Circulatory Physiology* **302**(12): H2545-H2552.
- Perel, S., Sadtler, P. T., Oby, E. R., Ryu, S. I., Tyler-Kabara, E. C., Batista, A. P. and Chase, S. M. (2015). "Single-unit activity, threshold crossings, and local field potentials

in motor cortex differentially encode reach kinematics." *J Neurophysiol* **114**(3): 1500-1512.

Perez-Lluch, S., Blanco, E., Tilgner, H., Curado, J., Ruiz-Romero, M., Corominas, M. and Guigo, R. (2015). "Absence of canonical marks of active chromatin in developmentally regulated genes." *Nat Genet* **47**(10): 1158-1167.

Perlin, J. B., Gerwin, C. M., Panchision, D. M., Vick, R. S., Jakoi, E. R. and DeLorenzo, R. J. (1993). "Kindling produces long-lasting and selective changes in gene expression of hippocampal neurons." *Proc Natl Acad Sci U S A* **90**(5): 1741-1745.

Polesskaya, A., Duquet, A., Naguibneva, I., Weise, C., Vervisch, A., Bengal, E., . . . Harel-Bellan, A. (2000). "CREB-binding protein/p300 activates MyoD by acetylation." *J Biol Chem* **275**(44): 34359-34364.

Pott, S. and Lieb, J. D. (2015). "What are super-enhancers?" *Nat Genet* **47**(1): 8-12.

Pramparo, T., de Gregori, M., Gimelli, S., Ciccone, R., Frondizi, D., Liehr, T., . . . Guerrini, R. (2008). "A 7 Mb duplication at 22q13 in a girl with bipolar disorder and hippocampal malformation." *Am J Med Genet A* **146A**(13): 1754-1760.

Puri, P. L., Sartorelli, V., Yang, X. J., Hamamori, Y., Ogryzko, V. V., Howard, B. H., . . . Levrero, M. (1997). "Differential roles of p300 and PCAF acetyltransferases in muscle differentiation." *Mol Cell* **1**(1): 35-45.

Qiu, Y., Sharma, A. and Stein, R. (1998). "p300 mediates transcriptional stimulation by the basic helix-loop-helix activators of the insulin gene." *Mol Cell Biol* **18**(5): 2957-2964.

Rada-Iglesias, A., Bajpai, R., Swigut, T., Brugmann, S. A., Flynn, R. A. and Wysocka, J. (2011). "A unique chromatin signature uncovers early developmental enhancers in humans." *Nature* **470**(7333): 279-283.

Raisner, R., Kharbanda, S., Jin, L., Jeng, E., Chan, E., Merchant, M., . . . Gascoigne, K. E. (2018). "Enhancer Activity Requires CBP/P300 Bromodomain-Dependent Histone H3K27 Acetylation." *Cell Rep* **24**(7): 1722-1729.

Rajagopal, N., Ernst, J., Ray, P., Wu, J., Zhang, M., Kellis, M. and Ren, B. (2014). "Distinct and predictive histone lysine acetylation patterns at promoters, enhancers, and gene bodies." *G3 (Bethesda)* **4**(11): 2051-2063.

Ramalho-Santos, M., Yoon, S., Matsuzaki, Y., Mulligan, R. C. and Melton, D. A. (2002). "'Stemness': transcriptional profiling of embryonic and adult stem cells." *Science* **298**(5593): 597-600.

Ramón y Cajal, S. (1909). *Histologie du système nerveux de l'homme & des vertébrés*, Paris : Maloine.

Ramos, Y. F., Hestand, M. S., Verlaan, M., Krabbendam, E., Ariyurek, Y., van Galen, M., . . . t Hoen, P. A. (2010). "Genome-wide assessment of differential roles for p300 and CBP in transcription regulation." *Nucleic Acids Res* **38**(16): 5396-5408.

- Rando, O. J. (2012). "Combinatorial complexity in chromatin structure and function: revisiting the histone code." Curr Opin Genet Dev **22**(2): 148-155.
- Ransohoff, J. D., Wei, Y. and Khavari, P. A. (2018). "The functions and unique features of long intergenic non-coding RNA." Nat Rev Mol Cell Biol **19**(3): 143-157.
- Rao, S. S. P., Huang, S. C., Glenn St Hilaire, B., Engreitz, J. M., Perez, E. M., Kieffer-Kwon, K. R., . . . Aiden, E. L. (2017). "Cohesin Loss Eliminates All Loop Domains." Cell **171**(2): 305-320 e324.
- Raposo, A. A., Vasconcelos, F. F., Drechsel, D., Marie, C., Johnston, C., Dolle, D., . . . Castro, D. S. (2015). "Ascl1 Coordinately Regulates Gene Expression and the Chromatin Landscape during Neurogenesis." Cell Rep.
- Rea, S., Eisenhaber, F., O'Carroll, D., Strahl, B. D., Sun, Z. W., Schmid, M., . . . Jenuwein, T. (2000). "Regulation of chromatin structure by site-specific histone H3 methyltransferases." Nature **406**(6796): 593-599.
- Rebel, V. I., Kung, A. L., Tanner, E. A., Yang, H., Bronson, R. T. and Livingston, D. M. (2002). "Distinct roles for CREB-binding protein and p300 in hematopoietic stem cell self-renewal." Proc Natl Acad Sci U S A **99**(23): 14789-14794.
- Rinn, J. L. and Chang, H. Y. (2012). "Genome regulation by long noncoding RNAs." Annu Rev Biochem **81**: 145-166.
- Risca, V. I. and Greenleaf, W. J. (2015). "Unraveling the 3D genome: genomics tools for multiscale exploration." Trends Genet **31**(7): 357-372.
- Robison, A. J. and Nestler, E. J. (2011). "Transcriptional and epigenetic mechanisms of addiction." Nat Rev Neurosci **12**(11): 623-637.
- Ross, S. E., Greenberg, M. E. and Stiles, C. D. (2003). "Basic helix-loop-helix factors in cortical development." Neuron **39**(1): 13-25.
- Roth, J. F., Shikama, N., Henzen, C., Desbaillets, I., Lutz, W., Marino, S., . . . Eckner, R. (2003). "Differential role of p300 and CBP acetyltransferase during myogenesis: p300 acts upstream of MyoD and Myf5." Embo j **22**(19): 5186-5196.
- Roundtree, I. A., Evans, M. E., Pan, T. and He, C. (2017). "Dynamic RNA Modifications in Gene Expression Regulation." Cell **169**(7): 1187-1200.
- Rubinstein, J. H. and Taybi, H. (1963). "Broad thumbs and toes and facial abnormalities. A possible mental retardation syndrome." Am J Dis Child **105**: 588-608.
- Sabari, B. R., Tang, Z., Huang, H., Yong-Gonzalez, V., Molina, H., Kong, H. E., . . . Allis, C. D. (2015). "Intracellular crotonyl-CoA stimulates transcription through p300-catalyzed histone crotonylation." Mol Cell **58**(2): 203-215.
- Sabari, B. R., Zhang, D., Allis, C. D. and Zhao, Y. (2017). "Metabolic regulation of gene expression through histone acylations." Nat Rev Mol Cell Biol **18**(2): 90-101.

- Saha, R. N., Jana, M. and Pahan, K. (2007). "MAPK p38 regulates transcriptional activity of NF-kappaB in primary human astrocytes via acetylation of p65." J Immunol **179**(10): 7101-7109.
- Saksouk, N., Simboeck, E. and Dejardin, J. (2015). "Constitutive heterochromatin formation and transcription in mammals." Epigenetics Chromatin **8**: 3.
- Samanich, J., Montagna, C., Morrow, B. E. and Babcock, M. (2012). "Interstitial duplication of 22q13.2 in a girl with short stature, impaired speech and language, and dysmorphism." J Pediatr Genet **1**(1): 47-53.
- Sartorelli, V. and Puri, P. L. (2018). "Shaping Gene Expression by Landscaping Chromatin Architecture: Lessons from a Master." Mol Cell **71**(3): 375-388.
- Sauer, J. F. and Bartos, M. (2010). "Recruitment of early postnatal parvalbumin-positive hippocampal interneurons by GABAergic excitation." J Neurosci **30**(1): 110-115.
- Scandaglia, M., Lopez-Atalaya, J. P., Medrano-Fernandez, A., Lopez-Cascales, M. T., Del Blanco, B., Lipinski, M., . . . Barco, A. (2017). "Loss of Kdm5c Causes Spurious Transcription and Prevents the Fine-Tuning of Activity-Regulated Enhancers in Neurons." Cell Rep **21**(1): 47-59.
- Schaukowitch, K., Joo, J. Y., Liu, X., Watts, J. K., Martinez, C. and Kim, T. K. (2014). "Enhancer RNA facilitates NELF release from immediate early genes." Mol Cell **56**(1): 29-42.
- Schiebinger, G., Shu, J., Tabaka, M., Cleary, B., Subramanian, V., Solomon, A., . . . Lander, E. S. (2019). "Optimal-Transport Analysis of Single-Cell Gene Expression Identifies Developmental Trajectories in Reprogramming." Cell **176**(4): 928-943 e922.
- Schröder, S., Herker, E., Itzen, F., He, D., Thomas, S., Gilchrist, D. A., . . . Ott, M. (2013). "Acetylation of RNA polymerase II regulates growth-factor-induced gene transcription in mammalian cells." Mol Cell **52**(3): 314-324.
- Schuettengruber, B., Bourbon, H. M., Di Croce, L. and Cavalli, G. (2017). "Genome Regulation by Polycomb and Trithorax: 70 Years and Counting." Cell **171**(1): 34-57.
- Schwab, M. H., Druffel-Augustin, S., Gass, P., Jung, M., Klugmann, M., Bartholomae, A., . . . Nave, K. A. (1998). "Neuronal basic helix-loop-helix proteins (NEX, neuroD, NDRF): spatiotemporal expression and targeted disruption of the NEX gene in transgenic mice." J Neurosci **18**(4): 1408-1418.
- Semple, B. D., Blomgren, K., Gimlin, K., Ferriero, D. M. and Noble-Haeusslein, L. J. (2013). "Brain development in rodents and humans: Identifying benchmarks of maturation and vulnerability to injury across species." Prog Neurobiol **106-107**: 1-16.
- Sener, R. N. (1995). "Rubinstein-Taybi syndrome: cranial MR imaging findings." Comput Med Imaging Graph **19**(5): 417-418.

- Seo, S., Lim, J. W., Yellajoshiyula, D., Chang, L. W. and Kroll, K. L. (2007). "Neurogenin and NeuroD direct transcriptional targets and their regulatory enhancers." Embo j **26**(24): 5093-5108.
- Shachar, S., Voss, T. C., Pegoraro, G., Sciascia, N. and Misteli, T. (2015). "Identification of Gene Positioning Factors Using High-Throughput Imaging Mapping." Cell **162**(4): 911-923.
- Sheikh, B. N. and Akhtar, A. (2018). "The many lives of KATs - detectors, integrators and modulators of the cellular environment." Nat Rev Genet.
- Shekhar, K., Lapan, S. W., Whitney, I. E., Tran, N. M., Macosko, E. Z., Kowalczyk, M., . . . Sanes, J. R. (2016). "Comprehensive Classification of Retinal Bipolar Neurons by Single-Cell Transcriptomics." Cell **166**(5): 1308-1323 e1330.
- Shi, D., Pop, M. S., Kulikov, R., Love, I. M., Kung, A. L. and Grossman, S. R. (2009). "CBP and p300 are cytoplasmic E4 polyubiquitin ligases for p53." Proc Natl Acad Sci U S A **106**(38): 16275-16280.
- Shi, Y., Lan, F., Matson, C., Mulligan, P., Whetstine, J. R., Cole, P. A., . . . Shi, Y. (2004). "Histone demethylation mediated by the nuclear amine oxidase homolog LSD1." Cell **119**(7): 941-953.
- Shi, Y. and Mello, C. (1998). "A CBP/p300 homolog specifies multiple differentiation pathways in *Caenorhabditis elegans*." Genes Dev **12**(7): 943-955.
- Shikama, N., Lutz, W., Kretzschmar, R., Sauter, N., Roth, J. F., Marino, S., . . . Eckner, R. (2003). "Essential function of p300 acetyltransferase activity in heart, lung and small intestine formation." Embo j **22**(19): 5175-5185.
- Shikama, N., Lyon, J. and La Thangue, N. B. (1997). "The p300/CBP family: integrating signals with transcription factors and chromatin." Trends Cell Biol **7**(6): 230-236.
- Shin, J., Ming, G. L. and Song, H. (2014). "DNA modifications in the mammalian brain." Philos Trans R Soc Lond B Biol Sci **369**(1652).
- Smith, Z. D. and Meissner, A. (2013). "DNA methylation: roles in mammalian development." Nat Rev Genet **14**(3): 204-220.
- Son, H., Kim, S., Jung, D. H., Baek, J. H., Lee, D. H., Roh, G. S., . . . Kim, H. J. (2019). "Insufficient glutamine synthetase activity during synaptogenesis causes spatial memory impairment in adult mice." Sci Rep **9**(1): 252.
- Song, C. Z., Keller, K., Chen, Y., Murata, K. and Stamatoyannopoulos, G. (2002). "Transcription coactivator CBP has direct DNA binding activity and stimulates transcription factor DNA binding through small domains." Biochem Biophys Res Commun **296**(1): 118-124.
- Soo, K., O'Rourke, M. P., Khoo, P. L., Steiner, K. A., Wong, N., Behringer, R. R. and Tam, P. P. (2002). "Twist function is required for the morphogenesis of the cephalic

- neural tube and the differentiation of the cranial neural crest cells in the mouse embryo." Dev Biol **247**(2): 251-270.
- Soshnev, A. A., Josefowicz, S. Z. and Allis, C. D. (2016). "Greater Than the Sum of Parts: Complexity of the Dynamic Epigenome." Mol Cell **62**(5): 681-694.
- Soufi, A., Garcia, M. F., Jaroszewicz, A., Osman, N., Pellegrini, M. and Zaret, K. S. (2015). "Pioneer transcription factors target partial DNA motifs on nucleosomes to initiate reprogramming." Cell **161**(3): 555-568.
- Spruijt, C. G., Gnerlich, F., Smits, A. H., Pfaffeneder, T., Jansen, P. W., Bauer, C., . . . Vermeulen, M. (2013). "Dynamic readers for 5-(hydroxy)methylcytosine and its oxidized derivatives." Cell **152**(5): 1146-1159.
- Stark, R. and Brown, G. (2011). DiffBind differential binding analysis of ChIP-Seq peak data, Bioconductor. **100**.
- Stefanakis, N., Carrera, I. and Hobert, O. (2015). "Regulatory Logic of Pan-Neuronal Gene Expression in *C. elegans*." Neuron **87**(4): 733-750.
- Stessman, H. A., Xiong, B., Coe, B. P., Wang, T., Hoekzema, K., Fenckova, M., . . . Eichler, E. E. (2017). "Targeted sequencing identifies 91 neurodevelopmental-disorder risk genes with autism and developmental-disability biases." Nat Genet **49**(4): 515-526.
- Stevens, C. A. (2002). Rubinstein-Taybi Syndrome. GeneReviews((R)). M. P. Adam, H. H. Ardinger, R. A. Pagon et al. Seattle (WA).
- Stiehl, D. P., Fath, D. M., Liang, D., Jiang, Y. and Sang, N. (2007). "Histone deacetylase inhibitors synergize p300 autoacetylation that regulates its transactivation activity and complex formation." Cancer Res **67**(5): 2256-2264.
- Stilling, R. M. and Fischer, A. (2011). "The role of histone acetylation in age-associated memory impairment and Alzheimer's disease." Neurobiol Learn Mem **96**(1): 19-26.
- Strahl, B. D. and Allis, C. D. (2000). "The language of covalent histone modifications." Nature **403**(6765): 41-45.
- Stroud, H., Su, S. C., Hrvatin, S., Greben, A. W., Renthal, W., Boxer, L. D., . . . Greenberg, M. E. (2017). "Early-Life Gene Expression in Neurons Modulates Lasting Epigenetic States." Cell **171**(5): 1151-1164 e1116.
- Struhl, K. (1998). "Histone acetylation and transcriptional regulatory mechanisms." Genes Dev **12**(5): 599-606.
- Sugimoto, Y., Furuno, T. and Nakanishi, M. (2009). "Effect of NeuroD2 expression on neuronal differentiation in mouse embryonic stem cells." Cell Biol Int **33**(2): 174-179.
- Sun, Y., Nadal-Vicens, M., Misono, S., Lin, M. Z., Zubiaga, A., Hua, X., . . . Greenberg, M. E. (2001). "Neurogenin Promotes Neurogenesis and Inhibits Glial Differentiation by Independent Mechanisms." Cell **104**(3): 365-376.

Swank, M. W. and Sweatt, J. D. (2001). "Increased histone acetyltransferase and lysine acetyltransferase activity and biphasic activation of the ERK/RSK cascade in insular cortex during novel taste learning." *J Neurosci* **21**(10): 3383-3391.

Tahiliani, M., Koh, K. P., Shen, Y., Pastor, W. A., Bandukwala, H., Brudno, Y., . . . Rao, A. (2009). "Conversion of 5-Methylcytosine to 5-Hydroxymethylcytosine in Mammalian DNA by MLL Partner TET1." *Science* **324**(5929): 930-935.

Takahashi, K., Tanabe, K., Ohnuki, M., Narita, M., Ichisaka, T., Tomoda, K. and Yamanaka, S. (2007). "Induction of pluripotent stem cells from adult human fibroblasts by defined factors." *Cell* **131**(5): 861-872.

Takahashi, K. and Yamanaka, S. (2006). "Induction of pluripotent stem cells from mouse embryonic and adult fibroblast cultures by defined factors." *Cell* **126**(4): 663-676.

Takahashi, K. and Yamanaka, S. (2015). "A developmental framework for induced pluripotency." *Development* **142**(19): 3274-3285.

Tanaka, Y., Naruse, I., Hongo, T., Xu, M., Nakahata, T., Maekawa, T. and Ishii, S. (2000). "Extensive brain hemorrhage and embryonic lethality in a mouse null mutant of CREB-binding protein." *Mech Dev* **95**(1-2): 133-145.

Tanaka, Y., Naruse, I., Maekawa, T., Masuya, H., Shiroishi, T. and Ishii, S. (1997). "Abnormal skeletal patterning in embryos lacking a single Cbp allele: a partial similarity with Rubinstein-Taybi syndrome." *Proc Natl Acad Sci U S A* **94**(19): 10215-10220.

Tapias, A. and Wang, Z. Q. (2017). "Lysine Acetylation and Deacetylation in Brain Development and Neuropathies." *Genomics Proteomics Bioinformatics* **15**(1): 19-36.

Tapscott, S. J. (2005). "The circuitry of a master switch: Myod and the regulation of skeletal muscle gene transcription." *Development* **132**(12): 2685-2695.

Tasic, B., Menon, V., Nguyen, T. N., Kim, T. K., Jarsky, T., Yao, Z., . . . Zeng, H. (2016). "Adult mouse cortical cell taxonomy revealed by single cell transcriptomics." *Nat Neurosci* **19**(2): 335-346.

Telley, L., Govindan, S., Prados, J., Stevant, I., Nef, S., Dermitzakis, E., . . . Jabaudon, D. (2016). "Sequential transcriptional waves direct the differentiation of newborn neurons in the mouse neocortex." *Science* **351**(6280): 1443-1446.

Thakurela, S., Sahu, S. K., Garding, A. and Tiwari, V. K. (2015). "Dynamics and function of distal regulatory elements during neurogenesis and neuroplasticity." *Genome Res* **25**(9): 1309-1324.

Thienpont, B., Bena, F., Breckpot, J., Philip, N., Menten, B., Van Esch, H., . . . Devriendt, K. (2010). "Duplications of the critical Rubinstein-Taybi deletion region on chromosome 16p13.3 cause a novel recognisable syndrome." *J Med Genet* **47**(3): 155-161.

- Thomas, P. D., Campbell, M. J., Kejariwal, A., Mi, H., Karlak, B., Daverman, R., . . . Narechania, A. (2003). "PANTHER: a library of protein families and subfamilies indexed by function." Genome Res **13**(9): 2129-2141.
- Thomas, P. D. and Kahn, M. (2016). "Kat3 coactivators in somatic stem cells and cancer stem cells: biological roles, evolution, and pharmacologic manipulation." Cell Biol Toxicol **32**(1): 61-81.
- Thompson, P. R., Wang, D., Wang, L., Fulco, M., Pediconi, N., Zhang, D., . . . Cole, P. A. (2004). "Regulation of the p300 HAT domain via a novel activation loop." Nat Struct Mol Biol **11**(4): 308-315.
- Tillotson, R., Selfridge, J., Koerner, M. V., Gadalla, K. K. E., Guy, J., De Sousa, D., . . . Bird, A. (2017). "Radically truncated MeCP2 rescues Rett syndrome-like neurological defects." Nature **550**(7676): 398-401.
- Tsien, J. Z., Chen, D. F., Gerber, D., Tom, C., Mercer, E. H., Anderson, D. J., . . . Tonegawa, S. (1996). "Subregion- and cell type-restricted gene knockout in mouse brain." Cell **87**(7): 1317-1326.
- Tsonis, P. A., Madhavan, M., Tancous, E. E. and Del Rio-Tsonis, K. (2004). "A newt's eye view of lens regeneration." Int J Dev Biol **48**(8-9): 975-980.
- Tsui, D., Voronova, A., Gallagher, D., Kaplan, D. R., Miller, F. D. and Wang, J. (2014). "CBP regulates the differentiation of interneurons from ventral forebrain neural precursors during murine development." Dev Biol **385**(2): 230-241.
- Tsunemoto, R., Lee, S., Szucs, A., Chubukov, P., Sokolova, I., Blanchard, J. W., . . . Baldwin, K. K. (2018). "Diverse reprogramming codes for neuronal identity." Nature **557**(7705): 375-380.
- Tyagi, M., Imam, N., Verma, K. and Patel, A. K. (2016). "Chromatin remodelers: We are the drivers!!" Nucleus **7**(4): 388-404.
- Tyssowski, K. M., DeStefino, N. R., Cho, J. H., Dunn, C. J., Poston, R. G., Carty, C. E., . . . Gray, J. M. (2018). "Different Neuronal Activity Patterns Induce Different Gene Expression Programs." Neuron **98**(3): 530-546 e511.
- Ugai, H., Uchida, K., Kawasaki, H. and Yokoyama, K. K. (1999). "The coactivators p300 and CBP have different functions during the differentiation of F9 cells." J Mol Med **77**(6): 481-494.
- Uszczyńska-Ratajczak, B., Lagarde, J., Frankish, A., Guigo, R. and Johnson, R. (2018). "Towards a complete map of the human long non-coding RNA transcriptome." Nat Rev Genet **19**(9): 535-548.
- Vakoc, C. R., Mandat, S. A., Olenchock, B. A. and Blobel, G. A. (2005). "Histone H3 lysine 9 methylation and HP1 gamma are associated with transcription elongation through mammalian chromatin." Mol Cell **19**(3): 381-391.

- Valor, L. M., Guiretti, D., Lopez-Atalaya, J. P. and Barco, A. (2013a). "Genomic landscape of transcriptional and epigenetic dysregulation in early onset polyglutamine disease." *J Neurosci* **33**(25): 10471-10482.
- Valor, L. M., Pulopulos, M. M., Jimenez-Minchan, M., Olivares, R., Lutz, B. and Barco, A. (2011). "Ablation of CBP in forebrain principal neurons causes modest memory and transcriptional defects and a dramatic reduction of histone acetylation but does not affect cell viability." *J Neurosci* **31**(5): 1652-1663.
- Valor, L. M., Viosca, J., Lopez-Atalaya, J. P. and Barco, A. (2013b). "Lysine acetyltransferases CBP and p300 as therapeutic targets in cognitive and neurodegenerative disorders." *Curr Pharm Des* **19**(28): 5051-5064.
- Vanyushin, B. F. and Ashapkin, V. V. (2017). History and Modern View on DNA Modifications in the Brain. *DNA Modifications in the Brain*. T. W. Bredy. San Diego, Academic Press: 1-25.
- Vanyushin, B. F., Tushmalova, N. A. and Guskova, L. V. (1974). "Метилирование ДНК мозга как показатель участия генома в механизмах индивидуально приобретенной памяти (Brain DNA methylation as an index of genome participation in mechanisms of individually acquired memory)." *Dokl Akad Nauk SSSR* **219**(3): 742-744.
- Vanzan, L., Sklias, A., Herceg, Z. and Murr, R. (2017). Mechanisms of Histone Modifications. *Handbook of Epigenetics*: 25-46.
- Victor, M., Bei, Y., Gay, F., Calvo, D., Mello, C. and Shi, Y. (2002). "HAT activity is essential for CBP-1-dependent transcription and differentiation in *Caenorhabditis elegans*." *EMBO Rep* **3**(1): 50-55.
- Viosca, J., Lopez-Atalaya, J. P., Olivares, R., Eckner, R. and Barco, A. (2010). "Syndromic features and mild cognitive impairment in mice with genetic reduction on p300 activity: Differential contribution of p300 and CBP to Rubinstein-Taybi syndrome etiology." *Neurobiol Dis* **37**(1): 186-194.
- Visel, A., Blow, M. J., Li, Z., Zhang, T., Akiyama, J. A., Holt, A., . . . Pennacchio, L. A. (2009). "ChIP-seq accurately predicts tissue-specific activity of enhancers." *Nature* **457**(7231): 854-858.
- Vo, N. and Goodman, R. H. (2001). "CREB-binding protein and p300 in transcriptional regulation." *J Biol Chem* **276**(17): 13505-13508.
- Voigt, P., Tee, W. W. and Reinberg, D. (2013). "A double take on bivalent promoters." *Genes Dev* **27**(12): 1318-1338.
- Vojtek, A. B., Taylor, J., DeRuiter, S. L., Yu, J. Y., Figueroa, C., Kwok, R. P. and Turner, D. L. (2003). "Akt regulates basic helix-loop-helix transcription factor-coactivator complex formation and activity during neuronal differentiation." *Mol Cell Biol* **23**(13): 4417-4427.
- Voss, A. K. and Thomas, T. (2018). "Histone Lysine and Genomic Targets of Histone Acetyltransferases in Mammals." *Bioessays* **40**(10): e1800078.

- Waddington, C. H. (1942). "The epigenotype." Endeavor **1**: 18-20.
- Waddington, C. H. (1957). The strategy of the genes. A discussion of some aspects of theoretical biology. With an appendix by H. Kacser, London: George Allen & Unwin, Ltd.
- Waddington, C. H. (2012). "The epigenotype. 1942." Int J Epidemiol **41**(1): 10-13.
- Wagner, A., Regev, A. and Yosef, N. (2016). "Revealing the vectors of cellular identity with single-cell genomics." Nat Biotechnol **34**(11): 1145-1160.
- Wang, A., Yue, F., Li, Y., Xie, R., Harper, T., Patel, N. A., . . . Sander, M. (2015). "Epigenetic priming of enhancers predicts developmental competence of hESC-derived endodermal lineage intermediates." Cell Stem Cell **16**(4): 386-399.
- Wang, C., Lee, J. E., Lai, B., Macfarlan, T. S., Xu, S., Zhuang, L., . . . Ge, K. (2016). "Enhancer priming by H3K4 methyltransferase MLL4 controls cell fate transition." Proc Natl Acad Sci U S A **113**(42): 11871-11876.
- Wang, F., Marshall, C. B. and Ikura, M. (2013a). "Transcriptional/epigenetic regulator CBP/p300 in tumorigenesis: structural and functional versatility in target recognition." Cellular and Molecular Life Sciences **70**(21): 3989-4008.
- Wang, J., Weaver, I. C., Gauthier-Fisher, A., Wang, H., He, L., Yeomans, J., . . . Miller, F. D. (2010). "CBP histone acetyltransferase activity regulates embryonic neural differentiation in the normal and Rubinstein-Taybi syndrome brain." Dev Cell **18**(1): 114-125.
- Wang, S., Sun, H., Ma, J., Zang, C., Wang, C., Wang, J., . . . Liu, X. S. (2013b). "Target analysis by integration of transcriptome and CHIP-seq data with BETA." Nat Protoc **8**(12): 2502-2515.
- Wang, X., Zhang, C., Szabo, G. and Sun, Q. Q. (2013c). "Distribution of CaMKIIalpha expression in the brain in vivo, studied by CaMKIIalpha-GFP mice." Brain Res **1518**: 9-25.
- Wang, Z., Zang, C., Cui, K., Schones, D. E., Barski, A., Peng, W. and Zhao, K. (2009). "Genome-wide mapping of HATs and HDACs reveals distinct functions in active and inactive genes." Cell **138**(5): 1019-1031.
- Wang, Z., Zang, C., Rosenfeld, J. A., Schones, D. E., Barski, A., Cuddapah, S., . . . Zhao, K. (2008). "Combinatorial patterns of histone acetylations and methylations in the human genome." Nat Genet **40**(7): 897-903.
- Wapinski, O. L., Lee, Q. Y., Chen, A. C., Li, R., Corces, M. R., Ang, C. E., . . . Chang, H. Y. (2017). "Rapid Chromatin Switch in the Direct Reprogramming of Fibroblasts to Neurons." Cell Rep **20**(13): 3236-3247.
- Wapinski, O. L., Vierbuchen, T., Qu, K., Lee, Q. Y., Chanda, S., Fuentes, D. R., . . . Wernig, M. (2013). "Hierarchical mechanisms for direct reprogramming of fibroblasts to neurons." Cell **155**(3): 621-635.

- Warburton, E. C. and Brown, M. W. (2015). "Neural circuitry for rat recognition memory." Behav Brain Res **285**: 131-139.
- Weinert, B. T., Narita, T., Satpathy, S., Srinivasan, B., Hansen, B. K., Scholz, C., . . . Choudhary, C. (2018). "Time-Resolved Analysis Reveals Rapid Dynamics and Broad Scope of the CBP/p300 Acetylome." Cell **174**(1): 231-244 e212.
- Weintraub, H. and Groudine, M. (1976). "Chromosomal subunits in active genes have an altered conformation." Science **193**(4256): 848-856.
- Whyte, W. A., Orlando, D. A., Hnisz, D., Abraham, B. J., Lin, C. Y., Kagey, M. H., . . . Young, R. A. (2013). "Master transcription factors and mediator establish super-enhancers at key cell identity genes." Cell **153**(2): 307-319.
- Wolf, L., Harrison, W., Huang, J., Xie, Q., Xiao, N., Sun, J., . . . Cvekl, A. (2013). "Histone posttranslational modifications and cell fate determination: lens induction requires the lysine acetyltransferases CBP and p300." Nucleic Acids Res **41**(22): 10199-10214.
- Wong, C. K., Wade-Vallance, A. K., Luciani, D. S., Brindle, P. K., Lynn, F. C. and Gibson, W. T. (2018). "The p300 and CBP Transcriptional Coactivators Are Required for beta-Cell and alpha-Cell Proliferation." Diabetes **67**(3): 412-422.
- Wood, M. A., Attner, M. A., Oliveira, A. M., Brindle, P. K. and Abel, T. (2006). "A transcription factor-binding domain of the coactivator CBP is essential for long-term memory and the expression of specific target genes." Learn Mem **13**(5): 609-617.
- Wood, M. A., Kaplan, M. P., Park, A., Blanchard, E. J., Oliveira, A. M., Lombardi, T. L. and Abel, T. (2005). "Transgenic mice expressing a truncated form of CREB-binding protein (CBP) exhibit deficits in hippocampal synaptic plasticity and memory storage." Learn Mem **12**(2): 111-119.
- Wu, C. (1980). "The 5' ends of Drosophila heat shock genes in chromatin are hypersensitive to DNase I." Nature **286**(5776): 854-860.
- Xie, H., Xu, J., Hsu, J. H., Nguyen, M., Fujiwara, Y., Peng, C. and Orkin, S. H. (2014). "Polycomb repressive complex 2 regulates normal hematopoietic stem cell function in a developmental-stage-specific manner." Cell Stem Cell **14**(1): 68-80.
- Xu, H., Zhou, J., Lin, S., Deng, W., Zhang, Y. and Xue, Y. (2017). "PLMD: An updated data resource of protein lysine modifications." J Genet Genomics **44**(5): 243-250.
- Xu, W., Fukuyama, T., Ney, P. A., Wang, D., Rehg, J., Boyd, K., . . . Brindle, P. K. (2006). "Global transcriptional coactivators CREB-binding protein and p300 are highly essential collectively but not individually in peripheral B cells." Blood **107**(11): 4407-4416.
- Yang, N., Ng, Y. H., Pang, Z. P., Sudhof, T. C. and Wernig, M. (2011). "Induced neuronal cells: how to make and define a neuron." Cell Stem Cell **9**(6): 517-525.

Yao, T. P., Oh, S. P., Fuchs, M., Zhou, N. D., Ch'ng, L. E., Newsome, D., . . . Eckner, R. (1998). "Gene dosage-dependent embryonic development and proliferation defects in mice lacking the transcriptional integrator p300." Cell **93**.

Yeghiazaryan, M., Rutkowska-Wlodarczyk, I., Konopka, A., Wilczynski, G. M., Melikyan, A., Korkotian, E., . . . Figiel, I. (2014). "DP-b99 modulates matrix metalloproteinase activity and neuronal plasticity." PLoS One **9**(6): e99789.

Yi, P., Wang, Z., Feng, Q., Chou, C. K., Pintilie, G. D., Shen, H., . . . O'Malley, B. W. (2017). "Structural and Functional Impacts of ER Coactivator Sequential Recruitment." Mol Cell **67**(5): 733-743 e734.

Yi, P., Wang, Z., Feng, Q., Pintilie, G. D., Foulds, C. E., Lanz, R. B., . . . O'Malley, B. W. (2015). "Structure of a biologically active estrogen receptor-coactivator complex on DNA." Mol Cell **57**(6): 1047-1058.

Yun, M., Wu, J., Workman, J. L. and Li, B. (2011). "Readers of histone modifications." Cell Res **21**(4): 564-578.

Zaini, M. A., Muller, C., de Jong, T. V., Ackermann, T., Hartleben, G., Kortman, G., . . . Calkhoven, C. F. (2018). "A p300 and SIRT1 Regulated Acetylation Switch of C/EBPalpha Controls Mitochondrial Function." Cell Rep **22**(2): 497-511.

Zanger, K., Radovick, S. and Wondisford, F. E. (2001). "CREB binding protein recruitment to the transcription complex requires growth factor-dependent phosphorylation of its GF box." Mol Cell **7**(3): 551-558.

Zeisel, A., Muñoz-Manchado, A. B., Codeluppi, S., Lönnerberg, P., La Manno, G., Juréus, A., . . . Linnarsson, S. (2015). "Brain structure. Cell types in the mouse cortex and hippocampus revealed by single-cell RNA-seq." Science **347**(6226): 1138-1142.

Zeng, H. and Sanes, J. R. (2017). "Neuronal cell-type classification: challenges, opportunities and the path forward." Nat Rev Neurosci **18**(9): 530-546.

Zhang, H., Gao, L., Anandhakumar, J. and Gross, D. S. (2014). "Uncoupling transcription from covalent histone modification." PLoS Genet **10**(4): e1004202.

Zhang, M., Poplawski, M., Yen, K., Cheng, H., Bloss, E., Zhu, X., . . . Mobbs, C. V. (2009). "Role of CBP and SATB-1 in Aging, Dietary Restriction, and Insulin-Like Signaling." PLOS Biology **7**(11): e1000245.

Zhang, T. Y., Keown, C. L., Wen, X., Li, J., Vousden, D. A., Anacker, C., . . . Meaney, M. J. (2018). "Environmental enrichment increases transcriptional and epigenetic differentiation between mouse dorsal and ventral dentate gyrus." Nat Commun **9**(1): 298.

Zhang, Y., Liu, T., Meyer, C. A., Eeckhoute, J., Johnson, D. S., Bernstein, B. E., . . . Liu, X. S. (2008). "Model-based analysis of ChIP-Seq (MACS)." Genome Biol **9**(9): R137.

Zhang, Z., Hofmann, C., Casanova, E., Schutz, G. and Lutz, B. (2004). "Generation of a conditional allele of the CBP gene in mouse." Genesis **40**(2): 82-89.

Zhao, Y. and Garcia, B. A. (2015). "Comprehensive Catalog of Currently Documented Histone Modifications." Cold Spring Harb Perspect Biol **7**(9): a025064.

Zhou, Q. and Anderson, D. J. (2002). "The bHLH transcription factors OLIG2 and OLIG1 couple neuronal and glial subtype specification." Cell **109**(1): 61-73.

Zhou, Q., Wang, S. and Anderson, D. J. (2000). "Identification of a novel family of oligodendrocyte lineage-specific basic helix-loop-helix transcription factors." Neuron **25**(2): 331-343.

Zhou, Z., Enoch, M. A. and Goldman, D. (2014). "Gene expression in the addicted brain." Int Rev Neurobiol **116**: 251-273.

Zirkle, C. (1935). "The Inheritance of Acquired Characters and the Provisional Hypothesis of Pangenesis." The American Naturalist **69**(724): 417-445.



Annex





ANNEX I - Top 100 DEGs in the hippocampus of dKAT3-ifKO mice.

Notice that the top DEGs contain only downregulated genes because the adjusted p-values of upregulated genes were substantially lower.

log2Fold Change	p-adj	mg_i_symbol	mg_i_description
-5.1354601	4.15E-205	C1ql2	complement component 1, q subcomponent-like 2
-3.728353572	2.81E-195	Rgs14	regulator of G-protein signaling 14
-3.796424202	1.32E-183	Slc8a2	solute carrier family 8 (sodium/calcium exchanger), member 2
-3.659417326	2.63E-178	Nptx1	neuronal pentraxin 1
-3.31993458	1.13E-166	Stum	mechanosensory transduction mediator
-4.507557124	2.69E-163	Ddn	dendrin
-3.320700089	1.04E-152	Myo5b	myosin VB
-3.375272817	2.47E-150	Fam212b	family with sequence similarity 212, member B
-4.05885383	7.35E-148	Lrrc10b	leucine rich repeat containing 10B
-3.695214656	1.84E-142	Hpca	hippocalcin
-2.457388793	1.84E-142	Cpne6	copine VI
-2.593508089	6.01E-137	Ptk2b	PTK2 protein tyrosine kinase 2 beta
-3.092776234	1.46E-136	Slc30a3	solute carrier family 30 (zinc transporter), member 3
-2.820495981	2.40E-130	Fam131a	family with sequence similarity 131, member A
-2.978400629	5.12E-129	Itpka	inositol 1,4,5-trisphosphate 3-kinase A
-2.712936309	1.97E-126	Camk2a	calcium/calmodulin-dependent protein kinase II alpha
-2.882331399	9.07E-126	Wipf3	WAS/WASL interacting protein family, member 3
-3.517524883	3.49E-122	Rasd1	RAS, dexamethasone-induced 1
-2.985241085	1.85E-121	Rnf112	ring finger protein 112
-2.606375686	5.90E-121	Nrn1	neuritin 1
-3.58071256	5.51E-119	Rin1	Ras and Rab interactor 1
-2.616954917	3.47E-118	Sowaha	sosondawah ankyrin repeat domain family member A
-3.622650335	2.06E-115	Mdga1	MAM domain containing glycosylphosphatidylinositol anchor 1
-3.600427219	2.57E-115	Slc17a7	solute carrier family 17 (sodium-dependent inorganic phosphate cotransporter), member 7
-3.716710628	8.44E-114	Fam19a1	family with sequence similarity 19, member A1
-2.984790505	3.17E-112	Slit1	slit homolog 1 (Drosophila)
-3.731115482	8.14E-111	Plk5	polo like kinase 5
-2.209262392	8.32E-111	Phyhip	phytanoyl-CoA hydroxylase interacting protein
-2.61899844	1.80E-110	2010300C02Rik	RIKEN cDNA 2010300C02 gene
-3.181784318	7.11E-110	Kalrn	kalirin, RhoGEF kinase
-2.584644692	2.02E-108	Nrgn	neurogranin
-2.588041264	3.69E-108	Camkv	CaM kinase-like vesicle-associated
-4.612271886	4.23E-107	Spink8	serine peptidase inhibitor, Kazal type 8
-2.405765477	6.84E-105	Kcnip2	Kv channel-interacting protein 2
-2.474870034	2.55E-104	Lrrtm1	leucine rich repeat transmembrane neuronal 1
-3.358632877	1.77E-101	Thsd4	thrombospondin, type I, domain containing 4
-2.267979887	2.16E-101	Psd	pleckstrin and Sec7 domain containing
-2.599322744	1.99E-100	Enc1	ectodermal-neural cortex 1
-2.456642438	5.04E-99	3300002P13Rik	RIKEN cDNA 3300002P13 gene
-2.628220245	6.31E-99	Rasgrp1	RAS guanyl releasing protein 1
-2.53395747	7.15E-99	Mical2	microtubule associated monoxygenase, calponin and LIM

			domain containing 2
-2.816628447	1.26E-98	Kcnj4	potassium inwardly-rectifying channel, subfamily J, member 4
-2.264784423	2.29E-98	Olfm1	olfactomedin 1
-2.149559525	9.32E-97	Jph4	junctionophilin 4
-2.267624195	9.38E-96	Plch2	phospholipase C, eta 2
-2.120748079	2.08E-95	Rasgef1a	RasGEF domain family, member 1A
-2.455802995	5.19E-95	Chrm1	cholinergic receptor, muscarinic 1, CNS
-2.881345489	1.02E-94	Islr2	immunoglobulin superfamily containing leucine-rich repeat 2
-3.845135829	1.24E-94	Lct	lactase
-2.03526627	9.53E-94	Camkk1	calcium/calmodulin-dependent protein kinase kinase 1, alpha
-2.518627925	1.47E-92	Gabra5	gamma-aminobutyric acid (GABA) A receptor, subunit alpha 5
-4.38767441	2.20E-92	Crlf1	cytokine receptor-like factor 1
-2.724885335	4.20E-92	Adcy1	adenylate cyclase 1
-2.394125652	6.04E-90	Orai2	ORAI calcium release-activated calcium modulator 2
-3.339224143	1.60E-89	Robo3	roundabout guidance receptor 3
-2.294391644	2.01E-88	Nptxr	neuronal pentraxin receptor
-2.459840509	5.15E-88	Icam5	intercellular adhesion molecule 5, telencephalin
-2.294732659	5.29E-88	Prmt8	protein arginine N-methyltransferase 8
-1.886587457	1.76E-87	Ak5	adenylate kinase 5
-2.516074889	2.34E-86	Gm2115	predicted gene 2115
-1.923584515	3.24E-86	Kcnab2	potassium voltage-gated channel, shaker-related subfamily, beta member 2
-3.088434953	3.34E-86	Bdnf	brain derived neurotrophic factor
-2.245344967	1.10E-85	Cabp7	calcium binding protein 7
-2.261205962	3.72E-85	Neurod2	neurogenic differentiation 2
-2.07631434	6.12E-84	Dgkz	diacylglycerol kinase zeta
-2.270263487	6.15E-82	Fam163b	family with sequence similarity 163, member B
-2.379745281	2.00E-81	Rtn4r	reticulon 4 receptor
-3.884592207	1.34E-80	Sstr3	somatostatin receptor 3
-2.169613507	1.94E-80	Prkcg	protein kinase C, gamma
-2.235492361	1.73E-79	Plekhg5	pleckstrin homology domain containing, family G (with RhoGef domain) member 5
-2.68263127	3.61E-79	Crym	crystallin, mu
-2.631134031	1.62E-78	Gpd1	glycerol-3-phosphate dehydrogenase 1 (soluble)
-2.006829279	8.42E-76	Chn1	chimerin 1
-3.656390084	2.55E-75	Tnfrsf25	tumor necrosis factor receptor superfamily, member 25
-3.715164032	3.15E-75	A830036E02Rik	RIKEN cDNA A830036E02 gene
-3.50770691	5.48E-75	Smoc2	SPARC related modular calcium binding 2
-2.96857628	5.48E-75	Car7	carbonic anhydrase 7
-2.548008844	7.91E-75	Kcnq5	potassium voltage-gated channel, subfamily Q, member 5
-2.017832926	8.55E-75	Mast3	microtubule associated serine/threonine kinase 3
-2.723539775	1.08E-74	Grm2	glutamate receptor, metabotropic 2
-2.038888239	1.26E-74	Chst1	carbohydrate (keratan sulfate Gal-6) sulfotransferase 1
-1.931857494	3.93E-74	Gria1	glutamate receptor, ionotropic, AMPA1 (alpha 1)
-1.79400094	4.97E-74	Rab15	RAB15, member RAS oncogene family
-1.765879772	5.06E-74	Camk2b	calcium/calmodulin-dependent protein kinase II, beta
-1.822148295	8.34E-74	Pgbd5	piggyBac transposable element derived 5
-2.36671861	2.05E-73	Grin2a	glutamate receptor, ionotropic, NMDA2A (epsilon 1)
-2.974766367	2.25E-73	Rprm1	reprimin-like
-2.258798802	2.83E-73	Syt17	synaptotagmin XVII
-1.863581555	1.82E-72	Cplx2	complexin 2
-2.596865582	2.71E-72	Cck	cholecystokinin
-3.42464933	8.05E-72	Rtn4rl2	reticulon 4 receptor-like 2

-2.413890988	1.57E-71	Agap2	ArfGAP with GTPase domain, ankyrin repeat and PH domain 2
-2.011672068	2.12E-71	Ctxn1	cortexin 1
-1.763614949	4.21E-70	Nell2	NEL-like 2
-2.048282245	5.48E-69	Hpcal4	hippocalcin-like 4
-2.822240892	1.08E-67	Kcnv1	potassium channel, subfamily V, member 1
-2.062862446	1.08E-67	Gas7	growth arrest specific 7
-1.793060174	7.90E-67	Mmp17	matrix metalloproteinase 17
-2.689673774	9.70E-67	Adra1d	adrenergic receptor, alpha 1d
-2.163663625	2.08E-66	Egr1	early growth response 1



ANNEX II – Full publication list

In addition to the experiments presented in the two chapters of Results, I have participated in six publications relevant to this thesis. Two of these articles are presented in Annex III and Annex IV as part of this compendium of publications. The other four publications were not included as part of this thesis for various reasons.

- Scandaglia, M., **Lopez-Atalaya, J. P.**, Medrano-Fernandez, A., Lopez-Cascales, M. T., Del Blanco, B., **Lipinski, M.**, . . . **Barco, A.** (2017). "Loss of Kdm5c Causes Spurious Transcription and Prevents the Fine-Tuning of Activity-Regulated Enhancers in Neurons." *Cell Rep* 21(1): 47-59.
DOI: 10.1016/j.celrep.2017.09.014
- Galvão-Ferreira, P., **Lipinski, M.**, Santos, F., **Barco, A.** and Costa, R. M. (2017). "Skill Learning Modulates RNA Pol II Poising at Immediate Early Genes in the Adult Striatum." *eNeuro* 4(2).
DOI: 10.1523/ENEURO.0074-17.2017
- Del Blanco, B., Guiretti, D., Tomasoni, R., Lopez-Cascales, M. T., Muñoz-Viana, R., **Lipinski, M.**, . . . **Barco, A.** (2019). "CBP and SRF co-regulate dendritic growth and synaptic maturation." *Cell Death Differ.*
DOI: 10.1038/s41418-019-0285-x
- Fernandez-Albert, J., **Lipinski, M.**, Lopez-Cascales, M. T., Rowley, M. J., Martin-Gonzalez, A. M., Del Blanco, B., . . . **Barco, A.** (2019). "Integrative multi-omic analysis unveils the immediate and deferred epigenomic signature of neuronal activation." (Under review).
DOI: 10.1101/534115

ANNEX III – Authored article 1

The review article "CBP/p300 in brain development and plasticity: Disentangling the KAT's cradle." by Michal Lipinski, Beatriz del Blanco and Angel Barco has been recently published in *Curr Opin Neurobiol* 2019 Mar 8; 59:1-8.

DOI: 10.1016/j.conb.2019.01.023

This review directly derives from the bibliographic investigation conducted during the preparation of this thesis.



Title: CBP/p300 in brain development and plasticity: Disentangling the KAT's cradle

Authors: Michal Lipinski, Beatriz del Blanco and Angel Barco*

Author affiliations:

Instituto de Neurociencias (Universidad Miguel Hernández - Consejo Superior de Investigaciones Científicas). Av. Santiago Ramón y Cajal s/n. Sant Joan d'Alacant. 03550. Alicante, Spain.

* **Corresponding author:** Angel Barco, Instituto de Neurociencias (Universidad Miguel Hernández – Consejo Superior de Investigaciones Científicas). Av. Santiago Ramón y Cajal s/n. Sant Joan d'Alacant 03550, Alicante, Spain. Tel: +34 965 919232. Fax: +34 965 919492.

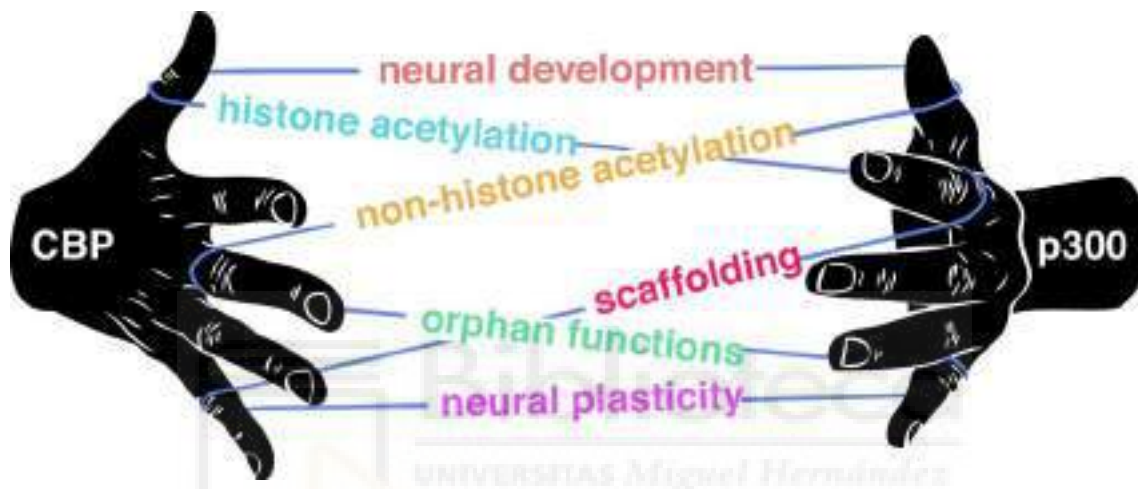
Email: abarco@umh.es

Running title: KAT3 in brain development and plasticity

Keywords: Transcriptional co-activator, lysine acetyltransferase, histone acetylation, CBP, p300, Rubinstein-Taybi syndrome, neuronal plasticity, nervous system development.

Abstract

The paralogous transcriptional co-activators CBP and p300 (*aka* KAT3A and KAT3B, respectively) contain a characteristic and promiscuous lysine acetyltransferase (KAT) domain and multiple independent protein-binding domains that enable them to interact with hundreds of proteins, possibly promoting the acetylation of thousands of target lysine residues. Both proteins play critical roles during the development of the nervous system and may also regulate stimuli-driven transcription and plasticity in postmitotic neurons. The multiplicity of functions, substrates and molecular partners, together with the redundancy and singularity of the two KAT3 paralogs, define a complex cat's cradle of relationships. In this review, we discuss the role of the KAT3 proteins in neurons and integrate recent information regarding their function and mode of action.



Word count: 118

1. The acetylation switch

During the development of multicellular organisms, cells with the same genome acquire unique features by switching on and off specific gene programs. This differentiation process is driven or supported by covalent changes in the chromatin that can be inherited along with the acquired gene expression profiles by daughter cells throughout successive rounds of division [1]. Among these epigenetic mechanisms, the acetylation of lysine (K) residues in nucleosome histones is thought to loosen up the contacts between histones and DNA, and facilitate the recruitment of transcription factors (TFs) and the RNA polymerase complex [2]. As a result, histone acetylation levels contribute in defining the transcriptional competence of the locus [3].

During neurogenesis and postmitotic maturation of fate-committed neurons, dynamic changes in the level and distribution of histone acetylation across the genome (which define the so-called histone acetylome) accompany the onset and maintenance of gene expression programs associated with neuronal function and plasticity [4]. After neuronal development, changes in neuronal histone acetylation are also associated with memory formation and other neuroadaptive processes in the adult brain [2,5]. As such, it is not surprising that altered levels of neuronal histone acetylation – both during neuronal development and in the adult brain – have been linked to adverse effects and neuropsychiatric disorders in humans and animal models [4,6].

Histone acetylation is regulated by the opposing actions of lysine acetyltransferases (KATs) and deacetylases (KDACs), which are also frequently referred to as histone acetyltransferases (HATs) and deacetylases (HDAC) although the substrate specificity of these enzymes is not restricted to histone proteins [7]. Different KATs are required depending on the stage of gene activation, with a high functional specificity needed in the early gene activation stage during development and less specific functionality needed in the later maintenance stage in adult animals [3,8].

2. CBP and p300: Key players of the neuronal histone acetylome

Among the different families of nuclear KATs [7], we will focus on CBP and p300. These two large (>250 kDa) and ubiquitously expressed proteins are the only members of the KAT3 family and play important roles in neurodevelopment. The knockout (KO) mouse embryos of *Crebbp* and *Ep300* (encoding for CBP and p300, respectively) exhibit defects in neural tube closure and die between E9 and E12.5 [9]. Further supporting the relevance of KAT3 proteins in the nervous system, heterozygous mutations in *CREBBP* and *EP300* cause Rubinstein-Taybi syndrome (RSTS1, OMIM #180849 and RSTS2, OMIM #613684, respectively), and a duplication of the same loci occur in 16p13.3 duplication syndrome (OMIM #613458) and in a few clinical cases linked to microduplication at 22q13.2 [10]. All these conditions are associated with intellectual disability and severe neurological symptoms [11,12]. The analysis of cells from RSTS patients indicates that the disorder could be caused by aberrant chromatin regulation [12] and defective neuronal functioning [13]. Furthermore, heterozygous *Crebbp* and *Ep300* mice exhibit neurological and cognitive deficits that recapitulate the RSTS phenotype [12].

Although early embryonic death of the conventional KOs initially prevented a precise study of the cellular and molecular function of CBP and p300 during brain development, the generation of conditional KO (cKO) mice has allowed to progress in the dissection of their specific contribution in different cell types and stages of development. For example, several studies have shown that CBP is required for the correct differentiation and integration of different classes of neurons into cortical, hippocampal, cerebellar neuronal and spinal cord circuits [14-18]. In addition, we have recently found that after differentiation, CBP is required to activate the gene programs underlying dendritic growth, spine maturation and activity-dependent synaptic changes in newborn neurons [19]. Similar studies should be conducted with p300 cKOs to evaluate if p300 also participates in neuron differentiation and maturation.

Although many, if not most, RSTS symptoms may result from impaired development of the central nervous system, several studies indicate that some aspects of the intellectual disability might result from the deficiency of CBP/p300 during adulthood [20-25]. In fact, the increase in histone acetylation associated with mnemonic processes has been ascribed to CBP given its interaction with CREB, a key TF involved in memory formation [26]. In line with this idea, postnatal forebrain-restricted bi-allelic CBP mutants display memory defects, although more modest than those observed in heterozygous mice [22-24]. Overall, these findings reveal a role for CBP both in progenitor cells and neurons (immature and mature), although similarly to other epigenetic enzymes, its relative importance seems to decrease along the differentiation process [27].

3. KAT3 proteins: Unique and overlapping functions

One of the most intriguing unresolved issues regarding CBP and p300 biology is the overlap of their functions. Structurally, they display 57% identity at the whole protein level and 88% similarity in their KAT domains (**Figure 1A**), and as indicated before, the elimination of either one of these two proteins results in early embryonic death. Notably, double heterozygosis caused an almost indistinguishable phenotype, which first pointed to overlapping and partially redundant functions [9]. The fact that heterozygous loss-of-function of either of these proteins causes similar syndromes in humans further supports a shared biological role [12].

However, in addition to overlapping functions, evidence also points towards unique roles and situations in which one of the KAT3 proteins is not as relevant as the other. For example p300, but not CBP, appears to be essential for the correct development of the heart [28,29]. Also, overexpression of just one p300 KAT inactive allele (but not a CBP KAT inactive allele) has a dominant negative effect on the development of the skeletal muscles, lungs and intestine *in vivo* [28,29]. Congenital heart anomalies and embryonic lethality could, in fact, explain a low prevalence of *EP300* mutations among RSTS patients (5% versus 60% of *CREBBP* mutations) [11]. On the other hand, the rare RSTS2 patients have milder cognitive deficits [30], which is consistent with observations in heterozygous mice [20,31]. While several studies in brain-restricted CBP cKOs [22-24] and transgenic mice expressing a KAT-inactive CBP variant [21] have shown mice with cognitive deficits, similar evidence in p300-

deficient mice is limited [25,32]. Further supporting a greater role for CBP in intellectual development and cognitive function, single cell RNA-seq data show that p300 is less expressed than CBP in neurons in both the developing [33] and adult brain [34] (**Figure 1B**). This difference in expression may be particularly relevant for proteins like CBP and p300 as they are thought to be present in limiting amounts with TFs competing for their recruitment [35]. The asymmetric importance of the two proteins in different organs and cell types suggests that the duplication of many gene families that occurred in the first vertebrate along with the emergence of a neural crest and cephalization resulted in the appearance of two KAT3 proteins [36] that acquired specialized functions throughout evolution but that maintained some ancestral shared functions as well (**Figure 1C**).

Notably, CBP and p300 widely bind to enhancer regions that are highly tissue specific [1,37]. The few studies that have compared the genomic distribution of CBP and p300 (not one of them conducted on neuronal tissue) have revealed a large overlap [38-40]. More precise genetic manipulations, single-cell genomics and the production of CBP/p300-specific inhibitors should help to elucidate the differences between the two KAT3 proteins [41].

4. The KATs in the HATs

Since the discovery of their KAT activity, it has been clear that both CBP and p300 can acetylate an assortment of proteins beyond histones. Many of these proteins are TFs (e.g., MyoD, p65, STAT3 and GATA2) and transcriptional regulators, including the RNA Polymerase 2 (RNAPII) itself [42] (**Figure 2A**). Thanks to quantitative proteomics techniques and the use of different KAT3 inhibitors, thousands of proteins have recently been identified as substrates of CBP/p300 [43]. This pinpoints these proteins as two of the main KATs of the mammalian proteome. Of note, the separate roles of CBP and p300 in protein acetylation remain to be investigated because current KAT3 inhibitors are not specific for either protein [44]. The contribution of the so-called “orphan” functions of CBP/p300 [45] also remains largely unexplored *in vivo*. Apart from a possible role as cytoplasmic E4 polyubiquitin ligases [46], CBP and p300 can drive non-acetylation acylations of K residues. For instance, crotonylation of histone H3 (H3K18Cr) [47,48] and 2-hydroxyisobutyrylation of histone H4 (H4K8Hib) [49] and non-histone proteins [50] may represent alternative mechanisms by which KAT3 proteins affect transcription.

Even though histone tails are certainly not the only targets of these KAT3 proteins, it is widely considered that they affect gene expression through histone acetylation. In particular, the acetylation of K27 in histone H3 (H3K27ac) is highly dependent on CBP/p300. This histone posttranslational modification (PTM) has been shown to mark active enhancers and correlate with gene expression [1,51]. The reduction of KAT3-dependent H3K27ac results in impaired enhancer activation and associated transcription, with the production of both mRNA and eRNA being affected [52]. Further supporting an active role for KAT3-dependent acetylation in promoting transcription, recent experiments using CRISPR technology and an inactivated Cas9 (dCas9) protein fused to p300's KAT domain confirmed that driving lysine acetylation

either to enhancers or promoters increases the expression of the associated gene [53]. In turn, CBP's KAT activity is positively regulated by the binding of eRNA to a highly disordered activation loop domain [54], which suggests the existence of an auto-regulatory mechanism potentially important for enhancer function and maintenance. Neuronal activity is also likely to modulate KAT activity because both KAT3 proteins are found downstream of numerous signaling cascades and are targets of multiple PTMs that may influence their transactivation potential and their ability to interact with specific TFs [6]. Nonetheless, the significance of these regulatory mechanisms in neurons and *in vivo* remains to be elucidated (**Figure 2B**).

5. Scaffolding and lysine acetylation – two mechanisms behind transcriptional activation?

The lack of a direct correlation between transcription and CBP/p300 presence at promoters and enhancers suggests that the co-activation mechanism is complex and incompletely understood [40,55]. Both CBP and p300 contain at least nine protein-binding sites for a huge variety of proteins (**Figure 1A**), including TFs, kinases, chromatin remodelers, structural proteins and others [55]. The principal domains of KAT3 are separated by highly flexible, intrinsically disordered, linker domains [35]. Even these linker regions, apart from playing a structural role, have been reported to bind transcription factors [56]. As a result, KAT3 proteins can potentially bind to multiple proteins at the same time [55,57]. This ability is considered essential for their function as a transcriptional co-activator, which is achieved either by creating a scaffold for multiple proteins that bind synergistically to perform their function [57-59] or by forming a “bridge” between TFs and RNAPII [60,61]. Structural evidence coming from chromatin conformation capture (3C) experiments supports this view and indicates that CBP and p300 may create multi-kilobase spanning complexes. However, loss of these complexes resulted in relatively limited changes in gene expression, thereby undermining the direct implication of these complexes in transcription [62].

Unambiguous evidence for the scaffolding function could come from experiments in which the KAT domain is inactivated or eliminated. In the early 2000s, multiple biochemical assays overexpressing catalytically dead CBP or p300 suggested that their KAT activity is either not required [63-65] or only partially required [66] for their transcriptional co-activator function. Although these experiments suggest that KAT function is not always necessary, these conclusions are based on protein overexpression *in vitro* rather than in a natural setting. Moreover, these studies did not investigate the consequences of simultaneously eliminating the KAT activity of both KAT3 proteins. This leaves open the possibility that one protein compensates for the other and thereby results in little or no noticeable phenotype. Mixed messages also came from experiments in animals whose genome encodes for just one KAT3. While studies on the KAT3 homolog in *Drosophila*, known as *nejire*, have produced inconsistent results regarding the importance of KAT activity [67-69], the KAT activity of *cbp-1* seems to be crucial for cell differentiation in *C. elegans* [70]. Experiments in embryonic stem cells (ESC) have also shown that KAT activity is essential for their self-renewal [62]. Furthermore, the transcriptional changes that occur upon treating with

KAT inhibitors are similar to those observed in CBP/p300 null KOs [43], which also suggests that K acetylation may be the main mechanism through which CBP and p300 regulate transcription.

Based on the available evidence, we believe that the scaffolding and KAT functions are likely parts of the same mechanism of action *in vivo*. The exact way in which these mechanisms collaborate is still elusive and the specific contribution of K acetylation to the formation of transcriptional complexes requires further investigation. On one hand, the KAT activity is crucial for the recruitment of RNAPII to active promoters [71]. On the other hand, KAT3 proteins are recruited to specific genomic locations through the interaction with TFs [35,55] and the recruitment itself may be critical for KAT activity [72]. A recent study has shown that the catalytic activity of p300 directly depends on the dimerization status of its TF ligands, which can explain the coordination between transcription and chromatin acetylation [72]. Therefore, one could imagine KAT3 proteins as partially redundant, quasi-universal co-activators that can activate a multitude of transcriptional programs depending on the specific genomic setting and the TF repertoire of the cell (**Figure 2C**). It has been proposed that, in the absence of membrane-delimited sub-compartments in the interphase nucleus, phase separation can give rise to non-membrane-bound compartments in which movement is constrained and biochemical reactions are concentrated [73,74]. The abundance and coincidental acetylation of histone and non-histone K residues in euchromatin, along with the ubiquitous presence of acetyl-binding bromodomains (BrD) in proteins involved in transcriptional regulation, may define such sub-compartments. Consistent with this notion, the interaction of KAT3 bromodomains with acetylated K residues increases the aggregation state of acetylated proteins [72,75]. CBP and p300 could thus create patches of transcriptionally active chromatin, contributing to physically separate permissive and non-permissive chromatin stretches.

6. Future directions

Recent advances have provided us with new tools to investigate the roles of CBP/p300 in brain development, function and disease. The potential that CBP and p300 hold as drug targets in cancer has led to great efforts in producing KAT3-specific inhibitors [41], albeit these compounds have not yet been used extensively in neurobiology. There is also ongoing work aimed at developing specific activators to stimulate KAT3 activity in RSTS and other disorders (e.g., Huntington's disease) associated with reduced histone acetylation [6,76]. Given the likely pleotropic effects of such compounds, their safety will require serious scrutiny. For instance, if KAT3 inhibitors in cancer therapy pass the blood-brain barrier, they might trigger adverse secondary effects with respect to the intellectual capacity of the patient [77,78]. Similarly, the use of KAT3 activators may have undesirable effects in cell differentiation and proliferations. Nonetheless, the availability of novel and more specific KAT inhibitors and activators, particularly if they can differentiate between CBP and p300, open up new and exciting possibilities to investigate the role of KAT3 proteins in neurons. Complementing these studies, the novel CRISPR-based techniques for epi-editing and the development of new sequencing techniques to investigate genome biology should help us to understand the complex

interplay between CBP/p300 protein-binding and KAT activities in different cell types and cell states. Despite the continuous progress it is possible that we are still missing essential aspects of CBP/p300 regulation in neurons.

Acknowledgements: A.B. research is supported by grants SAF2017-87928-R, PCIN-2015-192-C02-01 (part of the ERA-NET NEURON JTC2015 project ChromISyn) and SEV-2017-0723 from MICINN co-financed by ERDF, PROMETEO/2016/026 from the Generalitat Valenciana, and RGP0039/2017 from the Human Frontiers Science Program Organization (HFSPO). The Instituto de Neurociencias is a “Centre of Excellence Severo Ochoa”.

Bibliography

1. Gallegos DA, Chan U, Chen LF, West AE: **Chromatin Regulation of Neuronal Maturation and Plasticity.** *Trends Neurosci* 2018, **41**:311-324.
2. Lopez-Atalaya JP, Barco A: **Can changes in histone acetylation contribute to memory formation?** *Trends Genet* 2014, **30**:529-539.
3. Kurdستاني SK, Grunstein M: **Histone acetylation and deacetylation in yeast.** *Nat Rev Mol Cell Biol* 2003, **4**:276-284.
4. Tapias A, Wang ZQ: **Lysine Acetylation and Deacetylation in Brain Development and Neuropathies.** *Genomics Proteomics Bioinformatics* 2017, **15**:19-36.
5. Graff J, Tsai LH: **Histone acetylation: molecular mnemonics on the chromatin.** *Nat Rev Neurosci* 2013, **14**:97-111.
6. Valor LM, Viosca J, Lopez-Atalaya JP, Barco A: **Lysine acetyltransferases CBP and p300 as therapeutic targets in cognitive and neurodegenerative disorders.** *Curr Pharm Des* 2013, **19**:5051-5064.
7. Sheikh BN, Akhtar A: **The many lives of KATs - detectors, integrators and modulators of the cellular environment.** *Nat Rev Genet* 2018, **Nov 2**. doi: **10.1038/s41576-018-0072-4**.
- * Very recent and updated review discussing the role of KATs, including CBP and p300, in transcription regulations and other important cellular functions.
8. Anamika K, Krebs AR, Thompson J, Poch O, Devys D, Tora L: **Lessons from genome-wide studies: an integrated definition of the coactivator function of histone acetyl transferases.** *Epigenetics Chromatin* 2010, **3**:18.
9. Yao TP, Oh SP, Fuchs M, Zhou ND, Ch'ng LE, Newsome D, Bronson RT, Li E, Livingston DM, Eckner R: **Gene dosage-dependent embryonic development and proliferation defects in mice lacking the transcriptional integrator p300.** *Cell* 1998, **93**:361-372.
10. Samanich J, Montagna C, Morrow BE, Babcock M: **Interstitial duplication of 22q13.2 in a girl with short stature, impaired speech and language, and dysmorphism.** *J Pediatr Genet* 2012, **1**:47-53.
11. Roelfsema JH, Peters DJ: **Rubinstein-Taybi syndrome: clinical and molecular overview.** *Expert Rev Mol Med* 2007, **9**:1-16.
12. Lopez-Atalaya JP, Valor LM, Barco A: **Epigenetic factors in intellectual disability: the Rubinstein-Taybi syndrome as a paradigm of**

neurodevelopmental disorder with epigenetic origin. *Prog Mol Biol Transl Sci* 2014, **128**:139-176.

13. Alari V, Russo S, Terragni B, Ajmone PF, Sironi A, Catusi I, Calzari L, Concolino D, Marotta R, Milani D, et al.: **iPSC-derived neurons of CREBBP- and EP300-mutated Rubinstein-Taybi syndrome patients show morphological alterations and hypoexcitability.** *Stem Cell Res* 2018, **30**:130-140.
** The authors show that iPSC-derived neurons from RSTS patients display morphological changes and hypoexcitability, while proliferation and reprogramming potential are unaffected. This is the first study performed on iPSCs and iPSC-derived neurons from RSTS patients.
14. Wang J, Weaver IC, Gauthier-Fisher A, Wang H, He L, Yeomans J, Wondisford F, Kaplan DR, Miller FD: **CBP histone acetyltransferase activity regulates embryonic neural differentiation in the normal and Rubinstein-Taybi syndrome brain.** *Dev Cell* 2010, **18**:114-125.
15. Tsui D, Voronova A, Gallagher D, Kaplan DR, Miller FD, Wang J: **CBP regulates the differentiation of interneurons from ventral forebrain neural precursors during murine development.** *Dev Biol* 2014, **385**:230-241.
16. Merk DJ, Ohli J, Merk ND, Thatikonda V, Morrissy S, Schoof M, Schmid SN, Harrison L, Filser S, Ahlfeld J, et al.: **Opposing Effects of CREBBP Mutations Govern the Phenotype of Rubinstein-Taybi Syndrome and Adult SHH Medulloblastoma.** *Dev Cell* 2018, **44**:709-724 e706.
* The study shows that depending on the developmental stage of the cerebellar granule neuron, *CREBBP* KAT-inactivating mutations cause a different outcome. In the early development, CBP seems to be crucial for neuronal survival and correct neuronal migration. However, it primarily plays a tumor-suppressive role in postnatal development.
17. Medrano-Fernandez A, Delgado-Garcia JM, Del Blanco B, Llinares M, Sanchez-Campusano R, Olivares R, Gruart A, Barco A: **The Epigenetic Factor CBP Is Required for the Differentiation and Function of Medial Ganglionic Eminence-Derived Interneurons.** *Mol Neurobiol* 2018, **Oct 17**. doi: **10.1007/s12035-018-1382-4**.
* Recent study reporting a crucial role for CBP in interneuron differentiation *in vivo*. The changes in interneuron population that result from CBP elimination cause electrophysiological and behavioral impairments.
18. Lee S, Lee B, Lee JW, Lee SK: **Retinoid signaling and neurogenin2 function are coupled for the specification of spinal motor neurons through a chromatin modifier CBP.** *Neuron* 2009, **62**:641-654.
19. del Blanco B, Guiretti D, Tomasoni R, Lopez-Cascales MT, Muñoz-Viana R, Lipinski M, Scandaglia M, Coca Y, Olivares R, Valor LM, et al.: **CBP and SRF co-regulate dendritic growth and synaptic maturation** *Cell Death Differ* 2019, **In press**.
* The study shows that the KAT activity of CBP is essential for the normal growth and maturation of glutamatergic neurons both in culture and in vivo. It also identifies SRF as an important partner of CBP in the regulation of these processes.
20. Alarcon JM, Malleret G, Touzani K, Vronskaya S, Ishii S, Kandel ER, Barco A: **Chromatin acetylation, memory, and LTP are impaired in CBP+/- mice: a model for the cognitive deficit in Rubinstein-Taybi syndrome and its amelioration.** *Neuron* 2004, **42**:947-959.
21. Korzus E, Rosenfeld MG, Mayford M: **CBP histone acetyltransferase activity is a critical component of memory consolidation.** *Neuron* 2004, **42**:961-972.

22. Valor LM, Pulopulos MM, Jimenez-Minchan M, Olivares R, Lutz B, Barco A: **Ablation of CBP in forebrain principal neurons causes modest memory and transcriptional defects and a dramatic reduction of histone acetylation, but does not affect cell viability.** *J. Neurosci.* 2011, **31**:1652-1663.
23. Chen G, Zou X, Watanabe H, van Deursen JM, Shen J: **CREB binding protein is required for both short-term and long-term memory formation.** *J Neurosci* 2010, **30**:13066-13077.
24. Barrett RM, Malvaez M, Kramar E, Matheos DP, Arrizon A, Cabrera SM, Lynch G, Greene RW, Wood MA: **Hippocampal focal knockout of CBP affects specific histone modifications, long-term potentiation, and long-term memory.** *Neuropsychopharmacology* 2011, **36**:1545-1556.
25. Oliveira AM, Estevez MA, Hawk JD, Grimes S, Brindle PK, Abel T: **Subregion-specific p300 conditional knock-out mice exhibit long-term memory impairments.** *Learn Mem* 2011, **18**:161-169.
26. Benito E, Barco A: **CREB's control of intrinsic and synaptic plasticity: implications for CREB-dependent memory models.** *Trends Neurosci* 2010, **33**:230-240.
27. Iwase S, Berube NG, Zhou Z, Kasri NN, Battaglioli E, Scandaglia M, Barco A: **Epigenetic Etiology of Intellectual Disability.** *J Neurosci* 2017, **37**:10773-10782.
28. Shikama N, Lutz W, Kretzschmar R, Sauter N, Roth JF, Marino S, Wittwer J, Scheidweiler A, Eckner R: **Essential function of p300 acetyltransferase activity in heart, lung and small intestine formation.** *EMBO J* 2003, **22**:5175-5185.
29. Roth JF, Shikama N, Henzen C, Desbaillets I, Lutz W, Marino S, Wittwer J, Schorle H, Gassmann M, Eckner R: **Differential role of p300 and CBP acetyltransferase during myogenesis: p300 acts upstream of MyoD and Myf5.** *Embo J* 2003, **22**:5186-5196.
30. Fergelot P, Van Belzen M, Van Gils J, Afenjar A, Armour CM, Arveiler B, Beets L, Burglen L, Busa T, Collet M, et al.: **Phenotype and genotype in 52 patients with Rubinstein-Taybi syndrome caused by EP300 mutations.** *Am J Med Genet A* 2016, **170**:3069-3082.
31. Viosca J, Lopez-Atalaya JP, Olivares R, Eckner R, Barco A: **Syndromic features and mild cognitive impairment in mice with genetic reduction on p300 activity: Differential contribution of p300 and CBP to Rubinstein-Taybi syndrome etiology.** *Neurobiol Dis* 2010, **37**:186-194.
32. Oliveira AM, Wood MA, McDonough CB, Abel T: **Transgenic mice expressing an inhibitory truncated form of p300 exhibit long-term memory deficits.** *Learn Mem* 2007, **14**:564-572.
33. Telley L, Govindan S, Prados J, Stevant I, Nef S, Dermitzakis E, Dayer A, Jabaudon D: **Sequential transcriptional waves direct the differentiation of newborn neurons in the mouse neocortex.** *Science* 2016, **351**:1443-1446.
34. Zeisel A, Munoz-Manchado AB, Codeluppi S, Lonnerberg P, La Manno G, Jureus A, Marques S, Munguba H, He L, Betsholtz C, et al.: **Brain structure.** *Cell*

- types in the mouse cortex and hippocampus revealed by single-cell RNA-seq.** *Science* 2015, **347**:1138-1142.
35. Dyson HJ, Wright PE: **Role of Intrinsic Protein Disorder in the Function and Interactions of the Transcriptional Coactivators CREB-binding Protein (CBP) and p300.** *J Biol Chem* 2016, **291**:6714-6722.
- * Recent overview of the structure of KAT3 proteins and the functionality of the different protein-binding domains.
36. Giles RH, Dauwerse HG, van Ommen GJ, Breuning MH: **Do human chromosomal bands 16p13 and 22q11-13 share ancestral origins?** *Am J Hum Genet* 1998, **63**:1240-1242.
37. Malik AN, Vierbuchen T, Hemberg M, Rubin AA, Ling E, Couch CH, Stroud H, Spiegel I, Farh KK-H, Harmin DA, et al.: **Genome-wide identification and characterization of functional neuronal activity-dependent enhancers.** *Nature Neuroscience* 2014, **17**:1330-1339.
38. Ramos YF, Hestand MS, Verlaan M, Krabbendam E, Ariyurek Y, van Galen M, van Dam H, van Ommen GJ, den Dunnen JT, Zantema A, et al.: **Genome-wide assessment of differential roles for p300 and CBP in transcription regulation.** *Nucleic Acids Res* 2010, **38**:5396-5408.
39. Wang Z, Zang C, Cui K, Schones DE, Barski A, Peng W, Zhao K: **Genome-wide mapping of HATs and HDACs reveals distinct functions in active and inactive genes.** *Cell* 2009, **138**:1019-1031.
40. Kasper LH, Qu C, Obenaus JC, McGoldrick DJ, Brindle PK: **Genome-wide and single-cell analyses reveal a context dependent relationship between CBP recruitment and gene expression.** *Nucleic Acids Res* 2014, **42**:11363-11382.
41. Breen ME, Mapp AK: **Modulating the masters: chemical tools to dissect CBP and p300 function.** *Curr Opin Chem Biol* 2018, **45**:195-203.
- * Recent review describing the progress in the development of chemical tools targeting CBP/p300 domains with selectivity, which should allow the discrimination of differential KAT3 usage.
42. Schroder S, Herker E, Itzen F, He D, Thomas S, Gilchrist DA, Kaehlcke K, Cho S, Pollard KS, Capra JA, et al.: **Acetylation of RNA polymerase II regulates growth-factor-induced gene transcription in mammalian cells.** *Mol Cell* 2013, **52**:314-324.
43. Weinert BT, Narita T, Satpathy S, Srinivasan B, Hansen BK, Scholz C, Hamilton WB, Zucconi BE, Wang WW, Liu WR, et al.: **Time-Resolved Analysis Reveals Rapid Dynamics and Broad Scope of the CBP/p300 Acetylome.** *Cell* 2018, **174**:231-244 e212.
- ** This publication provides a compelling database of KAT3-dependent acetylome in cultured cells by combining quantitative proteomics, next-generation sequencing methods and several KAT3 inhibitors. The study does not only identify thousands of targets of CBP/p300, it also unveils the kinetics of KAT3-mediated acetylation.
44. Dancy BM, Cole PA: **Protein lysine acetylation by p300/CBP.** *Chem Rev* 2015, **115**:2419-2452.
45. Montgomery DC, Sorum AW, Meier JL: **Defining the orphan functions of lysine acetyltransferases.** *ACS Chem Biol* 2015, **10**:85-94.

46. Shi D, Pop MS, Kulikov R, Love IM, Kung AL, Grossman SR: **CBP and p300 are cytoplasmic E4 polyubiquitin ligases for p53**. *Proc Natl Acad Sci U S A* 2009, **106**:16275-16280.
47. Sabari BR, Tang Z, Huang H, Yong-Gonzalez V, Molina H, Kong HE, Dai L, Shimada M, Cross JR, Zhao Y, et al.: **Intracellular crotonyl-CoA stimulates transcription through p300-catalyzed histone crotonylation**. *Mol Cell* 2015, **58**:203-215.
- * This review article discusses the latest evidence for the role of histone acylations in transcription, with a particular interest in the environment-epigenetics-transcription axis of regulation.
48. Sabari BR, Zhang D, Allis CD, Zhao Y: **Metabolic regulation of gene expression through histone acylations**. *Nat Rev Mol Cell Biol* 2017, **18**:90-101.
49. Dai L, Peng C, Montellier E, Lu Z, Chen Y, Ishii H, Debernardi A, Buchou T, Rousseaux S, Jin F, et al.: **Lysine 2-hydroxyisobutyrylation is a widely distributed active histone mark**. *Nat Chem Biol* 2014, **10**:365-370.
50. Huang H, Tang S, Ji M, Tang Z, Shimada M, Liu X, Qi S, Locasale JW, Roeder RG, Zhao Y, et al.: **EP300-Mediated Lysine 2-Hydroxyisobutyrylation Regulates Glycolysis**. *Mol Cell* 2018, **70**:663-678 e666.
51. Calo E, Wysocka J: **Modification of enhancer chromatin: what, how, and why?** *Mol Cell* 2013, **49**:825-837.
52. Raisner R, Kharbanda S, Jin L, Jeng E, Chan E, Merchant M, Haverty PM, Bainer R, Cheung T, Arnott D, et al.: **Enhancer Activity Requires CBP/P300 Bromodomain-Dependent Histone H3K27 Acetylation**. *Cell Rep* 2018, **24**:1722-1729.
- ** The study shows that a selective inhibitor of KAT3 bromodomain, GNE-049, selectively decreases H3K27, but not H3K18, acetylation. These changes result in the downregulation of eRNAs and enhancer-proximal genes, suggesting that KAT3-dependant H3K27ac is crucial for enhancer activity.
53. Hilton IB, D'Ippolito AM, Vockley CM, Thakore PI, Crawford GE, Reddy TE, Gersbach CA: **Epigenome editing by a CRISPR-Cas9-based acetyltransferase activates genes from promoters and enhancers**. *Nat Biotechnol* 2015, **33**:510-517.
54. Bose DA, Donahue G, Reinberg D, Shiekhattar R, Bonasio R, Berger SL: **RNA Binding to CBP Stimulates Histone Acetylation and Transcription**. *Cell* 2017, **168**:135-149 e122.
- ** Interesting and complete biochemical study providing a novel mechanism for CBP catalytic regulation in enhancers. The binding of eRNA to CBP displaces the autoregulatory loop increasing KAT activity. This eRNA-KAT3 feedback mechanism may be crucial for enhancer maintenance.
55. Bedford DC, Kasper LH, Fukuyama T, Brindle PK: **Target gene context influences the transcriptional requirement for the KAT3 family of CBP and p300 histone acetyltransferases**. *Epigenetics* 2010, **5**:9-15.
56. Contreras-Martos S, Piai A, Kosol S, Varadi M, Bekesi A, Lebrun P, Volkov AN, Gevaert K, Pierattelli R, Felli IC, et al.: **Linking functions: an additional role for an intrinsically disordered linker domain in the transcriptional coactivator CBP**. *Sci Rep* 2017, **7**:4676.
57. Yi P, Wang Z, Feng Q, Chou CK, Pintilie GD, Shen H, Foulds CE, Fan G, Serysheva I, Ludtke SJ, et al.: **Structural and Functional Impacts of ER Coactivator Sequential Recruitment**. *Mol Cell* 2017, **67**:733-743 e734.

* The same lab reported in 2015 the first 3D structure of both free and TF-bound p300 protein. Here, they further explore the sequential recruitment of different coactivators that results in conformational and functional changes in p300.

58. Merika M, Williams AJ, Chen G, Collins T, Thanos D: **Recruitment of CBP/p300 by the IFN beta enhanceosome is required for synergistic activation of transcription.** *Mol Cell* 1998, **1**:277-287.
59. Gu W, Roeder RG: **Activation of p53 sequence-specific DNA binding by acetylation of the p53 C-terminal domain.** *Cell* 1997, **90**:595-606.
60. Kee BL, Arias J, Montminy MR: **Adaptor-mediated recruitment of RNA polymerase II to a signal-dependent activator.** *J Biol Chem* 1996, **271**:2373-2375.
61. Shikama N, Lyon J, La Thangue NB: **The p300/CBP family: integrating signals with transcription factors and chromatin.** *Trends Cell Biol* 1997, **7**:230-236.
62. Fang F, Xu Y, Chew KK, Chen X, Ng HH, Matsudaira P: **Coactivators p300 and CBP maintain the identity of mouse embryonic stem cells by mediating long-range chromatin structure.** *Stem Cells* 2014, **32**:1805-1816.
63. Song CZ, Keller K, Murata K, Asano H, Stamatoyannopoulos G: **Functional interaction between coactivators CBP/p300, PCAF, and transcription factor FKLf2.** *J Biol Chem* 2002, **277**:7029-7036.
64. Harton JA, Zika E, Ting JP: **The histone acetyltransferase domains of CREB-binding protein (CBP) and p300/CBP-associated factor are not necessary for cooperativity with the class II transactivator.** *J Biol Chem* 2001, **276**:38715-38720.
65. Hecht A, Vleminckx K, M.P. S, van Roy F, Kemler R: **The p300/CBP acetyltransferases function as transcriptional coactivators of beta-catenin in vertebrates.** *Embo j* 2000, **19**:1839-1850.
66. Wang L, Grossman SR, Kieff E: **Epstein-Barr virus nuclear protein 2 interacts with p300, CBP, and PCAF histone acetyltransferases in activation of the LMP1 promoter.** *Proc Natl Acad Sci U S A* 2000, **97**:430-435.
67. Ludlam WH, Taylor MH, Tanner KG, Denu JM, Goodman RH, Smolik SM: **The Acetyltransferase Activity of CBP Is Required for wingless Activation and H4 Acetylation in Drosophila melanogaster.** *Molecular and Cellular Biology* 2002, **22**:3832-3841.
68. Kumar JP, Jamal T, Doetsch A, Turner FR, Duffy JB: **CREB binding protein functions during successive stages of eye development in Drosophila.** *Genetics* 2004, **168**:877-893.
69. Lilja T, Aihara H, Stabell M, Nibu Y, Mannervik M: **The acetyltransferase activity of Drosophila CBP is dispensable for regulation of the Dpp pathway in the early embryo.** *Dev Biol* 2007, **305**:650-658.
70. Victor M, Bei Y, Gay F, Calvo D, Mello C, Shi Y: **HAT activity is essential for CBP-1-dependent transcription and differentiation in Caenorhabditis elegans.** *EMBO Rep* 2002, **3**:50-55.
71. Boija A, Mahat DB, Zare A, Holmqvist PH, Philip P, Meyers DJ, Cole PA, Lis JT, Stenberg P, Mannervik M: **CBP Regulates Recruitment and Release of Promoter-Proximal RNA Polymerase II.** *Mol Cell* 2017, **68**:491-503 e495.

* The study shows that the KAT activity of CBP in *Drosophila* is crucial for RNAPII recruitment at promoters and release RNAPII from pausing.

72. Ortega E, Rengachari S, Ibrahim Z, Hoghoughi N, Gaucher J, Holehouse AS, Khochbin S, Panne D: **Transcription factor dimerization activates the p300 acetyltransferase.** *Nature* 2018, **562**:538-544.

** This study demonstrates that the dimerization of TF ligands contribute to the activation of the catalytic activity of p300 by promoting trans-autoacetylation and the subsequent release of an autoinhibitory loop. This finding unveils a critical new mechanism for the interplay between transcription and chromatin acetylation.

73. Strom AR, Emelyanov AV, Mir M, Fyodorov DV, Darzacq X, Karpen GH: **Phase separation drives heterochromatin domain formation.** *Nature* 2017, **547**:241-245.

74. Sabari BR, Dall'Agnesse A, Boija A, Klein IA, Coffey EL, Shrinivas K, Abraham BJ, Hannett NM, Zamudio AV, Manteiga JC, et al.: **Coactivator condensation at super-enhancers links phase separation and gene control.** *Science* 2018, **361**.

75. Olzscha H, Fedorov O, Kessler BM, Knapp S, La Thangue NB: **CBP/p300 Bromodomains Regulate Amyloid-like Protein Aggregation upon Aberrant Lysine Acetylation.** *Cell Chem Biol* 2017, **24**:9-23.

76. Chatterjee S, Cassel R, Schneider-Anthony A, Merienne K, Cosquer B, Tzeplaeff L, Halder Sinha S, Kumar M, Chaturbedy P, Eswaramoorthy M, et al.: **Reinstating plasticity and memory in a tauopathy mouse model with an acetyltransferase activator.** *EMBO Mol Med* 2018, **10**.

** The study shows that treatment with a small-molecule activator of CBP/p300, CSP-TTK21, can rescue tauopathy-induced memory impairments in mice. This is the first evidence *in vivo* that suggest that increasing KAT3 activity could be a valid therapeutic approach in diseases related with histone hypoacetylation.

77. Korb E, Herre M, Zucker-Scharff I, Darnell RB, Allis CD: **BET protein Brd4 activates transcription in neurons and BET inhibitor Jq1 blocks memory in mice.** *Nat Neurosci* 2015, **18**:1464-1473.

78. Maddox SA, Watts CS, Schafe GE: **p300/CBP histone acetyltransferase activity is required for newly acquired and reactivated fear memories in the lateral amygdala.** *Learn Mem* 2013, **20**:109-119.

79. Park S, Stanfield RL, Martinez-Yamout MA, Dyson HJ, Wilson IA, Wright PE: **Role of the CBP catalytic core in intramolecular SUMOylation and control of histone H3 acetylation.** *Proc Natl Acad Sci U S A* 2017, **114**:E5335-E5342.

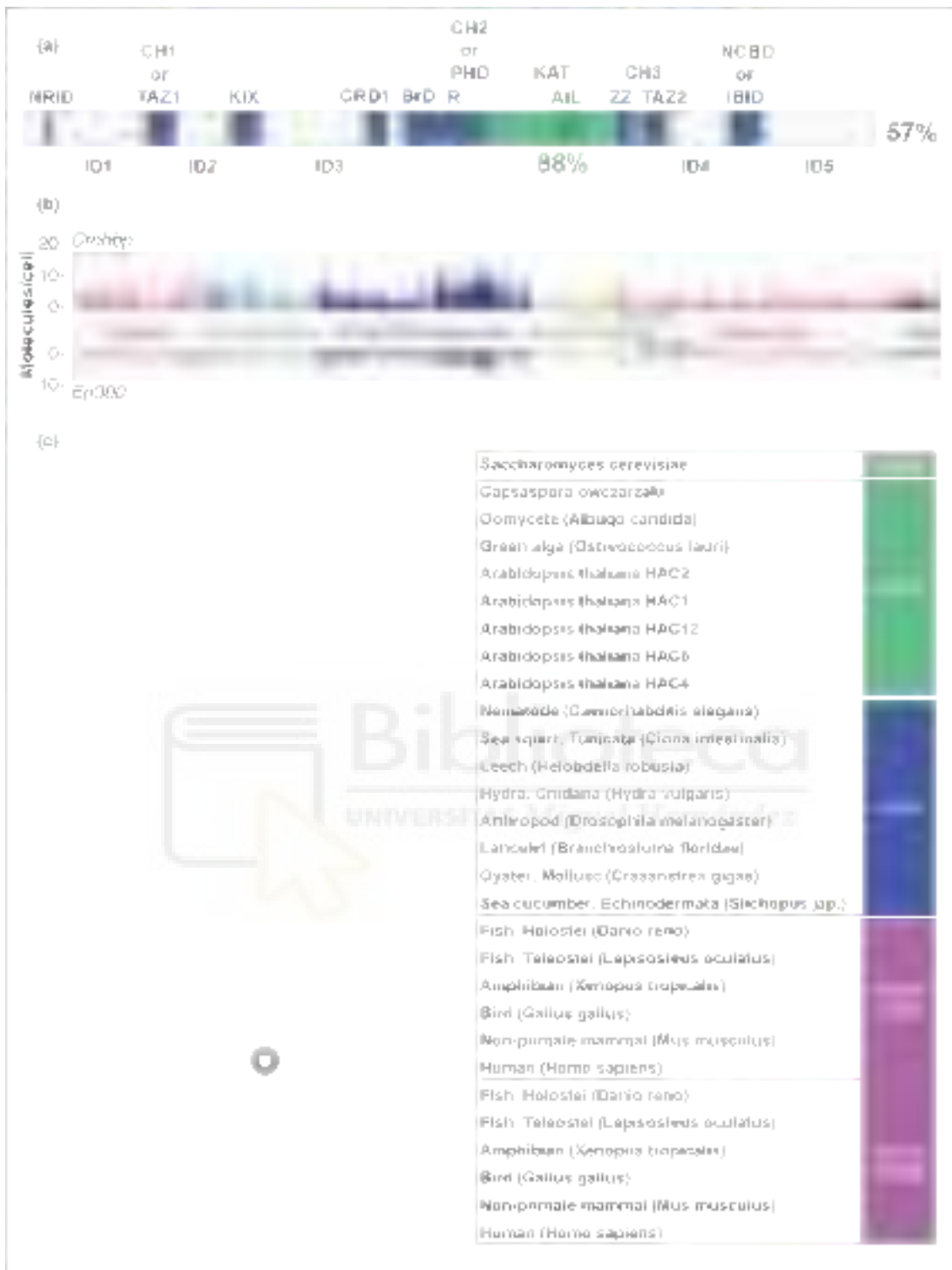


Figure 1. KAT3 structure and evolution. A. *CREBBP* gene structure based on INTERPRO software results with integrated data from [35,56,79]. NRID: nuclear receptor interaction domain; TAZ1-2: transcriptional adapter zinc-binding motifs 1 and 2; KIX: kinase-inducible domain for interaction with CREB; CRD1: cyclin-dependent kinase inhibitor-reactive domain; BrD: bromodomain; PHD domain is discontinued by the RING finger domain (R); KAT: lysine acetyltransferase domain; AIL: autoinhibitory loop; ZZ: dystrophin-like small zinc-binding domain; NCBD: nuclear receptor co-activator binding domain, also called IRF-3 binding domain (IBID); CH1-3: cysteine-histidine-rich domain 1-3; ID1-5: intrinsically disordered regions 1-5.

Percentage values represent the identity between KAT3 proteins for the entire protein and the KAT domain alone. **B.** CBP and p300 expression in different cell types according to single-cell transcriptomic data in the mouse cortex generated by the Linnarsson's lab [34]. **C.** Phylogenetic tree for KAT3 and KAT3-like proteins in different organisms throughout evolution. KAT3 ortholog protein sequences of representative species were extracted from the [INTERPRO](#) database. Multiple sequence alignment was performed using Clustal Omega (EMBL-EBI) and the tree generated using [MEGA](#) software. Gray: the protein closest to KAT3 common ancestor; green: KAT3 genes, non-Animalia; blue: single KAT3 gene, Animalia; magenta: two KAT3 paralog genes, Animalia. Notice that KAT3 duplication seems to coincide with the emergence of vertebrates.



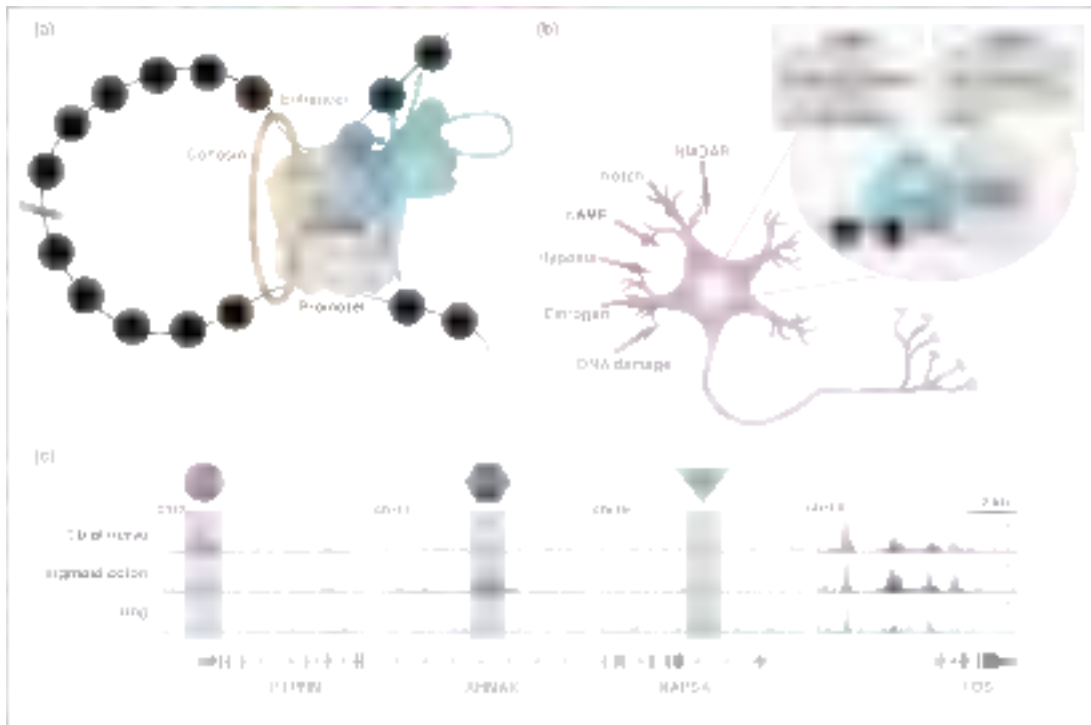


Figure 2. Mechanisms of action of KAT3 proteins. **A.** KAT3 proteins are very proficient lysine acetyltransferases. Within the promoter-enhancer structure, KAT3s engage in an across-the-board acetylation of all kinds of proteins including the four nucleosome histones, transcription factors (TF), structural proteins, the RNAPII complex and KAT3 proteins themselves (asterisks represent these different acetylation events). This provides a broad range of options for influencing transcription, even if not every acetylation event is required for each step or mechanism. **B.** Multiple signaling transduction pathways can potentially affect the transcriptional co-activator function of KAT3 proteins (red arrows). In addition, different studies have identified PTMs and ligands that can either inhibit or stimulate KAT3 activity (square boxes), although the existence or role of most of them has not been investigated in neurons. **C.** The chromatin occupancy profile of KAT3 proteins is highly tissue-specific. ChIP-seq profiles of p300 in three different human tissues (information extracted from the ENCODE project repository) show examples of specific binding in the chromatin of the tibial nerve, sigmoid colon and the upper lobe of left lung, as well as loci occupied in the three tissues. As p300 does not directly bind to DNA, its binding is likely mediated by a different, tissue-specific TF (TF1-3) in each case. The cell type-specific TF interactome of KAT3 proteins thereby drives KAT activity to sculpt a cell type-specific histone acetylome.

ANNEX IV – Authored article 2

The article " Loss of neuronal 3D chromatin organization causes transcriptional and behavioural deficits related to serotonergic dysfunction." by Ito S, Magalska A, Alcaraz-Iborra M, **Lopez-Atalaya JP**, Rovira V, Contreras-Moreira B, **Lipinski M**, Olivares R, Martinez-Hernandez J, Ruszczycki B, Lujan R, Geijo-Barrientos E, Wilczynski GM, **Barco A**. *Nat Commun*. 2014 Jul 18; 5:4450.

DOI: 10.1038/ncomms5450. PMID: 25034090

This article introduced me to the different techniques used in the preparation of this thesis and to basic aspects of the relationship between the chromatin structure and behavioral outcome.



Title: Loss of neuronal 3D chromatin organization causes transcriptional and behavioral deficits related to serotonergic dysfunction

Authors: Satomi Ito^{1,5,6}, Adriana Magalska^{2,5}, Manuel Alcaraz-Iborra¹, Jose P. Lopez-Atalaya¹, Victor Rovira¹, Bruno Contreras-Moreira³, Michal Lipinski¹, Roman Olivares¹, Jose Martinez-Hernandez⁴, Blazej Rusczycki², Rafael Lujan⁴, Emilio Geijo-Barrientos¹, Grzegorz Wilczynski² and Angel Barco^{1,*}

Affiliations

¹ Instituto de Neurociencias (Universidad Miguel Hernández - Consejo Superior de Investigaciones Científicas). Av. Santiago Ramón y Cajal s/n. Sant Joan d'Alacant. 03550. Alicante, Spain.

² Nencki Institute of Experimental Biology. Pasteura 3, 02-093, Warsaw, Poland.

³ Laboratory of Computational Biology, Estación Experimental de Aula Dei (Consejo Superior de Investigaciones Científicas) and Fundación ARAID, Av.Montañana 1.005. 50059 Zaragoza, Spain.

⁴ Instituto de Investigación en Discapacidades Neurológicas (IDINE), Departamento de Ciencias Médicas, Facultad de Medicina, Universidad de Castilla-La Mancha, Campus Biosanitario, C/ Almansa, 14. 02006 Albacete, Spain.

⁵ Equal contribution

⁶ Current address: Information Processing Biology Unit, Okinawa Institute of Science and Technology (OIST) Graduate University, 1919-1 Tancha, Onna-son, Kunigami, Okinawa 904-049, Japan.

* Correspondence: Angel Barco, Instituto de Neurociencias de Alicante (Universidad Miguel Hernández – Consejo Superior de Investigaciones Científicas), Av. Santiago Ramon y Cajal s/n, Sant Joan d'Alacant 03550, Alicante, Spain. Tel: +34 965 919232; Fax: +34 965 919492. Email: abarco@umh.es.

Running title: 3D-chromatin organization and brain function

Abstract

The interior of the neuronal cell nucleus is a highly organized 3-dimensional (3D) structure where regions of the genome that are linearly millions of bases apart establishing sub-structures with specialized functions. To investigate neuronal chromatin organization and dynamics *in vivo*, we generated bi-transgenic mice expressing GFP-tagged histone H2B in principal neurons of the forebrain. Surprisingly, the expression of this chimeric histone in mature neurons caused chromocenter declustering and disrupted the association of heterochromatin with the nuclear lamina. The loss of these structures did not affect neuronal viability but was associated with specific transcriptional and behavioral deficits related to serotonergic dysfunction. Overall, our results demonstrate that the 3D-organization of chromatin within neuronal cells provides an additional level of epigenetic regulation of gene expression which critically impacts neuronal function. This in turn suggests that some loci associated with neuropsychiatric disorders may be particularly sensitive to changes in chromatin architecture.



Introduction

Research over the last decade indicates that epigenetic dysregulation importantly contributes to the etiology of neuropsychiatric disorders^{1, 2, 3}. Among the different epigenetic mechanisms of regulation of gene expression, the modulation of higher-order chromatin structures is one of the least understood. The interior of the eukaryotic cell nucleus is a highly organized 3D structure in which regions of the genome that are millions of bases apart, even belonging to different chromosomes, work together and define specialized sub-structures with dedicated functions^{4, 5}. Thus, in most interphase somatic cells, pericentromeric regions are organized in clusters referred to as chromocenters that consist of transcriptionally silent DNA and exhibit species- and cell type-specific features^{6, 7, 8}.

Chromatin architecture may have particular importance in neurons because these long-living cells are permanently arrested in interphase and the structures formed during neuronal differentiation are likely irreversible^{9, 10, 11}. During neuronal maturation, the nuclear architecture of neural precursors undergoes dramatic changes and passes from a small, heterochromatic nucleus with many small chromocenters to the large euchromatic nucleus with a few large chromocenters characteristic of mature neurons¹². Although the functional consequences of these changes are obscure, the conserved pattern in terminally differentiated neurons suggests that they are physiologically relevant. For instance, studies in Purkinje neurons have revealed a precise assembly process in which specific chromosomes always cluster together and adjacent neurons have similar spatial distribution of centromeric and telomeric clusters^{13, 14}. Furthermore, recent studies have shown that gene mutations associated with intellectual disability in humans affect chromatin compactation and the number and size of chromocenters in cortical neurons^{15, 16}. The reported changes in the spatial distribution of satellite DNA and active loci in hippocampal neurons after seizures or experimentally induced long-term potentiation also support a role for higher-order chromatin structures in neuronal function^{17, 18, 19}. Also consistent with this view, a recent study has revealed chromosomal conformation changes in the chromatin of the prefrontal cortex of schizophrenic patients that specifically affected the *GADI* locus²⁰.

Serendipitously, the generation of bitransgenic mice that express a histone H2B tagged with GFP (H2BGFP) in an inducible manner in principal neurons of the forebrain provided us with an unexpected and valuable approach to examine the consequences of interfering with 3D chromatin organization in neuronal gene expression and physiology. We found that the accumulation of H2BGFP causes dramatic changes in the nuclear architecture of pyramidal neurons, including chromocenter declustering and loss of peripheral heterochromatin. These changes are accompanied by highly specific transcriptional defects and behavioral abnormalities, including alterations associated with serotonin (5-HT) dysfunction. Our results suggest a new role for perinuclear heterochromatin and chromocenter organization in the epigenetic regulation of neuronal gene expression that may have relevance in the etiology of mental illness.

Results

Aberrant chromatin architecture in H2BGFP-expressing neurons

To label the nucleus of principal neurons in the forebrain, we used the doxycycline (dox)-regulated system of double transgenics²¹ to express a fusion protein between histone H2B and GFP (Fig. 1a). Double transgenics raised off dox expressed high levels of H2BGFP in principal neurons of the forebrain, particularly in the CA1 and DG subfields of the hippocampus, specific layers of the cortex and striatum (Fig. 1b). RT-qPCR and western blot assays indicated that the chimeric histone is expressed at a comparable level to endogenous histone H2B and is functionally integrated into chromatin (Fig. 1c-e). Nissl staining and immunostaining for different neuronal proteins demonstrated that H2BGFP did not cause neuronal death nor gross alterations in brain anatomy (Supplementary Fig. 1).

In the course of these initial experiments, we observed that H2BGFP accumulated in discrete structures in the interior of the neuronal nucleus that were strongly labeled with the DNA stain DAPI. While DAPI staining in the nucleus of CA1 neurons typically delineates the nuclear envelope and accumulates in a few large chromocenters, in bitransgenic animals DAPI fluorescence overlapped with GFP and provided a distinctive subnuclear pattern with numerous foci and without peripheral heterochromatin attached to the nuclear membrane (Fig. 1f). Similar but less pronounced differences were also observed in other neuronal types expressing H2BGFP, such as granular neurons in the dentate gyrus, and cortical and striatal neurons (Fig. 1g). Quantitative 3D analysis confirmed the increase in the number of intranuclear DAPI-stained foci in CA1 pyramidal neurons and revealed that these structures were larger and more irregular in bitransgenic than in control mice (Fig. 1h-j and Supplementary Movies 1 and 2).

To confirm these observations using a different approach that provides better spatial resolution, we used electron microscopy (EM). The comparison of EM images corresponding to the *stratum pyramidale* in the CA1 subfield revealed dramatic differences between H2BGFP and control littermates. In ultrathin sections, the nucleus of CA1 pyramidal neurons in control animals showed none or, at most, 1-2 heterochromatic regions (Fig. 1k), whereas bitransgenic mice exhibited multiple discrete heteropycnotic regions (Fig. 1l). Moreover, whereas the nuclei of control neurons show heterochromatin attached to the inner nuclear envelope, in H2BGFP mice this was detached (compare Fig. 1m and 1n). In fact, some neurons in bitransgenic mice exhibited nuclear body-like circular membranous structures that may have originated from invaginations of the nuclear lamina during heterochromatin detachment. We also observed a reorganization of the interchromatin compartment, which appeared much emptier in H2BGFP mice than in control animals (Fig. 1m-n, insets). These changes of nuclear ultrastructure did not alter the number or structure of synapses in the *stratum radiatum* (Fig. 1o-p: Control= 0.285 and H2BGFP= 0.272 syn μm^{-2}).

To characterize the extent of the nuclear disorganization, we next conducted colocalization experiments with proteins or protein modifications that are known to be enriched in specific nuclear sub-structures. In agreement with EM images, the nucleolar proteins fibrillarin and nucleolin revealed that nucleoli were normal in H2BGFP expressing neurons (Fig. 2a). The spliceosome protein Sam68 and the Cajal body

protein coilin also revealed a normal staining pattern indicating that these structures were preserved in bitransgenic mice (Fig. 2b-c). Lamina staining was also not affected except for the occasional invaginations reported above (Fig. 2d-e). In contrast, fluorescence in situ hybridization (FISH) using a pancentromeric probe revealed striking differences between genotypes; in control nuclei the FISH signal overlapped with chromocenters, whereas in H2BGFP-expressing neurons the signal was scattered in the form of dots embedded within the aberrant DNA foci, in addition to some normal-looking chromocenters (Fig. 2f). H3K9me2/3 (Fig. 2g) and methyl-Cytosine (mCyt, Fig. 2h), two modifications of the chromatin associated with a heterochromatic state, also exhibited an aberrant staining pattern that overlapped with GFP/DAPI foci. This redistribution was associated with a significant reduction of the signal for mCyt (Control= 1.00±0.38, H2BGFP= 0.7±0.03, $p < 0.0001$). Interestingly, the expression of H2BGFP caused a shifting of the signal for the intercalating agent propidium iodide (PI) in flow cytometry experiments (Fig. 2i) that disappeared when the nuclei were pre-incubated with HCl to extract chromatin proteins and allow the full access of PI to DNA, which suggests that the accessibility to PI in a fraction of the chromatin is larger in H2BGFP-expressing neurons. Immunostaining for H3K27me3, a histone posttranslational modification (PTM) that can be found in both active and inactive loci but not in silent chromatin, also revealed dramatic differences between genotypes. Whereas in control animals H3K27me3 showed a diffuse pattern that excluded the large chromocenters, in bitransgenics the signal partially overlapped with the aberrant DAPI foci (Fig. 2j). A similar but milder redistribution was also observed for the methyl CpG binding protein 2 (MeCP2), a transcriptional repressor that binds methylated DNA sequences (Fig. 2k). Finally, the staining patterns for several protein modifications associated with euchromatin were also altered. Thus, whereas the staining for histone acetylations (Fig. 2l) and phospho-Pol II S5P (Fig. 2j) filled most of the nucleus in normal neurons, concentrating at brighter spots (possibly transcription factories), they accumulated around GFP/DAPI foci in bitransgenic mice. This accumulation was particularly pronounced in the case of H3K9ac that showed a striking ring-like pattern around the foci. Together, these results demonstrate that H2BGFP expression is associated with an abnormal interaction between heterochromatin and the nuclear lamina, the declustering of pericentromeric chromatin and the reorganization of transcriptionally active domains.

Interference with heterochromatin structures

Previous studies indicate that H2BGFP does not interfere with most chromatin functions in dividing cells, including transcription and mitosis²². Our results, however, show that the continuous and robust expression of this chimeric histone can destabilize heterochromatin structures in the quiescent nuclei of forebrain neurons. The modeling of nucleosomes bearing H2BGFP instead of H2B indicates that the bulky GFP tag (a barrel with radius and height of approximately 30 Å) will prominently protrude from the chromatin fiber and may interfere with the folding of the chromatin fiber in highly compacted tertiary structures (Fig. 3a), such as the dense interdigitation of nucleosomal arrays that has been postulated as a possible arrangement for heterochromatin *in vivo*²³.

Based on this observation and the previous evidence indicating that H2BGFP molecules are rapidly exchanged in active nucleosomes during transcription but retained in non-active chromatin domains²⁴, we speculate that this chimeric histone would progressively accumulate into heterochromatin sterically destabilizing the highly compacted tertiary chromatin structures characteristic of fully differentiated neurons. Consistently with this view, the relative enrichment for H2BGFP in hippocampal chromatin at steady state was larger in silent genes, such as *Hbb-bh1*, than in highly expressed genes, such as *Gapdh* (Fig. 3b). Also, supporting the specificity of the effect of chronic H2BGFP expression in neuronal nuclear architecture, we found that H2BGFP did not alter DAPI staining in HEK293 cells or transiently transfected cultured hippocampal neurons (Fig. 3c). Most glial cells in bitransgenic mice generated by crossing tetO-H2BGFP mice with pGFAP-tTA also showed a normal DNA distribution (Supplementary Fig. 2). In contrast, neural crest-derived Neuro-2a (N2a) cells transfected with H2BGFP appeared initially normal but exhibited an aberrant chromatin distribution after dibutyryl-cAMP (dbcAMP)-induced differentiation to a neuronal phenotype (Fig. 3d). The latter experiment also revealed a good correlation between the level of H2BGFP expression and the strength of the chromatin phenotype.

Additional experiments in transgenic mice demonstrated that chromocenter declustering closely correlated with transgene expression. Thus, the neurons of 6-days old bitransgenic mice, in which transgene expression was nearly undetectable, exhibited a normal nuclear pattern with few large chromocenters, whereas 3 weeks later young bitransgenic animals already presented the aberrant staining described for adult mice (Fig. 3e). On the other hand, bitransgenic mice raised on a dox-supplemented diet did not express the transgene and exhibited normal DAPI staining (Fig. 1b, right panels), but incipient chromocenter disorganization became evident 1 week after transgene induction and was completed 2 weeks later (Fig. 3f). Consistently, transgene repression by continuous treatment with dox for several months led to the appearance of scattered neurons that showed the loss of both GFP fluorescence and the aberrant DAPI staining phenotype (Fig. 3g). Note that the very long half-life of this protein²⁵ caused that the rapid decrease of H2BGFP by dox transcripts was not followed by a similar reduction at the protein level (Fig. 3h).

Loss of chromatin architecture and transcription

We next investigated the consequences of aberrant chromatin organization in global gene expression using microarrays. This analysis revealed that the dramatic structural changes had a surprisingly modest impact on hippocampal gene expression (Fig. 4a). Heterochromatin disorganization did not cause the de-repression of non neuronal genes or transcriptionally repressed repetitive elements. In fact, most of the detected changes corresponded to genes downregulated in H2BGFP mice (Fig. 4b and Supplementary Table 1). The differential profiling retrieved transcript cluster (TC) IDs of particular relevance for neuronal function and behavior, such as *Drd5*, *Npy2r*, *Htr1a*, *Htr1b* and *Htr2a* that encode for a dopamine, a neuropeptide and three serotonin receptors, respectively. Indeed, *Negative regulation of glutamatergic synaptic transmission* (adj. $P= 7 \times 10^{-5}$), *Serotonin receptor signaling* (adj. $P= 1 \times 10^{-4}$) and

Dopamine secretion (adj. $P= 2 \times 10^{-4}$) were the most affected biological processes in the H2BGFP profile according to Gene Ontology (GO) analysis (Supplementary Table 2). The functional analysis also revealed a significant association with *abnormal anxiety-related response* (adj. $P= 3 \times 10^{-4}$), *abnormal spatial learning* (adj. $P= 6 \times 10^{-4}$), *abnormal locomotor activation* (adj. $P= 5 \times 10^{-3}$) phenotypes and a number of disturbances of the conduct in humans that included *Attention Deficit Disorder with Hyperactivity* (adj. $P= 2 \times 10^{-7}$) and other behavioral disorders (adj. $P < 1 \times 10^{-6}$).

RT-qPCR assays using independent samples confirmed the most relevant transcriptional changes, including the downregulation of 5-HT receptors (Fig. 4c), and the absence of significant changes in repetitive elements (Supplementary Fig. 3a).

Behavioral abnormalities in H2BGFP mice

We next examined whether animal's behavior was affected as predicted by our functional analysis of differential expression. No differences were observed between bitransgenic mice and control siblings in a battery of neurological tests assessing basic reflexes, strength and other parameters (Supplementary Table 3). Motor performance in an accelerated Rotarod task was also not affected (Supplementary Fig. 4a: $F_{(1, 16)} \text{ genotype} = 0.10$, $P= 0.75$). However, bitransgenic mice showed locomotor hyperactivity in an open arena measured as ambulatory distance (Fig. 5a: $F_{(1, 16)} \text{ genotype} = 24.92$, $P= 0.0001$; see also Supplementary Fig. 4b), reduced resting time (Fig. 5b: $F_{(1, 16)} \text{ genotype} = 24.46$, $P= 0.0001$) and faster speed (Fig. 5c: $F_{(1, 16)} \text{ genotype} = 23.46$, $P = 0.0002$). Bitransgenic mice also presented deficits in tasks evaluating their responsiveness to different sort of external stimuli, including reduced marble burying behavior (Fig. 5d: $F_{(1, 16)} \text{ genotype} = 10.67$, $P= 0.005$), larger latencies for exploring novel objects (Fig. 5e: $F_{(1, 16)} \text{ genotype} = 7.87$, $P= 0.01$), impaired social interaction (Fig. 5f: $F_{(1, 16)} \text{ genotype} = 5.42$, $P= 0.03$; Fig. 5g: $F_{(1, 16)} \text{ genotype} = 0.44$, $P= 0.02$), larger latencies in the hot plate task (Fig. 5h: $F_{(1, 16)} \text{ genotype} = 6.64$, $P= 0.02$) and deficits in sensorimotor gating (Fig. 5i: $F_{(1, 13)} \text{ genotype} = 6.06$, $P= 0.03$), but normal startle response (Supplementary Fig. 4c: $F_{(1, 13)} \text{ genotype} = 0.12$, $P= 0.73$).

H2BGFP mice were also impaired in several cognitive tasks. We should, however, note that the existence of underlying basic behavioral alterations, such as hyperlocomotion in the open field and reduced nociception, prevents a precise evaluation of cognitive capabilities. In the novel object recognition (NOR) task, control mice spent more time exploring a novel than a familiar object (Fig. 5j: $F_{(1, 8)} = 1.93$, $P= 0.05$), whereas H2BGFP mice explored similar time both objects showing no memory for previously explored objects ($F_{(1, 6)} = 0.93$, $P= 0.37$). Similarly, bitransgenic mice did not express a preference for interacting with a novel versus a previously encountered mouse in the 3-chambered social novelty task (Fig. 5g: $F_{(1, 16)} \text{ genotype} = 0.47$, $P= 0.02$). H2BGFP mice also exhibited significant deficits in contextual (Fig. 5k: $F_{(1, 14)} \text{ genotype} = 7.31$, $P= 0.02$) and cued ($F_{(1, 14)} \text{ genotype} = 6.16$, $P= 0.03$) fear conditioning and a reduced immediate response to the shock ($F_{(1, 14)} \text{ genotype} = 33.0$, $P < 0.001$). Furthermore, in the hidden platform water maze task, H2BGFP mice showed severe deficits in spatial learning manifested in the latency (Fig. 5l: $F_{(7, 84)} \text{ time} \times \text{genotype} = 1.89$, $P= 0.04$) and path length (Supplementary Fig. 4d: $F_{(7, 84)} \text{ time} \times \text{genotype} = 2.95$, $P= 0.008$) curves that led to

very poor performance in the probe trials assessing spatial memory (Fig. 5m: PT1_{TQ} $F_{(1, 12)} = 1.96$, $P = 0.19$; PT2_{TQ} $F_{(1, 12)} = 5.13$, $P = 0.04$; see also Supplementary Fig. 4e). Importantly, these mice also swam slower (Supplementary Fig. 4f: $F_{(1, 12)}^{\text{genotype}} = 5.44$, $P = 0.04$) and, starting after the visible platform task, were more prone to floating (Fig. 5n: $F_{(7, 84)}^{\text{time} \times \text{genotype}} = 2.39$, $P = 0.03$), which is consistent with the reduced responsiveness observed in other tasks.

These behavioral deficits are likely not caused by a failure in activity-driven transcription because the well-characterized and transient induction of immediate early genes (IEGs) upon novelty exposure, which includes genes involved in neuronal plasticity and memory consolidation such as *Fos*, *Arc* and *Npas4*²⁶, was preserved in the hippocampus of H2BGFP mice despite of the severe chromatin disorganization (Supplementary Fig. 3b).

Epigenetic dysregulation of serotonin receptor genes

Prompted by our functional analysis of differential gene expression, we examined in detail the genomic features of behaviorally relevant loci whose expression was altered in H2BGFP mice. We observed that the three 5-HT receptor genes downregulated in bitransgenic mice (*Htr1a*, *Htr1b* and *Htr2a*) had in common their location adjacent to desert islands (Fig. 6a-b). The examination of the hippocampal profiles for H3K4me3 and H3K9,14ac recently generated by our group²⁷ confirmed the large distance between these loci and the nearest active gene in hippocampal tissue (Fig. 6c). Consistently, the exploration of the profiles recently generated by Ren's lab in their screen for cis-regulatory sequences in the mouse cerebral cortex²⁸ did not identify any prominent putative regulatory element in these genomic regions (Supplementary Fig. 5a). The comparison with the same region in the human genome reveals high synteny and conserved spacing between the two species. Other genes at the edge of gene desert, such as *Fat4*, *Gpr101* and *Ptpru* were also downregulated in H2BGFP mice. Overall 13% of the genes in which the distance to one of its two neighbors is > 0.5 Mbp (660 genes, 59% of them showing a expression in hippocampal tissue higher than the median) were altered in H2BGFP mice (Fisher's exact test P -value = 0.01). The significance of this enrichment is even larger if we consider a neighbor distance > 250 Kb (P -value = 1.8×10^{-5}). The position of these genes in the interphase between eu- and heterochromatin might contribute to explain their larger susceptibility to changes in chromatin architecture, although additional gene features should lend specificity to this sensitivity because not all the genes located in the proximity of gene-free regions were affected by H2BGFP expression.

We next investigated the association of the most affected and clinically relevant of these loci, *Htr1a*, with peripheral heterochromatin and chromocenters through fluorescence in situ hybridization (FISH). Consistently with a recent screen for lamina-associated domains (Supplementary Fig. 5b), quantitative FISH analysis of *Htr1a* in control animals revealed a nonrandom spatial distribution in the nucleus of CA1 neurons, in which one of the two *Htr1a* alleles was frequently positioned at the nuclear margin, whereas the other was at the nucleus interior (Fig. 6d and Supplementary Fig. 6). This configuration was altered in neurons from H2BGFP mice, in which in the

absence of perinuclear heterochromatin, the two *Htr1a* alleles were positioned in the proximity of, or even within, the aberrant DNA-foci (Fig. 6d and Supplementary Fig. 6, note that *Htr1a* signal is consistently associated with the less bright foci originated after chromocenter declustering.). To assess the functional status of the locus, we performed immuno-FISH assays to simultaneously detect the *Htr1a* alleles and activated RNA Polymerase II phospho-epitopes p-Ser2 or p-Ser5 (Fig. 6e–f). In agreement with our gene expression data, the quantitative analysis revealed that the association of *Htr1a* with these two phospho-proteins was larger in control than in H2BGFP mice (Fig. 6g: Control S2P= 89±1.0%; H2BGFP S2P= 53±0.9%; Control S5P= 79±1.0%; H2BGFP S5P= 53±0.8%). Moreover, the reduced expression and intranuclear relocation was associated with the spreading of heterochromatin PTMs into this locus (Fig. 6h). Also consistently with gene expression data, similar results were obtained at the promoters of *Htr1b* and *Htr2a* (Fig. 6h). In our effort to investigate the relationship between the global changes in chromatin architecture and the, in contrast, highly specific transcriptional changes, we determined the genomic profile of H3K27me3 in the chromatin of H2BGFP mice and control littermates. This histone PTM is found at the boundaries of lamin-bound domains and has been traditionally considered a repressive chromatin mark although is mutually exclusive with H3K9 methylation. Although the intranuclear (3D) distribution of H3K27me3 is severely disrupted by H2BGFP expression (Fig. 2j), ChIP-seq analysis did not reveal dramatic alterations of its (2D) genomic profile (Fig. 6i and Supplementary Fig. 7a). Notably, the genomic screen confirmed the increase of H3K27me3 presence in *Htr* loci detected in locus-specific assays (Fig. 6j) but did not reveal any major change in the topography of this mark neither in the loci nor in the adjacent gene desert regions (Fig. 6c and Supplementary Fig. 7b). As expected from studies outside the brain, the larger enrichment for H3K27me3 was found in developmental homeobox genes silenced in adult tissue (Supplementary Fig. 7c).

To determine whether serotonin signaling was effectively reduced in H2BGFP-expressing CA1 pyramidal neurons, we performed electrophysiological recordings in CA1 pyramidal neurons of bitransgenic and control littermates. Serotonin binding to 5-HT_{1A} subtype receptors (encoded by *Htr1a*) in the membrane of CA1 neurons activates G protein-coupled inwardly-rectifying K⁺ channels causing cell hyperpolarization and the reduction of membrane resistance^{29, 30}. Both parameters were significantly reduced in the neurons of bitransgenic animals after serotonin application (Fig. 7a–b). Moreover, the administration of the partial agonist of 5-HT_{1A} receptors buspirone, which modulates locomotor activity in the open field (Fig. 7c: $F_{(1, 30)} \text{ drug treatment} = 10.31, P = 0.003$), restored the mobility of bitransgenic mice to control levels, and increased the percentage of time that the mice spent interacting with a stranger mouse and the duration of social contacts in the social interaction task (Fig. 7d–e). These results indicate that some of the behavioral alterations revealed in our comprehensive screen are related to serotonergic dysfunction.

Discussion

We demonstrate here that the robust expression of histone H2B tagged with EGFP in mature neurons causes a dramatic reorganization of chromatin that affected the association of heterochromatin with the nuclear lamina, the higher-order organization of pericentromeric heterochromatin in large chromocenters that is characteristic of mature cortical and hippocampal pyramidal neurons, and the subnuclear distribution of protein PTMs associated with active transcription. Although GFP-tagged histones are a common tool in cellular and developmental biology studies, our experiments indicate that caution is needed while using this tool in studies of the adult brain. Two unique features of our study led to this finding. First, most previous studies with GFP-tagged histone H2B have been performed after transient expression and/or in dividing cell, whereas we investigated the quiescent postmitotic nuclei of mature pyramidal neurons at the steady-state. Second, the aberrant DAPI pattern was first noted in mouse CA1 hippocampal neurons, which have a particularly prominent and characteristic chromocenter organization.

In differentiated cells, chromatin is spatially segregated in different types⁵. Chromocenters and peripheral heterochromatin represent the highest level of chromatin compactation and are labeled with epigenetic modifications associated with silent DNA (e.g., mCyt and H3K9me2/3), whereas transcriptionally active domains are located in the nucleoplasm and enriched in histone modifications associated with an open chromatin conformation, like the acetylation of histone tails and H3K4me3. This spatial configuration is profoundly disturbed by H2BGFP possibly as a result of its shuttling in active chromatin and retention in non-active domains where it sterically interferes with highly compacted heterochromatin conformations. These changes also affected less compacted forms of chromatin and, as a result, the characteristic dispersed pattern of H3K27me3 in interphase nuclei was replaced in bitransgenic mice by a patched pattern that overlapped with GFP/DAPI foci (although in the absence of apparent changes in its genomic distribution), whereas histone PTMs associated with active transcription clustered in the surface of these structures. Notably, other subnuclear structures, like the nucleolus or the Cajal bodies, were not affected by these changes of nuclear architecture. Taken together, our results indicate that the loss of one heterochromatin compartment has a broad impact on chromatin compartmentalization, and highlight the fine interplay between histone PTMs that regulate the transition between different chromatin configurations³¹.

The dramatic changes in chromatin architecture had a surprisingly subtle impact in gene expression. This observation indicates that either H2BGFP causes some specific transcriptional alterations that mediate the changes in chromatin distribution or, more likely, H2BGFP induces an aberrant chromatin conformation that leads to the transcriptional deregulation of specific loci. Given that none of the genes affected in H2BGFP mice is known to play a major role in chromatin organization, whereas H2BGFP is an integrant component of the chromatin in these neurons that has the potential to severely disrupt its packaging, we favor the second hypothesis. Intriguingly, the short list of genes affected by H2BGFP expression was enriched in genes that are adjacent to gene-free genomic regions. The large chromocenters in fully differentiated pyramidal neurons might represent the ultimate storage solution for DNA that will not

longer be replicated nor transcribed. Our results suggest that the functional state of this inert DNA did not change as a result of chromocenter destabilization, but its decompaction and the concurrent relocation of active domains in the surface of the DNA foci observed in our co-staining experiments (Fig. 2) may be responsible for the reduction in the transcription of active genes that are located in its immediate proximity. However, additional gene features should lend specificity to this epigenetic inactivation because not all the genes located in the proximity of gene-free regions were affected by H2BGFP expression. Future genome-wide chromosome conformational capture experiments might clarify this issue and relate specific changes in gene clustering to the transcriptional deficits reported here.

Our study complements recent research demonstrating that intellectual disability disorders in humans are frequently associated with mutations in genes encoding chromatin regulators³² and recent studies linking high-order chromatin organization and brain disease^{19,20}, contributing to a better understanding of the still obscure role of chromatin architecture in brain function and gene expression. It allows to discern for the first time between processes that depend, or not depend, on such organization. Thus, our results indicate that 3D chromatin organization is not essential for neuronal viability or to maintain neuronal identity, but also show that its loss triggers physiological and behavioral deficits that are reminiscent of endophenotypes found in important behavioral disorders in humans. Furthermore, our experiments identified specific misregulated genes likely involved in these behavioral alterations. In particular, the changes in 5-HT1A receptor expression are considered an important determinant of predisposition to mental illness³³ and, although the mechanisms underlying the variable expression of this locus between individuals remain unclear, transcriptional dysregulation has been suggested as a likely candidate³⁴. 5-HT2A and 5-HT1B receptors are also of great relevance for behavioral disorders^{35,36}. These three 5-HT receptors are particularly abundant in corticolimbic regions targeted for H2BGFP expression in bitransgenic animals. Intriguingly, additional loci associated with mental illness, such as *DRD5* and *TDO2*, are also affected in H2BGFP mice. Both *Drd5* (encoding for a dopamine receptor) and *Tdo2* (encoding for the rate-limiting enzyme in the synthesis of serotonin tryptophan 2,3-dioxygenase) play a role in serotonin signaling and have been related to attention deficit-hyperactivity disorder (ADHD) and autism spectrum disorder (ASD)^{37,38,39,40}. The case of Rett syndrome (RS) is particularly interesting because (i) this congenital disorder associated with intellectual disability and autism has been recently related to impaired heterochromatin clustering¹⁵ and chromocenter alterations during neuronal maturation¹⁶; (ii) RS is caused by mutations in the gene encoding MeCP2, one of the proteins showing abnormal distribution in H2BGFP-expressing neurons; (iii) the dysfunction of monoaminergic systems is known to be an important component of RS neuropathology⁴¹ and 5-HT1A agonists, like the one used in our study, prolong the life of mouse model of the disease⁴² and are useful in the treatment of respiratory dysfunction in RS patients⁴³; and (iv) recent transcriptomics analyses show that *Htr1a* and *Htr2a* are downregulated in the hippocampus of mouse models of RS⁴⁴. The transcriptional and behavioral deficits in H2BGFP mice also relate to negative symptoms in schizophrenia, such as prepulse

inhibition and cognitive impairments and reduced motivational drive. In fact, it has been proposed that alterations in serotonergic activity could be responsible for the dysregulation of dopaminergic function observed in schizophrenia and some of the receptors downregulated in H2BGFP mice are found also decreased in the prefrontal cortex of schizophrenia subjects ⁴⁵. We should, however, note that other relevant aspects of behavior related to serotonin dysfunction, like despair (Supplementary Fig. 4g-h) and anxiety (Supplementary Fig. 4i-k), were not altered in H2BGFP mice. The distinct actions of auto- and heteroreceptors ⁴⁶ and differential impact of impaired 5-HT signaling in immature and mature mood-related circuitry ^{47, 48} together with the spatial and temporal pattern of transgenic expression, which restricts H2BGFP to areas of high heteroreceptor expression and late developmental stages, may explain the selective impact. Although it is unlikely that the disorganization of higher-order chromatin structure is a widespread feature of neuropsychiatric disorders, the overlap between the transcriptional deficits found in H2BGFP mice and some gene associations in neuropsychiatric disorders is striking. Our synteny analysis revealed that the genes encoding the serotonin receptors affected in H2BGFP mice are also located in the proximity of gene deserts in humans. It is, therefore, attractive to speculate that this topographic feature may underlie a larger susceptibility of the loci to epigenetic regulation in response to experience and environmental changes.



Methods

Animals and treatments

pCaMKII-tTA/line B²¹ and tetO-HIST1H2BJ/GFP²⁵ mice were crossed to produce CaMKII-tTA/tetO-H2BGFP bitransgenic mice that are referred to as “H2BGFP mice” in the text. Both parental strains are available at Jackson laboratories (stock number 7004 and 5104, respectively) and are maintained on a C57BL/6J genetic background (the second one after backcrossing to this background). H2BGFP mice were usually raised without doxycycline (dox) and transgene repression was achieved by dox administration (40 mg kg⁻¹ of food) for at least 1 week. In all our experiments, we used as control littermates mice carrying either no transgene or the tTA or tetO transgene alone. Behavioral testing and the ChIP-seq experiment were performed with males. In all other experiments, mice from both sexes were used keeping a balance between control and mutant groups. Mice were 2-4 months old mice at least that explicitly indicated otherwise, except for the electrophysiological recordings conducted in younger animals (4-5 weeks old). Experimenters were blind to genotypes and the result of the PCR-based genotyping (see Supplementary Table 4 for primers sequences) was provided as a factor for statistical analysis once the experiments were concluded. Sodium butyrate (1.2 g kg⁻¹) and buspirone (2 mg kg⁻¹) were dissolved in PBS and administered by intraperitoneal injection. Mice were maintained according to animal care standards established by the European Union; all experimental protocols were approved by the Institutional Animal Care and Use Committee..

Neuronal and cell line cultures

Primary hippocampal neurons from Swiss albino mouse embryos at E17.5-E18.5 were cultured in 24-well plates (Becton Dickinson 353047) on 12mm glass coverslips (VWR) coated with Poly-D-Lysine (Sigma Aldrich). After tissue homogenization, cells were counted in a Neubauer chamber and seeded at a density of ~130.000 cells per well. After 2-3 h, Plating Medium (DMEM supplemented with 10% FBS, 0.45% glucose, 2 mM glutamine and penicillin/streptomycin 100 U/ml-100 µg/ml) was replaced with defined Maintenance Medium (MM, Neurobasal supplemented with B27, 2 mM glutamine and penicillin/streptomycin 100 U/ml-100µg/ml). Transient transfection experiments in HEK293 cells, Neuro 2A (N2A) cells and primary hippocampal neurons with the plasmid pCAG-hH2BGFP were performed using Lipofectamin 2000 (Invitrogen). For N2A differentiation experiments, cells were transiently transfected with pCAG-hH2BGFP and planted on glass slides (1x10⁴ cells ml⁻¹) in DMEM + 1% FBS; dibutyryl-cAMP (dbcAMP 2.5 mM, Sigma) was added to the medium to stop proliferation and trigger differentiation towards a neuronal phenotype. Samples were fixed at indicated time points with 4% PFA and stained with Phalloidin-TRITC (10 µg ml⁻¹, Sigma) and DAPI (1nM, Invitrogen) to visualize cell actin and DNA respectively.

RT-qPCR and ChIP-qPCR assays

Extraction of hippocampal RNA and RT-qPCR assays were performed as previously described⁵². Primer sequences are listed in Supplementary Table 4. For chromatin immunoprecipitation (ChIP) assays, mice were sacrificed by decapitation and the whole

hippocampus was dissected, minced into small pieces and crosslinked in 1% formaldehyde for 15 min at room temperature (at least three independent tissue samples per condition). Chromatin samples were then sonicated with a bioruptor (Diagenode) and incubated overnight at 4°C in the presence of specific antibodies (Supplementary Table 5) or rabbit-derived pre-immune serum. ChIP-qPCR assays were performed using specific primers immediately upstream of the transcription start site (Supplementary Table 4).

Microarray, ChIP-seq and other genomic analyses

For microarray hybridization, total hippocampal RNA was extracted with TRI reagent (Sigma). Equal amounts of purified total RNA from a couple (one male and one female) of age and genotype-matched mice were pooled, treated with DNaseI and cleaned up using the RNeasy mini kit (Qiagen). Three independent pooled samples per genotype were hybridized to Mouse Gene 1.0 ST expression arrays (Affymetrix). Microarray data were analyzed using the Bioconductor R packages *oligo*, *genefilter* and *limma* ⁵³. More precisely, expression data were preprocessed with RMA using the median polish method for probe-set summarization ⁵⁴; then, control probes were removed and intensity filtering was applied to eliminate non-expressed probe-sets (intensity value below 20% percentile in all arrays); finally, differential expression analysis was performed with moderated *t*-statistics ⁵⁵. Adjusted P-values were used to rank and filter expression values. Functional genomics enrichment analyses were performed at *WebGestalt* (<http://bioinfo.vanderbilt.edu/webgestalt/>) ⁵⁶. ChIP-seq analysis was performed as in ²⁷. Briefly, we pooled hippocampal chromatin of twelve male mice per condition. The cross-linked and sonicated chromatin was immunoprecipitated using a ChIP-grade (ChIP-seq tested) antibody against H3K27me3 (Abcam, ab6002, 1:100 dilution) or rabbit-derived preimmune serum. DNA libraries were produced and sequenced using a HiSeq-2500 apparatus (Illumina, service provided by Fasteris S.L.) according to manufacturer instructions. Two independent sequencing runs (1 x 50 bp) were performed for each library (technical replicates). Reads were mapped onto the mouse genome (NCBIM37/mm9) using BWA ⁵⁷, BAM files were generated and parsed to filter uniquely mapped reads using SAMTOOLS ⁵⁸, and the heatmaps and k-means clustering analysis were performed on the merged replicates (library size > 25x10⁶ in all cases) using seqMINER ⁵⁹. Clusters showing H3K27me3 enrichment were merged for further analysis. Density plots showing intergenic distance were generated using the Refseq database after removal of overlapping genes. To evaluate a selective enrichment in genes with a long-distance neighbor among the differentially expressed genes in H2BGFP mice, we performed Fisher exact test against those genes contained in the array. The information about LADs was extracted from ⁶⁰, about cis-regulatory elements from ²⁸, and the enrichment profiles for H3K9,14ac and H3K4me3 from ²⁷. Microarray and ChIP-seq data is accessible through the Gene Expression Omnibus (GEO) database using the accession number GSE56810.

Molecular modeling

For GFP docking into the nucleosome model, a homology model of GFP plus the 8-residue linker was built with *MODELLER*⁴⁹ using as template Protein Data Bank entry 4en1 with a sequence identity of 95%. Then, the modeled GFP domain was docked to the C-terminus of H2B (chain D of PDB entry 1ZBB) with pyDockTET⁵⁰. Nucleosome radius increments were estimated by measuring interatomic distances, while volumes were calculated with help from *UnionBalls*⁵¹.

FISH and Immuno-FISH

The FISH procedure was performed in 40µm coronal brain cryosections of 4% paraformaldehyde-perfused animals. The pancentromeric probe (Chrombios), directly labeled with Texas-red and recognizing a conserved sequence in mouse centromeres, was used according to manufacturer's instructions. The CH29-584 BAC used as template for *Htr1a* probe was obtained from Children's Hospital Oakland Research Institute. For DNA amplification Illustra Genomi Phi V2 kit (GE Healthcare) was used according to manufacturers' protocol. The probe was directly labeled with Cy5-dUTP nucleotide using the Nick-Translation Mix (Roche). *Htr1a*-Cy5 labeled probe was verified on mouse metaphase spreads. The hybridization reaction was performed for 72 h with the probe diluted in buffer containing 50% formamide, 10% dextran and 2x SSC (Sigma), followed by a series of high-stringency washes with 2x SSC at 37°C and 0.1x SSC at 60°C⁶². In immuno-FISH experiments, FISH was followed by a rabbit polyclonal antibody directed against the phosphorylated RNA pol II C-terminal domain phosphorylated on S2, or phosphorylated on S5, (Abcam), followed by DyLight 488 conjugated goat anti-rabbit antibody (Invitrogen), according to our standard protocol⁶³. Nuclei were counterstained using Hoechst 33342 (Invitrogen). The quantitative analyses were performed using the public domain software Fiji (<http://fiji.sc/Fiji>) in 72 nuclei from control animals and in 86 nuclei from H2BGFP animals. Co-localization maps were made using the Fiji plugin parison with control group at least that indicated otherwise.

Other immunological methods

Hippocampal protein extracts and Western blot analysis were performed according to standard protocols. We used the primary antibodies listed in Supplementary Table 5 and HRP-conjugated secondary antibodies from Sigma-Aldrich. Flow cytometry experiments were performed in a BD FACSAriaTM III apparatus and analyzed using FACSDivaTM software. The initial steps of nuclei preparation for flow cytometry analysis were the same than in the ChIP procedure. To extract chromatin proteins and allow full access of propidium iodide (Sigma, P4170) to DNA, fixed nuclei were pre-incubated with 0.1N HCl for 1 minute⁶¹. For immunohistochemistry (IHC), mice were anaesthetized with a ketamine/xylazine mixture and perfused with paraformaldehyde (4% in 0.1M phosphate buffer); brains were postfixed overnight and cut in a vibratome. Brain slices were washed with PBS, permeabilized with PBS containing 0.25% Triton X-100, incubated with the primary antibodies listed in Supplementary Table 5, and counterstained with a 1 nM DAPI (Invitrogen). For image acquisition, fluorescent specimens were examined under Carl Zeiss LSM780 Spectral Confocal using diode

laser 405nm (CW/pulsed), DPSS diode 561nm and HeNe 633nm laser, at room temperature. Cross talk between the fluorophores was avoided by adjustment of the spectral ranges of the detectors and sequential scanning of the images. Signal intensity quantification in individual nuclei (at least 20-30 nuclei per condition) was performed using the free open source application ImageJ64 as described⁶². Image-stacks were acquired at the sampling density of 80 nm/pixel, and Z-spacing of 200 nm, using Plan Apochromat 63x/1.4 Oil DIC objective. To reduce noise and improve resolution, the stacks were 3D deconvolved by means of Huygens Professional software (Scientific Volume Imaging). Three-dimensional (3D) image analysis was performed in 221 nuclei from control animals and in 284 nuclei from H2BGFP animals using the custom-written software “Segmentation magick” essentially as described in¹⁹, except that the nucleus boundary had to be enhanced using anti-lamin B immunostaining because of the aberrant chromatin pattern in H2BGFP mice. The 3D reconstructions and movies were made using *Imaris* software (Bitplane).

Other histological techniques

For Nissl staining, brain slices were incubated with cresylviolet for 30 min, then dipped briefly in dH₂O, washed briefly in 0.1% acetate in 95% ethanol, washed in 95% EtOH, washed in 100% EtOH, dipped in xylene twice for 3 min, and quick mounted with Neo-Mount. For electron microscopy, bitransgenic and control littermates were perfused with 4% paraformaldehyde and 1% glutaraldehyde in 0.1M phosphate buffer (PB). Coronal sections were cut with a thickness of 60 μ m at the level of the dorsal hippocampus. After several washes in PB, the sections were postfixed with osmium tetroxide (1% in PB) and block stained with uranyl acetate (1% in distilled water). The sections were then dehydrated in ascending series of ethanol to 100% followed by propylene oxide and flat embedded on glass slides in *Durcupan*. The CA1 region of the hippocampus was cut at 70–90 nm on an ultramicrotome and collected on 200-mesh nickel grids. Staining was performed on drops of 1% aqueous uranyl acetate followed by Reynolds’s lead citrate. Ultrastructural analyses were performed with a Jeol-1010 electron microscope.

Electrophysiology

Cortical slices of 300 μ m thickness were prepared from H2BGFP and control littermates aged 4-5 weeks according to routine methods used in our laboratory⁶³. Animals were killed by cervical dislocation and coronal slices in which the hippocampus was present were cut with a Vibratome (Leica VT1000) in ice-cold cutting solution (composition in mM: NaCl, 124; KCl, 2.5; PO₄H₂Na, 1.25; Mg Cl₂, 2.5; CaCl₂, 0.5; NaCO₃H, 26; glucose, 10; pH 7.4 when saturated with 95% O₂ and 5% CO₂). The slices were transferred to artificial cerebrospinal fluid (ACSF; composition in mM: NaCl, 124; KCl 2.5; PO₄H₂Na, 1.25; Mg Cl₂, 1; CaCl₂, 2; NaCO₃H, 26; glucose, 10; pH 7.4 when saturated with 95% O₂ and 5% CO₂) where they were incubated at 37° during 30 min and thereafter kept at room temperature until use. For recording, the slices were placed in a submersion type chamber, placed on the stage of an upright microscope (Olympus BX50WI), and superfused at a flow rate of 3-5 ml min⁻¹ with

ACSF at 33-34°C. Hippocampal CA1 pyramidal neurons were identified visually with DIC optics and infrared illumination. Intracellular recordings were obtained with glass microelectrodes pulled in a Sutter P-97 electronic puller (Sutter Instruments, USA) that had a resistance of 3-7 MOhm when filled with intracellular solution (Composition in mM: KMeSO₄, 135; NaCl, 8; HEPES, 10; Mg₂ATP, 2; Na₃GTP, 0.3; PH 7.3 adjusted with KOH; osmolality 295 mOsm kg⁻¹). Current clamp recordings were acquired with a two channel Multiclamp 700B amplifier (Axon Instruments, Molecular Devices, USA), low pass filtered at 6KHz and digitized at 20 KHz with a Digidata 1322A (Axon Instruments, Molecular Devices, USA). Serotonin was obtained from Sigma-Aldrich (USA) and applied dissolved in ASCF at a final concentration of 5 µM. Each slice was used only for the recording of a single neuron to avoid possible long-term effects of the serotonin on the electrophysiological properties of CA1 pyramidal neurons. Membrane input resistance was measured using hyperpolarizing current pulses of 25 pA and 250 ms. In some recordings, during the serotonin application the membrane potential was adjusted to the resting level with direct current injection. Statistical comparisons were made with SigmaStat 3.2 (Systat Software Inc.); Student's t-test for unpaired and paired samples were used after checking for the normality and equal variance of the samples; data are given as mean ± s.e.m.

Behavioral analysis

Three independent cohorts of adult (3-6 months old) bitransgenic and control littermate males were tested in series of behavioral tasks. Cohort 1: Open field (OF), Elevated Plus Maze (EPM), Rotarod, SHIRPA, Forced Swim Test (FST), Tail Suspension Test (TST) and Hot Plate test; Cohort 2: Morris Water Maze (MWM, including visible and hidden platform tasks), Stress-induced Hyperthermia (SIH), Social Interaction, Marble Burying and Novel Object Exploration tests; Cohort 3: Startle response (SR) and Prepulse inhibition (PPI), Novel Object Recognition (NOR) memory test, Three-chambered Social Approach test and Fear Conditioning (FC, including contextual and cued tests). Mice from the three cohorts were finally used in experiment evaluating the interaction of the 5-HT_{1A} receptor agonist buspirone with relevant behaviors. Buspirone (2 mg kg⁻¹) was administered 20 min before a new 30 min-OF session to examine the impact in locomotor hyperactivity. Immediately after, one 3-weeks old mouse was brought in the center of the chamber to evaluate social interaction. The SHIRPA primary screen, OF, EPM and FC tasks were performed as previously described⁶⁴. To study motor coordination and learning, mice were trained on a Rotarod (Ugo Basile) at a constant speed (4 rpm) four times per day during 2 days. On the testing day, the Rotarod was set to increase its speed 1 rpm every 16 s starting at 4 rpm, and the latency to fall was measured. To evaluate nociception and sensitivity to thermal stimulus, mice were placed in the test chamber of a hot plate (IITC Life Science) set at 54°C, and the latency until the animal exhibited paw licking was recorded. All mice were tested three times with 1 h interval between each measurement. Spatial learning in the MWM was assessed in a circular tank (170 cm diameter) filled with opaque white water as described previously⁶⁴. Mice were monitored throughout the training and testing sessions with the video-tracking software SMART (Panlab S.L.). A platform of

10 cm diameter was submerged 1 cm below the water surface in the center of the target quadrant. The training protocol, both when the platform was visible (5 d: V1 to V5) and hidden (8 d: H1 to H8), consisted of four trials per day with a 45 min intertrial interval. If the mice did not find the platform after 120 s, they were gently guided to it. Mice were transferred to their cages only after remaining on the platform for at least 10 s. Memory retention trials of 60 s were performed at the beginning of day H5 (probe trial 1) and 24 h after concluding the training on day H8 (probe trial 2). The NOR task was performed as previously described⁶⁵ with a 10-min training session and a 10-min testing session 24 h after training. For FST, mice were placed into clear plastic buckets 2/3 filled with 26°C water and videotaped from the side. After 2 min pretest period, the activity of the mice the following 4 min was scored. TST was performed with Med associates Inc. equipment; mice were suspended by the tail with adhesive tape to a hook connected to a strain gauge during 6 min and their activity recorded. To evaluate physiological mild stress, SIH was evaluated by measuring rectal temperature twice with an intertrial interval of 10 min in which the mice were placed in a new cage; the difference ($\Delta T=T2-T1$) reflects the SIH response. In both the social interaction test and novel object tests, mice were placed in a white acrylic box (48 x 48 x 30 cm) for 30 min of habituation; then, either a 3-weeks old mouse or a novel object was introduced in the cage and the number of contacts and the latency until the first investigation were measured. In the marble burying task, 16 opaque marbles placed in a 4x4 arrangement (5 cm separation between marbles) on top of fresh sawdust; then, the number of marbles with more than 2/3 of their surface covered with sawdust (buried) during the 30 min test session was scored. PPI was carried as previously described⁶⁴ but using different intensity for the prepulse (PP): 20-ms PP trials of 83 dB, 86 dB and 92 dB. In the three-chambered social approach test, mice were initially placed in the center chamber with access to two side chambers containing one empty cylinder; after 5 min of freely exploring this environment (Hab), an unfamiliar C57BL/6J male mouse (Mouse1) was placed in one of the empty cylinders for 10 min and the time spent interacting with the empty or the occupied cylinder was scored (Test1). Immediately after, a second unfamiliar male (Mouse2) was placed inside the empty cylinder to evaluate social novelty during 10 min; the time spent interacting with stranger 1 and 2 was scored (Test2).

Accession code: Microarray and ChIP-seq data is accessible through the Gene Expression Omnibus (GEO) database using the accession number GSE56810.

References

1. Jakovcevski M, Akbarian S. Epigenetic mechanisms in neurological disease. *Nat Med* **18**, 1194-1204 (2012).
2. Sun H, Kennedy PJ, Nestler EJ. Epigenetics of the depressed brain: role of histone acetylation and methylation. *Neuropsychopharmacology : official publication of the American College of Neuropsychopharmacology* **38**, 124-137 (2013).
3. Schaefer A, Tarakhovskiy A, Greengard P. Epigenetic mechanisms of mental retardation. *Prog Drug Res* **67**, 125-146 (2011).
4. Schoenfelder S, Clay I, Fraser P. The transcriptional interactome: gene expression in 3D. *Curr Opin Genet Dev* **20**, 127-133 (2010).
5. Politz JC, Scalzo D, Groudine M. Something Silent This Way Forms: The Functional Organization of the Repressive Nuclear Compartment. *Annu Rev Cell Dev Biol* **29**, 241-270 (2013).
6. De Boni U. The interphase nucleus as a dynamic structure. *Int Rev Cytol* **150**, 149-171 (1994).
7. Solovei I, *et al.* Nuclear architecture of rod photoreceptor cells adapts to vision in mammalian evolution. *Cell* **137**, 356-368 (2009).
8. Clowney EJ, *et al.* Nuclear aggregation of olfactory receptor genes governs their monogenic expression. *Cell* **151**, 724-737 (2012).
9. Takizawa T, Meshorer E. Chromatin and nuclear architecture in the nervous system. *Trends Neurosci* **31**, 343-352 (2008).
10. Mitchell AC, *et al.* The Genome in Three Dimensions: A New Frontier in Human Brain Research. *Biol Psychiatry*, (2013).
11. Wilczynski G. Significance of higher-order nuclear architecture for neuronal function and dysfunction. *Neuropharmacology*, (2014).
12. Aoto T, Saitoh N, Ichimura T, Niwa H, Nakao M. Nuclear and chromatin reorganization in the MHC-Oct3/4 locus at developmental phases of embryonic stem cell differentiation. *Dev Biol* **298**, 354-367 (2006).
13. Martou G, De Boni U. Nuclear topology of murine, cerebellar Purkinje neurons: changes as a function of development. *Exp Cell Res* **256**, 131-139 (2000).
14. Vadakkan KI, Li B, De Boni U. Trend towards varying combinatorial centromere association in morphologically identical clusters in Purkinje neurons. *Cell Chromosome* **5**, 1 (2006).
15. Agarwal N, *et al.* MeCP2 Rett mutations affect large scale chromatin organization. *Hum Mol Genet* **20**, 4187-4195 (2011).
16. Singleton MK, *et al.* MeCP2 is required for global heterochromatic and nucleolar changes during activity-dependent neuronal maturation. *Neurobiol Dis* **43**, 190-200 (2011).
17. Borden J, Manuelidis L. Movement of the X chromosome in epilepsy. *Science* **242**, 1687-1691 (1988).
18. Billia F, Baskys A, Carlen PL, De Boni U. Rearrangement of centromeric satellite DNA in hippocampal neurons exhibiting long-term potentiation. *Brain Res Mol Brain Res* **14**, 101-108 (1992).
19. Walczak A, *et al.* Novel Higher-Order Epigenetic Regulation of the Bdnf Gene upon Seizures. *J Neurosci* **33**, 2507-2511 (2013).
20. Bharadwaj R, *et al.* Conserved chromosome 2q31 conformations are associated with transcriptional regulation of GAD1 GABA synthesis enzyme and altered in prefrontal cortex of subjects with schizophrenia. *J Neurosci* **33**, 11839-11851 (2013).

21. Mayford M, Bach ME, Huang YY, Wang L, Hawkins RD, Kandel ER. Control of memory formation through regulated expression of a CaMKII transgene. *Science* **274**, 1678-1683 (1996).
22. Kanda T, Sullivan KF, Wahl GM. Histone-GFP fusion protein enables sensitive analysis of chromosome dynamics in living mammalian cells. *Curr Biol* **8**, 377-385 (1998).
23. Luger K, Dechassa ML, Tremethick DJ. New insights into nucleosome and chromatin structure: an ordered state or a disordered affair? *Nat Rev Mol Cell Biol* **13**, 436-447 (2012).
24. Kimura H, Cook PR. Kinetics of core histones in living human cells: little exchange of H3 and H4 and some rapid exchange of H2B. *J Cell Biol* **153**, 1341-1353 (2001).
25. Tumber T, *et al.* Defining the epithelial stem cell niche in skin. *Science* **303**, 359-363 (2004).
26. Flavell SW, Greenberg ME. Signaling mechanisms linking neuronal activity to gene expression and plasticity of the nervous system. *Annu Rev Neurosci* **31**, 563-590 (2008).
27. Lopez-Atalaya JP, Ito S, Valor LM, Benito E, Barco A. Genomic targets, and histone acetylation and gene expression profiling of neural HDAC inhibition. *Nucleic Acids Res* **41**, 8072-8084 (2013).
28. Shen Y, *et al.* A map of the cis-regulatory sequences in the mouse genome. *Nature* **488**, 116-120 (2012).
29. Andrade R, Malenka RC, Nicoll RA. A G protein couples serotonin and GABAB receptors to the same channels in hippocampus. *Science* **234**, 1261-1265 (1986).
30. Andrade R, Nicoll RA. Pharmacologically distinct actions of serotonin on single pyramidal neurones of the rat hippocampus recorded in vitro. *J Physiol* **394**, 99-124 (1987).
31. Pinheiro I, *et al.* Prdm3 and Prdm16 are H3K9me1 methyltransferases required for mammalian heterochromatin integrity. *Cell* **150**, 948-960 (2012).
32. Kleefstra T, Schenck A, M. KJ, van Bokhoven H. The genetics of cognitive epigenetics. *Neuropharmacology*, (2014).
33. Lanzenberger RR, *et al.* Reduced serotonin-1A receptor binding in social anxiety disorder. *Biol Psychiatry* **61**, 1081-1089 (2007).
34. Albert PR, Le Francois B, Millar AM. Transcriptional dysregulation of 5-HT1A autoreceptors in mental illness. *Mol Brain* **4**, 21 (2011).
35. Barnes NM, Sharp T. A review of central 5-HT receptors and their function. *Neuropharmacology* **38**, 1083-1152 (1999).
36. Quist JF, *et al.* The serotonin 5-HT1B receptor gene and attention deficit hyperactivity disorder. *Molecular psychiatry* **8**, 98-102 (2003).
37. Comings DE. Clinical and molecular genetics of ADHD and Tourette syndrome. Two related polygenic disorders. *Ann N Y Acad Sci* **931**, 50-83 (2001).
38. Hsu CD, Tzang RF, Liou YJ, Hong CJ, Tsai SJ. Family-based association study of tryptophan hydroxylase 2 and serotonin 1A receptor genes in attention deficit hyperactivity disorder. *Psychiatric genetics* **23**, 38 (2013).
39. Shim SH, *et al.* A case-control association study of serotonin 1A receptor gene and tryptophan hydroxylase 2 gene in attention deficit hyperactivity disorder. *Progress in neuro-psychopharmacology & biological psychiatry* **34**, 974-979 (2010).

40. Nabi R, Serajee FJ, Chugani DC, Zhong H, Huq AH. Association of tryptophan 2,3 dioxygenase gene polymorphism with autism. *Am J Med Genet B Neuropsychiatr Genet* **125B**, 63-68 (2004).
41. Santos M, *et al.* Monoamine deficits in the brain of methyl-CpG binding protein 2 null mice suggest the involvement of the cerebral cortex in early stages of Rett syndrome. *Neuroscience* **170**, 453-467 (2010).
42. Abdala AP, Dutschmann M, Bissonnette JM, Paton JF. Correction of respiratory disorders in a mouse model of Rett syndrome. *Proc Natl Acad Sci U S A* **107**, 18208-18213 (2010).
43. Andaku DK, Mercadante MT, Schwartzman JS. Bupirone in Rett syndrome respiratory dysfunction. *Brain & development* **27**, 437-438 (2005).
44. Baker SA, Chen L, Wilkins AD, Yu P, Lichtarge O, Zoghbi HY. An AT-hook domain in MeCP2 determines the clinical course of Rett syndrome and related disorders. *Cell* **152**, 984-996 (2013).
45. Meltzer HY, Massey BW, Horiguchi M. Serotonin receptors as targets for drugs useful to treat psychosis and cognitive impairment in schizophrenia. *Current pharmaceutical biotechnology* **13**, 1572-1586 (2012).
46. Richardson-Jones JW, *et al.* 5-HT1A autoreceptor levels determine vulnerability to stress and response to antidepressants. *Neuron* **65**, 40-52 (2010).
47. Gross C, *et al.* Serotonin1A receptor acts during development to establish normal anxiety-like behaviour in the adult. *Nature* **416**, 396-400 (2002).
48. Audero E, Mlinar B, Baccini G, Skachokova ZK, Corradetti R, Gross C. Suppression of serotonin neuron firing increases aggression in mice. *J Neurosci* **33**, 8678-8688 (2013).
49. Eswar N, *et al.* Comparative protein structure modeling using Modeller. *Current protocols in bioinformatics / editorial board, Andreas D Baxevanis [et al]* **Chapter 5**, Unit 5 6 (2006).
50. Cheng TM, Blundell TL, Fernandez-Recio J. Structural assembly of two-domain proteins by rigid-body docking. *BMC Bioinformatics* **9**, 441 (2008).
51. Mach P, Koehl P. Geometric measures of large biomolecules: surface, volume, and pockets. *Journal of computational chemistry* **32**, 3023-3038 (2011).
52. Lopez-Atalaya JP, *et al.* CBP is required for environmental enrichment-induced neurogenesis and cognitive enhancement. *Embo J* **30**, 4287-4298 (2011).
53. Gentleman RC, *et al.* Bioconductor: open software development for computational biology and bioinformatics. *Genome Biol* **5**, R80 (2004).
54. Irizarry RA, Bolstad BM, Collin F, Cope LM, Hobbs B, Speed TP. Summaries of Affymetrix GeneChip probe level data. *Nucleic Acids Res* **31**, e15 (2003).
55. Smyth G. *Limma: linear models for microarray data*. Springer, New York (2005).
56. Wang J, Duncan D, Shi Z, Zhang B. WEB-based GEne SeT AnaLysis Toolkit (WebGestalt): update 2013. *Nucleic Acids Res* **41**, W77-83 (2013).
57. Li H, Durbin R. Fast and accurate long-read alignment with Burrows-Wheeler transform. *Bioinformatics* **26**, 589-595 (2010).
58. Li H, *et al.* The Sequence Alignment/Map format and SAMtools. *Bioinformatics* **25**, 2078-2079 (2009).
59. Ye T, *et al.* seqMINER: an integrated ChIP-seq data interpretation platform. *Nucleic Acids Res* **39**, e35 (2011).
60. Guelen L, *et al.* Domain organization of human chromosomes revealed by mapping of nuclear lamina interactions. *Nature* **453**, 948-951 (2008).

61. Darzynkiewicz Z, Traganos F, Kapuscinski J, Staiano-Coico L, Melamed MR. Accessibility of DNA in situ to various fluorochromes: relationship to chromatin changes during erythroid differentiation of Friend leukemia cells. *Cytometry* **5**, 355-363 (1984).
62. Valor LM, Pulopulos MM, Jimenez-Minchan M, Olivares R, Lutz B, Barco A. Ablation of CBP in forebrain principal neurons causes modest memory and transcriptional defects and a dramatic reduction of histone acetylation, but does not affect cell viability. *J Neurosci* **31**, 1652-1663 (2011).
63. Troca-Marin JA, Geijo-Barrientos E. Inhibition by 5-HT of the synaptic responses evoked by callosal fibers on cortical neurons in the mouse. *Pflugers Archiv : European journal of physiology* **460**, 1073-1085 (2010).
64. Viosca J, Schuhmacher AJ, Guerra C, Barco A. Germline expression of H-Ras(G12V) causes neurological deficits associated to Costello syndrome. *Genes Brain Behav* **8**, 60-71 (2009).
65. Puighermanal E, Marsicano G, Busquets-Garcia A, Lutz B, Maldonado R, Ozaita A. Cannabinoid modulation of hippocampal long-term memory is mediated by mTOR signaling. *Nat Neurosci* **12**, 1152-1158 (2009).



End Notes

Acknowledgments: The authors thank Matias Pulpulos and Alessandro Ciccarelli for preliminary observations on the behavior of H2BGFP mice. We also thank Francesc Artigas, Cornelius Gross, Eloisa Herrera, Christoph Kellendonk and Luis M. Valor for critical reading of the manuscript.

Funding: SI held a Juan de la Cierva contract from the Spanish Ministry of Economy and Competitiveness (MINECO). JLA held a postdoctoral contract (JAE-DOC) from the Program “Junta para la Ampliación de Estudios” co-funded by the Fondo Social Europeo (FSE). AM is supported by a postdoctoral fellowship from BIO-IMAGINE (EU FP7 Capacities Programme). Research at AB’s lab is supported by grants from MINECO (SAF2011-22855) and the Generalitat Valenciana (Prometeo/2012/005). Research at EG’s lab is supported by the grant BFU2011-27326 and research at RL’s lab is supported by the CONSOLIDER grant CSD2008-00005 both given by MINECO. Research at GW’s lab is supported by the grant POIG 01.01.02-00-008/08 from the European Regional Development Fund.

Author contributions: SI, AM and ML performed cellular and molecular biology experiments and analyzed the data. MA conducted the behavioral characterization, VR the electrophysiological recordings and JMH the electron microscopy experiments. BCM conducted the GFP docking modeling, BR developed the software for 3D reconstruction and quantification of confocal images, JLA performed bioinformatics analysis. AB, GW, EGB, and RL directed the work and analyzed the data. AB designed the experiments and wrote the manuscript.

Conflict of interest statement: The authors do not express any conflict of interest.

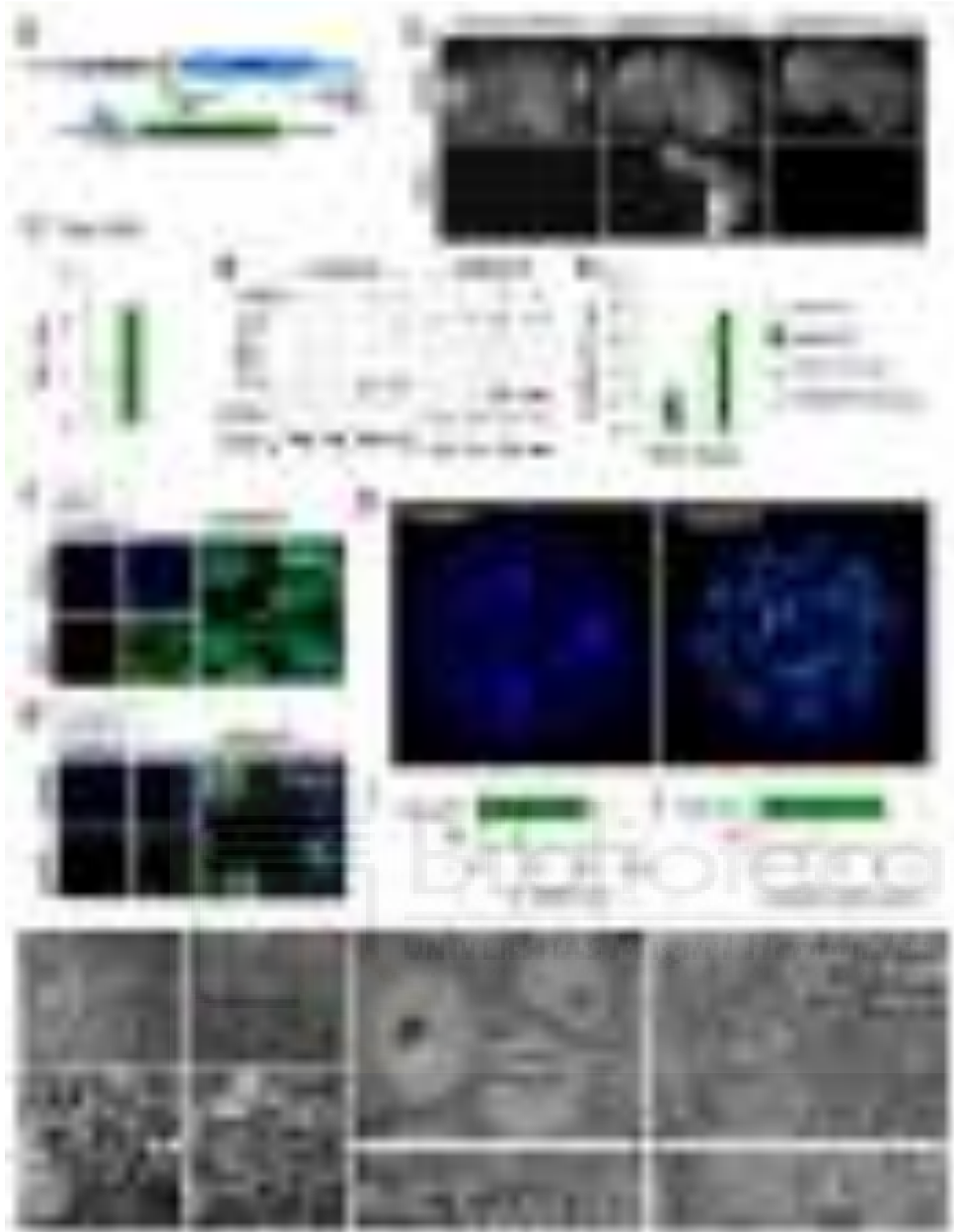


Figure 1. Regulated expression of H2BGFP in the brain of transgenic mice is associated with aberrant DNA staining. **a.** Bitransgenic approach used in this study. **b.** GFP immunostaining of brain sagittal sections from H2BGFP mice, fed or not with dox, and a control littermate. DAPI was used for nuclear counterstaining. **c.** qPCR assays using a primer pair that recognizes a highly conserved sequence present in both mouse and human H2B transcripts. **d.** Western-blot analyses using antibodies against H2Bac, GFP and H2B (top to bottom). H2BGFP was hyperacetylated like endogenous histone H2B after treatment with the inhibitor of histone deacetylases sodium butyrate (NaBt). **e.** Relative intensity quantification of H2BGFP acetylation. **f-g.** GFP and DAPI patterns in CA1 (f) and cortical (g) neurons of H2BGFP and control mice. **h.** 3D reconstruction of confocal images illustrating both chromocenters declustering and the loss of peripheral heterochromatin in CA1 pyramidal neurons of H2BGFP mice. **i-j.** Quantification of the number (i) and size (j) of DAPI-stained foci in H2BGFP and control littermates. **k-p.** Electron micrographs of pyramidal neurons in the CA1 subfield of control (k) and H2BGFP mice (l). The higher magnification images of disorganized heterochromatin and insets illustrate the emptiness of nucleoplasm space and occasional

presence of internal membranous structures in H2BGFP nuclei (n) compared to control littermates (m). In contrast, there is no apparent difference in the *stratum radiatum* of control (o) and H2BGFP mice (p).

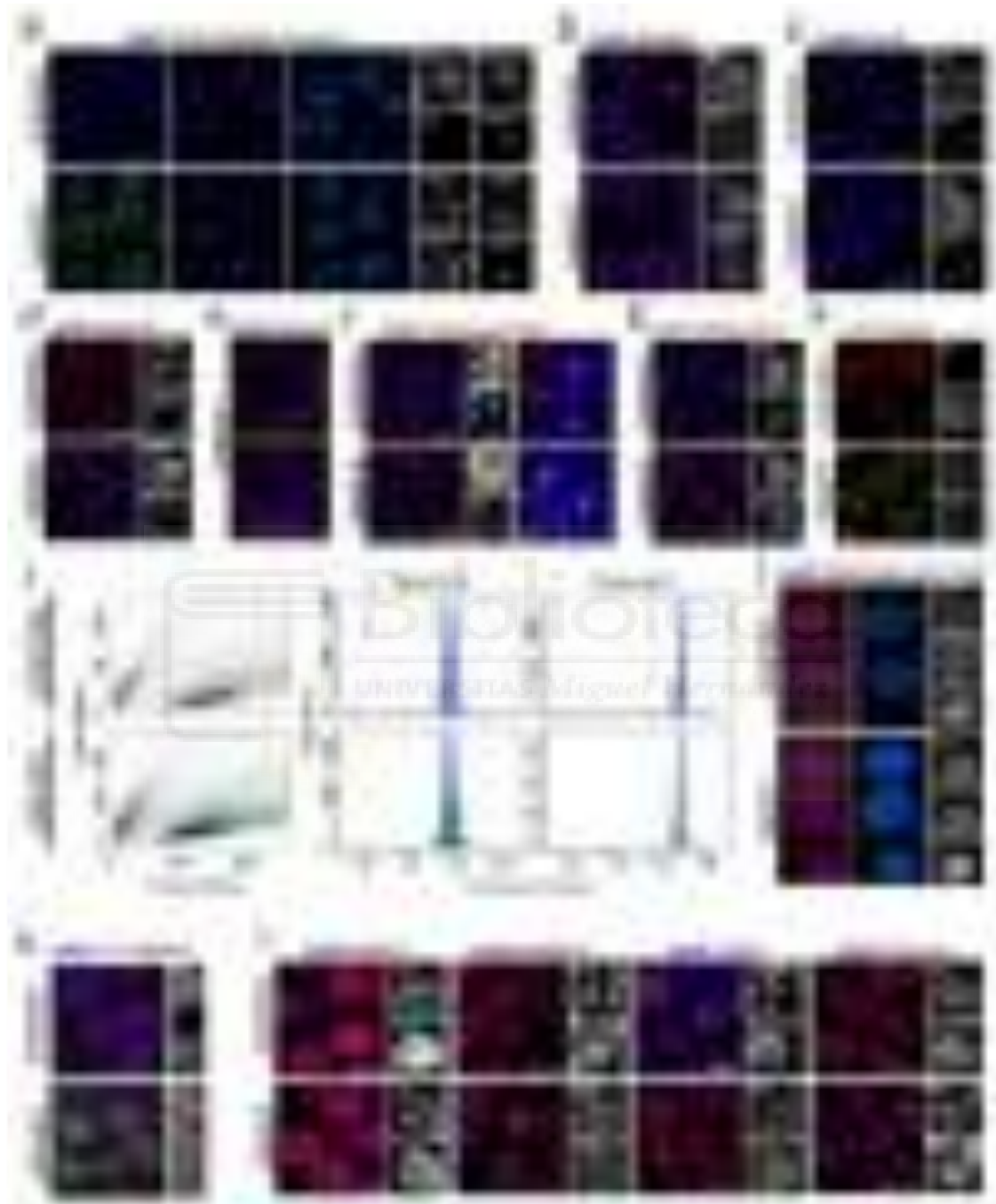


Figure 2. H2BGFP expression alters heterochromatin and euchromatin organization in hippocampal CA1 neurons. **a.** Quadruple fluorescent imaging of brain slices from control and H2BGFP mice detecting native GFP fluorescence, immunostaining for two nucleolar proteins (fibrilarin and nucleolin) and DNA counterstaining with DAPI. **b.** Immunostaining against Sam68, a protein enriched at the spliceosome, revealed no difference between control and H2BGFP mice. **c.** Immunostaining against coilin, a protein located at Cajal bodies, revealed no difference. **d-e.** Immunostaining with lamin B was normal in most cells (d), although a small

percentage of H2BGFP-expressing neurons exhibited lamin B invaginations (e, arrows). **f.** Pancentromeric probe FISH revealed the declustering of centromeres in H2BGFP mice. Note the association of centromere label with numerous DNA foci in bitransgenic mice (arrows). **g.** Immunostaining of brain slices using antibodies against the heterochromatin-associated histone modification H3K9me2/3. **h.** Double immunostaining using antibodies against GFP and mCyt. **i.** Flow cytometry of H2BGFP nuclei from hippocampal cells. The difference in PI signal observed in GFP⁺ cells disappeared upon HCl treatment. **j.** Double immunostaining using antibodies against H3K27me3 and phospho-pol II S5P. **k.** Double immunostaining using antibodies against GFP and MeCP2. **l.** Immunostaining against H3K9,14ac, H2AK5ac, pan-H2Bac and H4K12ac. Bars: 10 μ m. Nuclei were counterstained with DAPI except when indicated otherwise.

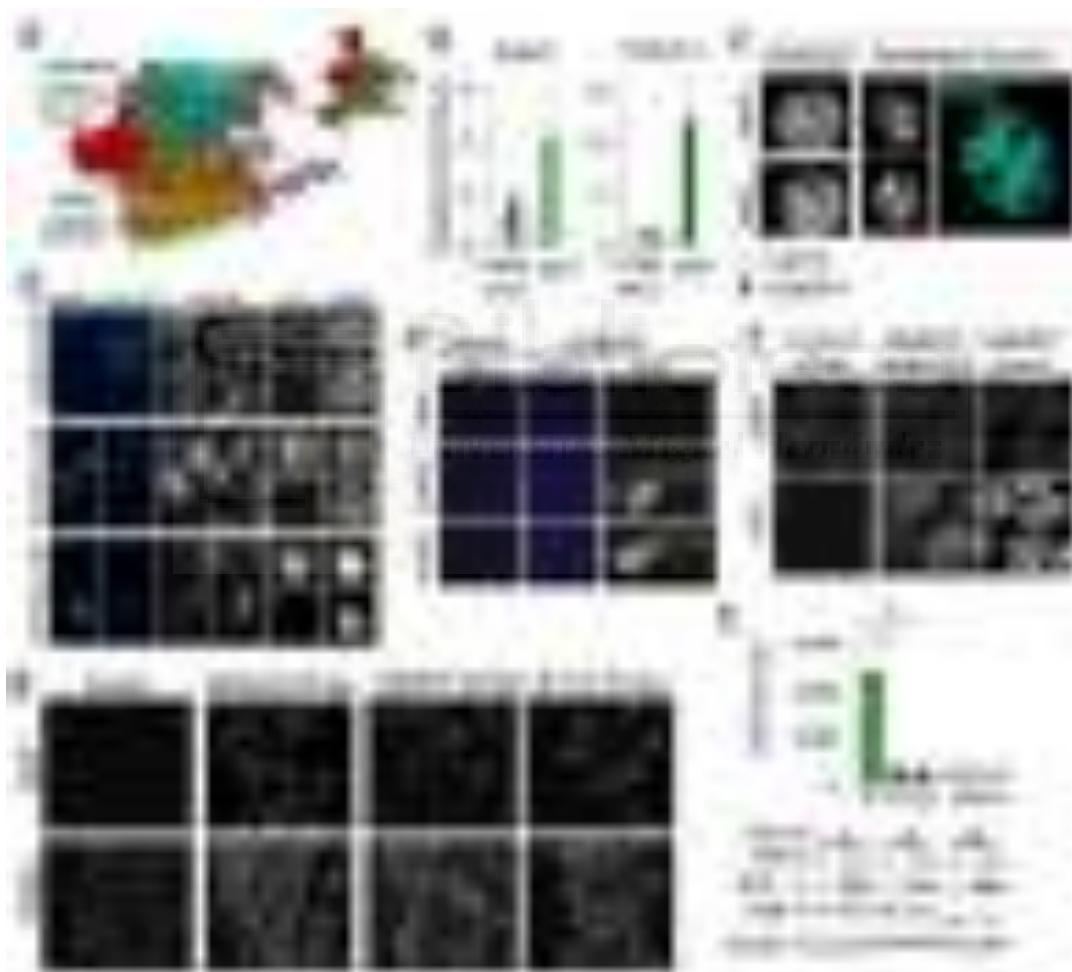


Figure 3. H2BGFP accumulation destabilizes highly compacted chromatin structures. **a.** Model of nucleosome sandwich incorporating a single H2BGFP molecule. The steric difficulty to accommodate the GFP tag increases if we consider that each nucleosome may contain up to 2 molecules of GFP (upper right inset). **b.** ChIP assays using anti-GFP antibody indicate that H2BGFP is incorporated into chromatin and enriched in silent genes. Data are represented as mean \pm s.e.m.; $n=9$ for both genotypes in H3K4me3 analysis; $n=4$ (control) and 5 (H2BGFP) in GFP analysis; *: $p<0.05$. **c.** HEK293 cells and primary hippocampal neurons (10DIV) 24 h after transfection with a H2BGFP-expressing construct show normal DNA staining. **d.**

Neuro-2a cells were transfected with an H2BGFP-expressing construct and then treated with dbcAMP to stop proliferation and promote neuronal differentiation. H2BGFP expression was associated with progressive loss of chromatin architecture in differentiating cells (pictures correspond to 3 and 9 days after adding dbcAMP to the medium). **e.** At postnatal day 6 (PND6), CA1 neurons of bitransgenic mice express very low or no GFP and exhibit a normal intranuclear organization. At PND30, CA1 neurons of bitransgenic mice express strong GFP fluorescence and show the same aberrant pattern described for adult mice (PND90). **f.** Induction of transgene expression in adult mice triggers a progressive disruption of chromocenter organization. **g.** GFP expression is still detected in the nucleus of CA1 neurons in H2BGFP mice 4 months after dox addition to the mouse diet. Note that the neurons that do not express GFP fluorescence have recovered a normal DNA staining pattern with few large chromocenters and peripheral heterochromatin. Images correspond to 9-month old mice that were either kept out of dox (Control and H2BGFP Off dox images) or in which dox was added to the diet when the animals were 5-month old. The two sets of images under the “H2BGFP Off dox 4 m On dox” label correspond to two independent animals. **h.** RT-qPCR (up) and western-blot (down) assays indicates that although RNA levels were severely reduced in mice fed with dox for 4 or 10 days, protein levels were not reduced. Data are represented as mean \pm s.e.m.; n= 2 per group; *: p<0.05.



Figure 4. Transcriptional dysregulation in H2BGFP mice. **a.** MA plot summarizing differential expression in H2BGFP mice. **b.** Heatmap showing the top 50 TCIDs differentially expressed in H2BGFP mice. Gene downregulations (blue) were much more abundant than upregulations (red); several upregulated TCIDs recognizes histone H2B transcripts and likely report transgene expression. **c.** Biological validation of candidate genes by RT-qPCR analysis. *: p < 0.05 (Student’s t test), n= 5 per group.

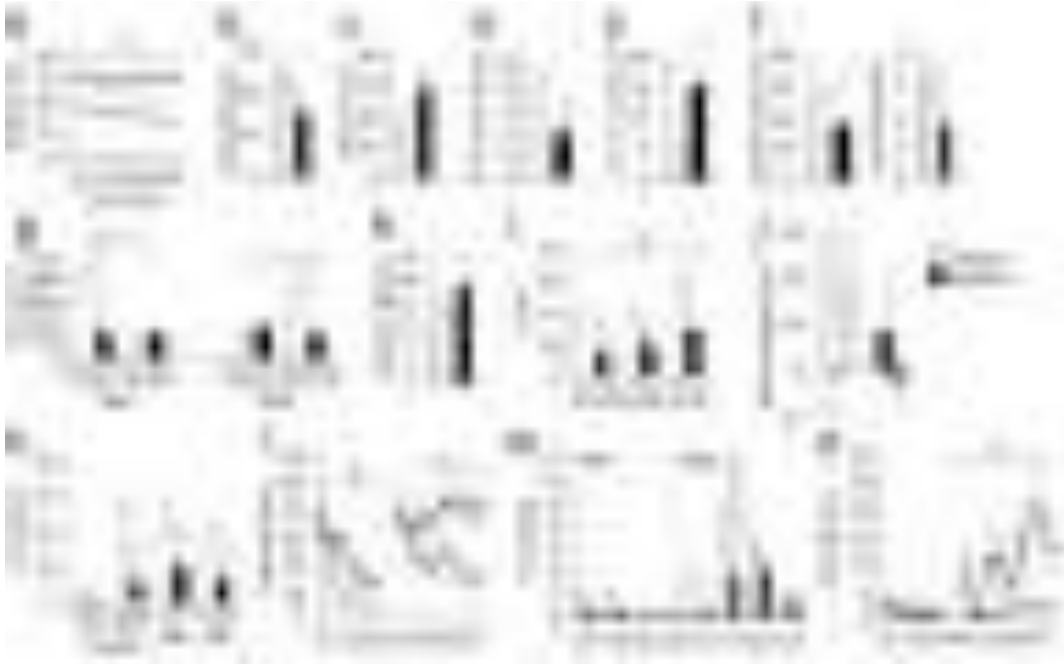


Figure 5. Behavioral consequences of the loss of chromatin architecture. **a-c.** Total travelled distance (a), resting time (b) and speed (c) in an open arena. **d.** Performance in the marble burring task. **e.** Time taken to first approach a novel object in a familiar arena. **f.** Performance in social interaction task. **g.** Performance in the three-chambered social approach task (Test1), and social novelty preference task (Test2). **h.** Latency for first reaction in the hot plate test. **i.** Performance in the PPI test. **j.** Performance in the NOR task. **k.** Performance in the fear conditioning task. **l-n.** Visible and hidden platform watermaze tasks: Latency to find the platform (l); number of crossing in the two probe trials (PT1 and PT2) (m); and time floating (n). TQ: target quadrant. #: genotype effect < 0.05 (repeated-measure ANOVA); *: $p < 0.05$. **a-h:** $n = 9$, both groups; **i:** 8 control and 7 H2BGFP; **j-k:** 9 control and 7 H2BGFP; **l-n:** $n = 7$, both groups. H2BGFP: dark squares; control: open circles. See Supplementary Fig. 4 for additional details.

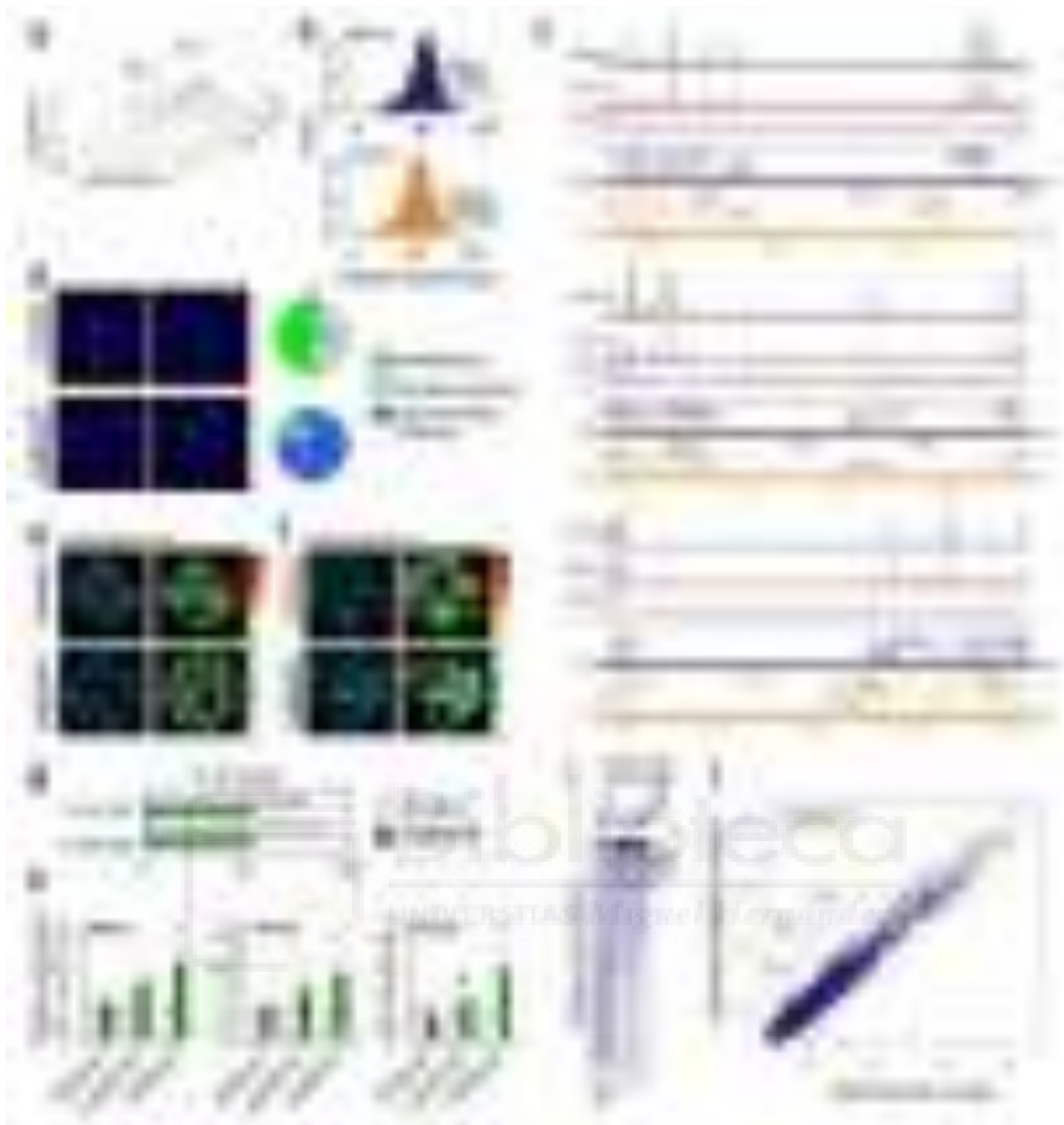


Figure 6. Epigenetic dysregulation of serotonin receptor genes. **a.** Plot presenting the fold change, p-value and distance to farthest neighbor of genes in Fig. 4B. **b.** The distance between *Htr1a*, *Htr1b* and *Htr2a* and, at least, one of the two adjacent genes is far above the median, both in mice (blue) and humans (orange). **c.** Genomic view of the *Htr1a*, *Htr1b* and *Htr2a* loci in the mouse (blue) and human (orange) genome and the profiles in hippocampal chromatin for H3K4me3 and H3K9,14ac and H3K27me3 histone marks. **d.** FISH for *Htr1a* (red, arrow heads) with Hoechst counterstaining. The sector graphs show the percentage of *Htr1a* alleles located at the nuclear periphery, associated with chromocenter/internal DNA foci or the nucleoplasm. **e-f.** Association of *Htr1a* alleles (red, arrow heads) with the activated forms of Pol II S2P (e) and S5P (f), both labeled in green. Color maps represent the correlation coefficient between intensities of PolII signal and hybridization signal. **g.** Quantification of the experiments in panels e and f. **h.** ChIP assays at the *Htr1a*, *Htr1b* and *Htr2a* promoters. Data are represented as mean \pm s.e.m.; n= 3 per group; *: p<0.05; #: p= 0.07. **i.** Heatmap of read densities across Refseq TSSs (10 kb window around TSS) in input and H3K27me3 datasets. Red bar: 5647 genes. **j.** Scatter plot of H3K27me3 enrichment in the hippocampus of H2BGFP and control mice. The regression line (green dotted line) and coefficient of determination are shown.

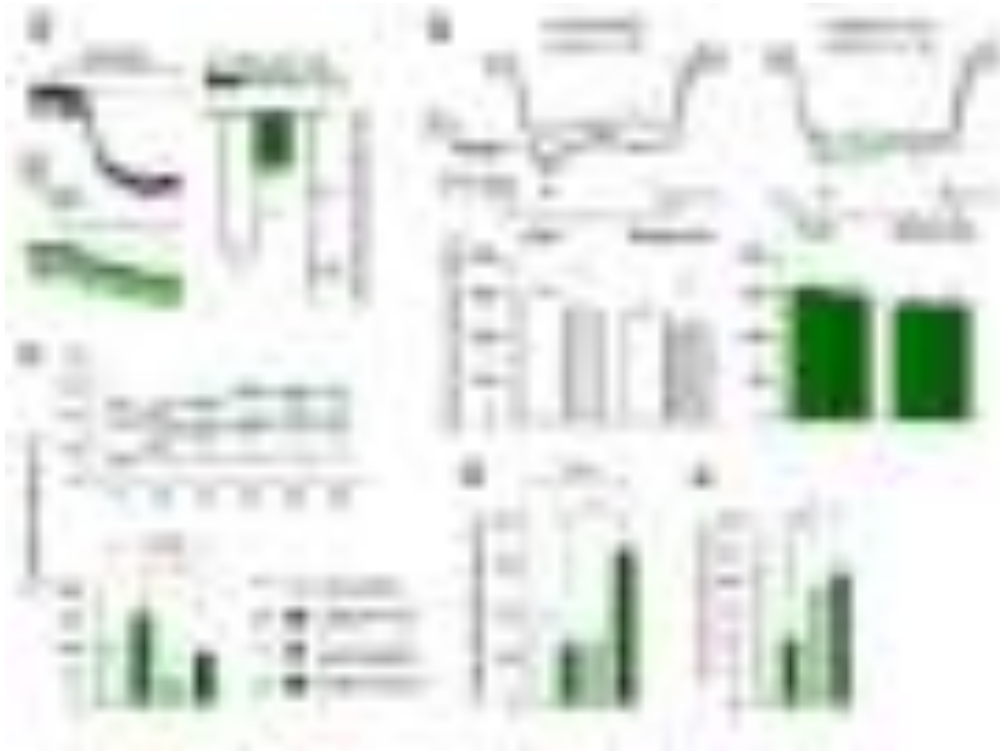


Figure 7. Serotonin signaling is impaired in H2BGFP mice. **a.** Effect of the application of 5 μ M 5-HT on the resting membrane potential of CA1 pyramidal neurons from a control (black trace) or a H2BGFP (green trace) mouse. Dashed lines indicate the resting membrane potential (Control= -64.4 ± 1.4 mV, $n = 10$; H2BGFP= -63.8 ± 1.4 mV, $n = 7$; $p = 0.77$). The bar graph shows the average hyperpolarization caused by 5-HT (*: $p = 0.005$, $n = 10$ control, 7 H2BGFP). **b.** Representative responses to 25 pA hyperpolarizing current pulses. Bar graphs show the average values of membrane input resistance in control ($n = 10$, $p_{(\text{peak})} = 0.002$, $p_{(\text{steady state})} = 0.007$) and H2BGFP neurons ($n = 7$, non significant) treated (hatched bars) or not (open bars) with in 5-HT, at the peak of the hyperpolarizing response and at the end of the pulse (arrows). **c.** Locomotor activity in an open arena (8 mice per group; #: genotype effect < 0.05 ; \$: drug effect < 0.05). **d-e.** Interaction time (E) and duration of social contacts (D) in a social interaction task ($n = 12$ for vehicle (VEH), $n = 13$ for buspirone (BUSP) groups; #: genotype effect < 0.05 ; \$: drug effect; &: drug x genotype interaction < 0.05 ; *: $p < 0.05$, Student t-test comparison with control group at least that indicated otherwise).

